UNIVERSITY OF SOUTHAMPTON

FACULTY OF PHYSICAL AND APPLIED SCIENCES

Physics

On Leptogenesis, Flavour Effects and the Low Energy Neutrino Parameters

by

Luca Marzola

Thesis for the degree of Doctor of Philosophy

13th November 2012

UNIVERSITY OF SOUTHAMPTON

ABSTRACT

FACULTY OF PHYSICAL AND APPLIED SCIENCES
Physics

Doctor of Philosophy

ON LEPTOGENESIS, FLAVOUR EFFECTS AND THE LOW ENERGY NEUTRINO PARAMETERS

by **Luca Marzola**

Contemporary Physics is testing the boundaries of one of its existent paradigms, the Standard Model of Particle Physics. In recent years many attempts have been made in order to overcome the difficulties arising within this well-known framework. Along with the effort made on the experimental side, for example the search for the Higgs boson at the Large Hadron Collider, there is a present requirement for testable theoretical scenarios describing Physics beyond the current paradigms. To this purpose we consider the type I Seesaw extension of the Standard Model, in which the neutrino mass puzzle is possibly solved and the baryon asymmetry of the Universe explained via Leptogenesis. After reviewing the basis of the Seesaw mechanism and its recent developments we present a rigorous investigation which confirms the validity of the adopted description. Encouraged by this success we then employ the interplay of light and heavy neutrino flavour effects to address the problem of initial conditions in Leptogenesis. Our analysis identifies the τ N_2-dominated scenario as the only possible answer, proposing a well defined setup in which successful strong thermal Leptogenesis is achieved. Attracted by the properties of our solution we consequently investigate its compatibility with the $SO(10)$-inspired model of Leptogenesis. The result is indeed intriguing: the strong thermal solutions of the $SO(10)$-inspired model deliver sharp predictions on the low-energy neutrino parameters that fall within the reach of future neutrino experiments, opening up the possibility of a full test of this attractive Leptogenesis scenario.

Contents

List of Figures

List of Tables

Declaration of Authorship

I, **Luca Marzola**, declare that the thesis entitled *On Leptogenesis, Flavour Effects and the Low Energy Neutrino Parameters* and the work presented in the thesis are both my own, and have been generated by me as the result of my own original research. I confirm that:

- this work was done wholly or mainly while in candidature for a research degree at this University;
- where any part of this thesis has previously been submitted for a degree or any other qualification at this University or any other institution, this has been clearly stated;
- where I have consulted the published work of others, this is always clearly attributed;
- where I have quoted from the work of others, the source is always given. With the exception of such quotations, this thesis is entirely my own work;
- I have acknowledged all main sources of help;
- where the thesis is based on work done by myself jointly with others, I have made clear exactly what was done by others and what I have contributed myself;
- parts of this work have been published as: [1], [2] and [3].

Date:13/09/2012

Acknowledgements

It is indeed a hard task to mention all the people that directly or indirectly contributed to the present Thesis, therefore I apologise in advance should I forget somebody. Let me start by acknowledging the support of the NExT institute and SEPnet, who funded my research during these years. I also wish to express my gratitude to the School of Physics and Astronomy of the University of Southampton, the SHEP group in particular, for providing the friendly and informal environment in which I could develop my studies. In this regard, beside my advisor S. F. King, I thank my office mates, especially B. Samways, K. Mimasu, M. Brown, J. Callaghan, J. Lyon, D. Becciolini and P. Svantesson for the interesting discussions – sometimes also – about Physics.
Obviously, for this work I am most indebted to my supervisor, P. Di Bari, who kindly guided me during the years of my PhD in Southampton. I also wish to thank D. A Jones, S. Blanchet and E. Bertuzzo for clarifying my doubts during our collaborations. Last but not least, I wish to thank my wife and my family for supporting me during the drafting of the present work.

Conventions and abbreviations

In the present Thesis we adopt the natural system of units setting $\hbar = c = k_B \equiv 1$. What is written is therefore meant multiplied by an appropriate combination of these constants yielding to the correct dimensions. Throughout our study we also consistently refer to the Lagrangian density as the Lagrangian. The convention adopted for the particles of the Standard Model are presented in Appendix A.
A list of the abbreviations we employ follows:

BAO	baryon acoustic oscillations
BAU	(the) baryon asymmetry of the Universe
BBN	Big Bang Nucleosynthesis
CC	charged current (interactions)
CKM	(the) Cabibbo-Kobayashi-Maskawa (matrix)
CL	confidence level
CMB	(the) Cosmic Microwave Background
Diag(X), D_X	diagonal form of the matrix X
ES	elastic scattering
EW	Electro-Weak (interactions)
GUT	grand unified theory
IO	inverted order (of the light neutrino mass spectrum)
LH	left-handed
LHC	(the) Large Hadron Collider
LHS	left-hand side (of an equation)
NO	normal order (of the light neutrino mass spectrum)
PMNS	(the) Pontecorvo-Maki-Nakagawa-Sakata (matrix)
QCD	Quantum Chromo Dynamics
RH	right-handed
RHS	right-hand side (of an equation)
SM	Standard Model (of Particle Physics)
Tr(X)	trace of the matrix X

Chapter 1

Introduction: two limitations of the Standard Model

Since the discovery of the neutral current interactions in 1973, the Standard Model [4–6] has been increasingly regarded as the paradigm of modern Particle Physics. The theoretical setup of this framework proposes two types of fermionic fields, quarks and leptons, which interact with the gauge bosons imposed by the local $SU(3)_C \times SU(2)_L \times U(1)_Y$ symmetry group. The particle content of the model is completed by a further field, associated to the Higgs boson, which triggers the breaking of the $SU(2)_L \times U(1)_Y$ symmetry group down to the $U(1)_Q$ of Quantum ElectroDynamics. After the phase transition, the Weak Interaction gauge bosons, as well as quarks and leptons acquire a mass proportional to the characteristic energy scale of the symmetry breaking, in a way that preserves the gauge-invariance of the original theory [7]. On the experimental side, the extensive examination of Standard Model led to an impressive list of achievements. For example the mass of Z and W bosons, measured for the first time in 1983 [8–11], are in striking agreement with the predictions of the theory. On top of that, also the third generation of quarks and leptons involved in this framework has been experimentally confirmed, with the discovery of the bottom quark in 1977 [12], the top quark in 1995 [13, 14] and the τ neutrino in the year 2000 [15]. The latest success of the Standard Model is indeed the recent discovery of the Higgs boson at the LHC [16, 17], which concludes the experimental search of the particle content proposed by this theory.

Yet, despite the appealing theoretical framework and the numerous experimental confirmations, the Standard Model is not an exhaustive description of Nature. For instance, the Standard Model does not explain one of the fundamental forces, Gravity, being substantially incompatible with the theory of General Relativity. On top of that, recent cosmological observations revealed that the particles of the Standard Model account only for a small fraction of the energy budget of the Universe. The biggest contributions

into the latter are in fact provided by the Dark Energy and the Dark Matter, two mysterious agents that remain unexplained within this framework. Further issues arise also on the theoretical side, with the strong-CP and the hierarchy problems for example. The former concerns strong interactions, which respect the CP symmetry despite the underlying theory, the Quantum Chromo Dynamics (QCD), presenting no arguments preventing the violation of this quantity. The hierarchy problem regards instead the mass of the Higgs boson, detected well below the Grand Unified Theory and Planck scales where the relevant quantum correction seem to push it.
In this Thesis we will focus on two further problems that the Standard Model leaves unsolved, connected respectively to the observation of an asymmetry between matter and antimatter in our Universe, reviewed in Section 1.2, and to the properties of neutrinos, as depicted by the neutrino oscillation experiments discussed below.

1.1 A first puzzle: neutrino oscillations

Neutrinos have always been a puzzle to physicists. Even nowadays, after more than forty years of dedicated studies, some fundamental properties and the exact number of neutrino species are still unknown[1]. This Section is dedicated to the analysis of neutrino oscillations, originally proposed by B. Pontecorvo in 1968 [18]. After presenting a basic review of the mechanism and the supporting experimental evidences, we will discuss the compatibility of neutrino oscillations with the framework of the Standard Model.

1.1.1 Neutrino oscillations: basics and experimental evidences

Neutrinos are indeed elusive particles, bearing no colour nor electric charges. They are only involved in Weak Interactions, coupled to the charged leptons and the gauge bosons of the broken $SU(2)_L$ symmetry in the specific case of charge current interactions – Section A.2:

$$\mathcal{L}_{cc}^{m_\nu \neq 0} = -\frac{g}{\sqrt{2}} \sum_{\substack{i=1,2,3 \\ \alpha=e,\mu,\tau}} \left[\overline{n_{iL}}\, \gamma^\mu \, (U^\dagger)_{i\alpha}\, l_{\alpha L} \right] W_\mu + \text{H.c.}. \tag{1.1.1}$$

Here the subscript "L" denotes the left-handed components of the involved fields, remarking the chiral nature of Weak Interactions. Considering three neutrinos species, the Pontecorvo-Maki-Nakagawa-Sakata (PMNS) matrix U [19, 20] is a unitary 3×3 matrix which regulates the mixing of the fields n_i, diagonalising the neutrino mass term, into

[1] The results obtained by the LEP experiment on the invisible decay width of the Z boson indicate the existence of three species of neutrinos, associated to masses $m_i \lesssim m_Z/2$. The existence of further neutrino species characterised by a higher mass scale cannot consequently be excluded. Similarly, also the presence of additional sterile neutrinos, which are not directly involved in the Weak Interactions, is not disproved by the LEP result.

the *flavour neutrinos* ν_α that diagonalise eq. (1.1.1) in the flavour space:

$$\nu_{\alpha L} \coloneqq \sum_{i=1}^{3} U_{\alpha i}\, n_{iL}, \qquad \alpha = e, \mu, \tau \tag{1.1.2}$$

To understand the basics of neutrino oscillations we focus on the evolution of a one-particle state generated by one of the above flavour neutrino fields. For sake of simplicity we will neglect the complications brought by the presence of matter and simplify our notation by leaving the subscript "L" understood. Furthermore, for the rest of the Section, greek subscripts will run on the three flavours (e, μ, τ) while the latin subscripts are reserved for $(1, 2, 3)$.
The definition of flavour neutrino fields in eq. (1.1.2) induces an analogous mixing on the corresponding particle states denoted by a ket[2]:

$$|\nu_\alpha\rangle = \sum_{i=1}^{3} U^*_{\alpha i}\, |n_i\rangle\,. \tag{1.1.3}$$

Notice that the neutrino particles $|\nu_\alpha\rangle$ that experiments involve, should be therefore regarded as superpositions of the mass eigenstates $|n_i\rangle$, satisfying the orthogonality condition

$$\langle n_i | n_j \rangle = \delta_{ij} \tag{1.1.4}$$

and corresponding to physical particles of mass m_i. The Schrödinger equation controls the time evolution of these particle states, hence after a time t we have:

$$|\nu_\alpha(t)\rangle = \sum_{i=1}^{3} U^*_{\alpha i}\, e^{-iE_i t}\, |n_i\rangle\,. \tag{1.1.5}$$

With the term *neutrino oscillations* we refer to flavour transitions related to variations in the flavour of a neutrino state. For this effect a neutrino co-emitted with a charged lepton of flavour α, $|\nu_\alpha\rangle$, could subsequently be measured as a neutrino $|\nu_\beta\rangle$ of flavour $\beta \neq \alpha$. Experimentally these processes are detected in reactions as $\nu_\alpha(t) + N' \to l_\beta + N$, where $\alpha \neq \beta$, with transition probability proportional to the *oscillation probability*

$$P_{\nu_\alpha \to \nu_\beta}(t) = |\langle \nu_\beta | \nu_\alpha(t) \rangle|^2 = \left| \sum_{i,j=1}^{3} U_{\beta j} U^*_{\alpha i}\, e^{-iE_i t}\, \delta_{ij} \right|^2 \tag{1.1.6}$$

where the orthogonality condition in eq. (1.1.4) was used. Notice that the typical energy spectrum of neutrino fluxes is peaked around $(1 - 10^3)$ MeV, hence neutrinos can be regarded as relativistic particles with $E_i \simeq E + \frac{m_i^2}{2E}$. In addition to that, we can here identify $t = L$, being L the length that the particle travelled during the time t of its

[2] In the next Sections this notation is left understood when we unambiguously refer to one-particle states.

evolution. Finally, by defining $\Delta m^2_{ik} \coloneqq m^2_i - m^2_k$, the oscillation probability becomes:

$$P_{\nu_\alpha \to \nu_\beta}(t) = \sum_{i,k=1}^{3} U_{\beta i}\, U^*_{\alpha i}\, U^*_{\beta k}\, U_{\alpha k}\, e^{-i\frac{\Delta m^2_{ik} L}{2E}}. \tag{1.1.7}$$

Some remarks follow:

- the neutrino squared mass differences Δm^2_{ik} drive the oscillations. Consequently, in a framework involving three neutrinos, at least two non-degenerate mass eigenstates are required in order to provide a non-zero oscillation mode. Furthermore, the independence of the presented mechanism from the absolute neutrino mass scale implies, on the experimental side, the impossibility of detecting the latter through neutrino oscillation experiments.
- The PMNS matrix elements set the amplitude of the oscillations. We emphasise also that the quartic product in eq. (1.1.7) is invariant under the rephasing $U_{\alpha k} \to e^{i\psi_\alpha} U_{\alpha k} e^{i\phi_k}$. Consequently, as the explicit form of the PMNS matrix in eq. (1.1.12) will make clear, neutrino oscillation experiments cannot probe the Majorana phases ρ and σ in U.

Having said that, the final formula for the oscillation probability follows from eq. (1.1.7) after some algebra:

$$\begin{aligned} P_{\nu_\alpha \to \nu_\beta}(t) = \delta_{\alpha\beta} - 4\mathrm{Re} \sum_{\substack{i>k \\ i,k=1,2,3}} U_{\beta i}\, U^*_{\alpha i}\, U^*_{\beta k}\, U_{\alpha k}\, \sin^2\left(\frac{\Delta m^2_{ik} L}{2E}\right) + \\ + 2\mathrm{Im} \sum_{\substack{i>k \\ i,k=1,2,3}} U_{\beta i}\, U^*_{\alpha i}\, U^*_{\beta k}\, U_{\alpha k}\, \sin\left(\frac{\Delta m^2_{ik} L}{2E}\right). \end{aligned} \tag{1.1.8}$$

We now discuss the experimental evidences supporting the neutrino oscillation mechanism sketched above. A first hint that neutrino oscillations are realised in Nature dates back to the 1960s, with the Homestake experiment.

By employing a chlorine-based detector, sensitive to electron neutrinos via the charged current (CC) interaction $\nu_e + {}^{37}\mathrm{Cl} \to e^- + {}^{37}\mathrm{Ar}$, this experiment measured for the first time the flux of electron neutrinos emitted by the Sun[3]. The result was a puzzling evidence: the Homestake experiment revealed a serious deficit in the observed particles [21] with respect to the Standard Solar Model predictions [22]. In this way the *solar neutrino problem* was born.
To understand the origin of this anomaly several experiments repeated the measurement in the following years, employing different technologies for the detection of the

[3] During nuclear fusions protons are converted into neutrons through the reaction $p + e^- \to n + \nu_e$. The Sun is therefore a source of electron neutrinos with $E \sim$MeV.

neutrino flux. On one hand water Cherenkov detectors, as Kamiokande [23] and Super-Kamiokande [24], measured the high-energy part of the spectrum relying on elastic scattering (ES) processes $\nu_\alpha + e^- \to \nu_\alpha + e^-$, mainly sensitive to electron neutrinos due to the enhanced cross section. On the other, the radiochemical Gallium-based experiments GALLEX/GNO [25, 26] and SAGE [27] were sensitive to low-energy neutrinos, observed through the CC interaction $\nu_e + {}^{71}\mathrm{Ga} \to e^- + {}^{71}\mathrm{Ge}$.
All the experiments confirmed the deficit in the detected flux. Furthermore, the dependence of the phenomena on the energy of neutrinos was emphasised owing to the different detection techniques.
The fundamental importance of the solar neutrino problem became explicit in the year 1998, when the Super-Kamiokande experiment measured a similar anomaly in the atmospheric neutrino fluxes[4]. In particular, the observation was performed by comparing the number of detected particles for incoming directions with opposite zenith angles. This revealed a zenith-depenent deficit of neutrinos, which found in a $\nu_\mu - \nu_\tau$ mixing the most convincing explanation [28]. The Super-Kamiokande result was therefore strongly supporting the solution of the solar neutrino problem in favour of the neutrino oscillation mechanism. The conclusive evidence was given three years later, when the SNO experiment published its analysis of the solar neutrino flux [29]. By using a heavy water Cherenkov detector relying on ES, CC interactions and the neutral current interactions $\nu_\alpha + d \to p + n + \nu_\alpha$, SNO measured both the electron and the $\mu - \tau$ components of the neutrino flux. While an anomaly was once again detected in the electron channel, the measurements of the total flux were found in agreement with the Standard Solar Model. This resulted in a direct evidence for neutrino flavour transformations, confirming the neutrino oscillation mechanism as the correct answer to the solar neutrino problem.

In the following years, further evidence supporting this solution was provided by the so called *reactor and accelerator experiments*. These involve the detection of terrestrial antineutrinos generated in the β-decay chains of the heavy nuclei in fission reactors and particle accelerators. For the former category we mention here the KamLAND experiment, which corroborated the large mixing angle solution of the solar neutrino problem [30]. Amongst the accelerator experiments we recall instead K2K and MINOS, that verified the result on the atmospheric neutrinos previously obtained by the Super-Kamiokande experiment and confirmed the oscillation mechanism is the only cause behind the detected flux anomaly [31], [32].

1.1.2 Neutrino oscillations and the Standard Model

Having sketched the basics of neutrino oscillations and reviewed the numerous supporting evidences, we can now discuss the compatibility of this mechanism with the Standard

[4]Protons from cosmic rays collide on the nuclei in the atmosphere, resulting in hadronic showers containing especially pions. The pions then decay into muons $\pi^- \to \mu^- + \overline{\nu_\mu}$, $\pi^+ \to \mu^+ + \nu_\mu$ generating neutrinos with energies $E \sim$GeV.

Model of Particle Physics.

In theories presenting degenerate neutrinos, and likewise for the Standard Model (SM), the PMNS matrix U in eq. (1.1.2) can be reabsorbed by performing a redefinition of the neutrino fields – more details are presented in Section A.2, after eq. (A.2.6) –

$$\mathcal{L}_{cc}^{m_\nu \neq 0} = -\frac{g}{\sqrt{2}} \sum_{\substack{i=1,2,3 \\ \alpha=e,\mu,\tau}} \left[\overline{n_{iL}}\, \gamma^\mu\, (U^\dagger)_{i\alpha}\, l_{\alpha L}\right] W_\mu + \text{H.c.} \rightarrow \tag{1.1.9}$$

$$\rightarrow \mathcal{L}_{cc}^{SM} = -\frac{g}{\sqrt{2}} \sum_{\alpha=e,\mu,\tau} \left[\overline{n_{\alpha L}}\, \gamma^\mu\, l_{\alpha L}\right] W_\mu + \text{H.c.} \tag{1.1.10}$$

Notice that the eq. (1.1.9) hence implies

$$U_{\alpha i} \Big|_{SM} \equiv \delta_{\alpha i} \tag{1.1.11}$$

and that massless or degenerate neutrinos require as well $\Delta m^2_{ik} \equiv 0$.

Clearly, these predictions can be investigated through neutrino oscillation experiments and, in regard to this, our discussion in Section 1.1.1 has already revealed the outcome: the description of neutrinos within the Standard Model is clearly in disagreement with the outcomes of neutrino oscillation experiments.
In order to quantify this disagreement we focus now on the PMNS mixing matrix, as delineated by experiments.

1.1.2.1 The PMNS mixing matrix

A general parametrization of a unitary 3×3 matrix is given by three mixing angles and six phases. The number of the latter can be further reduced to one or three by rephasing the lepton fields in the Lagrangian, depending on the Dirac/Majorana nature of neutrinos. As a consequence the a general form of the PMNS matrix is

$$U = \begin{pmatrix} c_{12}c_{13} & s_{12}c_{13} & s_{13}e^{-i\delta} \\ -s_{12}c_{23} - c_{12}s_{23}s_{13}e^{i\delta} & c_{12}c_{23} - s_{12}s_{23}s_{13}e^{i\delta} & s_{23}c_{13} \\ s_{12}s_{23} - c_{12}c_{23}s_{13}e^{i\delta} & -c_{12}s_{23} - s_{12}c_{23}s_{13}e^{i\delta} & c_{23}c_{13} \end{pmatrix} \cdot \begin{pmatrix} e^{i\rho} & 0 & 0 \\ 0 & 1 & 0 \\ 0 & 0 & e^{i\sigma} \end{pmatrix} \tag{1.1.12}$$

where the $c_{ij} \equiv \cos(\theta_{ij})$, $s_{ij} \equiv \sin(\theta_{ij})$ and $\rho = \sigma = 0$ for Dirac particles.

As remarked before, neutrino oscillations are not sensitive to the absolute neutrino mass scale. In terms of the neutrino mass spectrum this leads to a further complication: beside the normal ordering (NO) of neutrino masses for which eq. (1.1.12) holds, a second pattern, the inverted ordering (IO), is allowed by current experiments. As shown in Figure 1.1, maintaining the convention $m_1 < m_2 < m_3$, IO corresponds to a permutation

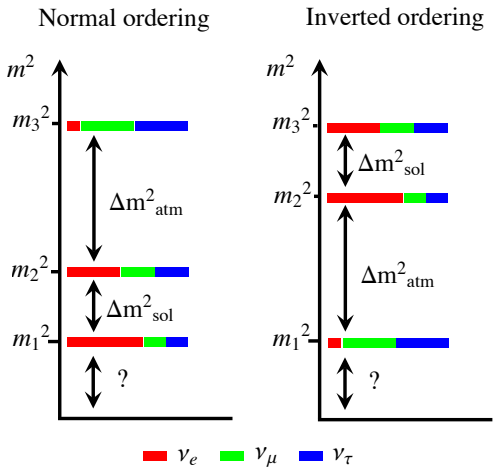

Figure 1.1: Normal ordering and inverted ordering compared, adapted from [33]. The colour code represents the approximate flavour composition of the neutrino mass eigenstates n_i.

of the involved neutrinos and the appropriate mixing matrix is consequently obtained from eq. (1.1.12) through a permutation of the corresponding columns.

The current status of the parameters measured through neutrino oscillation experiments is presented in Table 1.1.

Parameter	Best fit	1σ range	3σ range
$(\Delta m^2_{sol} = \delta^2 m)/10^{-5}$ eV^2 (NO and IO)	7.54	7.32 - 7.80	6.99 - 8.18
$(\Delta m^2_{atm} \simeq \Delta^2 m)/10^{-3}$ eV^2 (NO)	2.43	2.33 - 2.49	2.19 - 2.62
$(\Delta m^2_{atm} \simeq \Delta^2 m)/10^{-3}$ eV^2 (IO)	2.42	2.31 - 2.49	2.17 - 2.61
$\sin^2\theta_{12}/10^{-1}$ (NO and IO)	3.07	2.91 - 3.25	2.59 - 3.59
$\sin^2\theta_{13}/10^{-2}$ (NO)	2.41	2.16 - 2.66	1.69 - 3.13
$\sin^2\theta_{13}/10^{-2}$ (IO)	2.44	2.19 - 2.67	1.71 - 3.15
$\sin^2\theta_{23}/10^{-1}$ (NO)	3.86	3.65 - 4.10	3.31 - 6.37
$\sin^2\theta_{23}/10^{-1}$ (IO)	3.92	3.70 - 4.31	3.35 - 6.63

Table 1.1: The current status of oscillation parameters for inverted ordering (IO) and normal ordering (NO), from [34].

The investigations report two non-zero squared mass differences, Δm^2_{atm} and Δm^2_{sol}, respectively measured in atmospheric and solar neutrino oscillations. The picture is consistent with a framework including three neutrino species, but these non-zero squared mass differences imply a first contrast with the requirement $\Delta m^2_{ik} \equiv 0$ of the Standard Model. As for the mixing angles, all the best values differ from null with a significance of at least 5σ, implying that also the prediction $U_{\alpha i} = \delta_{\alpha i}$ of the theory is rejected.
Indeed a substantial inconsistency is found between the Standard Model and the data that neutrino oscillation experiments present. This contrast is arising from the proposed

description of neutrinos, which involving purely massless particles precludes the possibility of accounting for neutrino oscillations. The experimental confirmation of the latter thus underlines the necessity of additional mechanisms to address the neutrino mass puzzle, providing in this way a first evidence for Physics beyond the Standard Model. In this regard we postpone a possible solution to the next Chapter, focusing for the moment once again on the neutrino phenomenology.

In commenting on Table 1.1, it would be a serious shortfall not mentioning the recent merits of reactor experiments in relation to the first measurements of θ_{13}. This is the only mixing angle that solar and atmospheric oscillations cannot test, constrained during the last decade only by the upper bound resulting from the CHOOOZ experiment [35]. A first 2σ indication for a non-zero θ_{13} was presented by the MINOS experiment [36] in 2011, followed by the 3σ evidence reported by the T2K collaboration [37] a few months later. Finally, in 2012, the Daya Bay [38] and the Reno [39] collaborations confirmed a non-zero mixing angle quoting a significance of respectively 5.2 and 4.9 standard deviations. The conclusive plots of the two investigations, involving the survival probability

$$P_{\overline{\nu_e}\to\overline{\nu_e}} := 1 - \sum_{\alpha=\mu,\tau} P_{\overline{\nu_e}\to\overline{\nu_\alpha}} \tag{1.1.13}$$

are reported in Figure 1.2. We insist on the cruciality of these results for a complete understanding of leptons, as the inferred values of θ_{13} remarkably allow for a direct measurement of the CP violation in the sector, encoded in the Dirac phase δ of the PMNS Matrix.

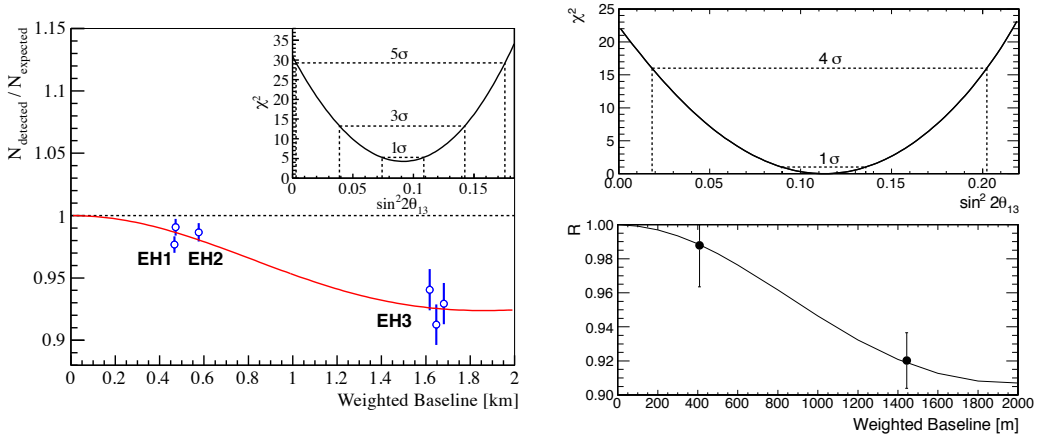

Figure 1.2: Experimental evidences for non-zero θ_{13}. Left panel: results from the Daya Bay experiment, [38]. Right panel: results from Reno experiment, [39]. The upper parts of both the panels show the χ^2 plot for the measured parameter $\sin^2(2\theta_{13})$. The remaining parts compare the measured neutrino events to the expected number given by the no-oscillation predictions. In particular the ratio $R := N_{detected}/N_{expected}$ is plotted against the detector distance L. The solid line corresponds to the best fit for the survival probability $P_{\overline{\nu_e}\to\overline{\nu_e}}$. The no-oscillations hypothesis requires $R \equiv 1$.

1.1.3 Exploring the neutrino mass scale

We analyse now another important aspect of neutrino phenomenology, related to the detection of the mass scale associated to these particles.

As shown in Section 1.1.1 and confirmed by Table 1.1, neutrino oscillations provide important informations on the neutrino mass hierarchy and the PMNS mixing parameters, with no sensitivity to the absolute neutrino masses scale. The complementary experiments, dedicated to a direct measurement of this parameter, hunt distortions near the kinematic endpoints of electron energy spectrums associated to allowed β-decays, for which the nuclear matrix elements generate no energy dependence. The results constrain the effective electron neutrino mass

$$m_\beta^2 \coloneqq \sum_{i=1}^{3} |U_{ei}|^2 \, m_i^2 \tag{1.1.14}$$

and latest upper bound

$$m_\beta \lesssim 2.4 \text{ eV} \quad (95\% \text{ CL}) \tag{1.1.15}$$

is due to the Mainz [40] and Troitzk [41] tritium experiments. The same collaborations are currently preparing a new joint experiment, KATRIN, aiming to reach a sensitivity of about 0.2 eV at 90% CL.

Beside m_β, neutrino Physics is in principle sensitive to another energy scale: the *effective Majorana mass* of neutrinoless double β-decays, m_{ee}.
The relevant process consists of two simultaneous β-decays with no emission of antineutrinos, as illustrated in the left panel of Figure 1.3. Each neutrinoless double β-decay therefore leads to a lepton number violation of two units[5], underlining that only Majorana neutrinos are involved. Clearly the process is forbidden in the Standard Model, hence the observation of these events would provide further evidence for new Physics. In particular, notice that neutrinoless double β-decay experiment can potentially decide on the fundamental problem of the Dirac/Majorana nature of neutrinos.

Currently no positive signals have been observed and the Majorana effective mass

$$m_{ee} \coloneqq \left| \sum_{i=1}^{3} U_{ei}^2 \, m_i \right| \tag{1.1.16}$$

[5]The Standard Model presents an accidental $U(1)_e \times U(1)_\mu \times U(1)_\tau$ symmetry associated to the three generations of lepton doublets. For the Noether theorem this symmetry corresponds to the conservation of three charges, *the family lepton numbers* L_e, L_μ, and L_τ. *The total lepton number* $L = \sum_\alpha L_\alpha$ is therefore conserved as well. With respect to the latter, a lepton carries a charge $L = +1$ while antileptons are associated to negative charges. If Majorana particles are involved no lepton number is conserved as the accidental symmetry is completely broken, while for Dirac massive neutrinos the symmetry breaks to $U(1)_L$, corresponding to the conservation of the total lepton number defined above [42].

has been constrained to

$$m_{ee} \lesssim (0.3 - 1.0) \text{ eV} \quad (90\%\text{CL}). \tag{1.1.17}$$

Nevertheless, it should be stressed that future experiments as MAJORANA [43] and GERDA [44] declare sensibilities below the 0.05 eV level. As shown in the right panel of Figure 1.3 this would constrain the neutrino mass spectrum, performing a complete test of the region associated to quasi-degenerate neutrinos and probing a part of the one associated to the inverted ordering.

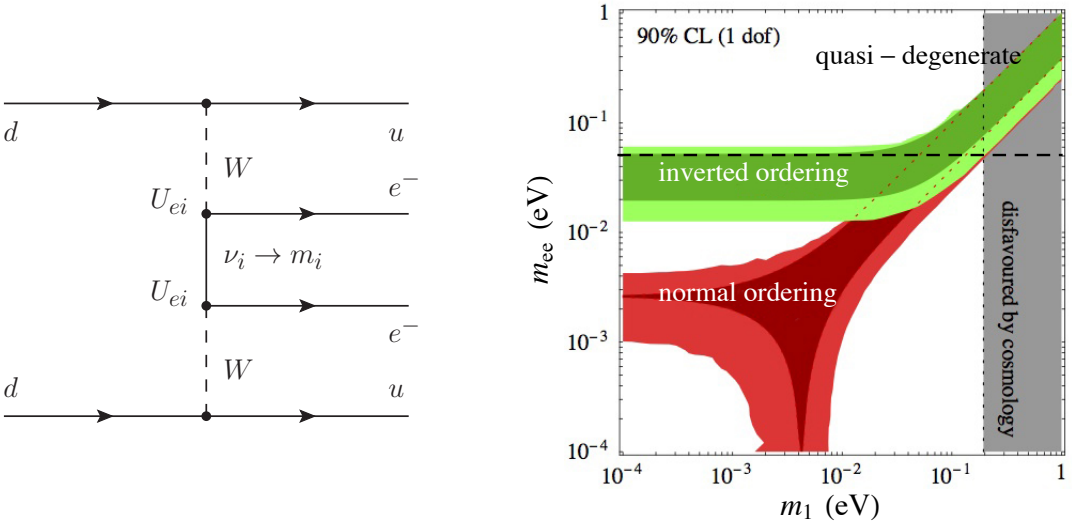

Figure 1.3: Neutrinoless double β-decay. Left panel: the tree level contribution to the process. Majorana neutrinos are required in order to observe the lepton number-violating transition.
Right panel: m_{ee} as a function of the lightest neutrino mass m_1, adapted from [45]. Regions corresponding to quasi-degenerate, normal-ordered and inverted-ordered neutrinos are presented. The dashed line corresponds to $m_{ee} = 0.05$ eV while the grey exclusion region is due to eq. (1.1.19).

Finally, a different probe of the neutrino mass scale is remarkably provided by Cosmology. The Baryon Acoustic Oscillations are in fact sensitive to the sum of the neutrino masses. Hence, using the 7-years WMAP data and the latest measurements of H_0 [46] yields

$$\sum_{i=1}^{3} m_i < 0.58 \text{ eV} \quad (95\%\text{CL}) \tag{1.1.18}$$

which, falling in the quasi degenerate regime $m_1 \gg \sqrt{|\Delta m^2_{atm}|}$, simply implies

$$m_1 \lesssim 0.19 \text{ eV} \quad (95\%\text{CL}). \tag{1.1.19}$$

1.2 A cosmological puzzle: the baryon asymmetry of the Universe

During the last decades, the observations of the Cosmic Microwave Background Radiation (CMB), galaxies, supernova and the large scale structure of the Universe have been dramatically improved due to theoretical and technological progress. As a result Cosmology entered its precision era and the *Λ-CDM model*, describing the evolution of the Universe since few instants after its birth, was formulated.
For the precision of its predictions and the numerous connections to Particle Physics, the Λ-CDM model can be regarded nowadays as a fundamental phenomenological benchmark for theories of new Physics and the Standard Model itself. In this respect, we already met a first constraint that contemporary Cosmology imposes on Particle Physics in eq. (1.1.19), where the bound on the neutrino masses follows from pure cosmological arguments. For a second example, which concerns the limitations of the current framework, consider the energy budget of the Universe. The computation performed within the Λ-CDM model underlines that only a small share, about 5%, of the total energy density is connected to the particles of the Standard Model. The biggest contributions are due instead to two unknown agents, the Dark Energy and the Dark Matter, accounting respectively for the 73% and the 22% of the energy content of the Universe [47]. At the present time very little is known about these mysterious components. Dark Energy is supposed to drive the Universe expansion and its nature is still highly unclear. Dark Matter, in contrast, is tentatively modelled after new particles that theories beyond the Standard Model involve.

Let us focus now on a further issue that a comparison of the Standard Model to its cosmological counterpart reveals, concerning the existence of an asymmetry between baryonic matter and antimatter in our Universe. In fact, despite our laws of Physics maintaining a high degree of symmetry between particles and anti-particles since 1928, when P. A. M. Dirac proposed the existence of antimatter, Nature seems to have a different attitude.
The present Section is therefore dedicated to the baryon asymmetry of the Universe. Here we review the supporting experimental evidence and the conditions necessary for its formation. Our analysis then concludes by discussing the compatibility of the described scenario with the Standard Model.

1.2.1 Supporting evidences

The absence of proton-antiproton annihilations in our everyday life proves that our world is purely made of matter. On a larger scale, the exploration of the Solar System and the study of solar cosmic rays revealed that our moon, the Sun and the near planets are also made of matter. The first traces of antimatter appear in cosmic rays, which probe the composition of the Universe on a galactic distance.

The detected antiproton to proton abundance ratio is at most $\sim 10^{-4}$ – Figure 1.4 – suggesting a secondary production of the observed antimatter in proton-interstellar medium collisions. We can thus conclude that also our galaxy is entirely made of matter. The idea of dedicated antimatter galaxies is equally not correct, leading to annihilation signals in the γ-background within the cluster that are not observed [49]. For a similar reason, separated antimatter domains of a larger scale are also not viable: the annihilations taking place at the boundaries with the matter regions would result in distortions of the CMB spectrum actually not detected [49, 50].

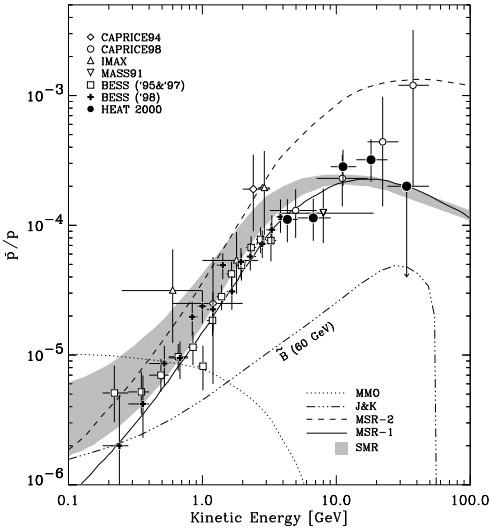

Figure 1.4: The antiproton content of cosmic rays, as reported after the HEAT experiment [48]. The ratio of antiproton to proton abundances, $\bar{p}/p$, is plotted against the detected energy and compared to the predictions of primary and secondary production mechanisms.

The asymmetry between matter and antimatter is therefore a fundamental characteristic of our Universe. To investigate this feature we define the *baryon asymmetry of the Universe* (BAU)

$$\eta_B := \frac{n_B - n_{\overline{B}}}{n_\gamma} \tag{1.2.1}$$

where n_B, $n_{\overline{B}}$ and n_γ are respectively the numerical density of baryons, antibaryons and photons. As all the observations are consistent with the hypothesis of a maximal asymmetry, $n_{\overline{B}} \equiv 0$, η_B is quantified by measuring the baryonic content of the Universe. To this purpose, we can avail ourself of two different phenomenologies that contemporary Cosmology offers: the Big Bang Nucleosynthesis and the Cosmic Microwave Background.

1.2.1.1 Big Bang Nucleosynthesis

The *Big Bang Nucleosynthesis* (BBN) describes the formation of nuclear abundances occurred in the primordial Universe for a temperature $T \lesssim 1$ MeV. [51, 52]. By assuming the nuclear reactions involved be in kinetic and chemical equilibrium, the nucleosynthesis

is sensitive to three parameters only: the number of neutrino species N_ν, the mean neutron lifetime τ_n and the same BAU.

- The number of neutrino species affects the Hubble parameter H

$$H \simeq 1.66\sqrt{g_\star}\frac{T^2}{m_{Pl}}, \qquad m_{Pl} = 1.22 \times 10^{19}\ \text{GeV} \tag{1.2.2}$$

  through $g_\star = g_\star(T)$, which represents the number of relativistic degrees of freedom in the plasma. Larger values of N_ν therefore result in a faster expansion rate and, in terms of BBN, in an earlier freeze-out of the neutron-to-proton ratio with a consecutive enhancement of the ^{4}He production.

- The rate of the proton to neutron conversion $e^- + p \to n + \nu_e$ is normalised by the neutron mean lifetime. A larger τ_n leads to a reduction of this rate, resulting once again in an earlier freeze-out of the neutron-to-proton ratio which increments the final abundance of ^{4}He.

- The mass fraction contribution X_A of an atomic species (A, Z)

$$X_A := \frac{A\, n_A}{n_p + n_n + \sum_i A_i n_{A_i}} \tag{1.2.3}$$

  is directly proportional to the baryon asymmetry:

$$X_A \propto \eta_B^{A-1}. \tag{1.2.4}$$

  Furthermore, notice that η_B also regulates the density of photons, which could inhibit the production of D and ^{3}He through photodissociation. Hence larger baryon asymmetries lead to enhanced light elements abundances, especially the deuterium one.

In this way, once the primordial nuclear abundances and the neutron mean life time have been measured, the baryon asymmetry of the Universe can be inferred through BBN in a given framework. In particular, by assuming three neutrino species the measured D/H abundance ratio yields [53]

$$\eta_B^{BBN} = \big(5.9 \pm 0.5\big) \times 10^{-10} \qquad (68\%\ \text{CL}). \tag{1.2.5}$$

1.2.1.2 The Cosmic Microwave Background Radiation

The Cosmic Microwave Background (CMB) is generated at the recombination era, when the temperature of the Universe allowed electrons and nuclei to combine into neutral atoms. The number of free electrons decreased dramatically, forcing the decoupling of

radiation from baryons at $T_{dec} \simeq 0.3$ eV. During the consecutive eras photons have travelled undisturbed through the Universe, constituting what today is detected as CMB. The analysis of CMB by the COBE satellite in 1992 [54] revealed an interesting feature of this background. On top of a perfect black body spectrum, corresponding to a temperature $T_\gamma \simeq 2.7$ K, CMB presents a peculiar pattern of anisotropies arising from local fluctuations of the temperature around the mean T_γ. This pattern is investigated by measuring correlations in the temperature fluctuations associated to different couples of points in the sky. Hence a correlation function can be obtained as a multipole expansion depending on a set of measured coefficients, *the angular power spectrum* $\mathcal{C}_\ell$, associated to the multiple components denoted by ℓ. As for the theoretical side, the angular power spectrum can be calculated within every cosmological model in terms of a number of fundamental parameters. By fitting the experimental measurements it is therefore possible to infer the latter. In the left panel of Figure 1.5 we present a comparison of the best-fit Λ-CDM model with the latest WMAP data [47].

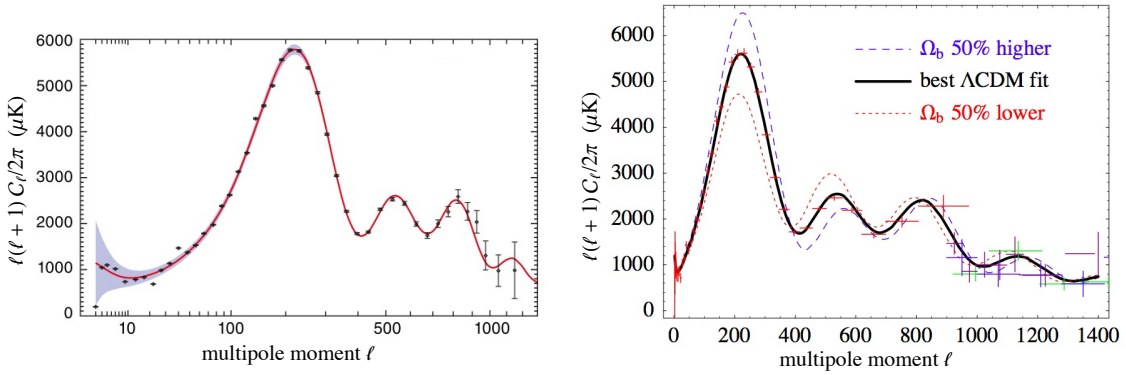

Figure 1.5: Left Panel: the angular power spectrum of CMB, adapted from [47]. The points correspond to the 7-year WMAP dataset while the solid line is the best-fit within the Λ-CDM model. The shaded region represents theoretical uncertainties due to the cosmic variance.
Right Panel: The sensitivity of the angular power spectrum to Ω_B, from [55].

In the proposed analysis the temperature fluctuations of CMB result in a characteristic series of peaks in the angular power spectrum. These correspond to oscillations of the original baryon-photon plasma driven by the contrast between the radiation pressure and gravity – the baryon acoustic oscillations (BAOs). As shown in the right panel of Figure 1.5, this mechanism is clearly sensitive to the abundance of baryons present in the plasma. Consequently, within the Λ-CDM model, CMB measurements constrain the baryon density parameter

$$\Omega_B := \frac{\rho_B}{\rho_c} \tag{1.2.6}$$

where ρ_c is the critical energy density, defined as $\rho_c := 3H^2 m_{Pl}^2/8\pi$. It is then easy to recast the bound on the density parameter as a measure of the baryon asymmetry.

Adopting the 7-year WMAP dataset, BAO and the latest measurement of the Hubble constant H_0 yields [46]

$$\eta_B^{CMB} = \frac{\rho_B}{n_\gamma m_p} = \frac{\Omega_B \rho_c}{n_\gamma m_p} = \left(6.19 \pm 0.15\right) \times 10^{-10} \qquad (68\%\ \text{CL}) \tag{1.2.7}$$

where m_p is the proton mass. Notice that for the observed thermal equilibrium of CMB, it is highly unlikely that some mechanism could modify the baryon asymmetry of the Universe after the recombination era. Consequently eq. (1.2.7) can also be regarded as a measure of the baryon asymmetry today.

To conclude the present Section we comment on the agreement between eq. (1.2.7) and (1.2.5). Beside being completely independent, the measurements that BBN and CMB provide also frame the baryon asymmetry of the Universe in totally different times. BBN probes this quantity for $T \sim (10^{-1} - 10)$ MeV, corresponding to an age of the Universe $t \sim (10^{-2} - 10^{2})$ *seconds*. Differently CMB tests the baryon asymmetry at the recombination, when $T \sim 1$ eV and $t \sim 10^6$ *years*. The fact that the two measurements are compatible is therefore not trivial at all and, as the Λ-CDM model strictly constrains the evolution of η_B between these two eras, the agreement of eq. (1.2.7) and (1.2.5) can indeed be regarded as a great success of this theory.

1.2.2 Generating the asymmetry

Persuaded of the baryon asymmetry existence by the BBN and CMB measurements, we now concentrate on the conditions which led to its formation in our Universe.

The first issue we have to confront is whether or not this asymmetry was actually generated. In fact, it could be sustained that the origin of the baryon asymmetry is an initial set-up of the Universe, which favoured matter over antimatter. No explanation would therefore be required to motivate the present value of η_B, owing to the initial condition involved. This hypothesis is however invalidated, within the Λ-CDM model, by a key ingredient in the evolution of the Universe: Inflation. During the inflationary stage the Universe undergoes an exponential expansion, which would quickly dilute any present asymmetry. As a consequence our observable Universe would then contain baryonic matter and antimatter in equal proportions after the Inflation era, contradicting the current experimental observations. Not spoiling the successes of Inflation therefore imposes the baryon asymmetry of the Universe be necessarily generated dynamically, after the considered inflationary stage.

The conditions that a mechanism must satisfy to dynamically produce such asymmetry were pointed out in 1967 by A. D. Sakharov [56]. The analysis underlined three fundamental requirements[6]:

I *Violation of the baryon number.*
This condition is somewhat intuitive: starting from a null asymmetry, the mechanism must account for the value of η_B we measure.
Notice that, in analogy to leptons, baryons and antibaryons are also associated to a charge provided by an accidental symmetry of the Standard Model: the *the baryon number* B. The above remark therefore trivially implies $\Delta B \neq 0$.

II *Violation of C and CP symmetries.*
Also this condition can be easily understood, as the mechanism must generate more matter than antimatter in order to give rise to the asymmetry. Violations of C and CP are then necessary to discriminate between particles and antiparticles. If this condition is not satisfied the B-violating interactions would produce baryons and antibaryons at the same rate, resulting in a null asymmetry.

III *Departure from equilibrium.*
The departure from equilibrium is required for a twofold reason. Entropy, in *chemical equilibrium*, is maximised when the chemical potentials of species associated to non-conserved quantum numbers vanish. The requirement (I) postulates the non-conservation of the baryon number, hence chemical equilibrium would enforce $\mu_B = 0$ and consequently a vanishing asymmetry, through the relation

$$n_X - n_{\overline{X}} = \frac{g_X T^3}{6} \begin{cases} \beta\mu_X + \mathcal{O}\big((\beta\mu_X)^3\big) & \text{X is a fermion} \\ 2\beta\mu_X + \mathcal{O}\big((\beta\mu_X)^3\big) & \text{X is a boson} \end{cases} \tag{1.2.8}$$

where $\beta \coloneqq 1/T$ and g_X accounts for the number of internal degrees of freedom of the species X.

On top of that, in *thermal equilibrium* the baryon number satisfies

$$\langle B(t)\rangle = \frac{\mathrm{Tr}\big(e^{-H/T}B(t)\big)}{Z} = \frac{\mathrm{Tr}\big(e^{-H/T}e^{-iHt}B(t=0)e^{iHt}\big)}{Z} \equiv \langle B(t=0)\rangle \tag{1.2.9}$$

and clearly no baryon asymmetry can be generated as far as thermal equilibrium is maintained – after the Inflation $B(t=0) = 0$.

[6] In our analyses we will assume that the sphaleron processes, discussed in the upcoming Section, be active during the Leptogenesis process. This implies a further condition quantified in a lower bound on the temperature of the Universe of order of the Electro-Weak symmetry breaking scale: $T \gtrsim 10^2$ GeV. In the framework we propose this requirement will always be satisfied and consequently we disregard the possibilities offered by low scale Leptogenesis scenarios, in which the BAU asymmetry is generated below the Electro-weak symmetry breaking scale through different mechanisms.

The Sakharov conditions specified above clearly identify the requirements that the production of a baryon asymmetry imposes. Our next step is to analyse whether these prerequisites are satisfied within the specific framework provided by the Standard Model.

1.2.3 The Standard Model scenario: Electro-Weak Baryogenesis

To discuss how the Standard Model fulfils the above requirements we address each point separately.

- *Baryon number violations in the Standard Model: the sphaleron process.*
  As mentioned before, B and L conservations are respectively introduced in the Standard Model by the accidental $U(1)_B$ and $U(1)_L$ symmetries. Strictly speaking this is not correct, as non perturbative effects – the *instantons* – break these symmetries [57]. Instantons are related to transitions between topologically different vacuum states of Yang-Mills theories, accompanied by a violation of baryon and lepton numbers. The typical transition rate is however negligible, hence the above accidental symmetries are recovered.
  The situation is different if we consider non-zero temperatures, as another non-perturbative effect is driving these transitions: the *sphaleron* [58]. The rate of these processes is related to the free energy of the sphaleron-type configuration, a saddle point in the gauge-Higgs bosons configuration space. The effective operator corresponding to the Electro-Weak sphaleron transitions couples all the left-handed fields of the Standard Model

$$\mathrm{O}_{sph} = \prod_i \left(Q_{iL} Q_{iL} Q_{iL} \ell_{iL}\right). \tag{1.2.10}$$

  Hence when in thermal equilibrium, for 10^2 GeV $\lesssim T \lesssim 10^{14}$ GeV, sphalerons induce a violation of baryon and lepton numbers

$$\Delta B = \Delta L = 3 \tag{1.2.11}$$

  and the first Sakharov condition is therefore satisfied within the Standard Model. Notice that the sphaleron transitions conserve the $B - L$ charge and also its individual components $B/3 - L_\alpha$, $\alpha = e, \mu, \tau$.

- *C and CP violations: Weak Interactions.*
  The Weak Interactions are responsible for breaking C and CP in the Standard Model. The former is explicitly broken, as Weak Interactions couple only particles –and antiparticles – with definite chirality. As for CP, the quark mixing mechanism [59] is regulated by the Cabibbo-Kobayashi-Maskawa (CKM) matrix which contains one CP-violating phase. Experiments investigating neutral K and B

mesons oscillations tested this phase [60], confirming the presence of CP-violation in the quark sector of the Standard Model.

- *Out of equilibrium dynamics: a strong phase transition.* The last ingredient necessary in the Standard Model is the departure form equilibrium. This is provided, at the Electro-Weak symmetry breaking, by a strong first-order phase transition proceeding through nucleation and growth of bubbles [61]. In this case the Electro-Weak symmetry is broken only inside the bubbles, hence particles and antiparticles would enter the latter at different rates generating an asymmetry.

In principle all the Sakharov conditions are satisfied by the Standard Model, delineating a straightforward solution to the puzzle posed by the existence of a baryon asymmetry in our Universe: *Electro-Weak Baryogenesis* [62]. Unfortunately, a first issue disfavouring this answer is brought by the same baryon asymmetry. In this regard, it was found that even by assuming the required departure from equilibrium and violation of the baryon number, the amount of CP asymmetry in the Standard Model is not enough to explain the measured value of η_B [63]. On top of that, a more radical problem is underlined by dedicated lattice simulations [64]. These proved that a first-order phase transition, as strong as required for non equilibrium dynamics, yields a strict upper bound on the mass of the Higgs boson $m_H \lesssim 45$ GeV. Clearly this condition is not satisfied by the latest measurements $m_H \simeq 126$ GeV [16, 17], implying inevitably the failure of the proposed scenario.

In conclusion, the Standard Model alone is not able to account for the baryon asymmetry of the Universe that BBN and CMB quantify. The failure of Electro-Weak Baryogenesis reveals the necessity of a new baryogenesis model, explaining the origin of such asymmetry. For this reason, the latter can be thus regarded as a strong evidence in favour of new Physics, further to the results of neutrino oscillation experiments that we considered before.

Currently, many scenarios beyond the Standard Model are proposing different mechanisms able to address the problems that we exposed in this Section. We mention for example, in connection to the neutrino mass puzzle, the possibilities offered by large extra-dimensions and by non-renormalizable operators. In the former approach, additional spatial dimensions are employed to address the hierarchy problem and provide an alternate explanation to the Seesaw mechanism for the generation of neutrino masses [65]. Regarding instead the Standard Model as an effective theory, valid up to the scale of new Physics Λ_{nP}, the underlying Lagrangian can be extended to non-renormalizable higher dimensional operators. These are suppressed by powers of $1/\Lambda_{nP}^{dim-4}$, with the largest effects at low energy arising from the $dim = 5$ operators which can provide a Majorana mass term to the ordinary neutrinos [66]. As for the problem concerning the generation of a BAU, beside the traditional Grand Unified Theory (GUT) baryogenesis scenarios

in which the decays of the GUT symmetry group bosons are responsible for the generation of the baryon asymmetry, we mention the solutions proposed by the Affleck-Dine scenario of inflation, within supersymmetric models, [67] and by the same Electro-Weak Baryogenesis. Differently from the Standard Model, scenarios of new Physics incorporating Supersymmetry or domain walls, for example, can in fact provide the strong first order phase transition that the third Sakharov condition imposes.
In the present work we will however disregard these possibilities in favour of a simple solution, which draws a connection between the neutrino mass puzzle and the observed baryon asymmetry of the Universe proposing a common solution.

1.3 An appealing solution

To summarise, in the present Chapter we focused on two problems that contemporary Physics is posing to the Standard Model, first with neutrino oscillation experiments, then through the baryon asymmetry of the Universe. The proposed evidences and the implied theoretical consequences underline the current necessity of new, testable, frameworks to address the problems disclosed. In this regard, in the remaining of this Thesis we will focus on a model yielding a possible answer.

The interesting feature of this solution is the nontrivial connection that it draws between neutrino Physics and contemporary Cosmology, addressing the problem of neutrino masses and the baryon asymmetry of the Universe at once. Chapter 2 is therefore dedicated to the Seesaw extension of the Standard Model, introducing the Seesaw mechanism and Leptogenesis to address respectively the neutrino mass puzzle and the problem of the baryon asymmetry generation. For sake of clarity we present here a first simplified scenario, N_1 Leptogenesis, which nevertheless is able to offer a significant insight into the Physics that the considered Seesaw extension proposes. In Chapter 3 we analyse the important consequences that flavour has within Leptogenesis. Flavours effects are exhaustively discussed within the classical Boltzmann-equations-approach to Leptogenesis, reserving to Chapter 4 a more precise formulation of the problem which employs the density matrix technology. In Chapter 5 we consider the problem of the initial conditions in Leptogenesis, employing the flavour effects to identify a particular strong thermal Leptogenesis scenario as the only possible solution. Then, considering the specific framework provided by the $SO(10)$-inspired model of Leptogenesis, in Chapter 6 we investigate the important phenomenological consequences that this strong thermal Leptogenesis scenario implies on the Seesaw parameter space. Finally, in Chapter 7, we conclude the present work summarising the results that our analyses of this fascinating scenario of new Physics highlighted.

Chapter 2

A possible answer: the Seesaw extension of the Standard Model

In the Introduction we exposed the present requirement for a new framework, to address the puzzle of neutrino oscillations and the baryon asymmetry of the Universe. The answer we consider is the Seesaw extension of the Standard Model, an interesting scenario of new Physics where these issues are linked by a common solution. The appeal of this framework is due to its twofold nature. On one hand we have the simplicity of the model, which offers a straightforward insight into the Physics beyond the Standard Model. On the other hand, for the non-trivial connection realised between Particle Physics and Cosmology, this solution yields important phenomenological implications. We will investigate the latter in the last Chapters of this work, focusing for the moment on the former point.

Before detailing the characteristics of the Seesaw mechanism that we employ in our analyses, we present a brief survey of the different variants proposed for this attractive mechanism.

- **Type I:**
  The type I is the simplest realisation of the Seesaw mechanism [68–71]. In this framework at least two right handed (RH) neutrinos are added as singlets to the content of the theory. The new particles are provided a Majorana mass term M and the associated mass scale is traditionally close to the scale of grand unification. These particles also couple to the lepton and Higgs doublets of the SM through a new set of Yukawa coupling h. Integrating the RH neutrinos out of the theory results in a dimension 5 operator which provides a Majorana mass to the usual neutrinos involved in the Weak Interactions. The emerging mass scale is of order $[m_\mu] \sim [v^2 h^2 / M]$, where v is proportional to the vacuum expectation value of the neutral Higgs component.

- **Type II:**
  In the type II Seesaw mechanism [72–74] a new Higgs $SU(2)_L$ triplet, Δ, couples to the lepton and Higgs doublets of the SM through the terms $\mathcal{L} \supset g\bar{\ell}\Delta\ell^c$ and $\mathcal{L} \supset g'\Phi^\dagger\Delta\Phi$ respectively, where c indicates a charge conjugated field. Once the neutral component of the Higgs triplet acquires a vacuum expectation value, v_Δ, a Majorana mass term of the order $[m_\mu] \sim [gv_\Delta]$ is generated for the neutrinos. We remark that the value of v_Δ is controlled by the coupling of the new triplet to the usual Higgs doublet of the SM: $v_\Delta \sim g'v^2/M_\Delta^2$. Hence, overall, the generated neutrino mass scale is given by $[m_\mu] \sim [gg'v^2/M_\Delta^2]$.

- **Type III:**
  The type III Seesaw mechanism [75] is a modification of the type I variant, where three RH neutrinos are considered and assigned to a triplet of $SU(2)_L$. Similarly to the case of type I, integrating out the RH neutrinos results in a dimension 5 effective operator which provides a Majorana mass term to the ordinary neutrinos. The mass scale recovered for these particles is the same as in the type I variant, $[m_\mu] \sim [v^2h^2/M]$, nevertheless within the type III Seesaw mechanism the RH neutrinos interact with the $SU(2)_L$ gauge bosons.

- **Radiative seesaw:**
  In the scenarios adopting a radiative seesaw mechanism, the dimension 5 operator which provides the neutrino mass term is generated through quantum corrections. These generally involve new heavy particles, which are charged under an imposed discrete symmetry. A specific example is provided by the Scotogenic models [76], in which the SM is extended by adding three neutral singlet fermions, the RH neutrinos, interacting with the lepton doublets through an additional scalar doublet. As the new particles are all odd under an exactly conserved Z_2 symmetry, while the SM content is kept even, the usual Dirac mass term for the neutrinos is forbidden in the theory and the type I Seesaw mechanism cannot be invoked. However, once the RH neutrinos are provided heavy Majorana masses, the coupling to the new scalar doublets results in a mass term for the ordinary neutrinos which is suppressed by the RH neutrino mass scale and proportional to the relevant loop factor. We remark that, owing to the Z_2 symmetry employed, the lightest of the new particle introduced in the theory is stable and, therefore, represents a suitable candidate for Dark Matter.

The scenario we consider is based on the *type-I seesaw mechanism* [68–71] and involves three new particles, the right-handed (RH) neutrinos ν_{iR} for $i = 1, 2, 3$, added to the content of the Standard Model[1]. Within the proposed framework, these RH neutrinos

[1] It is indeed possible to account for the current experimental observations also by considering two RH neutrino species only, in which case the lightest of the ordinary neutrino species is necessarily massless. Nevertheless, as we will explicitly show in Chapter 5, the presence of a third RH neutrino species is required within certain frameworks in order to explain the detected value of the BAU.

are Majorana particles which transform as singlets under the $SU(3)_C \times SU(2)_L \times U(1)_Y$ symmetry of the theory and couple to the lepton doublets of the SM through an additional Yukawa interaction term. The Lagrangian of the model is therefore given by

$$\mathcal{L} = \mathcal{L}_{SM} + \mathcal{L}_{Seesaw} \supset i \sum_{i=1}^{3} \overline{\nu_{iR}}\, \partial^{\mu}\, \gamma_{\mu}\, \nu_{iR} - \sum_{\alpha,\beta=e,\mu,\tau} y_{\alpha\beta}\, \overline{\ell'_{\alpha L}}\, l'_{\beta R}\, \Phi + \\ - \sum_{\substack{\alpha=e,\mu,\tau \\ i=1,2,3}} h'_{\alpha i}\, \overline{\ell'_{\alpha L}}\, \nu_{iR}\, \tilde{\Phi} - \frac{1}{2} \sum_{i,j=1,2,3} \overline{\nu^{c}_{iR}}\, M_{ij}\, \nu_{jR} + \text{ H.c.} \tag{2.0.1}$$

where $h'_{\alpha i}$ is a complex matrix containing the new set of Yukawa couplings while M_{ij} is the complex symmetric matrix of the RH neutrino masses. The RH neutrino fields satisfy

$$\nu^{c}_{iR} = \mathcal{C}\, \overline{\nu_{iR}}^{T} \tag{2.0.2}$$

$$\overline{\nu^{c}_{iR}} = -\nu^{T}_{iR}\, \mathcal{C}^{\dagger} \tag{2.0.3}$$

being $\mathcal{C}$ the representation of charge conjugation operator on the spinor space:

$$\mathcal{C}^{-1} = \mathcal{C}^{\dagger} \tag{2.0.4}$$

$$\mathcal{C}^{T} = -\mathcal{C} \tag{2.0.5}$$

$$\mathcal{C}(\gamma^{\mu})^{T}\mathcal{C}^{-1} = -\gamma^{\mu} \tag{2.0.6}$$

$$\mathcal{C}(\gamma^{5})^{T}\mathcal{C}^{-1} = \gamma^{5}. \tag{2.0.7}$$

The last field we introduce is $\tilde{\Phi}$, the negative Hypercharge Higgs doublet, defined in terms of the usual Higgs fields Φ – Section A.1 – as

$$\tilde{\Phi} \coloneqq i\sigma_2 \Phi^{*} = \begin{pmatrix} \phi^{0} \\ -\phi^{-} \end{pmatrix} \tag{2.0.8}$$

where $\phi^{-} \coloneqq (\phi^{+})^{\dagger}$ and σ_2 is the second Pauli matrix – eq. (A.1.3).

As in the previous Section, the greek subscripts are assigned to the charged-lepton flavours ($\alpha = e, \mu, \tau$) while the latin ones to the mass eigenstates ($i = 1, 2, 3$). Finally, the subscripts "L" and "R" refer to the chirality of the involved fields, with obvious meaning of the notation.

Without loss of generality, we can write our Lagrangian on a basis where both the charged-lepton Yukawa couplings and the RH neutrino mass matrix are diagonal. To this purpose we consider the bi-unitary diagonalisation of the former

$$y = U^{l\dagger}_{L}\, D_y\, U^{l}_{R} \tag{2.0.9}$$

where with D_X we indicate the diagonal form of a matrix X. The flavour lepton doublets are then defined according to

$$\ell_{\alpha L} \coloneqq (U_L^l)_{\alpha\beta}\, \ell'_{\beta L} = \begin{pmatrix} \nu_{\alpha L} \\ l_{\alpha L} \end{pmatrix} \tag{2.0.10}$$

while the RH components of the corresponding charged lepton mass eigenstates[2] are:

$$l_{\alpha R} \coloneqq (U_R^l)_{\alpha\beta}\, l'_{\beta R}. \tag{2.0.11}$$

As for the RH neutrinos, the diagonalisation of the complex symmetric matrix M proceeds through the *Takagi factorisation*

$$M = V_R^{\nu}\, D_M\, V_R^{\nu T}, \qquad D_M = \mathrm{Diag}(M_1, M_2, M_3) \tag{2.0.12}$$

where we assume $M_1 < M_2 < M_3$. The RH components of the corresponding Majorana mass eigenstates are then

$$N_{iR} \coloneqq (V_R^{\nu T})_{ij}\, \nu_{jR} \tag{2.0.13}$$

and by defining the Yukawa couplings h through

$$h' = h(V_R^{\nu})^T \tag{2.0.14}$$

the Lagrangian (2.0.1) can be finally recast as

$$\begin{aligned} \mathcal{L} \supset\, & i \sum_{i=1}^{3} \overline{N_{iR}}\, \partial^{\mu}\, \gamma_{\mu}\, N_{iR} - \sum_{\alpha=e,\mu,\tau} (D_y)_{\alpha}\, \overline{\ell_{\alpha L}}\, l_{\alpha R}\, \Phi - \sum_{\substack{\alpha=e,\mu,\tau \\ i=1,2,3}} h_{\alpha i}\, \overline{\ell_{\alpha L}}\, N_{iR}\, \tilde{\Phi} + \\ & - \frac{1}{2} \sum_{i}^{3} \overline{N_{iR}^c}\, (D_M)_i\, N_{iR} + \text{ H.c.}. \end{aligned} \tag{2.0.15}$$

It is now clear that the scenario we analyse adds 18 new parameters to the Standard Model: 15 entries[3] in the complex matrix h and the three RH neutrino masses M_i in D_M. As the phenomenologies we aim to describe provide currently only 6 observables, the value of η_B and the five parameters of Table 1.1, an issue concerning the predictivity of this framework can indeed be raised. We postpone our answer to Chapter 6, focusing for the moment on the basics of the presented scenario. In this regard, in the next section we show how the neutrino mass puzzle is addressed in a remarkable way.

[2] We implicitly intend the right-handed components of the fields corresponding to these particles. In the remaining part of the Thesis this remark will be understood.

[3] In general h is specified by nine real parameters and nine phases. The number of the latter can however be reduced to six through a rephasing of the three lepton doublets.

2.1 The Seesaw mechanism

Let us focus now on the last two terms in the Lagrangian (2.0.15), leading after the Electro-Weak symmetry breaking

$$\Phi(x) \xrightarrow{\langle\phi_0\rangle\neq 0} \begin{pmatrix} 0 \\ \frac{V+H}{\sqrt{2}} \end{pmatrix}, \qquad \tilde{\Phi} \xrightarrow{\langle\phi_0\rangle\neq 0} \begin{pmatrix} \frac{V+H}{\sqrt{2}} \\ 0 \end{pmatrix}, \qquad V \simeq 246 \text{ GeV} \tag{2.1.1}$$

to

$$\mathcal{L} \supset \mathcal{L}_M^{seesaw} = -v \sum_{\substack{\alpha=e,\mu,\tau \\ i=1,2,3}} h_{\alpha i}\, \overline{\nu_{\alpha L}}\, N_{iR} - \frac{1}{2} \sum_{i}^{3} \overline{N_{iR}^c}\, (D_M)_i\, N_{iR} + \text{ H.c.} \tag{2.1.2}$$

where $v \coloneqq V/\sqrt{2} \simeq 174$ GeV. The above equations clearly imposes a Dirac mass term $m_D \coloneqq vh$ to neutrinos. Consequently, even if we were to neglect any further implication of the Lagrangian (2.1.2) by setting $D_M \equiv 0$, we could in principle address the neutrino mass puzzle by picking an appropriate form for m_D. The latter would then yield a neutrino mass spectrum and a PMNS matrix in agreement with the current experimental bounds. Yet, even so, we would have to face a further complication. More explicitly, by adopting as a natural mass scale for neutrinos the one that oscillations experiments suggest $[m_\nu^{osc}] \sim (10^{-3} - 10^{-2})$ eV, given that $[v] \sim 10^5$ eV, in the above scheme the required Yukawa couplings result artificially small $[h] \sim (10^{-8} - 10^{-7})$. This is not the case within the Seesaw mechanism, which recovers the proposed neutrino mass scale even when natural Yukawa couplings of order $[h] \sim 1$ are considered, provided the RH neutrino mass scale is of the order of the typical Grand Unified Theory (GUT) scale $\Lambda_{GUT} \sim (10^{15} - 10^{16})$ GeV. In fact, restoring the Majorana mass term $D_M \neq 0$ in our Lagrangian, we gather now the involved fields into arrays of definite chirality and through the relation

$$\overline{\nu_{\alpha L}} N_{iR} = \overline{N_{iR}^c} \nu_{\alpha L}^c \tag{2.1.3}$$

the Lagrangian (2.1.2) can be written in a compact but meaningful form:

$$\mathcal{L}_M^{seesaw} = -\frac{1}{2} \begin{pmatrix} \overline{\nu_{eL}} & \dots & \overline{N_{3R}^c} \end{pmatrix} \begin{pmatrix} 0 & m_D \\ (m_D)^T & D_M \end{pmatrix} \begin{pmatrix} \nu_{eL}^c \\ \vdots \\ N_{3R} \end{pmatrix} + \text{ H.c.} \equiv \tag{2.1.4}$$

$$\equiv -\frac{1}{2} \sum_{j,k=1}^{6} \overline{\nu_{jL}}\, (M_{D+M})_{jk}\, \nu_{kL}^c + \text{ H.c..} \tag{2.1.5}$$

The formal structure of the above equation matches the one of the last term in eq. (2.0.1), therefore, for the viability of Seesaw mechanism, *neutrinos must be Majorana particles*. This clearly is an important prediction of the scenario, leading to a potential first test

through the neutrinoless double β-decay experiments presented in Section 1.1.3. Having said that, the neutrino mass eigenstates relevant for the oscillation mechanism are calculated by diagonalising the block matrix M_{D+M}. The resulting block eigenvalues, at the leading order, are

$$\lambda_1 = \frac{1}{2}\left(D_M - \sqrt{D_M^2 + 4m_D(m_D)^T}\right) \tag{2.1.6}$$

$$\lambda_2 = \frac{1}{2}\left(D_M + \sqrt{D_M^2 + 4m_D(m_D)^T}\right) \tag{2.1.7}$$

while the 6×6 matrix V^ν involved in the diagonalisation, again at the leading order, is

$$V^\nu \simeq \begin{pmatrix} 1 & m_D D_M^{-1} \\ -D_M^{-1} m_D^\dagger & 1 \end{pmatrix} \tag{2.1.8}$$

satisfying: $V^\nu (V^\nu)^\dagger \simeq (V^\nu)^\dagger V^\nu = 1 + \mathcal{O}(D_M^{-2})$. Until now we made no assumptions about the origin of the RH neutrinos. To this regard, notice that many GUTs propose the existence of these particles, which generally complete the representations of the GUT group occupied by matter. For example, within $SO(10)$ GUTs, the RH neutrinos appear in the 16 dimensional spinor representations associated to the three fermion families of the SM [77], while in $SU(6)$ theories the complete the 6 and $\overline{15}$ representations [78].
We can therefore expect the RH neutrino mass scale $[M]$ to be naturally of the required order $\Lambda_{GUT} \sim (10^{15} - 10^{16})$ GeV. In this case the *Seesaw limit* $[D_M] \gg [m_D] \sim 10^2$ GeV is satisfied and consequently:

$$V^{\nu\dagger} M_{D+M} V^{\nu *} \xrightarrow{\text{Seesaw limit}} \begin{pmatrix} m_\nu & 0 \\ 0 & D_M \end{pmatrix} \tag{2.1.9}$$

where

$$m_\nu \coloneqq -m_D\, D_M^{-1}\, (m_D)^T. \tag{2.1.10}$$

As clear from the above equation, imposing the Seesaw limit leads to a split neutrino mass spectrum presenting two sectors associated to different energy scales:

- *Low energy sector: light neutrinos.*
  The low energy sector contains three light neutrinos associated to the mass matrix in equation (2.1.10). Notice that for the above values of $m_D \sim [v]$ and $D_M \sim [M]$, the matrix m_ν matches the estimate provided by the oscillation experiments $[m_\nu] \sim (10^{-2} - 10^{-3})$ eV $\equiv [m_\nu^{osc}]$ in a natural way. On top of that, by ascribing the neutrino mass scale to the ratio of the Electro-Weak and GUT scales, the Seesaw mechanism potentially provides a way to test the high energy sector of the theory.
  From the above discussion on the merits of this attractive scenario, it should be clear that the proposed light neutrinos are suitable candidates to address the

neutrino oscillations puzzle. To calculate the corresponding mass eigenstates we therefore diagonalise the symmetric matrix m_ν

$$L^{\nu\dagger}\, m_\nu\, L^{\nu *} = -D_{m_\nu} \tag{2.1.11}$$

by means of the unitary 3×3 matrix L^ν. Hence, the 4-component Majorana fields associated to the eigenvalues m_i of D_{m_ν}, $n^l_i = n^l_{iL} + (n^l_{iL})^c$, are finally given by

$$n^l_{iL} \coloneqq \sum_{j=1,2,3} (L^{\nu\dagger})_{ij} \left[\sum_{k=1}^{6} \left(V^{\nu\dagger}\right)_{jk} \nu_{kL}\right], \qquad i = 1,2,3. \tag{2.1.12}$$

- *High energy sector: heavy neutrinos.*
  We consider now the lower block of the mass matrix in eq. (2.1.9). As no further diagonalisation is required, the heavy neutrino mass eigenstates are simply given by $n^h_i = n^h_{iL} + (n^h_{iL})^c$, where

$$n^h_{iL} \coloneqq \sum_{j=1}^{6} \left(V^{\nu\dagger}\right)_{(i+3)j} \nu_{jL}, \qquad i = 1,2,3. \tag{2.1.13}$$

With the complete neutrino mass spectrum given by the eigenvalues m_i and M_i associated to respectively to light and heavy neutrinos, we can now focus on the PMNS matrix that the Seesaw mechanism proposes.

2.1.1 The PMNS matrix in the Seesaw mechanism

To identify the leptonic mixing matrix we introduce the 6×6 matrix [79]

$$K \coloneqq \begin{pmatrix} L^\nu & 0 \\ 0 & 1 \end{pmatrix} \tag{2.1.14}$$

which relates the neutrino mass eigenstates to the array ν_{Lk} of eq. (2.1.4):

$$\begin{pmatrix} n^l_L \\ n^h_L \end{pmatrix}_j = \sum_{k=1}^{6} \left(K^\dagger\, V^{\nu\dagger}\right)_{jk} \nu_{kL}. \tag{2.1.15}$$

As the Lagrangian (2.1.2) is already written on a basis that diagonalises the charged lepton Yukawa couplings, the first three fields in the array ν_{Lk} correspond to the flavour neutrinos. Consequently eq.s (A.2.10) and (A.2.11) imply for the PMNS matrix

$$U_{\alpha k} \coloneqq \sum_{j=1}^{6} (V^\nu)_{\alpha j}\, (K)_{jk}\,. \tag{2.1.16}$$

Hence, within the proposed framework, the lepton mixing matrix is a 3×6 matrix satisfying $UU^\dagger = \mathbf{1}_{3\times 3}$, but $U^\dagger U \neq \mathbf{1}_{N\times N}$. As a result, the non unitarity of U breaks the Glashow-Iliopoulos-Maiani mechanism [80] and transitions between the different mass eigenstates are in principle possible via neutral current interactions – the flavour changing neutral currents.

We remark that the unitarity violation is in general a low-energy signal of the presence of new Physics. For instance, a possible source of non-unitary effects in the lepton mixing is the hypothetical existence of additional light neutrino species which are not involved in the Weak Interactions of the SM: the so-called sterile neutrinos. In more detail, the light sterile neutrinos are fermions with no ordinary Weak Interactions which could however mix significantly with ordinary neutrinos species. As a consequence the neutrino oscillation probabilities and all the astrophysical and cosmological mechanisms which involve neutrinos are potentially affected by the presence of sterile neutrinos. For example, as we saw in the previous Chapter, the same BBN is in principle sensitive to – and currently disfavours – the existence of additional neutrino species.

Another important consequence of a non-unitary lepton mixing is instead connected to the amount of CP violation present at low energy in the lepton sector, where these effects usually lead to a significant enhancement of this quantity. Finally, we remark that the observation of non-unitary effects within models presenting heavy sterile neutrinos could potentially provide a window to analyse the Physics of the associated high energy scale. For example, in the case of non-minimal Seesaw models, additional symmetry arguments are imposed in order to maintain the heavy neutrino massed around the TeV scale. This potentially gives rise to a significant light-heavy neutrino mixing and the consequent deviation from the unitarity could manifest itself in tree level processes like $\pi \to \mu + \nu$ or in the rare charged lepton flavour violating decays as $\mu \to e + \gamma$.

In this regard, for the Seesaw scenario we propose, considering the explicit form of the matrix

$$U = \begin{pmatrix} L^\nu & m_D D_M^{-1} \end{pmatrix} \tag{2.1.17}$$

the 3×3 block regulating the heavy neutrino mixing results clearly suppressed as D_M^{-1}. We thus expect the unitarity violation to be of order $\mathcal{O}(D_M^{-2})$ so, in the considered Seesaw limit, we can safely disregard this effect and identify the PMNS matrix with the 3×3 unitary matrix $L^\nu \equiv U$. In this way equation (2.1.11) is recast as

$$D_{m_\nu} = -U^\dagger m_\nu U^* \tag{2.1.18}$$

and the neutrino mass eigenstates of eq.s (2.1.12) and (2.1.13) satisfy

$$n_{iL}^l = n_{iL} \coloneqq \sum_{\alpha=e,\mu,\tau} \left(U^\dagger\right)_{i\alpha} \nu_{\alpha L}, \qquad i = 1,2,3 \tag{2.1.19}$$

and

$$n_{iL}^h = N_{iL} \equiv N_{iR}^c, \qquad i = 1,2,3. \tag{2.1.20}$$

The solution that the considered scenario proposes to the neutrino oscillations puzzle is therefore clear. In the Seesaw limit, the LH components of three Majorana neutrinos n_i are involved in the Weak Interactions. The mismatch between the basis diagonalising m_ν and the charged lepton Yukawa couplings y, quantified by U, gives rise to neutrino oscillations. As the latter do not involve the heavy neutrinos N_i, no sterile neutrinos appear in the present scheme. In Chapter 6, beside commenting on the predictivity of our framework, we also show the impact of the actual oscillation data on the Seesaw mechanism when a concrete model is considered. For the moment we focus again on the heavy neutrinos N_i and tackle the puzzle posed by the baryon asymmetry of the Universe.

2.2 Leptogenesis

By means of the usual chirality projection operators

$$P_R \coloneqq \frac{1+\gamma^5}{2}, \qquad P_L \coloneqq \frac{1-\gamma^5}{2} \tag{2.2.1}$$

the Yukawa interactions that the Seesaw extension introduced in the Lagrangian (2.0.15) can be written in terms of the heavy neutrinos $N_i = N_{iR} + N_{iR}^c$ that the Seesaw mechanism involves

$$\mathcal{L} \supset -\sum_{\substack{\alpha=e,\mu,\tau \\ i=1,2,3}} h_{\alpha i}\, \overline{\ell_\alpha} P_R\, N_i\, \tilde{\Phi} - \sum_{\substack{\alpha=e,\mu,\tau \\ i=1,2,3}} h_{\alpha i}^*\, \tilde{\Phi}^\dagger \overline{N_i} P_L\, \ell_\alpha. \tag{2.2.2}$$

Several new processes are therefore implied, for example we have:

- $|\Delta L| = 1$ decays and inverse-decays of the heavy neutrinos into lepton and Higgs doublets or antilepton and antiHiggs doublets
- $|\Delta L| = 1$ scatterings mediated by the Higgs doublets, involving mainly top quarks and gauge bosons
- $|\Delta L| = 2$ scatterings mediated by heavy neutrinos[4].

We can consequently sketch a new baryogenesis mechanism, *Leptogenesis*, in which the baryon asymmetry of the Universe is explained as a product of an original lepton asymmetry generated by the heavy neutrino decays. To illustrate the basics of this appealing scenario, we discuss now three fundamental points of the Leptogenesis process, closely related to Sakharov conditions of Section 1.2.2.

[4]The on-shell part of s-channel scatterings is already accounted for by decays and inverse-decays.

2.2.0.1 Lepton and baryon number violations in Leptogenesis: the role of $B - L$

To link lepton and baryon asymmetries, Leptogenesis clearly requires a connection between the lepton and baryon number violations that the first Sakharov condition imposes in the present framework[5]. The latter is provided again by the sphaleron processes of the Standard Model, while the Majorana mass term in eq. (2.0.15) ensures the explicit violation of the former. To investigate now the connection between the corresponding asymmetries we consider the processes that are active in the Early Universe, as well as the implications that chemical equilibrium has on the associated chemical potentials [81–83]:

Process	Corresponding condition
$W^- \longleftrightarrow \phi^- + \phi^0$	$\mu_W = \mu_{\phi^-} + \mu_{\phi^0}$
$W^- \longleftrightarrow \overline{u_{iL}} + d_{iL}$	$\mu_W = \mu_{d_{iL}} - \mu_{u_{iL}}$
$W^- \longleftrightarrow \overline{\nu_{\alpha L}} + l_{\alpha L}$	$\mu_W = \mu_{l_{\alpha L}} - \mu_{\nu_{\alpha L}}$
$\phi^0 \longleftrightarrow \overline{u_{iL}} + u_{iR}$	$\mu_{\phi^0} = \mu_{u_{iR}} - \mu_{u_{iL}}$
$\phi^0 \longleftrightarrow \overline{d_{iL}} + d_{iR}$	$\mu_{\phi^0} = \mu_{d_{iL}} - \mu_{d_{iR}}$
$\phi^0 \longleftrightarrow \overline{l_{\alpha R}} + l_{\alpha L}$	$\mu_{\phi^0} = \mu_{l_{\alpha L}} - \mu_{l_{\alpha R}}$

Table 2.1: Active processes in the Early Universe. The relevant reactions are presented in the left column. The right column shows the corresponding conditions that chemical equilibrium implies for the chemical potentials of the species involved. The subscript "i" labels the SM generations, u and d indicate respectively up-type and down-type quarks, while "α" is reserved for the lepton flavours.

Assuming now an *efficient particle mixing* due to

- quark mixing: $\mu_{u_{iL}} \to \mu_{u_L}$, $\mu_{u_{iR}} \to \mu_{u_R}$, $\mu_{d_{iL}} \to \mu_{d_L}$, $\mu_{d_{iR}} \to \mu_{d_R}$
- lepton mixing: $\mu_{l_{\alpha L}} \to \mu_{l_L}$, $\mu_{l_{\alpha R}} \to \mu_{l_R}$, $\mu_{\nu_{\alpha L}} \to \mu_{\nu_L}$

as well as *in-equilibrium* $SU(2)_L$ *gauge interactions*, which level the chemical potentials of species belonging to the same $SU(2)_L$ multiplet

$$\mu_{\phi^-} \equiv \mu_{\phi^0} = \mu_\Phi, \qquad \mu_{u_L} \equiv \mu_{d_L} = \mu_{Q_L}, \qquad \mu_{\nu_L} \equiv \mu_{l_L} = \mu_{\ell_L} \tag{2.2.3}$$

the reactions of Table 2.1 yield

$$\begin{cases} \mu_\Phi = \mu_{u_R} - \mu_{Q_L} \\ \mu_\phi = \mu_{q_L} - \mu_{d_R} \\ \mu_\phi = \mu_{\ell_L} - \mu_{l_R}. \end{cases} \tag{2.2.4}$$

[5] On top of the usual barion number violations, lepton number violations are required to generate the lepton asymmetry.

In addition to that, the Hypercharge neutrality of the Universe implies – Table A.1

$$\mu_{Q_L} + 2\mu_{u_R} - \mu_{d_R} - \mu_{\ell_L} - \mu_{l_R} + \frac{2}{3}\mu_\Phi = 0 \tag{2.2.5}$$

while the Electro-Weak sphaleron processes, in equilibrium for temperatures T 100 GeV $\lesssim T \lesssim 10^{14}$ GeV, impose

$$3\mu_{Q_L} + \mu_{\ell_L} = 0 \tag{2.2.6}$$

leading to a system of five equations for the six chemical potentials involved. Notice that owing to eq. (1.2.8), the latter actually measure the asymmetry densities between particles and antiparticles of the relative species. In particular, for baryons and leptons we consequently have

$$n_B - n_{\overline{B}} = 3\gamma\left(2\mu_{Q_L} + \mu_{u_R} + \mu_{d_R}\right), \qquad n_L - n_{\overline{L}} = 3\gamma\left(2\mu_{\ell_L} + \mu_{l_R}\right) \tag{2.2.7}$$

where $\gamma = T^2/6$ and the factor 3 is due to the considered number of generations. Then, by means of the system composed by eq.s (2.2.4, 2.2.5, 2.2.6), it follows

$$n_B - n_{\overline{B}} = -4\,\gamma\mu_{\ell_L}, \qquad n_L - n_{\overline{L}} = \frac{51}{7}\,\gamma\mu_{\ell_L} \tag{2.2.8}$$

showing explicitly the connection that the presented reactions established between baryon and lepton asymmetries. Going further, an effective measure for μ_{ℓ_L} is given by the $B-L$ *asymmetry density*, defined according to:

$$n_{B-L} \coloneqq n_B - n_{\overline{B}} - (n_L - n_{\overline{L}}) = -\frac{79}{7}\,\gamma\mu_{\ell_L} \tag{2.2.9}$$

Hence, by parametrizing the baryon and lepton asymmetry densities in terms of the above quantity

$$n_B - n_{\overline{B}} = \frac{28}{79}\,n_{B-L}, \qquad n_L - n_{\overline{L}} = -\frac{51}{79}\,n_{B-L} \tag{2.2.10}$$

it is evident that the first Sakharov condition actually implies the violation of the $B-L$ number within Leptogenesis. We anticipate that this will be a fundamental quantity in our analyses as, being conserved by all the Standard Model processes, it is purely determined by the Leptogenesis mechanism.
The way this scenario operates is therefore clear: by enforcing $\mu_{\ell_L} \neq 0$ through the heavy neutrino decays, the Leptogenesis process violates $B-L$ and results in an asymmetry that is partially converted into a baryon asymmetry, as prescript by eq. (2.2.10).

To conclude this Section, it should be stressed that the conversion factors in eq. (2.2.10) are valid only as far as the $B-L$ violation occurs in the temperature regime where Electro-Weak sphalerons are in equilibrium. This will always be the case in the present work, nevertheless we refer to the analysis in [82] for an expression of the same coefficients valid for temperatures below the Electro-Weak phase transitions.

2.2.0.2 C and CP violation in Leptogenesis: CP-asymmetries

The second point we consider is the violation of C and CP. Within the current framework, the former is still provided by the same Weak Interactions of the SM. As for the latter, notice that the heavy neutrino decays of Leptogenesis will result in a lepton asymmetry only if the leptonic and antileptonic decay channels do not compensate. Leptogenesis therefore explicitly requires a violation of the CP symmetry. Given the decay rates of the heavy neutrinos N_i

$$\Gamma_{i\alpha} = \Gamma_{i\alpha}\left(|N_i\rangle \to \sum_a \left(|\ell^a_\alpha\rangle + |\Phi^a\rangle\right)\right) \tag{2.2.11}$$

$$\overline{\Gamma}_{i\alpha} = \overline{\Gamma}_{i\alpha}\left(|N_i\rangle \to \sum_a \left(|\overline{\ell}^a_\alpha\rangle + |\overline{\Phi}^a\rangle\right)\right) \tag{2.2.12}$$

where $\alpha = e, \mu, \tau$ and $a = 1, 2$ is the $SU(2)_L$ index, such violation is then quantified through the CP-*asymmetries* introduced for GUT baryogenesis [84]:

$$\varepsilon_i \coloneqq \sum_{\alpha=e,\mu,\tau} \varepsilon_{i\alpha} = \sum_{\alpha=e,\mu,\tau} \left[-\frac{\Gamma_{i\alpha} - \overline{\Gamma}_{i\alpha}}{\sum\limits_\beta \left[\Gamma_{i\beta} + \overline{\Gamma}_{i\beta}\right]}\right]. \tag{2.2.13}$$

In the same context it was also noticed that non-zero CP-asymmetries arise form the interference between the tree-level and one-loop decay diagrams, provided tree level coupling constants be complex and on-shell particles run in the loops. In Leptogenesis these conditions are indeed satisfied, being $h_{\alpha i}$ a complex matrix and given the presence of more then one N_i. Hence an explicit calculation of the diagrams reported in Figure 2.1 yields [85, 86] for *hierarchical heavy neutrinos* $M_1 < M_2 < M_3$

$$\varepsilon_i = \sum_\alpha \varepsilon_{i\alpha} = \frac{3}{16\,\pi\,(h^\dagger h)_{ii}} \sum_{j\neq i} \mathrm{Im}\left[(h^\dagger h)^2_{ij}\right] \frac{\xi(x_j/x_i)}{\sqrt{x_j/x_i}} \tag{2.2.14}$$

where $x_i \coloneqq M_i^2/M_1^2$ and M_i is the mass of the heavy neutrino N_i. The function $\xi(x)$, which regulates the sensitivity of the CP-asymmetries on the heavy neutrino mass spectrum, is defined as [87]

$$\xi(x) := \frac{2}{3} x \left[(1+x)\ln\left(\frac{1+x}{x}\right) - \frac{2-x}{1-x}\right] \tag{2.2.15}$$

and represented in Figure 2.2.

It is therefore clear that beside satisfying the second Sakharov condition, Leptogenesis provides an additional source of CP violation that potentially addresses the issue raised by the magnitude of η_B proposed by CMB and BBN.

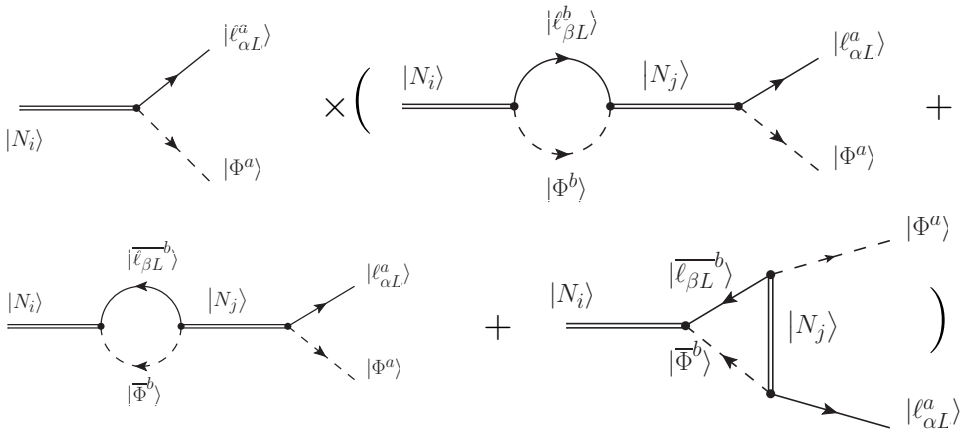

Figure 2.1: CP-asymmetry in Leptogenesis, the relevant diagrams. Double lines indicate the Majorana heavy neutrinos. The arrows are tracking the usual fermion flow along the fermion lines and the Hypercharge flow along the scalar ones.

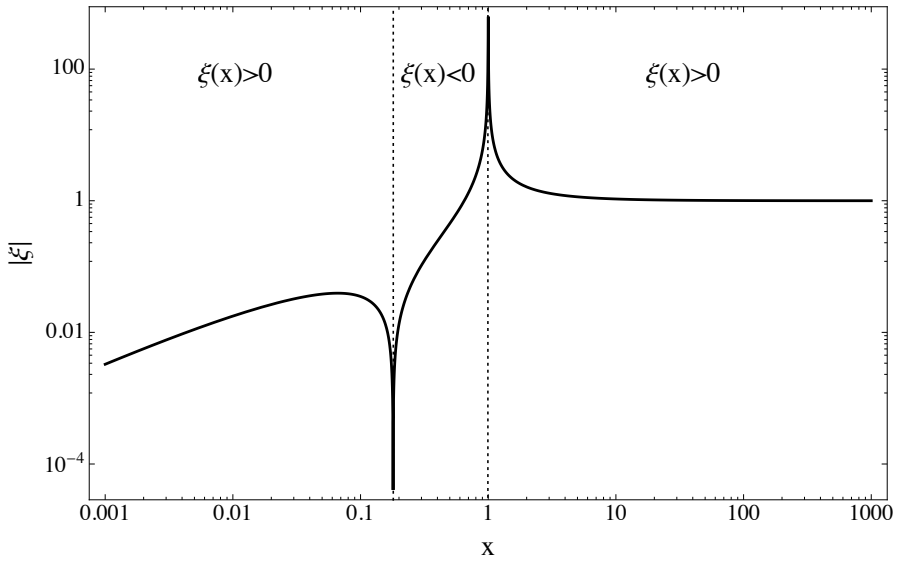

Figure 2.2: CP-asymmetry in Leptogenesis, the ξ function of eq. (2.2.14).

2.2.0.3 Out-of-equilibrium decays and departure from equilibrium

The last point we consider is the departure from equilibrium, which determined the non-viability of Electro-Weak Baryogenesis. We focused until now on the role that heavy neutrino decays have in Leptogenesis, neglecting the part of inverse-decays. Yet, when inverse-decays and decays are both active, through the reactions $N \longleftrightarrow \ell + \phi$ and $N \longleftrightarrow \overline{\ell} + \overline{\phi}$ chemical equilibrium implies:

$$\mu_N = \mu_{\ell_L} + \mu_\phi = 0. \tag{2.2.16}$$

Hence we are provided a sixth relation, that along with eq.s (2.2.4, 2.2.5, 2.2.6) forms a closed system having for solution

$$\mu_{\ell_L} = \mu_\phi = \mu_{u_R} = \mu_{l_R} = \mu_{d_R} = \mu_{q_L} \equiv 0 \tag{2.2.17}$$

and obviously no asymmetry can be generated. In addition, notice that the interplay of decays and inverse-decays forces the heavy neutrino abundance to track its equilibrium value, so thermal equilibrium is also realised. A departure from equilibrium must therefore occur, satisfying the third Sakharov condition.

Within Leptogenesis, out-of-equilibrium dynamics is provided by the expansion of Universe. A species will be able to maintain thermal and chemical equilibrium in this background only as far as all the rates $\Gamma_{\mathcal{I}}$, of the interactions $\mathcal{I}$ that thermalise its abundance, are fast enough to overcome the effects due to the expansion. Hence, with the Hubble parameter H quantifying the expansion rate, if $\Gamma_{\mathcal{I}} \gg H \ \forall \ \mathcal{I}$ thermal and chemical equilibrium are maintained. Conversely, when $\Gamma_{\mathcal{I}} \ll H$ reactions are said to *freeze-in* and the equilibrium regime is lost. In the specific case of Leptogenesis, focusing on a heavy neutrino N_i, the non-equilibrium-dynamics therefore results from the freeze-in of decay processes

$$\frac{\Gamma_{D,i}}{H} \ll 1 \tag{2.2.18}$$

or the freeze-in of inverse decays

$$\frac{\Gamma_{ID,i}}{H} \ll 1 \tag{2.2.19}$$

or from both the above conditions. Here $\Gamma_{D,i}$ is the total decay rate of the considered neutrino

$$\Gamma_{D,i} \coloneqq \sum_\alpha \left(\Gamma_{i\alpha} + \overline{\Gamma}_{i\alpha}\right) = \frac{\left(h^\dagger h\right)_{ii} M_i}{8\pi} \tag{2.2.20}$$

and the last equality holds at the tree-level. The inverse-decay rate is calculated through the condition $n_\ell^{eq}\,\Gamma_{ID,i} = \Gamma_{D,i}\,n_{N_i}^{eq}$. Introducing now the *decay parameter* K_i

$$K_i \coloneqq \frac{\Gamma_{D,i}(T=0)}{H(T=M_i)} \tag{2.2.21}$$

it is clear that this parameter discriminates between the above possibilities. In this regard, the limit cases $K_i \gg 1$ and $K_i \ll 1$ which respectively characterise the *strong washout regime* and the *weak washout regime*, correspond to separated regions of the Seesaw parameter space. The connection between K_i and the latter is made explicit by defining the *effective neutrino mass*

$$\tilde{m}_i \coloneqq \frac{8v^2\pi}{M_i^2}\Gamma_{D,i} = \frac{(m_D^\dagger m_D)_{ii}}{M_i} \tag{2.2.22}$$

and the *equilibrium neutrino mass*

$$m_\star \coloneqq \frac{8v^2\pi}{M_i^2} H(T = M_i) \simeq 1.08 \times 10^{-3} \quad \text{eV}. \tag{2.2.23}$$

Hence the decay parameters can be recast as

$$K_i = \frac{\tilde{m}_i}{m_\star}. \tag{2.2.24}$$

Notice that a natural value for $\tilde{m}_i$ is provided by $\tilde{m}_i \simeq m_\nu^{osc} \gtrsim m_\star$, excluding the weak washout regime. Attracted by this possibility, in the remaining part of this Thesis we will concentrate on Leptogenesis scenarios characterised by strong washout regimes. The *out-of-equilibrium-decays* that satisfy the third Sakharov condition will therefore be provided by the freeze-in of the inverse decays.

To summarise our discussion, Leptogenesis is indeed the explanation that the Seesaw extension proposes for the baryon asymmetry of the Universe. In this attractive scenario of baryogenesis, the out-of-equilibrium decays of the heavy neutrinos that the Seesaw mechanism involves break the CP symmetry, producing a lepton asymmetry. This process entails a violation of the $B - L$ number, which results in a partial conversion of the original lepton asymmetry into the desired baryon asymmetry.
As the connection between B, L and $B - L$ have already been disclosed, in the next Section we quantify the $B - L$ violation produced within the clear framework provided by N_1 Leptogenesis.

2.2.1 $\mathbf{N_1}$ Leptogenesis

N_1 Leptogenesis [81, 88, 89] is a simple scenario of Leptogenesis obtained by neglecting the contributions of the heaviest neutrinos N_2 and N_3 to the baryon asymmetry of the Universe. By focusing on the dynamics of a single neutrino, N_1 Leptogenesis provides a straightforward framework that nevertheless unfolds the fundamentals of more complex scenarios. Not to complicate this picture, in the present Section we discuss the evolution of the baryon asymmetry in a strong washout regime accounting only for the decays and inverse-decays of N_1. In particular we choose to disregard in our analyses the impact of scattering processes and flavour, discussing the modifications that the former introduces in a dedicated Subsection. A full analysis of Leptogenesis in relation to flavour effects is instead postponed to the next Chapter.

Under the proposed assumptions, the *Boltzmann equation* which regulates the abundance of N_1 in the expanding Universe is

$$\frac{\mathrm{d}\, N_{N_1}}{\mathrm{d}\, z} = -D_1(z) \left(N_{N_1}(z) - N_{N_1}^{eq}(z) \right) \tag{2.2.25}$$

where $z \coloneqq M_1/T$ and N_X denotes the abundance of particle or asymmetry X, normalised to a comoving volume which contains one heavy neutrino in ultra-relativistic regime and thermal equilibrium. The *decay factor* $D_1(z)$ is defined as

$$D_1(z) \coloneqq \frac{\Gamma_{D,1}(T)}{H\,z} = K_1\,z\left\langle\frac{\mathcal{K}_1(z)}{\mathcal{K}_2(z)}\right\rangle \tag{2.2.26}$$

and accounts for the effect of a non-zero temperature on the total decay width. The thermally averaged dilation factor is expressed through the modified Bessel functions of second kind $\mathcal{K}_i$. The equilibrium abundance $N_{N_1}^{eq}$ of the heavy neutrinos is also given on terms of Bessel functions

$$N_{N_1}^{eq}(z) = \frac{1}{2}z^2\mathcal{K}_2(z). \tag{2.2.27}$$

Hence, the abundance of N_1 is completely determined by two parameters: the decay parameter K_1 and the unknown initial abundance $N_{N_1}^{in} = N_{N_1}(z \ll 1)$.

The evolution of the baryon asymmetry is tracked by eq. (2.2.25) on top of the Boltzmann equations that regulate the modifications of B and L. As remarked before, we can restrict our analysis to the pure Leptogenesis processes by considering the $B-L$ number, non-anomalous within the Standard Model. Hence, by subtracting the equation for the evolution of the lepton asymmetry from the one controlling the baryon asymmetry, we obtain:

$$\frac{\mathrm{d}\,N_{B-L}}{\mathrm{d}\,z} = \epsilon_1\,D_1(z)\left(N_{N_1} - N_{N_1}^{eq}\right) - N_{B-L}\,W_1^{ID}(z). \tag{2.2.28}$$

The above formula is explained straightforwardly. The first term on the RHS accounts for the interplay of decays and inverse-decays. When an overabundance of heavy neutrinos arises – $N_{N_1} > N_{N_1}^{eq}$ – the $B-L$ asymmetry receives a positive contribution from the decay processes. Conversely, when $N_{N_1} < N_{N_1}^{eq}$, a negative contribution is originated from the inverse-decays which consume leptons and antileptons in different quantities to restore the N_1 abundance. The conversion factor between N_{B-L} and N_{N_1} is the CP-asymmetry ε_1, previously defined in eq.s (2.2.13) and (2.2.14). As for the second term on the RHS of eq. (2.2.28), the *washout factor* $W_1^{ID}(z)$ accounts for a statistical rebalancing which hinders the $B-L$ production and is driven by the inverse decays:

$$W_1^{ID}(z) \coloneqq \frac{1}{2}\frac{\Gamma_{ID,1}(z)}{H(z)z} = \frac{1}{4}K_1\,\mathcal{K}_1(z)z^3. \tag{2.2.29}$$

Here

$$\Gamma_{ID,1}\,N_\ell^{eq} = \Gamma_{D,1}\,N_{N_1}^{eq} \tag{2.2.30}$$

and for the adopted conventions it is $N_\ell^{eq} \equiv 1$. The Boltzmann equation for $B-L$ is then completely determined in terms of three parameters: K_1, $N_{N_1}^{in}$ and the initial $B-L$ abundance N_{B-L}^{preex}, which potentially comprises the contributions from N_2 and N_3.
Within this framework, the amount of baryon asymmetry of the Universe that Leptogenesis produced is completely determined by the final abundance of $B-L$ asymmetry, $N_{B-L}^f \equiv N_{B-L}(z \to \infty)$. In fact, by means of the conversion factor in eq. (2.2.10) and

accounting for the dilution factor in eq. (B.0.10) we obtain[6]

$$\eta_B(T=T_{rec}) = \frac{28}{79}\frac{n^f_{B-L}}{n_\gamma}\frac{g_{\star S}(T=T_{rec})}{g_{\star S}(T=T_{off})} = \frac{28}{79}\frac{N^f_{B-L}}{N_\gamma}\frac{g_{\star S}(T=T_{rec})}{g_{\star S}(T=T_{off})} = \\ = 0.96\times 10^{-2}\, N^f_{B-L} \tag{2.2.31}$$

where T_{rec} and T_{off} indicate the temperature of the Universe at the end of, respectively, recombination and Leptogenesis eras. To detail the $B-L$ production we consider now the following solution to eq. (2.2.28)

$$N_{B-L}(z) = N^{preex}_{B-L}(z=0)\,\exp\left[-\int_0^z W_1^{ID}(z')\,\mathrm{d}\,z'\right] + \varepsilon_1\kappa_1(z) \tag{2.2.32}$$

where the *efficiency factor* κ_i does not depend on the CP-asymmetries

$$\kappa_1(z) \coloneqq -\int_0^z \frac{\mathrm{d}\,N_{N_1}}{\mathrm{d}\,z'}\,\exp\left[-\int_{z'}^z W_1^{ID}(z'')\,\mathrm{d}\,z''\right]\mathrm{d}\,z' \tag{2.2.33}$$

and approximatively quantifies the number of heavy neutrinos which decay out of equilibrium. Notice that in a strong washout regime it is $K_1 \gg 1$, hence the preexisting component N^{preex}_{B-L} is exponentially washed out and the final $B-L$ abundance is consequently determined solely by the second term in the RHS of eq. (2.2.32), corresponding to the asymmetry that N_1 Leptogenesis produced. Therefore, given the expression for the CP-asymmetry in eq. (2.2.14), in order to calculate N^f_{B-L} we concentrate on the efficiency factor k_1, neglecting any preexisting contribution by setting $N^{preex}_{B-L} = 0$.

Suppose a vanishing initial abundance of N_1 and consider the resulting *thermal Leptogenesis* scenario in which the required heavy neutrinos are thermally produced through inverse-decays and, more in general, also through scatterings. By defining z_{eq} as the value of z for which the abundance of N_1 reaches its equilibrium value

$$N_{N_1}(z_{eq}) = N^{eq}_{N_1}(z_{eq}) \tag{2.2.34}$$

we can discriminate between two contributions that the efficiency factor comprises. The first one, κ_1^-, is due to the interplay of inverse-decays and washout processes. For $z < z_{eq}$ the effect of decays in eq. (2.2.25) is in fact negligible owing to the low N_1 abundance. Integrating this equation therefore yields

$$N_{N_1}(z<z_{eq}) = 2\int_0^z W_1^{ID}(z')\,\mathrm{d}\,z' \simeq \frac{K_1}{6}z^3 \tag{2.2.35}$$

[6]The presence of the dilution factor is necessary for a comparison with the experimental measurements of η_B. In this regard, for the higher precision reported, we will explicitly employ the CMB result (1.2.7) as our benchmark value.

where we used $\mathcal{K}_1(x) \simeq 1/x$ valid for $x < 1$. Hence $\kappa_1^- \coloneqq \kappa_1(z < z_{eq})$ is given by

$$\kappa_1^-(z, K) = -\int_0^z D_1(z')\, N_{N_1}^{eq}(z')\, \exp\left[-\int_{z'}^z W_1^{ID}(z'')\, \mathrm{d}\, z''\right] \mathrm{d}\, z' = \\ = -2\left(1 - \exp\left[-\frac{1}{12} K_1 z^3\right]\right). \tag{2.2.36}$$

The final value of this contribution, as found after the Leptogenesis process, is then calculated by accounting for the additional washout that will be performed for $z > z_{eq}$. An approximate expression is given by [89]

$$\kappa_1^{f-}(K_1) \coloneqq \kappa_1^-(z \to \infty, K_1) = -2e^{-\frac{1}{2}N(K_1)}\left(e^{\frac{1}{2}\bar{N}(K_1)} - 1\right) \tag{2.2.37}$$

which holds in the weak washout regime as well. In the above formula, the factor containing $N(K_1) \coloneqq 3\pi K_1/4$ represents the effect of the washout executed for $z > z_{eq}$, while

$$\bar{N}(K_1) \coloneqq \frac{N(K_1)}{\left(1 + \sqrt{N(K_1)}\right)^2} \tag{2.2.38}$$

extrapolates between $N_{N_1}(z_{eq}) = 1$, valid for[7] $K \gg 1$, and $N_{N_1}(z_{eq}) = N(K_1)$ of the weak washout regime.

The second contribution to the efficiency factor arises for $z > z_{eq}$, in connection to the decay processes of N_1. By defining $\Delta \coloneqq N_{N_1}(z) - N_{N_1}^{eq}(z)$ we can solve eq. (2.2.25) in powers of $1/K_1$

$$\Delta(z) \simeq -\frac{1}{D_1}\frac{\mathrm{d}\, N_{N_1}^{eq}}{\mathrm{d}\, z} \tag{2.2.39}$$

where we substituted $\mathrm{d}\, N_{N_1}/\mathrm{d}\, z \simeq \mathrm{d}\, N_{N_1}^{eq}/\mathrm{d}\, z$. For $z > z_{eq}$ the neutrino abundance is in fact tracking closely its equilibrium value, since $D_1 \propto K_1$ and $K_1 \gg 1$ owing to the strong washout regime. From eq. (2.2.29) it follows

$$\Delta(z) = \frac{1}{D_1}\frac{2}{K_1 z} W_1^{ID}(z) \tag{2.2.40}$$

and the contribution to the efficiency factor is therefore given by

$$\kappa_1^+(z, K_1) \coloneqq \int_{z_{eq}}^z D_1(z')\left(N_{N_1}(z') - N_{N_1}^{eq}(z')\right) e^{-\int_{z'}^z W_1^{ID}(z'')\,\mathrm{d}\, z''} \mathrm{d}\, z' = \\ = \frac{2}{K_1}\int_{z_0}^z \frac{1}{z'} W_1^{ID}(z')\, e^{-\int_{z'}^z W^{ID}(z'')\,\mathrm{d}\, z''} \mathrm{d}\, z'. \tag{2.2.41}$$

[7] From eq. (2.2.25) we expect the N_1 abundance to rapidly converge to its equilibrium value within a strong washout regime. This implies $z_{eq} < 1$ and therefore $N_{N_1}(z_{eq}) = 1$.

This integral is dominated by the contribution given by an interval around $z = z_L$, where the exponent is minimised. Requiring a stationary point yields the condition

$$W_1^{ID}(z_L) = \left\langle \frac{\mathcal{K}_2(z_L)}{\mathcal{K}_1(z_L)} \right\rangle - \frac{3}{z_L} \tag{2.2.42}$$

which consequently implies

$$z_L(K_1) \simeq 2 + 4K_1^{0.13} \exp\left(-\frac{2.5}{K_1}\right). \tag{2.2.43}$$

An expression for the final value of κ^+, which also holds in the weak washout regime, is given as [89]

$$\kappa_1^{f+}(K_1) \coloneqq \kappa_1^+(z \to \infty, K_1) = \frac{2}{z_L K_1}\left(1 - e^{-\frac{1}{2} z_L(K_1) K_1 \bar{N}(K_1)}\right) \tag{2.2.44}$$

where $\bar{N}$ was previously defined in eq. (2.2.38).
The final value of the total efficiency factor is therefore given by

$$\kappa_1^f(K_1) \coloneqq \kappa_1(z \to \infty, K_1) = \kappa_1^{f-}(K_1) + \kappa_1^{f+}(K_1) \tag{2.2.45}$$

and the produced $B - L$ asymmetry consequently is

$$N_{B-L}^{lept,f} = \epsilon_1 \, \kappa_1^f. \tag{2.2.46}$$

Three remarks follow:

- The signs of κ_1^{f-} and κ_1^{f+} are opposite. We will explain this disparity below, when commenting on the evolution of the $B - L$ asymmetry within N_1 Leptogenesis.
- As we anticipated, the washout processes hinder the $B - L$ production. In particular, notice that a strong washout regime enforces the exponential suppression of the asymmetry generated for $z < z_{eq}$ – eq. (2.2.37). Hence the asymmetry is effectively produced only for $z > z_{eq}$ where the suppression factor is $1/K_1$ – eq. (2.2.44).
- Imposing an initial thermal abundance $N_{N_1}^{in} = 1$ corresponds to neglecting the dynamics taking place for $z < z_{eq}$. As a result, the final efficiency factor in this case is simply given by eq. (2.2.45) with $\kappa_1^{f-} \equiv 0$.

A comprehensive description of N_1 Leptogenesis that builds on top of the presented analysis is given by Figure 2.3, where we plotted the numerical solutions of eq.s (2.2.25) and (2.2.28). We can clearly distinguish between three stages that characterise the evolution of the $B - L$ asymmetry:

I N_1 *production.*
In the first step, for $z < z_d$, decays are not active – Figure 2.4 – and the neutrino abundance is being produced by the inverse-decays. The latter consume leptons and antileptons in different quantities, resulting in a first $B - L$ asymmetry that we parametrized through $\kappa_1^-(z)$. For $z > z_{in}$ the washout process is also active – Figure 2.4.

II *Decays, inverse-decays and washout.*
For $z > z_d$ decays are finally active and at $z = z_{eq}$ the heavy neutrino abundance reaches its thermal equilibrium value. The $B-L$ asymmetry is now generated from an interplay of decays, inverse decays and washout processes accounted by $\kappa_1^+(z)$. The asymmetry generated in the previous step is quickly depleted as, on top of the exponential suppression that the washout process enforces, decays contribute to the $B - L$ asymmetry with opposite sign.

III *Out-of-equilibrium decays.*
The interplay between decays, inverse-decays and washout processes breaks down at $z = z_{out}$, where W_1^{ID} drops below the rate of the Universe expansion quantified by H – Figure 2.4 – and the inverse-decays freeze-in. The consequent deviation from equilibrium satisfies the third Sakharov condition and the $B - L$ asymmetry stabilises to its final abundance. The final value of the relevant contribution to the efficiency factor, κ_1^{f+}, is therefore mainly determined by the out-of-equilibrium decays which take place for $z > z_{out} \simeq z_L$[8] and the disparity of sign between κ_1^{f+} and κ_1^{f-} is consequently explained.

[8]The last step follows from eq. (2.2.42) in a strong washout regime.

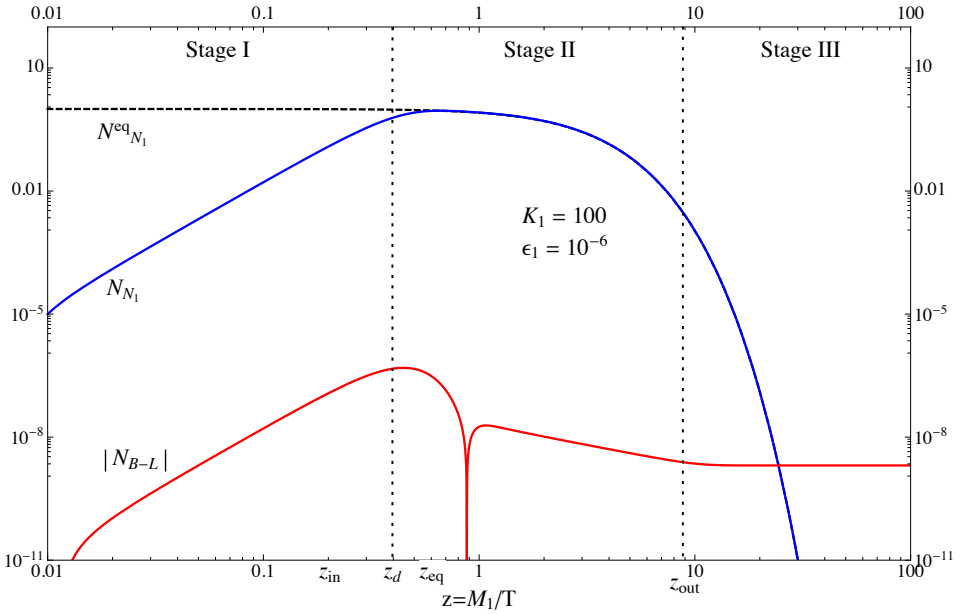

Figure 2.3: The $B-L$ asymmetry evolution in N_1 Leptogenesis and the three stages it comprises, adapted from [89]. The black dashed line corresponds to $N^{eq}_{N_1}(z)$ of eq. (2.2.27), while the blue line represents the actual N_1 abundance. The evolution of $|N_{B-L}|$ is tracked by the red line for the typical value $\varepsilon_1 = 10^{-6}$.

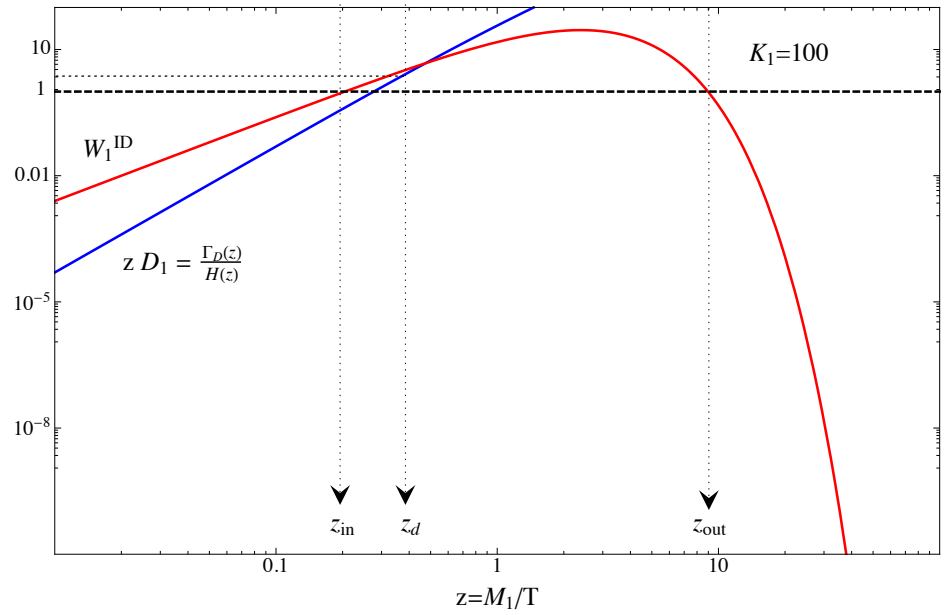

Figure 2.4: Washout and decay processes in Leptogenesis, adapted from [89]. The red line is associated to the washout term $W_1^{ID}(z)$ defined in eq. (2.2.29), the blue line represents instead $z\,D_1(z)$, where the decay factor $D_1(z)$ is given in eq. (2.2.26). The values of z_{in} and z_{out}, enclosing the interval where the inverse-decays and washout processes are in equilibrium, is revealed by the condition $W_z^{ID} = 1$. Similarly, the condition $zD_1(z) \geq 2$ identified the region $z > z_d$ where the decay processes of N_1 are in equilibrium.

2.2.1.1 Constraining N_1 Leptogenesis

We describe now the impact that the measurements reported in Chapter 1 have on N_1 Leptogenesis. In this regard, considering the *strong hierarchic limit* $M_3 \gg M_2 \gg M_1$ the eq. (2.2.13) for ε_1 simplifies due to the behaviour of $\xi(x_j/x_i)$. Hence we have

$$\varepsilon_1 = \frac{3M_1}{16\pi(h^\dagger h)_{11}} \sum_{j=1}^{3} \mathrm{Im}\left[\left(h^\dagger h\right)^2_{1j}\right] = -\frac{3M_1}{16v^2\pi(h^\dagger h)_{11}} \mathrm{Im}\left[\left(h^\dagger m^\nu h^*\right)_{11}\right] \tag{2.2.47}$$

where the summation in the first step has been extended to the null term that arises for $j = 1$. Introducing now the orthogonal matrix Ω [90]

$$\Omega := v\, D_{m^\nu}^{-1/2}\, U^\dagger\, h\, D_M^{-1/2} \tag{2.2.48}$$

we have

$$\mathrm{Im}(\Omega^T\Omega)_{11} = 0 \Rightarrow \frac{v^2}{M_1}\mathrm{Im}\left[h^T U^* D_m^{-1} U^\dagger h\right]_{11} = 0 \tag{2.2.49}$$

and the consequent identity

$$\frac{1}{m_1}\mathrm{Im}\left[(U^\dagger h)^2_{11}\right] = -\sum_{j\neq 1}\frac{1}{m_j}\mathrm{Im}\left[(U^\dagger h)^2_{j1}\right]. \tag{2.2.50}$$

Finally, by rewriting

$$\mathrm{Im}\left[h^\dagger m^\nu h^*\right]_{11} = -m_1 \mathrm{Im}\left[(U^\dagger h)^*_{11}(U^\dagger h)^*_{11}\right] - \mathrm{Im}\sum_{j\neq 1}\left[(U^\dagger h)^*_{j1}(U^\dagger h)^*_{j1}\right] \tag{2.2.51}$$

we have [91]

$$\epsilon_1 = -\frac{3M_1}{16\, v^2\, \pi}\sum_{j\neq 1}\frac{m_j^2 - m_1^2}{m_j}\frac{\mathrm{Im}\left[(\tilde{h})^2_{j1}\right]}{(\tilde{h}^\dagger\tilde{h})_{11}} \tag{2.2.52}$$

where we defined $\tilde{h} := U^\dagger h$. It is therefore possible to constrain the CP-asymmetry through the mass spectrum of the light neutrinos n_i [87, 92]. In particular, for normal ordered neutrinos we have the upper bound

$$|\varepsilon_1| \leqslant \varepsilon_1^{max} := \frac{3}{16\,\pi}\frac{M_1(\Delta m^2_{atm})^{1/2}}{v^2} \tag{2.2.53}$$

where $\Delta^2 m_{atm}$ is given in Table 1.1[9]. In this way, considering the value of the baryon asymmetry of the Universe as measured by CMB (1.2.7) for instance, through the relation

$$\eta_B^{lept} := 0.96\times 10^{-2} N_{B-L}^{lept,f} = 0.96\times 10^{-2}\varepsilon_1\, k_1^f \tag{2.2.54}$$

[9] The corresponding upper bound for inverted ordering is straightforwardly obtained by considering that in such scheme $m_2 \sim m_3$. This results in an extra factor of 2 in the RHS of eq. (2.2.53).

the upper bound on the CP-asymmetry can be recast as a lower bound on the mass of N_1. Hence, requiring $\eta_B^{lept} \geq \eta_B^{CMB}$ yields

$$M_1 \gtrsim 6.34 \times 10^8 \text{ GeV} \left(\frac{\eta_B^{CMB}}{6 \times 10^{-10}}\right) \left(\frac{0.05 \text{ eV}}{(\Delta m^2_{atm})^{1/2}}\right) \frac{1}{k_f} \tag{2.2.55}$$

representing a first condition that neutrino oscillation experiments and the measurements of the baryon asymmetry of the Universe impose to the Seesaw parameter space.

2.2.1.2 The impact of scattering processes

We neglected so far the impact that scatterings have on Leptogenesis. In order to account for these processes the Boltzmann equations for N_1 Leptogenesis are modified as follows

$$\frac{\mathrm{d}\, N_{N_1}}{\mathrm{d}\, z} = -\left(D_1(z) + S_1(z)\right)\left(N_{N_1} - N_{N_1}^{eq}\right) \tag{2.2.56}$$

$$\frac{\mathrm{d}\, N_{B-L}}{\mathrm{d}\, z} = \epsilon_1 \left(D_1(z) + S_1(z)\right)\left(N_{N_1} - N_{N_1}^{eq}\right) - N_{B-L}\, W_1(z) \tag{2.2.57}$$

where the scattering factor S_1 is defined similarly to the counterpart of decay processes

$$S_1(z) = \frac{\Gamma_s^{|\Delta L|=1}}{Hz} \tag{2.2.58}$$

and the washout factor is generalised to

$$W_1(z) = W_1^{ID} + W_1^{|\Delta L|=1} + W_1^{|\Delta L|=2} \tag{2.2.59}$$

with clear meaning of the notation.

The $|\Delta L| = 1$ processes, mediated by the Higgs boson in t and s channels, mainly involve top quarks and gauge bosons. Nevertheless, as the present situation concerning the reaction densities of the latter is controversial [93, 94], we will not discuss here this component. The main effect of $|\Delta L| = 1$ quark scatterings is to boost the heavy neutrino production, leading to an enhanced efficiency factor in the weak washout regime. On top of that, through the term $W_1^{|\Delta L|=1}$ these processes contribute also to the washout and therefore correct the efficiency factor in the strong washout regime as well. A detailed analysis yields [89]

$$D_1 + S_1 \simeq 0.1\, K_1 \left[1 + \ln\left(\frac{M_1}{m_H}\right) z^2 \ln\left(1 + \frac{a}{z}\right)\right] \tag{2.2.60}$$

where

$$a \coloneqq \frac{10}{\ln(M_1/m_H)} \tag{2.2.61}$$

and m_H, the mass of the Higgs boson, regularises the infra-red divergence of the t channel. The washout factor satisfies instead

$$W_1^{|\Delta L|=1} = j(z)\, W_1^{ID} \tag{2.2.62}$$

where the function $j(z)$ is defined as

$$j(z) = \left[\frac{z}{a}\ln\left(1+\frac{a}{z}\right) + \frac{r}{z}\right]\left(1+\frac{15}{8z}\right) \tag{2.2.63}$$

and $r = 1,\ 2/3$ respectively in strong and weak washout regime. A numerical analysis of the efficiency factor that eq. (2.2.57) implies reveals that within a strong washout regime the impact of $|\Delta L| = 1$ scattering described above is limited. In the following Chapters we therefore choose to neglect these processes, in favour of the simpler picture that decays and inverse decays provide.

The $|\Delta L| = 2$ scatterings can also be safely neglected for reasonable values of $M_1 < 10^{14}$ GeV, provided the light neutrinos n_i are hierarchical [89, 95]. By net these processes modify the washout parameter only in the non-relativistic regime, for $z \gg 1$, where the relative contribution is modelled in:

$$W_1^{|\Delta L|=2} = \frac{\omega}{z^2}\frac{M_1}{10^{10}\ \text{GeV}}\frac{\bar{m}^2}{(\text{eV})^2}. \tag{2.2.64}$$

Here $\omega \simeq 0.186$ while $\bar{m}$ defines the light neutrino mass scale: $\bar{m}^2 \coloneqq m_1^2 + m_2^2 + m_3^2$. We remarked before that, beside the necessary initial conditions, the Boltzmann equations for N_{N_1} and N_{B-L} are completely determined by one parameter, K_1, which involves the mass scale $\tilde{m}_1$ and the equilibrium mass $m_\star$. Clearly, when $|\Delta L| = 2$ scatterings are considered, this is no longer the case and the $B-L$ production is sensitive to M_1 and $\bar{m}$ through the above factor. The efficiency factor is affected by the extra washout that $|\Delta L| = 2$ scatterings perform in the following way

$$\kappa_1^f(K) \longrightarrow \kappa_1^{f,|\Delta L|=2}(K, M_1, \bar{m}) \coloneqq \kappa_1^f(K) e^{-\int_{z_L}^{\infty} W_1^{|\Delta L|=2}(z)\,\mathrm{d}\,z} \tag{2.2.65}$$

and the requirement of *successful Leptogenesis*, $\eta_B^{Lept} \sim \eta_B^{CMB}$, therefore selects now a region in the M_1 , $\bar{m}$ and $\tilde{m}_1$ parameter space associated to the N_1 Leptogenesis model. As a result it is possible to impose a second experimental constraint, quantified in the upper bound [87, 96]:

$$\bar{m} < (0.20 - 0.30) \quad \text{eV}. \tag{2.2.66}$$

Chapter 3

Flavour effects in Leptogenesis

N_1 Leptogenesis has been regarded as the classic scenario of Leptogenesis until the year 2006, when two independent groups underlined the radical impact that flavour has on this mechanism [97, 98]. The analyses we proposed in the previous Chapter excluded the consequences of flavour by focusing on the evolution of the total $B - L$ asymmetry abundance, as well as by disregarding the flavour composition of the leptons that the decays of N_1 produce. In this Chapter we therefore intend to rectify our description, moving away from the simplicity of N_1 Leptogenesis in favour of a more complex scenario where the effects of flavour are completely exploited.
To this purpose, in our analysis we distinguish between heavy neutrino flavour effects and light flavour effects when addressing the modifications that the considered neutrino and charged-lepton Yukawa interactions respectively impose to the theory.

3.1 Heavy neutrino flavour effects

As a first step toward the description of flavour effects we generalise the framework of N_1 Leptogenesis, accounting for the contributions of the heaviest neutrinos that we previously neglected. To simplify our treatment, again we neglect the effect of scattering processes and focus only on *hierarchical Leptogenesis scenarios*, where the heavy neutrino mass spectrum respects the condition

$$M_{i+1} \gtrsim 3M_i, \qquad i = 1, 2 \tag{3.1.1}$$

in a way that the processes associated to different heavy neutrino species do not overlap [99]. The Leptogenesis process consequently comprises three separated eras, each presenting the dynamics of a singular heavy neutrino species N_i, taking place for $T \sim M_i$. The three resulting stages all resemble the scenario of N_1 Leptogenesis described in the previous Chapter through the Boltzmann equations given for N_{N_1}, eq. (2.2.25), and

N_{B-L}, eq. (2.2.28). Hence, with clear meaning of the notation, for the heavy neutrino abundances we have

$$\frac{\mathrm{d}\, N_{N_i}}{\mathrm{d}\, z_i} = -D_i(z_i)\left(N_{N_i}(z_i) - N_{N_i}^{eq}(z_i)\right), \qquad i = 1,2,3 \tag{3.1.2}$$

where $z_i \coloneqq M_i/T$. Introducing again $x_i \coloneqq M_i^2/M_1^2$, it follows $z_i = z\sqrt{x_i}$ and the below expressions for the decay factors and the equilibrium abundances generalise those of Section 2.2.1:

$$D_i(z) \coloneqq K_i\, z_i \left\langle \frac{\mathcal{K}_1(z)}{\mathcal{K}_2(z)} \right\rangle \tag{3.1.3}$$

$$N_{N_i}^{eq}(z_i) = \frac{1}{2} z_i^2 \mathcal{K}_2(z_i). \tag{3.1.4}$$

The decay parameters K_i were instead already presented in eq. (2.2.21).
Focusing now on the $B-L$ asymmetry that Leptogenesis produces, the condition (3.1.1) neglects on one hand the possibilities that resonant Leptogenesis offers [100]. On the other, it effectively prevents the overlapping of the Leptogenesis processes associated to different heavy neutrinos [99]. In this way the final abundance of $B-L$ asymmetry is determined by the asymmetries N_{Δ_i}, resulting from the separated stages we mentioned. The relevant Boltzmann equations, analogous to eq. (2.2.28), are therefore

$$\frac{\mathrm{d}\, N_{\Delta_i}}{\mathrm{d}\, z} = \epsilon_i\, D_i(z)\left(N_{N_i} - N_{N_i}^{eq}\right) - N_{\Delta_i} W_i^{ID}(z), \qquad i = 1,2,3 \tag{3.1.5}$$

and represent three independent relations that, together with eq.s (3.1.2), form three decoupled systems of equations for N_{N_i}, N_{Δ_i} and $i = 1,2,3$. The CP-asymmetries ε_i are given according to eq. (2.2.14), while the washout factor are generalised to

$$W_i^{ID}(z_i) = \frac{1}{4} K_i\, \mathcal{K}_1\sqrt{x_i}\,(z_i)\, z_i^3. \tag{3.1.6}$$

Then, in analogy to eq. (2.2.32), we have

$$N_{\Delta_i}(z) = N_{B-L}(z_{0_i})\, \exp\left[-\int_{z_{0_i}}^{z} W_i^{ID}(z')\, \mathrm{d}\, z'\right] + \epsilon_i \kappa_i(z; K_i) \tag{3.1.7}$$

where $z_{0_i} \simeq z_{in,i}$ indicates the beginning of the considered Leptogenesis stage and the contributions of heavier neutrinos $N_{j>i}$ to the $B-L$ asymmetry are contained in $N_{B-L}(z_{0_i})$. The expression for the efficiency factor generalises the one previously given within N_1 Leptogenesis:

$$\kappa_i(z; K_i) \coloneqq -\int_{z_{0i}}^{z} \frac{\mathrm{d}\, N_{N_i}}{\mathrm{d}\, z'}\, \exp\left[-\int_{z'}^{z} W_i^{ID}(z'')\, \mathrm{d}\, z''\right] \mathrm{d}\, z'. \tag{3.1.8}$$

Imposing for simplicity a vanishing preexisting asymmetry $N_{B-L}^{preex}(z=0)=0$, the final value of N_{B-L} is given by

$$N_{B-L}^{f} = \varepsilon_1 \kappa_1^f + \varepsilon_2 \kappa_2^f e^{-\frac{3\pi}{8} K_1} + \varepsilon_3 \kappa_3^f e^{-\frac{3\pi}{8}(K_1+K_2)}. \tag{3.1.9}$$

Clearly, considering a strong washout regime, the asymmetries generated by the heaviest neutrinos are erased by the washout performed by the lightest and the dynamics of the whole Leptogenesis process therefore recovers the proposed N_1 Leptogenesis scenario.

An alternative formulation of the proposed Leptogenesis process is given by focusing on the total $B-L$ asymmetry. In this case, from the linearity of the involved Boltzmann equations, it follows [101, 102]

$$\frac{\mathrm{d}\, N_{B-L}}{\mathrm{d}\, z} = \sum_{i=1}^{3} \left[\epsilon_i \, D_i(z) \left(N_{N_i} - N_{N_i}^{eq} \right) \right] - N_{B-L} \sum_{i=1}^{3} W_i^{ID}(z) \tag{3.1.10}$$

and employing eq. (3.1.2) we have

$$N_{B-L}^{f} = N_{B-L}^{preex}(z=0) \, \exp\left[- \sum_{i=1}^{3} \int_{z_{0_i}}^{z} W_i^{ID}(z') \, \mathrm{d}\, z' \right] + \sum_{i=1}^{3} \varepsilon_i \kappa_i^f(K_1, K_2, K_3) \tag{3.1.11}$$

where the efficiency factor κ is here defined as

$$\kappa_i(z; K_1, K_2, K_3) \coloneqq - \int_{z_{0_i}}^{z} \frac{\mathrm{d}\, N_{N_i}}{\mathrm{d}\, z'} \, \exp\left[- \sum_{j=1}^{3} \int_{z'}^{z} W_j^{ID}(z'', K_j) \, \mathrm{d}\, z'' \right] \mathrm{d}\, z' \tag{3.1.12}$$

and implicitly accounts for the washout that lighter neutrinos N_i perform on the $B-L$ asymmetries that heavier neutrinos $N_{j>i}$ generate.

3.1.1 The origin of heavy neutrino flavour effects

The heavy neutrino flavour states designate the quantum states that the dynamics of a heavy neutrino species involves. Consider again, in this regard, the neutrino Yukawa term in the Seesaw Lagrangian:

$$\mathcal{L} \supset - \sum_{\substack{\alpha=e,\mu,\tau \\ i=1,2,3}} h_{\alpha i} \, \overline{\ell_\alpha} P_R \, N_i \, \tilde{\Phi} - \sum_{\substack{\alpha=e,\mu,\tau \\ i=1,2,3}} h_{\alpha i}^{*} \, \tilde{\Phi}^{\dagger} \overline{N_i} P_L \, \ell_\alpha. \tag{3.1.13}$$

Here ℓ_α are the flavour lepton doublets, $\alpha = e, \mu, \tau$, while $\tilde{\Phi}$ has been previously defined in eq. (2.0.8). For the proposed structure, at the tree-level each heavy neutrino couples only to the particular combination of lepton doublets that the corresponding column of the Yukawa coupling matrix states. Then, at one-loop level, according to the diagrams of Figure 2.1 the decay process of N_i receives additional contributions from the other heavy

neutrino species N_j. The flavour compositions of the lepton and antilepton states that the decays of N_i produce can therefore be specified, suggesting the following definitions for the *heavy neutrino flavour states* $|\ell_i\rangle$ and $|\overline{\ell_i}\rangle$:

$$|N_i\rangle \longrightarrow |\ell_i\rangle \coloneqq \sum_{\alpha=e,\mu,\tau} \mathcal{C}_{i\alpha}\,|\ell_\alpha\rangle\,, \qquad \mathcal{C}_{i\alpha} \coloneqq \langle \ell_\alpha|\ell_i\rangle \tag{3.1.14}$$

$$|N_i\rangle \longrightarrow |\overline{\ell_i}\rangle \coloneqq \sum_{\alpha=e,\mu,\tau} \overline{\mathcal{C}}_{i\alpha}\,|\overline{\ell_\alpha}\rangle\,, \qquad \overline{\mathcal{C}}_{i\alpha} \coloneqq \langle \overline{\ell_\alpha}|\overline{\ell_i}\rangle\,. \tag{3.1.15}$$

The heavy neutrino flavour states thus correspond to the coherent superpositions of flavour lepton or antilepton doublets associated to the processes of a specific heavy neutrino N_i. Due to the loop correction of Figure 2.1, in general $\overline{\mathcal{C}}_{i\alpha} \neq \mathcal{C}^*_{i\alpha}$ and therefore the heavy neutrino flavour states associated to a heavy neutrino do not form a CP-conjugated couple: $CP(|\ell_i\rangle) \neq |\overline{\ell_i}\rangle$. The coefficients $\mathcal{C}_{i\alpha}$ and $\overline{\mathcal{C}}_{i\alpha}$, discussed extensively in the Appendix C, correspond to the normalised amplitudes for the processes $|N_i\rangle \longrightarrow |\ell_\alpha\rangle + |\Phi\rangle$ and $|N_i\rangle \longrightarrow |\overline{\ell_\alpha}\rangle + |\overline{\Phi}\rangle$, in a way that

$$\sum_{\alpha=e,\mu,\tau} |\mathcal{C}_{i\alpha}|^2 = 1, \qquad \sum_{\alpha=e,\mu,\tau} |\overline{\mathcal{C}}_{i\alpha}|^2 = 1. \tag{3.1.16}$$

We underline that, barring special situations, the heavy neutrino flavour states do not satisfy any orthogonality condition [98]

$$\langle \ell_i|\ell_j\rangle \neq \delta_{ij}, \qquad i,j = 1,2,3. \tag{3.1.17}$$

The states $|\ell_\alpha\rangle$, appearing in eq. (3.1.14) and (3.1.15), are associated to the usual flavours e, μ and τ and within the present context are referred to as *light flavour states*. Differently form the heavy neutrino flavour states, $|\ell_\alpha\rangle$ and $|\overline{\ell_\alpha}\rangle$ satisfy

$$CP(|\ell_\alpha\rangle) = |\overline{\ell_\alpha}\rangle \tag{3.1.18}$$

and are necessarily orthogonal

$$\langle \ell_\alpha|\ell_\beta\rangle = \langle \overline{\ell_\alpha}|\overline{\ell_\beta}\rangle = \delta_{\alpha\beta}, \qquad \alpha,\beta = e,\mu,\tau. \tag{3.1.19}$$

A handy depiction of heavy neutrino flavour states that we will employ later is obtained by introducing the leptonic (antileptonic) flavour space, spanned by light flavours e,μ,τ ($\overline{e},\overline{\mu},\overline{\tau}$). In this space the heavy neutrinos are associated to *decay directions* i, $i = 1,2,3$, which reflect the flavour compositions of the resulting leptons (antileptons) and that, generally, are therefore neither mutually orthogonal nor parallel – Figure 3.1. The abundances N_{ℓ_i} ($N_{\overline{\ell_i}}$) of the leptons (antileptons) described through the heavy neutrino flavour states can then be represented by arrows along the relative decay directions.

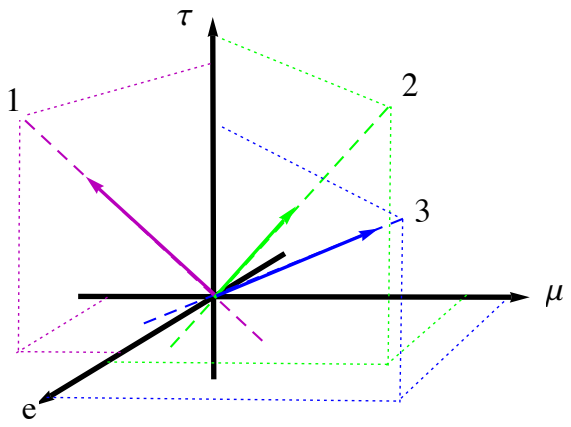

Figure 3.1: A depiction of leptonic light flavour and heavy neutrino flavour states in the flavour space. The former, corresponding to the charged lepton flavours e, μ and τ, are mutually orthogonal and can be chosen as a basis for the flavour space. The latter are instead associated to the directions characterising the flavour compositions of the leptons that the heavy neutrinos N_i, $i = 1, 2, 3$, produce. These heavy neutrino decay directions "i", $i = 1, 2, 3$, generally possess no peculiar mutual alignment. The abundances of the leptons that the heavy neutrino flavour lepton states describe are represented through arrows along the associated decay directions.
A similar depiction holds for the antileptons, in which case the flavour space is spanned by $\overline{e}, \overline{\mu}, \overline{\tau}$ and the directions of the heavy neutrino flavour states refer to the flavour compositions of the produced antileptons.

As remarked before, the heavy neutrino flavour states $|\ell_i\rangle$ and $|\overline{\ell_i}\rangle$, $i = 1, 2, 3$, thus designate the quantum states that the dynamics of the corresponding heavy neutrino N_i involves. In particular, for the resulting heavy neutrino flavour effects, the decays and inverse-decays of a heavy neutrino species therefore only affect leptons and antileptons associated to the relative heavy neutrino flavour states. Nevertheless, as the latter generally are not mutually orthogonal[1], some interplay between the processes and particles associated to different heavy neutrinos is still possible.
Consider for instance the coherent state $|\ell_i\rangle$ ($|\overline{\ell_i}\rangle$), describing the leptons (antileptons) which participate in the processes of N_i. As soon as active, the inverse processes of a different heavy neutrino $N_{j\neq i}$ are fast enough to effectively resolve in the considered state a component which lies along the flavour direction of the N_j decays. This leads to the *decoherence* of $|\ell_i\rangle$ ($|\overline{\ell_i}\rangle$), and the resulting incoherent mixture comprises a state $|\ell_j\rangle$ ($|\overline{\ell_j}\rangle$), involved in the dynamics of N_j, and an orthogonal state $|\ell_{j_i^\perp}\rangle$ ($|\overline{\ell_{j_i^\perp}}\rangle$). The latter, having no projection along the decay direction of N_j, is not involved by the dynamics of this heavy neutrino species. [103, 104]. The described interplay clearly depends on the probabilities p_{ij} for a lepton, or antilepton, on the heavy neutrino decay direction i to

[1]It should be stressed that the quantum corrections leading to non-zero CP asymmetries require at lest two heavy neutrino flavour states be non mutually orthogonal.

be actually measured as the corresponding particle on a heavy neutrino decay direction j. These probabilities are clearly regulated by the overlap of the associated states

$$p_{ij} \coloneqq |\langle \ell_j | \ell_i \rangle|^2 = \left| \sum_\alpha \mathcal{C}^*_{j\alpha} \mathcal{C}_{i\alpha} \right|^2$$
$$\overline{p}_{ij} \coloneqq \left| \langle \overline{\ell}_j | \overline{\ell}_i \rangle \right|^2 = \left| \sum_\alpha \overline{\mathcal{C}}^*_{j\alpha} \overline{\mathcal{C}}_{i\alpha} \right|^2 \tag{3.1.20}$$

and satisfy

$$p_{ij} + p_{ij_i^\perp} = 1, \qquad \overline{p}_{ij} + \overline{p}_{ij_i^\perp} = 1 \tag{3.1.21}$$

for $i, j = 1, 2, 3$. An explicit expression for these quantities, at the tree-level, is then given by

$$p^0_{ij} = \overline{p}^0_{ij} = \frac{\left|(m_D^\dagger m_D)_{ij}\right|^2}{(m_D^\dagger m_D)_{ii}(m_D^\dagger m_D)_{jj}} = \frac{|\sum_k m_h \Omega^*_{ki} \Omega_{kj}|^2}{\tilde{m}_i \tilde{m}_j} \tag{3.1.22}$$

where for the last step we employed the orthogonal parametrization in eq. (2.2.48) and defined $\tilde{m}_i$ as in eq. (2.2.22). As we are going to show now, these probabilities quantify the heavy neutrino flavour effects within Leptogenesis.

3.1.2 Leptogenesis with heavy neutrino flavour effects

We focus here on the modifications that heavy neutrino flavour effects impose on the Leptogenesis process. To this purpose we describe the three stages the latter comprises, disregarding for sake of simplicity the differences in flavour composition between leptons and antileptons associated to the same heavy neutrino species[2]. In this way $\overline{\mathcal{C}}_{i\alpha} = \mathcal{C}^*_{i\alpha}$ and it follows $\overline{p}_{ij} = p_{ij}$. Furthermore, to further simplify our description, we impose a vanishing preexisting asymmetry $N^{preex}_{B-L}(z = 0) = 0$, postponing to Chapter 5 a detailed discussion of this component.

I **$T \sim M_3$: N_3 Leptogenesis.**
The first stage of the Leptogenesis process takes pace for $T \sim M_3$, when the processes involving N_3 are active. The relevant Boltzmann equations are

$$\frac{\mathrm{d}\, N_{N_3}}{\mathrm{d}\, z} = -D_3(z) \left(N_{N_3}(z) - N^{eq}_{N_3}(z) \right) \tag{3.1.23}$$

$$\frac{\mathrm{d}\, N_{\Delta_3}}{\mathrm{d}\, z} = \epsilon_3\, D_3(z) \left(N_{N_3} - N^{eq}_{N_3} \right) - N_{\Delta_3} W^{ID}_3(z) \tag{3.1.24}$$

[2] A more general treatment of heavy neutrino flavour effects which does not impose this simplification is shown in the next Chapter, where we employ a rigorous density matrix formalism to describe Leptogenesis with flavour effects.

and clearly the dynamics of this stage resembles the one previously proposed within N_1 Leptogenesis. Hence, by imposing $N_{\Delta_3}(z=0)=0$ and $N_{N_3}(z=0)=0$ we have

$$N_{B-L}(M_3 > T > M_2) \equiv N^f_{\Delta_3} = \varepsilon_3\, \kappa^f_3(K_3, z_{L3}) \tag{3.1.25}$$

where $z_{L3} = z_L(K_3)$ – cf. eq. (2.2.43). Notice that heavy neutrino flavour effects ascribe the above asymmetry to the disparity between the abundances of particles associated to two specific quantum states: the heavy neutrino flavour lepton states $|\ell_3\rangle$ and antilepton states $|\overline{\ell_3}\rangle$, corresponding to the decay products of N_3.

II **$\mathbf{T \sim M_2}$: $\mathbf{N_2}$ Leptogenesis.**

For the condition imposed on the heavy neutrino mass spectrum by eq. (3.1.1), the evolution of the $B-L$ asymmetry is frozen until the temperature reaches $T \sim M_2$, where the second stage of Leptogenesis is active. The processes involving N_2 are regulated by a system of Boltzmann equations analogous to the one of the previous stage, nevertheless a non-zero initial asymmetry is stored in the quantum states $|\ell_3\rangle$ and $|\overline{\ell_3}\rangle$ as a result of N_3 Leptogenesis. According to our description of the interplay between different heavy neutrino flavour states, consequently to the N_2 inverse-decays $|\ell_3\rangle$ and $|\overline{\ell_3}\rangle$ break down to incoherent mixtures of states $|\ell_2\rangle$, $|\overline{\ell_2}\rangle$ and $|\ell_{2^\perp_3}\rangle$, $|\overline{\ell_{2^\perp_3}}\rangle$ respectively parallel and orthogonal to the decay direction of N_2 – Figure 3.2. The inverse decays of N_2 affect only the leptons and antileptons *measured* along the heavy neutrino decay direction "2", hence only the component of $N^f_{\Delta_3}$ associated to these particles is washed out during the considered processes. The $B-L$ asymmetry arising form the states $|\ell_{2^\perp_3}\rangle$ and $|\overline{\ell_{2^\perp_3}}\rangle$, orthogonal to $|\ell_2\rangle$, is protected from the washout and therefore left unmodified. We refer to this important consequence of the interplay between heavy neutrino flavour states as the *projection effect*.

With clear meaning of the notation, the Boltzmann equations to be solved in the present Leptogenesis stage are

$$\frac{\mathrm{d}\, N_{N_2}}{\mathrm{d}\, z} = -D_2(z)\left(N_{N_2}(z) - N^{eq}_{N_2}(z)\right) \tag{3.1.26}$$

and

$$\frac{\mathrm{d}\, N_{\Delta_2}}{\mathrm{d}\, z} = \varepsilon_2\, D_2(z)\left(N_{N_2} - N^{eq}_{N_2}\right) - N_{\Delta_2} W^{ID}_2(z) \tag{3.1.27}$$

$$\frac{\mathrm{d}\, N_{\Delta_{2^\perp}}}{\mathrm{d}\, z} = 0 \tag{3.1.28}$$

which describe the evolution of the asymmetries respectively due to states along the decay direction of N_2 and the orthogonal ones. The relevant initial conditions follow from eq. (3.1.20) as well as our initial assumptions:

$$\begin{aligned} N_{\Delta_2}(z_{0_2}) &= p_{32}\, N^f_{\Delta_3} \\ N_{\Delta_{2^\perp}}(z_{0_2}) &= (1-p_{32})\, N^f_{\Delta_3} \end{aligned} \tag{3.1.29}$$

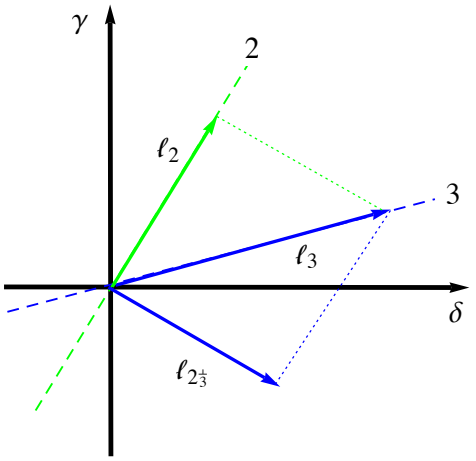

Figure 3.2: A depiction of the decoherence effects resulting from the interplay between heavy neutrino flavour states. Here γ and δ are specific superpositions of light flavours spanning the plane that contains the heavy neutrino decay directions 2 and 3. The washout processes of N_2 break the coherence of the heavy neutrino flavour leptonic states $|\ell_3\rangle$. The resulting incoherent mixture is composed by leptons associated to the state $|\ell_2\rangle$, on the decay direction of N_2, or to $|\ell_{2_3^\perp}\rangle$, orthogonal to the latter. The inverse decays of N_2 clearly affect only the former component.

In this way, at the end of the second Leptogenesis stage we have

$$\begin{aligned} N_{B-L}(M_2 > T > M_1) &= N^f_{\Delta_2} + N^f_{\Delta_{2^\perp}} = \\ &= \varepsilon_2\kappa^f_2 + p_{32}\,\varepsilon_3\kappa^f_3\, e^{-\frac{3\pi}{8}K_2} + (1-p_{32})\varepsilon_3\kappa^f_3. \end{aligned} \tag{3.1.30}$$

III **$\mathbf{T \sim M_1}$: $\mathbf{N_1}$ Leptogenesis.**

The heavy neutrino hierarchy prevents again the evolution of the $B-L$ asymmetry until $T \sim M_1$, where the last stage of the Leptogenesis process begins. The N_1 processes are active and, in analogy to the previous steps, a $B-L$ asymmetry is generated by the out-of-equilibrium decays of these heavy neutrinos along the corresponding decay direction. At the same time the coherence of the leptonic and antileptonic states inherited from the previous Leptogenesis stages is broken by the inverse-decays of N_1. For the projection effect, the consequent washout affects only the preexisting asymmetries arising from leptons and antileptons measured along the decay direction "1". The amount of $B-L$ asymmetry found at the end of the

Leptogenesis process is therefore given by

$$\begin{aligned} N^f_{B-L} &= N^f_{\Delta_1} + N^f_{\Delta_{1^\perp}} = \\ &= \varepsilon_1\kappa_1 + p_{21}\varepsilon_2\,\kappa_2\,e^{-\frac{3\pi}{8}K_1} + p_{21}\,p_{32}\,\varepsilon_3\,\kappa_3\,e^{-\frac{3\pi}{8}(K_2+K_1)} + (1-p_{21})\,\varepsilon_2\kappa_2 + \\ &+ (1-p_{21})\,p_{32}\,\varepsilon_3\,\kappa_3\,e^{-\frac{3\pi}{8}K_2} + p_{2_{\tilde{3}}^\perp 1}\,(1-p_{32})\,\varepsilon_3\,\kappa_3\,e^{-\frac{3\pi}{8}K_1} + \\ &+ (1-p_{2_{\tilde{3}}^\perp 1})\,(1-p_{32})\,\varepsilon_3\,\kappa_3. \end{aligned} \tag{3.1.31}$$

As anticipated, the effect of the interplay between heavy neutrino flavour states is encapsulated in the probabilities previously introduced by eq. (3.1.20). A comparison to the unflavoured calculation reveals that eq. (3.1.9), supporting N_1 Leptogenesis, is recovered only for the special case $p_{ij} = 1$. This implies the total alignment of the three decay directions. For more general configurations, in light of flavour effects, the correct description of the generated $B-L$ asymmetry is provided by eq. (3.1.31). We underline that due to the projection effect parts of the asymmetries generated by the heaviest neutrinos evade the washout performed by N_1. In this sense the heavy neutrino flavour effects show the limitations of N_1 Leptogenesis and require, at the same time, more complete models in which the dynamics of the other heavy neutrinos are considered. We also remark that in the limit of negligible washout, for $K_i \ll 1$, the results of equations (3.1.9) and (3.1.31) coincide again. In this regard, as we will see in the next Section, non-negligible washout processes are a necessary condition for both light flavour and heavy neutrino flavour effects to have an impact on the Leptogenesis process.
Notice furthermore that within every thermal Leptogenesis scenario, a strong washout regime is an essential prerequisite for the heavy neutrino abundance that Leptogenesis requires to be built thermally, independently of its initial value. Consequently, owing to the strong washout regime, the amount of baryon asymmetry that the Leptogenesis process generates is also independent of the value of the initial heavy neutrino abundance. In scenarios of Leptogenesis which propose a weak washout regime, on the contrary, the initial heavy neutrino abundance plays a central role in the determination of the final asymmetry.

3.2 Light flavour effects

Focusing on one heavy neutrino species, we further modify our formalism to address the light flavour effects that originate from the SM charged-lepton Yukawa interactions:

$$\mathcal{L} \supset -\sum_{\alpha=e,\mu,\tau} (D_y)_\alpha\,\overline{\ell_{\alpha L}}\,l_{\alpha R}\,\Phi + \text{ H.c.}. \tag{3.2.1}$$

Assuming a Higgs mass $m_H = 120$ GeV, the reaction rate of the corresponding processes $\ell_{\alpha L} + l_{\alpha R} \longleftrightarrow \Phi$, $\alpha = e, \mu, \tau$, is quantified in [105]

$$\Gamma_\alpha \simeq 5 \times 10^{-3} \, (D_y)^2_\alpha \, T \tag{3.2.2}$$

and due to the presence of the Yukawa couplings $(D_y)_\alpha$ is manifestly flavour sensitive. Notice that for the expression of the Hubble rate H given in eq. (1.2.2), the equilibrium criterion already introduced in Section 2.2.0.3 respects

$$\frac{\Gamma_\alpha}{H} \propto \frac{1}{T}. \tag{3.2.3}$$

Hence, as the temperature in the Universe drops consequently to the ongoing expansion, the Yukawa interactions progressively come into equilibrium. In particular the τ interactions satisfy $\Gamma_\tau > H$ for $T \lesssim 10^{12}$ GeV, while, due to the hierarchy in the relevant couplings, the μ interactions satisfy an analogous equilibrium condition only for $T \lesssim 10^9$ GeV. Finally, the electron Yukawa interactions enter their equilibrium regime when $T \lesssim 10^6$ GeV.

If the charged-lepton Yukawa interactions are in equilibrium and the condition

$$\Gamma_\alpha \gtrsim \sum_i \Gamma_{ID,i}, \qquad \alpha = e, \mu, \tau \tag{3.2.4}$$

is also satisfied [106], the effects of light flavours on the Leptogenesis process cannot be neglected. In fact consequently to eq. (3.2.4) the heavy neutrino flavour lepton states (antilepton states) generated by the decays of N_i interact, on average, first with the RH components of the charged-lepton (antilepton) fields of flavour α and then with a Higgs doublet. The involved charged-lepton Yukawa interactions are therefore fast enough to break the coherence of the heavy neutrino flavour states $|\ell_i\rangle$ ($|\overline{\ell_i}\rangle$) prior to their absorption in inverse-decay processes.

The lepton Yukawa interactions that our model proposes are thus competing in the determination of the relevant quantum states: the neutrino ones support the heavy neutrino flavour states while the charged-lepton Yukawa interactions select the light flavour ones.

In the full decoherence limit, which defines a *fully flavoured regime*, only one kind of lepton Yukawa interaction dominates. Should this be the charged-lepton one, the inverse-decays would then involve the Higgs doublets and an incoherent mixture that comprises the following statistically independent components: the light flavour states $|\ell_\alpha\rangle$ ($|\overline{\ell_\alpha}\rangle$), of definite light flavour α, and any remaining orthogonal state $|\ell_{\alpha_i^\perp}\rangle$ ($|\overline{\ell_{\alpha_i^\perp}}\rangle$) remnant of the original heavy neutrino flavour states. The evolution of these particle species must consequently be tracked individually and the associated $B-L$ asymmetries are therefore regulated by dedicated Boltzmann equations. In this regard, recall that beside $B-L$, the sphaleron transitions also conserve the flavoured quantities $B/3-L_\alpha$. To account for the

effects of light flavours it is therefore convenient to introduce the *flavoured asymmetries* $N_{\Delta_\alpha} \coloneqq N_{B/3-L_\alpha}$, which satisfy

$$N_{B-L} = \sum_{\alpha=e,\mu,\tau} N_{\Delta_\alpha}. \tag{3.2.5}$$

For the hierarchy presented by the charged lepton Yukawa couplings we therefore distinguish between the following fully flavoured regimes and relative flavoured asymmetries:

- **$T \gtrsim 10^{12}$ GeV: heavy neutrino flavour regime**.
  For $T > 10^{12}$ GeV all the Yukawa interactions associated to light flavours are out of equilibrium. The Leptogenesis process is therefore subject only to heavy neutrino flavour effects and the relevant asymmetries are N_{Δ_i} and $N_{\Delta_{i^\perp}}$.

- **10^{12} GeV $\gtrsim T \gtrsim 10^{9}$ GeV: two-flavour regime.**
  In this regime the τ Yukawa interactions are in equilibrium and fast enough to break the quantum coherence of the heavy neutrino flavour states:

  $$\begin{aligned} |\ell_i\rangle &\longrightarrow |\ell_\tau\rangle\,,\ |\ell_{\tau_i^\perp}\rangle \\ |\overline{\ell_i}\rangle &\longrightarrow |\overline{\ell_\tau}\rangle\,,\ |\overline{\ell_{\tau_i^\perp}}\rangle \end{aligned} \tag{3.2.6}$$

  Notice that the states orthogonal to the flavour "τ" are still a coherent superposition of e and μ leptons. The relevant flavoured asymmetries are here N_{Δ_τ} and $N_{\Delta_{\tau_i^\perp}}$.

- **10^{9} GeV $\gtrsim T \gtrsim 10^{6}$ GeV: three-flavour regime.**
  On top of τ reactions also the μ Yukawa interactions satisfy the equilibrium condition. The heavy neutrino flavour states are completely projected on the three light flavours

  $$\begin{aligned} |\ell_i\rangle &\longrightarrow |\ell_\tau\rangle\,,\ |\ell_\mu\rangle\,,\ |\ell_e\rangle \\ |\overline{\ell_i}\rangle &\longrightarrow |\overline{\ell_\tau}\rangle\,,\ |\overline{\ell_\mu}\rangle\,,\ |\overline{\ell_e}\rangle \end{aligned} \tag{3.2.7}$$

  as the electronic component of $|\ell_i\rangle$ ($|\overline{\ell_i}\rangle$) is effectively measured in this regime as a non-τ, non-μ state. The relevant asymmetries are therefore the three N_{Δ_α} already introduced in eq. (3.2.5).

3.2.1 Quantifying the effect

The impact of charged-lepton Yukawa interactions on the Leptogenesis process can be modelled in a set of *flavoured probabilities* [97, 98], defined by

$$p_{i\alpha} \coloneqq |\langle \ell_\alpha | \ell_i \rangle|^2 \tag{3.2.8}$$

$$\overline{p}_{i\alpha} \coloneqq \left|\langle\overline{\ell_\alpha}|\overline{\ell_i}\rangle\right|^2 \tag{3.2.9}$$

where $\alpha = \tau, \tau_i^{\perp}$ or $\alpha = e, \mu, \tau$ depending on the considered fully flavoured regime. In terms of the definitions given for the heavy neutrino flavour states

$$|\ell_i\rangle \coloneqq \sum_{\alpha=e,\mu,\tau} \mathcal{C}_{i\alpha}\,|\ell_\alpha\rangle\,, \qquad\qquad |\overline{\ell_i}\rangle \coloneqq \sum_{\alpha=e,\mu,\tau} \overline{\mathcal{C}}_{i\alpha}\,|\overline{\ell_\alpha}\rangle \tag{3.2.10}$$

the flavoured probabilities are given as

$$p_{i\alpha} = |\mathcal{C}_{i\alpha}|^2\,, \qquad\qquad \overline{p}_{i\alpha} = \left|\overline{\mathcal{C}}_{i\alpha}\right|^2 \tag{3.2.11}$$

and consequently quantify the relative probabilities of observing the reactions $N_i \longrightarrow |\ell_\alpha\rangle + |\Phi\rangle$ and $N_i \longrightarrow |\overline{\ell_\alpha}\rangle + |\overline{\Phi}\rangle$ within a fully flavoured regime. In this regard, considering the flavoured rates $\Gamma_{i\alpha}$ and $\overline{\Gamma}_{i\alpha}$ of eq. (2.2.11) and (2.2.12) and by introducing the heavy neutrinos decay rates

$$\Gamma_i \coloneqq \sum_{\alpha=e,\mu,\tau} \Gamma_{i\alpha} \tag{3.2.12}$$

$$\overline{\Gamma}_i \coloneqq \sum_{\alpha=e,\mu,\tau} \overline{\Gamma}_{i\alpha} \tag{3.2.13}$$

an alternative expression for the flavoured probabilities is in fact given by

$$p_{i\alpha} = \frac{\Gamma_{i\alpha}}{\Gamma_i} \tag{3.2.14}$$

$$\overline{p}_{i\alpha} = \frac{\overline{\Gamma}_{i\alpha}}{\overline{\Gamma}_i}. \tag{3.2.15}$$

Hence, correctly, these quantities satisfy the completeness relations

$$\sum_{\alpha=e,\mu,\tau} p_{i\alpha} = 1 \tag{3.2.16}$$

$$\sum_{\alpha=e,\mu,\tau} \overline{p}_{i\alpha} = 1. \tag{3.2.17}$$

It is useful to introduce the following parameterisation

$$p_{i\alpha} = p^0_{i\alpha} + \delta p_{i\alpha} \tag{3.2.18}$$

$$\overline{p}_{i\alpha} = p^0_{i\alpha} + \delta\overline{p}_{i\alpha} \tag{3.2.19}$$

which isolates the tree-level contribution $p^0_{i\alpha}$ [3] from the one given by the quantum corrections depicted in Figure 2.1. Evaluating the relevant decay rates at the tree-level,

[3] At the tree-level $(\mathcal{C}^0_{i\alpha})^* = \overline{\mathcal{C}}^0_{i\alpha}$ and from eq. (3.2.11) it thus follows $\overline{p}^0_{i\alpha} = p^0_{i\alpha}$.

denoted by the subscript "0", therefore yields

$$p^0_{i\alpha} \equiv \left|\mathcal{C}^0_{i\alpha}\right|^2 = \frac{|h_{\alpha i}|^2}{(h^\dagger h)_{ii}} \tag{3.2.20}$$

or, in terms of the orthogonal matrix Ω of eq. (2.2.48):

$$p^0_{i\alpha} = \frac{\left|\sum_k \sqrt{m_k} U_{\alpha k} \Omega_{\beta i}\right|^2}{\sum_j m_j \left|\Omega_{ji}\right|^2}. \tag{3.2.21}$$

These quantities then also satisfy a completeness relation:

$$\sum_{\alpha=e,\mu,\tau} p^0_{i\alpha} = 1. \tag{3.2.22}$$

Differently form the tree-level contribution, the quantum corrections in $\delta p_{i\alpha}$ and $\delta\overline{p}_{i\alpha}$ are generally different for leptons and antileptons as a consequence of CP-violation. Hence, as already remarked, $\mathcal{C}^*_{i\alpha} \neq \overline{\mathcal{C}}_{i\alpha}$ and the flavour composition of the heavy neutrino flavour lepton states differs from that of the corresponding flavour antilepton states. Within a fully flavoured regime these particles consequently originate two different incoherent mixtures, comprising the relevant light flavour states in different abundances.
From the properties of $p_{i\alpha}$ and $p^0_{i\alpha}$ the quantum correction contributions obey

$$\sum_\alpha \delta p_{i\alpha} = 0, \qquad \sum_\alpha \delta\overline{p}_{i\alpha} = 0 \tag{3.2.23}$$

and, by defining

$$\Delta p_{i\alpha} \coloneqq p_{i\alpha} - \overline{p}_{i\alpha} \tag{3.2.24}$$

it follows

$$\sum_\alpha \Delta p_{i\alpha} = 0. \tag{3.2.25}$$

The importance of these flavour probabilities is exposed by introducing the *flavoured CP-asymmetries*, which measure the asymmetry potentially stored in each light flavour

$$\varepsilon_{i\alpha} \coloneqq -\frac{\Gamma_{i\alpha} - \overline{\Gamma}_{i\alpha}}{\sum_\beta \left[\Gamma_{i\beta} + \overline{\Gamma}_{i\beta}\right]}. \tag{3.2.26}$$

Adopting the definitions proposed we can then decompose $\varepsilon_{i\alpha}$ as follows:

$$\varepsilon_{i\alpha} = \frac{p_{i\alpha} + \overline{p}_{i\alpha}}{2}\varepsilon_i - \frac{\Delta p_{i\alpha}}{2}. \tag{3.2.27}$$

The first term on the RHS represents the averaged flavour branching of the usual unflavoured contribution, quantified by ε_i, that the CP-asymmetry receives from the disparity between the leptonic and antileptonic decay rates of an heavy neutrino. The novelty of the flavoured CP-asymmetries then consists in the second term that the RHS

of eq. (3.2.27) presents. This contribution is in fact a *new source of CP-asymmetry*, driven by the possible differences in the flavour compositions of $|\ell_i\rangle$ and $|\overline{\ell_i}\rangle$ quantified by $\Delta p_{i\alpha}$. Notice that, for eq. (3.2.25), the term we are analysing automatically vanishes when considering the total CP-asymmetry

$$\varepsilon_i = \sum_\alpha \varepsilon_{i\alpha} \tag{3.2.28}$$

and therefore it is a unique feature of the flavoured CP-asymmetries. Furthermore, we also remark that whereas the first term in eq. (3.2.27) is subject to the same bounds and limitations that the total CP-asymmetry ε_i respects, $\Delta p_{i\alpha}$ is not. The relative contribution could then potentially dominate the flavoured asymmetry, yielding significant modifications to the bounds which hold within N_1 Leptogenesis [107].

The new contribution found in the expression for $\varepsilon_{i\alpha}$ is not the only effect that fast charged-lepton Yukawa interactions have on the Leptogenesis process. Consider again, in this regard, the proposed picture of full decoherence that applies to the fully flavoured regimes. The washout processes which take place under this condition involve, as a consequence of decoherence, the flavour states $|\ell_\alpha\rangle$ and $|\overline{\ell_\alpha}\rangle$ rather than the original heavy neutrino flavour states $|\ell_i\rangle$ and $|\overline{\ell_i}\rangle$, $i = 1, 2, 3$. The dynamics affecting the flavoured asymmetries N_{Δ_α} are then independent one of the others and, also, sensitive only to the processes that involve the leptonic and antileptonic states of the corresponding light flavour. In particular, focusing for example on one light flavour generically denoted by "γ", the inverse-decays that can potentially erase the asymmetry N_{Δ_γ} are only those which involve the Higgs doublets and the leptons (antileptons) $|\ell_\gamma\rangle$ ($|\overline{\ell_\gamma}\rangle$). Since the relative abundance of the latter is suppressed by a factor $p_{i\gamma}$ ($\overline{p}_{i\gamma}$), with respect to the unflavoured case, it follows that the rate of the washout process acting on N_{Δ_γ} is also *reduced* by the same factor with respect to W_i^{ID}.

3.2.1.1 The flavoured Boltzmann equations

In light of the twofold effect that the charged-lepton Yukawa interactions have on the Leptogenesis process, we modify our Boltzmann equations to provide a description valid within the fully flavoured regimes which involve light flavours. The relations we seek must track the evolution of the flavoured asymmetries N_{Δ_α} and account for the reduction of the relevant washout rate that $p_{i\alpha}$ regulates. On top of that, the contribution of $\Delta p_{i\alpha}$ to the CP-asymmetry is also to be included.
Within the SM, beside $B - L$, also the quantities $B/3 - L_\alpha$ are not-anomalous. Consequently, the amount of N_{Δ_α} asymmetry present in the Universe at the end of the Leptogenesis process is solely determined by the latter. The relevant Boltzmann equations are then written by considering the evolution of leptonic and antileptonic states of definite light flavour, subtracting consecutively the Boltzmann equation regulating the

baryon number suitably weighted by the factor 1/3. In this way the effects due to the sphaleron process cancel out and focusing on one heavy neutrino species we have [97,98]

$$\frac{\mathrm{d}\, N_{N_i}}{\mathrm{d}\, z_i} = -D_i(z_i)\left(N_{N_i}(z_i) - N_{N_i}^{eq}(z_i)\right), \qquad i = 1,2,3 \tag{3.2.29}$$

and

$$\frac{\mathrm{d}\, N_{\Delta_\alpha}}{\mathrm{d}\, z} = \varepsilon_{i\alpha}\, D_i(z_i)\left(N_{N_i}(z_i) - N_{N_i}^{eq}(z_i)\right) - p^0_{i\alpha}\, W_i^{ID}(z)\,(N_{\ell_\alpha} + N_\Phi) \tag{3.2.30}$$

where $\alpha = \tau, \tau_i^\perp$ or e, μ, τ[4].
The structure of the above equation indeed resembles that of eq. (3.1.5). The possible differences in the flavour compositions of the involved states are addressed by the flavoured CP-asymmetries

$$\varepsilon_{i\alpha} \coloneqq \frac{3}{16\,\pi\,(h^\dagger h)_{ii}} \sum_{j\neq i} \left\{ \mathrm{Im}[h^*_{\alpha i} h_{\alpha j} (h^\dagger h)_{ij}] \frac{\xi(x_j/x_i)}{\sqrt{x_j/x_i}} + \frac{2}{3(x_j/x_i - 1)} \mathrm{Im}[h^*_{\alpha i} h_{\alpha j} (h^\dagger h)_{ji}] \right\} \tag{3.2.31}$$

where, as usual, $x_i \coloneqq M_i^2/M_1^2$ and

$$\xi(x) := \frac{2}{3} x \left[(1+x) \ln\left(\frac{1+x}{x}\right) - \frac{2-x}{1-x} \right]. \tag{3.2.32}$$

Equation (3.2.30) also accounts for the desired reduction of the washout rate. In this regard, notice that $\delta p_{i\alpha}$, $\delta \overline{p}_{i\alpha} \propto \varepsilon_{i\alpha} \sim \mathcal{O}(N_{\Delta_\alpha})$ – cf. eq. (3.2.27) – hence, neglecting terms of order $\mathcal{O}((N_{\Delta_\alpha})^2)$, we approximated $p_{i\alpha}, \overline{p}_{i\alpha} \simeq p^0_{i\alpha}$ in the washout term. Some care is however still required, as the latter is currently formulated in terms of the lepton and Higgs asymmetries N_ℓ and N_Φ.

To disentangle the washout term we introduce the *flavour coupling matrices* [97,98,103,108] C^ℓ and C^Φ which satisfy

$$N_{\ell_\alpha} = (\mathrm{C}^\ell)_{\alpha\beta}\, N_{\Delta_\beta}, \qquad N_\Phi = (\mathrm{C}^\Phi)_\beta\, N_{\Delta_\beta} \tag{3.2.33}$$

and determine the relative entries through a procedure similar to the one proposed in Section 2.2.0.1. We need in fact to identify the connections between the asymmetries stored in the different species, hence we consider again the network that the reactions active in the early Universe form. For $T > T_{EW}$ the active processes comprise

- Lepton Yukawa interactions:

$$\mu_{\ell_{\alpha L}} - \mu_\Phi - \mu_{l_{\alpha R}} = 0, \qquad \alpha = e, \mu, \tau.$$

[4] In cases where more heavy neutrinos participate to the Leptogenesis process within the same fully flavoured regime, eq. (3.2.30) is generalised by summing over the involved species.

- Quark down-type Yukawa interactions:

$$\mu_{Q_{iL}} - \mu_{\Phi} - \mu_{d_{iR}} = 0, \qquad i = 1, 2, 3.$$

- Quark up-type Yukawa interactions:

$$\mu_{Q_{iL}} + \mu_{\Phi} - \mu_{u_{iR}} = 0, \qquad i = 1, 2, 3.$$

Here $\mu_{\ell_{\alpha L}}$ and $\mu_{Q_{iL}}$ respectively indicate the chemical potentials associated to each component of the lepton and quark $SU(2)_L$ doublets. On top of these reactions we have

- Hypercharge neutrality:

$$\sum_{i=1}^{3} [\mu_{Q_{iL}} + 2\mu_{u_{iR}} - \mu_{d_{iR}}] - \sum_{\alpha=e,\mu,\tau} [\mu_{\ell_{\alpha L}} + \mu_{l_{\alpha R}}] + 2\mu_{\Phi} = 0$$

- QCD and EW sphaleron processes:

$$\sum_{i=1}^{3} [2\mu_{Q_{iL}} - \mu_{u_{iR}} - \mu_{d_{iR}}] = 0$$

$$\sum_{x} [2\mu_{Q_{xL}} - \mu_{\ell_{xL}}] = 0.$$

  Notice that the EW sphaleron processes populate the SM generations equally, effectively levelling the baryon asymmetries associated to different generations: $B_i = B_j$, $i \neq j$.

Through the relations imposed by the Yukawa interactions, as far as the equilibrium condition is maintained, the asymmetry that Leptogenesis stores in the LH doublets is partially transferred to the relative RH counterparts, to the Higgs doublets and to the quarks through the latter. Nevertheless, in the fully flavoured regimes we aim to describe, not all of the above Yukawa interactions are actually in equilibrium. Within a three-flavour regime, in fact, the rates of electron, down and up-quark reactions do not respect the condition $\Gamma_x > H$. Furthermore, in the temperature range interested by the two-flavour regime, also the μ and strange interactions are out of equilibrium. The associated chemical potentials therefore no longer respect the relations that these Yukawa interactions imply, and the latter are then replaced by the following conditions:

- *leptons:* $\mu_{l_{\alpha R}} = 0$, if $\Gamma_\alpha < H$.
- *quarks:* $\mu_{d_{iR}} = \mu_{d_{jR}} = \mu_{u_{iR}} = \mu_{u_{jR}}$, if $\Gamma_i, \Gamma_j < H$.

When equilibrium is lost the asymmetry stored in the lepton RH singlets simply vanishes. The different treatment reserved for quarks is due to the QCD sphaleron processes,

which still allow the transfer of some asymmetry form the $SU(2)_L$ doublets to the RH counterparts. As QCD sphalerons create an equal number of singlets in each SM generation, the given condition is implied.
Introducing now the matrix $\mathrm{C} \coloneqq \mathrm{C}^{\ell} + \mathrm{C}^{\Phi}$, by solving for constraints the presented reaction network leads to the following expressions, holding respectively for a three-flavour and a two-flavour regime[5]

$$\mathrm{C}^{(3)} = \begin{pmatrix} -151/358 & 10/179 & 10/179 \\ 25/716 & -172/537 & -7/537 \\ 25/716 & -7/537 & -172/537 \end{pmatrix} \tag{3.2.34}$$

$$\mathrm{C}^{(2)} = \begin{pmatrix} -417/1178 & 60/589 \\ 15/589 & -195/589 \end{pmatrix}. \tag{3.2.35}$$

In deriving the matrix for the two-flavour regime we summed over the rows corresponding to $N_{\Delta e}$ and N_{Δ_μ}, consequenlty averaging of the columns associated to N_{ℓ_e} and N_{ℓ_μ}.

Given the above expressions for the C matrix and eq. (3.2.30), we could in principle calculate the flavoured asymmetries N_{Δ_α}. For the hierarchy that the entries of these matrices present, it is however usual to approximate $\mathrm{C} \simeq \mathrm{I}$ and consequently simplify the Boltzmann equations. We shell respect this tradition and describe the evolution of the flavoured asymmetries through

$$\frac{\mathrm{d}\, N_{N_i}}{\mathrm{d}\, z_i} = -D_i(z_i) \left(N_{N_i}(z_i) - N^{eq}_{N_i}(z_i) \right), \qquad i = 1, 2, 3 \tag{3.2.36}$$

and

$$\frac{\mathrm{d}\, N_{\Delta_\alpha}}{\mathrm{d}\, z} = \varepsilon_{i\alpha}\, D_i(z_i) \left(N_{N_i}(z_i) - N^{eq}_{N_i}(z_i) \right) - p^0_{i\alpha}\, W^{ID}_i(z) N_{\Delta_\alpha}. \tag{3.2.37}$$

The corresponding solution is then written as

$$N_{\Delta_\alpha}(z) = \varepsilon_{i\alpha} \kappa_i(z; K_i, p^0_{i\alpha}) + N_{\Delta_\alpha}(z_{0_i})\, e^{-p^0_{i\alpha} \int\limits_{z_{0_i}}^{z} W^{ID}_i(z')\, \mathrm{d}\, z'} \tag{3.2.38}$$

where the flavoured CP-asymmetries are given as in eq. (3.2.31) and the efficiency factor is defined by

$$\kappa_i(z; K_1, p^0_{i\alpha}) \coloneqq - \int\limits_{z_{0_i}}^{z} \frac{\mathrm{d}\, N_{N_i}}{\mathrm{d}\, z'}\, e^{-p^0_{i\alpha} \int\limits_{z'}^{z} W^{ID}_i(z'')\, \mathrm{d}\, z''}\, \mathrm{d}\, z'. \tag{3.2.39}$$

Once again we disregard the impact of any preexisting asymmetry by imposing $N_{\Delta_\alpha}(z_{0_i}) = 0$. Neglecting the effects due to other heavy neutrino species then yields

$$N^f_{\Delta_\alpha} \coloneqq N_{\Delta_\alpha}(z = \infty) = \varepsilon_{i\alpha} \kappa^f_i(K_i, p^0_{i\alpha}) \tag{3.2.40}$$

[5] As in [97], our abundances have been normalised to one degree of freedom.

with the final value of the efficiency factor comprising two contributions [109]

$$\kappa_i^f(K_i, p^0_{i\alpha}) = \kappa_i(z=\infty; K_i, p^0_{i\alpha}) = \kappa_i^{f-}(K_i, p^0_{i\alpha}) + \kappa_i^{f+}(K_i, p^0_{i\alpha}) \tag{3.2.41}$$

which generalise the counterparts of N_1 Leptogenesis – eq. (2.2.45):

$$\kappa_i^{f-}(K_i, p^0_{i\alpha}) = -\frac{2}{p^0_{i\alpha}} e^{-\frac{3\pi}{8}K_{i\alpha}} \left(e^{\frac{p^0_{i\alpha}}{2}\bar{N}(K_i)} - 1 \right) \tag{3.2.42}$$

$$\kappa_i^{f+}(K_i, p^0_{i\alpha}) = \frac{2}{z_L(K_{i\alpha})K_{i\alpha}} \left(1 - e^{-\frac{1}{2}z_L(K_{i\alpha})K_{i\alpha}\bar{N}(K_1)} \right). \tag{3.2.43}$$

In the present context we also introduced the *flavoured decay parameters*

$$K_{i\alpha} \coloneqq p^0_{i\alpha} K_i = \frac{v^2}{M_i}\frac{|h_{i\alpha}|^2}{m_\star} = \left| \sum_j \sqrt{\frac{m_j}{m_\star}} U_{\alpha j} \Omega_{ji} \right|^2 \tag{3.2.44}$$

while z_L and $\bar{N}$ are respectively given by eq. (2.2.43) and eq. (2.2.38). Notice that the latter still depends on the unflavoured decay parameter K_1: the heavy neutrino production is not affected by the light flavour effects.
For the orthogonality of the involved light flavours, $\alpha = \tau, \tau_i^\perp$ or $\alpha = e, \mu, \tau$, the total $B-L$ asymmetry that is produced within a fully flavoured regime is then given by

$$N^f_{B-L} = \sum_\alpha N^f_{\Delta_\alpha} \tag{3.2.45}$$

and finally the corresponding amount of BAU generated follows, as usual, from eq. (2.2.31):

$$\eta_B = 0.96 \times 10^{-2}\, N^f_{B-L}. \tag{3.2.46}$$

To conclude the Chapter we present now a detailed calculation of the final $B-L$ asymmetry within a two-flavour regime. This exercise has the purpose of illustrating the light flavour effects which are hidden in the above formalism. Starting with the relevant equations

$$\frac{\mathrm{d}\, N_{N_i}}{\mathrm{d}\, z_i} = -D_i(z_i)\left(N_{N_i}(z_i) - N^{eq}_{N_i}(z_i) \right), \qquad i = 1,2,3 \tag{3.2.47}$$

and

$$\frac{\mathrm{d}\, N_{\Delta_\tau}}{\mathrm{d}\, z_i} = \varepsilon_{i\tau}\, D_i(z_i)\left(N_{N_i}(z_i) - N^{eq}_{N_i}(z_i) \right) - p^0_{i\tau}\, W_i^{ID}(z_i) N_{\Delta\tau} \tag{3.2.48}$$

$$\frac{\mathrm{d}\, N_{\Delta_{\tau_i^\perp}}}{\mathrm{d}\, z_i} = \varepsilon_{i\tau_i^\perp}\, D_i(z_i)\left(N_{N_i}(z_i) - N^{eq}_{N_i}(z_i) \right) - p^0_{i\tau_i^\perp}\, W_i^{ID}(z_i) N_{\Delta\tau_i^\perp} \tag{3.2.49}$$

we disregard again possible preexisting asymmetries and, for the relations (3.2.38) to (3.2.45), the solution we seek therefore is

$$N^f_{B-L} = \varepsilon_{i\tau}\kappa^f_i(K_i, p^0_{i\tau}) + \varepsilon_{i\tau_i^\perp}\kappa^f_i(K_i, p^0_{i\tau_i^\perp}). \tag{3.2.50}$$

The light flavour effects are then disclosed by employing the parametrization of the flavoured CP-asymmetries proposed in eq. (3.2.27). Approximating $(p_{i\alpha} + \overline{p}_{i\alpha})/2 \simeq p^0_{i\alpha}$ and considering that $\Delta p_{i\tau} = -\Delta p_{i\tau_i^\perp}$ it follows

$$N^f_{B-L} = \sum_{\alpha=\tau,\tau_i^\perp} \left[p^0_{i\alpha}\, \varepsilon_i\, \kappa_i(K_i, p^0_{i\alpha})\right] - \frac{\Delta p_{i\tau}}{2}\left[\kappa(K_i, p^0_{i\tau}) - \kappa(K_i, p^0_{i\tau_i^\perp})\right] \tag{3.2.51}$$

and some remarks are to be given:

- For the definitions given in eq.s (3.2.42) and (3.2.43), the final expressions of the flavoured efficiency parameters satisfy the relation

$$\kappa^f_i(K_i, p^0_{i\alpha}) \simeq \frac{1}{p^0_{i\alpha}} \kappa^f_i(K_i) \tag{3.2.52}$$

  where $\kappa^f_i(K_i)$ was first introduced in eq. (3.1.7). The first term on the RHS of eq. (3.2.51) then reads

$$\sum_{\alpha=\tau,\tau_i^\perp} \left[p^0_{i\alpha}\, \varepsilon_i\, \kappa_i(K_i, p^0_{i\alpha})\right] \simeq 2\varepsilon_i\, \kappa_i(K_i) \tag{3.2.53}$$

  leading to an enhancement of a factor 2 with respect to the unflavoured calculation. In general, the light flavour effects thus amplify the $B-L$ asymmetry production by a factor equal to the number of light flavours interested by the considered regime.

- If the condition $p^0_{i\tau} \neq p^0_{i\tau_i^\perp}$ is satisfied, the different flavour composition of the involved heavy neutrino lepton and antilepton states yields an additional contribution to the final $B-L$ asymmetry. As we underlined before, the terms $\Delta p_{i\alpha}$ are not subject to the bounds that ε_i respects. In the general case we consequently expect large flavour effects arise if the following condition are both satisfied:

  I the heavy neutrino flavour lepton and antilepton states originating the incoherent mixtures comprising the light flavour states have different flavour compositions: $\delta_{i\alpha} \neq \overline{\delta}_{i\alpha} \neq 0$

  II the washout process is asymmetric: the washout rates for the involved flavoured asymmetries must be different. As we will see in Chapter 6 for a specific model, this condition is verified in large regions of the Seesaw parameter space.

- Likewise heavy neutrino flavour effects, also the light flavour effects require a non negligible washout to have an impact on the Leptogenesis process. In the weak washout regime, $K_{i\tau}, K_{i\tau_i^\perp} \ll 1$, eq. (3.2.51) recovers in fact the unflavoured expression for the final asymmetry.

- In schemes where more than one heavy neutrino species are involved, the asymmetric washout proposed by a flavoured treatment of Leptogenesis and the condition (3.2.22) imply that part of the asymmetry created by the heaviest neutrinos could survive the washout processes performed by the lighter, at least for particular configurations [98, 99]. In this sense the light flavour effects therefore provide a further reason to move beyond the N_1 Leptogenesis scenario.

Chapter 4

Light and heavy neutrino flavour effects in a density matrix approach

The description of the heavy neutrino dynamics we considered so far relies on the Boltzmann equations. In most cases this classical picture is sufficient for the calculation of the final asymmetry [89, 91, 94, 95, 102, 103, 110, 111]. Yet, when the flavour effects are taken into account [94, 98, 112], the different sets of Boltzmann equations described in the previous Chapter are to be employed depending on whether the asymmetry is generated in the heavy-flavour, two-flavour or in the three-flavour regime. These specialised Boltzmann equations still provide a good description of the $B - L$ asymmetry in the above *classical regimes*, where the decoherence of the involved quantum states can be interpreted as an instantaneous collapse of the relative wave functions due to a measurement process. On the contrary, in the transition regimes characterised by $M_i \sim 10^9\,\mathrm{GeV}$ or $M_i \sim 10^{12}\,\mathrm{GeV}$ where the dynamics of the decoherence process is actually relevant, the Boltzmann equations fail in reproducing the correct results.

The importance of an alternative description covering these last cases could indeed be questioned. In this regard, consider that when light flavour effects and heavy neutrino flavour effects are both taken into account, a reliable calculation of the final asymmetry cannot neglect the contributions of the heaviest neutrino species [103, 113]. The classical regimes mentioned above consequently define a large number of possible heavy neutrino mass patterns in an implicit way [2] – Figure 4.1 – and the requirement that all the neutrino masses do not fall within a transition regime clearly becomes quite restrictive. Furthermore, consider that each of the proposed mass patterns involves different sets of Boltzmann equations, hence the need for a more general formalism is also clearly evident.

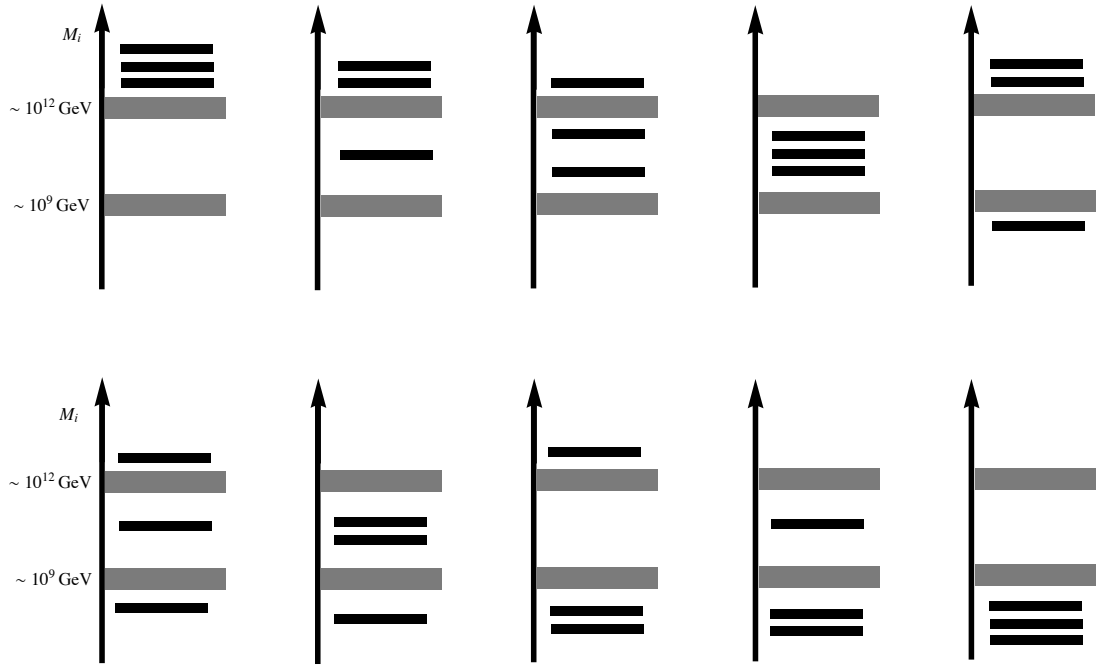

Figure 4.1: The possible mass pattern that the fully-flavoured regimes define for three heavy neutrino species. The grey areas for $M_i \simeq 10^9$ GeV and $M_i \simeq 10^{12}$ GeV denote the transition regimes.

The natural choice in tackling these problems is to employ density matrix methods and in this Chapter we therefore aim to generalise the density matrix treatment already proposed within N_1 Leptogenesis [103, 112, 114]. In particular, we intend to account for the heavy neutrino flavour effects and multiple neutrino species in the calculation of the final asymmetry, which should now hold for an arbitrary choice of the mass pattern. Beside that, in light of this improved formalism, we also intend to verify the results that we previously obtained within the simple description that an instantaneous quantum-collapse proposes. We will then focus on the projection effect that plays a main role in the next Chapter, addressing also the elusive phantom terms which we introduce below.

4.1 N_1 Leptogenesis revisited and phantom terms

We begin by recalling the basic steps behind the derivation of the Boltzmann equation that regulates the $B - L$ asymmetry within N_1 Leptogenesis. Considering that the sphaleron processes conserve this quantity, we can write

$$\frac{\mathrm{d}\, N_{B-L}}{\mathrm{d}\, z} = \frac{\mathrm{d}\, N_{\overline{\ell_1}}}{\mathrm{d}\, z} - \frac{\mathrm{d}\, N_{\ell_1}}{\mathrm{d}\, z} \tag{4.1.1}$$

where the variation rates of the lepton and antilepton abundances are given by the difference between the production rate, due to the heavy neutrino decays, and the depletion rate driven by the inverse decays. Neglecting the reprocessing action of sphalerons, which eventually cancels out in the equation for $B-L$, we therefore have

$$\frac{\mathrm{d}\, N_{\ell_1}}{\mathrm{d}\, z} = \frac{\Gamma_1}{H\, z}\, N_{N_1} - \frac{\Gamma_{ID,1}}{H\, z}\, N_{\ell_1} \tag{4.1.2}$$

while for the antileptons it is

$$\frac{\mathrm{d}\, N_{\overline{\ell_1}}}{\mathrm{d}\, z} = \frac{\overline{\Gamma}_1}{H\, z}\, N_{N_1} - \frac{\overline{\Gamma}_{ID,1}}{H\, z}\, N_{\overline{\ell_1}}. \tag{4.1.3}$$

As showed in Section 2.2.1, the inverse-decay rate is related to the decay rate through

$$\Gamma_{ID,1} = \Gamma_1\, \frac{N^{eq}_{N_1}}{N^{eq}_{\ell_1}}, \qquad\qquad \overline{\Gamma}_{ID,1} = \overline{\Gamma}_1\, \frac{N^{eq}_{N_1}}{N^{eq}_{\overline{\ell}_1}} \tag{4.1.4}$$

where $N^{eq}_{\ell_1} = N^{eq}_{\overline{\ell_1}} = 1$ quantify the number of leptons ℓ_1 and antileptons $\overline{\ell_1}$ at the thermal equilibrium for a vanishing $B-L$ asymmetry. These quantities can respectively be recast as

$$N_{\ell_1} \;=\; \frac{1}{2}\left(N_{\ell_1} + N_{\overline{\ell_1}}\right) + \frac{1}{2}\left(N_{\ell_1} - N_{\overline{\ell_1}}\right) = N^{eq}_{\ell_1} - \frac{1}{2}\, N_{B-L} + \mathcal{O}(N^2_{B-L}) \tag{4.1.5}$$

and

$$N_{\overline{\ell_1}} \;=\; \frac{1}{2}\left(N_{\ell_1} + N_{\overline{\ell_1}}\right) - \frac{1}{2}\left(N_{\ell_1} - N_{\overline{\ell_1}}\right) = N^{eq}_{\ell_1} + \frac{1}{2}\, N_{B-L} + \mathcal{O}(N^2_{B-L}) \tag{4.1.6}$$

hence, by inserting the above relations into eq. (4.1.1), we obtain the familiar equation governing the $B-L$ asymmetry already introduced in Section 2.2.1:

$$\frac{\mathrm{d}\, N_{B-L}}{\mathrm{d}\, z} = \epsilon_1\, D_1(z)\left(N_{N_1} - N^{eq}_{N_1}\right) - N_{B-L}\, W_1(z). \tag{4.1.7}$$

Notice that in writing our final result we neglected terms of order $\mathcal{O}(N^2_{B-L})$ and we defined, as usual,

$$D_1(z) \coloneqq \frac{\Gamma_{D,1}(T)}{H\, z} = K_1\, z \left\langle \frac{\mathcal{K}_1(z)}{\mathcal{K}_2(z)} \right\rangle \tag{4.1.8}$$

and

$$W_1(z) \simeq W_1^{ID}(z) \coloneqq \frac{1}{2}\frac{\Gamma_{ID,1}(z)}{H(z) z} = \frac{1}{4} K_1\, \mathcal{K}_1(z) z^3. \tag{4.1.9}$$

On top of reproducing the above results, the formalism we seek must be able to generalise our description of the Leptogenesis process by addressing the asymmetry evolution in the intermediate regimes. Here the lepton quantum states are interacting with the thermal bath via the charged-lepton Yukawa interactions, but the latter are not efficient enough for the instantaneous collapse approximation to hold. In this cases the ensemble of

lepton and antilepton quantum states is neither to be described in terms of pure states, nor as an incoherent mixture and clearly the classical description encapsulated in the Boltzmann equations cannot be employed. As remarked before, during the Leptogenesis process the neutrino and the charged-lepton Yukawa interactions compete with each other in determining the average properties of the quantum states, but in these transition regimes the outcome is actually a draw. Consequently, a complete description of the system cannot regard the involved leptons and antileptons as decoupled from the thermal bath and the density matrix formalism results particularly appropriate [115]. Such a formulation allows in fact the description of the lepton-antilepton subsystem in a separate way, neglecting back-reaction effects and encoding the coupling with the thermal bath in the evolution of the off-diagonal terms in the lepton and antilepton density matrices [103, 112, 114].

Attracted by these features, we derive now a density matrix equation that reproduces eq. (4.1.6) when the charged-lepton Yukawa interactions are negligible. To this purpose we consider the heavy neutrino flavour states [1]

$$|\ell_1\rangle = \mathcal{C}_{1\tau}\,|\ell_\tau\rangle + \mathcal{C}_{1\tau_1^\perp}\,|\ell_{\tau_1^\perp}\rangle\,, \qquad \mathcal{C}_{1\alpha} \coloneqq \langle \ell_\alpha|\ell_1\rangle \tag{4.1.10}$$

$$CP\,|\overline{\ell_1}\rangle = \overline{\mathcal{C}}_{1\tau}\,|\ell_\tau\rangle + \overline{\mathcal{C}}_{1\tau_1^\perp}\,|\ell_{\tau_1^\perp}\rangle\,, \qquad \overline{\mathcal{C}}_{1\alpha} \coloneqq \langle \ell_\alpha|\,(CP\,|\overline{\ell_1}\rangle) \tag{4.1.11}$$

defined with respect to the flavours $\alpha = \tau, \tau_1^\perp$.
We remark that the notation adopted in this Chapter is slightly different from the one presented in the rest of the Thesis. The rescaled amplitudes $\overline{\mathcal{C}}_{i\alpha}$ quantify here the flavour composition of the *lepton state* $CP\,|\overline{\ell_1}\rangle$, obtained through the CP-conjugation of the state $|\overline{\ell_1}\rangle$ that the N_1 decays identify. With respect to the quantities introduced in the previous Chapter and discussed in Appendix C, the $\overline{\mathcal{C}}_{i\alpha}$ present an extra complex-conjugation. Hence, for example, the one-loop contributions of Figure 2.1 imply here $\overline{\mathcal{C}}_{i\alpha} \neq \mathcal{C}_{i\alpha}$, underlining as usual the different flavour compositions of the above states.
In order to define a complete basis on which we can specify our density matrix, we introduce now the states $|\ell_{1^\perp}\rangle$ and $CP\,|\overline{\ell_{1^\perp}}\rangle$, respectively orthogonal to $|\ell_1\rangle$ and $CP\,|\overline{\ell_1}\rangle$:

$$|\ell_{1^\perp}\rangle = -\mathcal{C}^*_{1\tau_1^\perp}\,|\ell_\tau\rangle + \mathcal{C}^*_{1\tau}\,|\ell_{\tau_1^\perp}\rangle \tag{4.1.12}$$

$$CP\,|\overline{\ell_{1^\perp}}\rangle = -\overline{\mathcal{C}}^*_{1\tau_1^\perp}\,|\ell_\tau\rangle + \overline{\mathcal{C}}^*_{1\tau}\,|\ell_{\tau_1^\perp}\rangle\,. \tag{4.1.13}$$

In the bases $1, 1^\perp$ and $CP(1, 1^\perp)$ the lepton and antilepton density matrices are therefore given by

$$\rho^\ell_{ij} = |\ell_1\rangle\,\langle\ell_1| \equiv \begin{pmatrix} 1 & 0 \\ 0 & 0 \end{pmatrix}, \qquad \rho^{\overline{\ell}}_{ij} = CP\,|\overline{\ell_1}\rangle\,\langle\overline{\ell_1}|\,CP \equiv \begin{pmatrix} 1 & 0 \\ 0 & 0 \end{pmatrix} \tag{4.1.14}$$

Here we are implicitly disregarding the presence of leptons and antileptons which are not produced by the N_1 decays, assuming furthermore that the latter thermalised through the Yukawa interactions only. These assumptions clearly hold only in the heavy neutrino flavour regime, where $M_1 > 10^{12}$ GeV, provided that the considered Yukawa interactions are efficient and in absence of other thermalisation mechanisms. For the moment we will maintain this approximation, promising to discuss in a second time the important role that gauge interactions play in this framework.
By introducing now the density matrices which quantify the lepton and antilepton abundances respectively as

$$N^{\ell}_{ij} \equiv N_{\ell_1}\, \rho^{\ell}_{ij} \tag{4.1.15}$$

and

$$N^{\overline{\ell}}_{ij} \equiv N_{\overline{\ell}_1}\, \rho^{\overline{\ell}}_{ij} \tag{4.1.16}$$

for $T \sim T_{L1}$ we have

$$\frac{\mathrm{d}\, N^{\ell}_{ij}}{\mathrm{d}\, z} = \left(\frac{\Gamma_1}{H\, z}\, N_{N_1} - \frac{\Gamma_{ID,1}}{H\, z}\, N_{\ell_1}\right) \rho^{\ell}_{ij}, \qquad \frac{\mathrm{d}\, N^{\overline{\ell}}_{ij}}{\mathrm{d}\, z} = \left(\frac{\overline{\Gamma}_1}{H\, z}\, N_{N_1} - \frac{\overline{\Gamma}_{ID,1}}{H\, z}\, N_{\overline{\ell}_1}\right) \rho^{\overline{\ell}}_{ij}. \tag{4.1.17}$$

In order to obtain an equation for the total $B-L$ asymmetry matrix, $N_{B-L} \coloneqq N^{\overline{\ell}} - N^{\ell}$, these equations must be written in the same flavour basis so that their difference can be performed. In this regard, we choose for convenience the basis $\tau, \tau_1^{\perp}$ and define the rotation matrices

$$R^{(1)}_{i\alpha} = \begin{pmatrix} \mathcal{C}^{*}_{1\tau} & \mathcal{C}^{*}_{1\tau_1^{\perp}} \\ -\mathcal{C}_{1\tau_1^{\perp}} & \mathcal{C}_{1\tau} \end{pmatrix}, \qquad \overline{R}^{(1)}_{i\alpha} = \begin{pmatrix} \overline{\mathcal{C}}^{*}_{1\tau} & \overline{\mathcal{C}}^{*}_{1\tau_1^{\perp}} \\ -\overline{\mathcal{C}}_{1\tau_1^{\perp}} & \overline{\mathcal{C}}_{1\tau} \end{pmatrix} \tag{4.1.18}$$

acting respectively on the leptons and on the CP-conjugated states of the original antileptons. For example, the representations of the state $|\ell_1\rangle$ therefore satisfy

$$\begin{pmatrix} 1 \\ 0 \end{pmatrix} = R \begin{pmatrix} \mathcal{C}_{1\tau} \\ \mathcal{C}_{1\tau_1^{\perp}} \end{pmatrix}. \tag{4.1.19}$$

For the adopted notation, the superscript enclosed in round brackets indicates the heavy neutrino decay direction index for a matrix. Since we are dealing with leptons and the CP-conjugated of antilepton states, we also employ the same flavour labels to distinguish between the entries of the matrices associated to both these species. We nevertheless emphasise that due to the different flavour compositions of the states involved *the two rotation matrices generally do not coincide* and, in particular, N^{ℓ}_{ij} and $N^{\overline{\ell}}_{ij}$ are diagonal on different bases.
A common expression for the rotation matrices, in fact, can only be given by neglecting the one-loop contributions in the heavy neutrino decay process. At the tree-level we

consequently have

$$R^{0(1)}_{i\alpha} = \begin{pmatrix} \mathcal{C}^{0*}_{1\tau} & \mathcal{C}^{0*}_{1\tau_1^\perp} \\ -\mathcal{C}^{0}_{1\tau_1^\perp} & \mathcal{C}^{0}_{1\tau} \end{pmatrix} \equiv \overline{R}^{0(1)}_{i\alpha}. \tag{4.1.20}$$

In the charged-lepton flavour basis, the equation for the $B-L$ asymmetry matrix consequently reads

$$\frac{\mathrm{d}\, N^{B-L}_{\alpha\beta}}{\mathrm{d}\, z} = \left(\overline{R}^{(1)\dagger}\right)_{\alpha i} \frac{\mathrm{d}\, N^{\overline{\ell}}_{ij}}{\mathrm{d}\, z}\, \overline{R}^{(1)}_{j\beta} - (R^{(1)\,\dagger})_{\alpha i} \frac{\mathrm{d}\, N^{\ell}_{ij}}{\mathrm{d}\, z}\, R^{(1)}_{j\beta} \tag{4.1.21}$$

and the trace gives the $B-L$ asymmetry N_{B-L}.
Moving further, we now define the projectors

$$\mathcal{P}^{(1)}_{\alpha\beta} \coloneqq \left(R^{(1)\dagger}\right)_{\alpha i} \begin{pmatrix} 1 & 0 \\ 0 & 0 \end{pmatrix} R^{(1)}_{j\beta} = \begin{pmatrix} p_{1\tau} & \mathcal{C}^{*}_{1\tau_1^\perp}\, \mathcal{C}_{1\tau} \\ \mathcal{C}^{*}_{1\tau}\, \mathcal{C}_{1\tau_1^\perp} & p_{1\tau_1^\perp} \end{pmatrix} \tag{4.1.22}$$

and

$$\overline{\mathcal{P}}^{(1)}_{\alpha\beta} \coloneqq \left(\overline{R}^{(1)\dagger}\right)_{\alpha i} \begin{pmatrix} 1 & 0 \\ 0 & 0 \end{pmatrix} \overline{R}^{(1)}_{j\beta} = \begin{pmatrix} \overline{p}_{1\tau} & \overline{\mathcal{C}}^{*}_{1\tau_1^\perp}\, \overline{\mathcal{C}}_{1\tau} \\ \overline{\mathcal{C}}^{*}_{1\tau}\, \overline{\mathcal{C}}_{1\tau_1^\perp} & \overline{p}_{1\tau_1^\perp} \end{pmatrix} \tag{4.1.23}$$

whose diagonal elements are the same flavoured probabilities introduced in Chapter 3. At tree level these quantities are also given by a common expression:

$$\mathcal{P}^{0(1)}_{\alpha\beta} = \left(R^{0(1)\dagger}\right)_{\alpha i} \begin{pmatrix} 1 & 0 \\ 0 & 0 \end{pmatrix} R^{0(1)}_{j\beta} = \overline{\mathcal{P}}^{(1)0}_{\alpha\beta} = \frac{1}{(h^\dagger h)_{11}} \begin{pmatrix} |h_{\tau 1}|^2 & h_{\tau 1} h^*_{\tau_1^\perp 1} \\ h^*_{\tau 1} h_{\tau_1^\perp 1} & \left|h_{\tau_1^\perp 1}\right|^2 \end{pmatrix}. \tag{4.1.24}$$

Using these results we can now rewrite eq. (4.1.21) as

$$\frac{\mathrm{d}\, N^{B-L}_{\alpha\beta}}{\mathrm{d}\, z} = \left(\frac{\overline{\Gamma}_1}{H\, z}\, N_{N_1} - \frac{\overline{\Gamma}_{ID,1}}{H\, z}\, N_{\overline{\ell_1}}\right) \overline{\mathcal{P}}^{(1)}_{\alpha\beta} - \left(\frac{\Gamma_1}{H\, z}\, N_{N_1} - \frac{\Gamma_{ID,1}}{H\, z}\, N_{\ell_1}\right) \mathcal{P}^{(1)}_{\alpha\beta} \tag{4.1.25}$$

and by means of eqs. (4.1.5) and (4.1.6) it is:

$$\frac{\mathrm{d}\, N^{B-L}_{\alpha\beta}}{\mathrm{d}\, z} = \varepsilon^{(1)}_{\alpha\beta}\, D_1 \left(N_{N_1} - N^{eq}_{N_1}\right) - W_1\, N_{B-L} \left[\frac{\mathcal{P}^{(1)}_{\alpha\beta}\, \Gamma_1 + \overline{\mathcal{P}}^{(1)}_{\alpha\beta}\, \overline{\Gamma}_1}{\Gamma_1 + \overline{\Gamma}_1}\right]. \tag{4.1.26}$$

Finally, neglecting terms of order $\mathcal{O}(\varepsilon_1\, N_{B-L})$ and $\mathcal{O}(\Delta p\, N_{B-L})$, it follows

$$\frac{\mathrm{d}\, N^{B-L}_{\alpha\beta}}{\mathrm{d}\, z} = \varepsilon^{(1)}_{\alpha\beta}\, D_1\, (N_{N_1} - N^{eq}_{N_1}) - W_1\, N_{B-L}\, \mathcal{P}^{0(1)}_{\alpha\beta}. \tag{4.1.27}$$

The CP asymmetry matrix $\varepsilon^{(1)}_{\alpha\beta}$ is defined according to [103]

$$\varepsilon^{(1)} = \frac{\overline{\mathcal{P}}^{(1)}\, \overline{\Gamma}_1 - \mathcal{P}^{(1)}\, \Gamma_1}{\Gamma_1 + \overline{\Gamma}_1} = \varepsilon_1\, \frac{\overline{\mathcal{P}}^{(1)} + \mathcal{P}^{(1)}}{2} - \frac{\Delta\mathcal{P}^{(1)}}{2} \tag{4.1.28}$$

where $\Delta\mathcal{P}^{(1)} \coloneqq \mathcal{P}^{(1)} - \overline{\mathcal{P}}^{(1)}$, and generalises eq. (3.2.27) that still holds for the diagonal terms: $\varepsilon^{(1)}_{\alpha\alpha} \equiv \varepsilon_{1\alpha}$. The off-diagonal terms obey instead the relation $\varepsilon^{(1)}_{\alpha\beta} = (\varepsilon^{(1)}_{\beta\alpha})^*$ and are not necessarily real. Explicitly we have [116]

$$\begin{aligned}\varepsilon^{(i)}_{\alpha\beta} &= \frac{3}{32\pi(h^\dagger h)_{ii}} \sum_{j\neq i} \left\{ \mathrm{i} \left[h_{\alpha i} h^*_{\beta j} (h^\dagger h)_{ji} - h^*_{\beta i} h_{\alpha j} (h^\dagger h)_{ij} \right] \frac{\xi(x_j/x_i)}{\sqrt{x_j/x_i}} \right. \\ &\left. + \mathrm{i} \frac{2}{3(x_j/x_i - 1)} \left[h_{\alpha i} h^*_{\beta j} (h^\dagger h)_{ij} - h^*_{\beta i} h_{\alpha j} (h^\dagger h)_{ji} \right] \right\} \end{aligned} \tag{4.1.29}$$

where the ξ function was already defined in eq. (2.2.15). Notice that the presented expression for the flavoured asymmetry matrix correctly vanishes if $\epsilon_1 = 0$ and, at the same time, $\mathcal{C}_{i\alpha} = \overline{\mathcal{C}}_{i\alpha}$ prevents the possibility offered by differences in the flavour compositions of $|1\rangle$ and $CP\,|\overline{1}\rangle$.

The diagonal components of eq. (4.1.27) offer a flavoured insight in the N_1 Leptogenesis process, yielding for the considered heavy neutrino flavour regime:

$$\frac{\mathrm{d}\, N^{B-L}_{\tau\tau}}{\mathrm{d}\, z} = \varepsilon^{(1)}_{\tau\tau}\, D_1\, (N_{N_1} - N^{eq}_{N_1}) - p^0_{1\tau}\, W_1\, N_{B-L} \tag{4.1.30}$$

$$\frac{\mathrm{d}\, N^{B-L}_{\tau_1^\perp\tau_1^\perp}}{\mathrm{d}\, z} = \varepsilon^{(1)}_{\tau_1^\perp\tau_1^\perp}\, D_1\, (N_{N_1} - N^{eq}_{N_1}) - p^0_{1\tau_1^\perp}\, W_1\, N_{B-L}. \tag{4.1.31}$$

Notice that, with respect to eq. (3.2.48) and (3.2.49) which hold in a two-flavour regime, here the washout factor is multiplying the total $B-L$ asymmetry. By summing these equations we achieve our first goal, correctly reproducing eq. (4.1.7) for the total $B-L$ asymmetry $N_{B-L} = \mathrm{Tr}[N^{B-L}_{\alpha\beta}]$. On the top of that, from the relations (4.1.30) and (4.1.31), it follows

$$\frac{1}{p^0_{1\tau}} \frac{\mathrm{d}\, N^{B-L}_{\tau\tau}}{\mathrm{d}\, z} - \frac{1}{p^0_{1\tau_1^\perp}} \frac{\mathrm{d}\, N^{B-L}_{\tau_1^\perp\tau_1^\perp}}{\mathrm{d}\, z} = -\frac{\Delta p_{1\tau}}{2} \left(\frac{1}{p^0_{1\tau}} + \frac{1}{p^0_{1\tau_1^\perp}} \right) D_1\, (N_{N_1} - N^{eq}_{N_1}) \tag{4.1.32}$$

which, together with eq. (4.1.7) and

$$\frac{\mathrm{d}\, N_{N_1}}{\mathrm{d}\, z} = -D_1\, (N_{N_1} - N^{eq}_{N_1}) \tag{4.1.33}$$

form a system of equations for the flavoured asymmetries $N^{B-L}_{\alpha\alpha}$ that can be solved analytically.

At the end of the Leptogenesis process, for $T \ll T_{L1} \ll M_1$ and $T_{L1} \coloneqq M_1/z_{L1}$, we therefore have [117]:

$$\begin{aligned} N^{B-L,f}_{\tau\tau} &\simeq p^0_{1\tau}\, N^f_{B-L} - \frac{\Delta p_{1\tau}}{2}\, N^{in}_{N_1} \\ N^{B-L,f}_{\tau_1^\perp\tau_1^\perp} &\simeq p^0_{1\tau_1^\perp}\, N^f_{B-L} + \frac{\Delta p_{1\tau}}{2}\, N^{in}_{N_1}. \end{aligned} \tag{4.1.34}$$

These solutions show the flavour composition of the asymmetry produced by N_1 in

the considered heavy neutrino flavour regime. The sum of the first terms on the RHS correctly reproduces the total $B-L$ asymmetry that the out-of-equilibrium decays produced

$$N^f_{B-L} = \varepsilon_1 \kappa^f_1(K_1) \tag{4.1.35}$$

which, as usual, is washed out at the production – eq. (2.2.45). The remaining contributions are instead the so-called *phantom terms* [117]: flavoured asymmetries which are proportional to the initial abundance of heavy neutrinos $N^{in}_{N_1}$ and *avoid the washout* at the production. In the considered heavy neutrino flavour regime, where under the current assumptions the flavoured asymmetries are not measured by any process, the phantom terms do not result in any physical effect and effectively compensate in the calculation of the total asymmetry N_{B-L}. Yet, within setups in which the present Leptogenesis phase is followed by a further stage, the phantom terms could affect this quantity provided an asymmetric washout prevent the mutual cancellation.

4.1.1 Turning gauge and τ Yukawa interactions on

We investigate now the impact that charged-lepton Yukawa interactions and gauge interactions have on the picture presented above. To account for these effects we therefore generalise the eq.s (4.1.17) to [112, 116, 118]

$$\begin{aligned}
\frac{\mathrm{d}\, N^{\ell}_{\alpha\beta}}{\mathrm{d}\, z} &= \frac{\Gamma_1}{H\, z}\, N_{N_1}\, \mathcal{P}^{(1)}_{\alpha\beta} - \frac{1}{2}\, \frac{\Gamma_{ID,1}}{H\, z}\, \left\{ \mathcal{P}^{(1)}, N^{\ell} \right\}_{\alpha\beta} + \Lambda_{\alpha\beta} + G_{\alpha\beta} \\
\frac{\mathrm{d}\, N^{\bar{\ell}}_{\alpha\beta}}{\mathrm{d}\, z} &= \frac{\overline{\Gamma}_1}{H\, z}\, N_{N_1}\, \overline{\mathcal{P}}^{(1)}_{\alpha\beta} - \frac{1}{2}\, \frac{\overline{\Gamma}_{ID,1}}{H\, z}\, \left\{ \overline{\mathcal{P}}^{(1)}, N^{\bar{\ell}} \right\}_{\alpha\beta} + \overline{\Lambda}_{\alpha\beta} + G_{\alpha\beta}
\end{aligned} \tag{4.1.36}$$

where $\Lambda_{\alpha\beta}$ and $\overline{\Lambda}_{\alpha\beta}$ describe the effects of charged-lepton Yukawa interactions:

$$\Lambda_{\alpha\beta} = -\mathrm{i}\, \frac{\mathrm{Re}(\Lambda_\tau)}{H\, z} \left[\begin{pmatrix} 1 & 0 \\ 0 & 0 \end{pmatrix}, N^{\ell} \right]_{\alpha\beta} - \frac{\mathrm{Im}(\Lambda_\tau)}{H\, z} \begin{pmatrix} 0 & N^{\ell}_{\tau\tau_1^{\perp}} \\ N^{\ell}_{\tau_1^{\perp}\tau} & 0 \end{pmatrix} \tag{4.1.37}$$

$$\overline{\Lambda}_{\alpha\beta} = +\mathrm{i}\, \frac{\mathrm{Re}(\Lambda_\tau)}{H\, z} \left[\begin{pmatrix} 1 & 0 \\ 0 & 0 \end{pmatrix}, N^{\bar{\ell}} \right]_{\alpha\beta} - \frac{\mathrm{Im}(\Lambda_\tau)}{H\, z} \begin{pmatrix} 0 & N^{\bar{\ell}}_{\tau\tau_1^{\perp}} \\ N^{\bar{\ell}}_{\tau_1^{\perp}\tau} & 0 \end{pmatrix}. \tag{4.1.38}$$

Introducing the tau Yukawa coupling y_τ, the real and imaginary parts of the tau-lepton self-energy are respectively written as [105, 119]

$$\mathrm{Re}(\Lambda_\tau) \simeq \frac{y_\tau^2}{64}\, T, \qquad \mathrm{Im}(\Lambda_\tau) \simeq 8 \times 10^{-3}\, y_\tau^2\, T. \tag{4.1.39}$$

The former enters the commutator structure presented by third term on the RHS of eq. (4.1.36), consequently driving the flavour oscillations. The latter, instead, controls the damping of the off-diagonal elements in the involved density matrices.

Finally, the gauge interactions which have the effect of thermalising the above abundances in a way that equilibrium conditions can be assumed during the transition between heavy neutrino flavour and two-flavour regimes, are addressed by $G_{\alpha\beta}$. Notice that these reactions are CP conserving, hence both the total and flavoured asymmetries cannot be directly modified by the imposed thermalisation process. Nevertheless there is an indirect repercussion that gauge interactions yield.

4.1.1.1 Gauge interactions and the heavy neutrino flavour regime

We investigate here the impact of gauge interactions on the results of Section 4.1, derived for N_1 Leptogenesis within the heavy neutrino flavour regime.

As we have seen – cf. eq.s (4.1.5), (4.1.6) and (4.1.25) – assuming that the lepton abundances involved in the N_1 Leptogenesis are only thermalised through the Yukawa interactions results in the following density matrices:

$$N^{\ell} = N_{\ell_1}\, \mathcal{P}^{(1)} \tag{4.1.40}$$

and

$$N^{\bar{\ell}} = N_{\overline{\ell_1}}\, \overline{\mathcal{P}}^{(1)}. \tag{4.1.41}$$

Taking now into account the effects of gauge interactions, the above relations are modified as follows

$$\begin{aligned} N^{\ell} &= N_{\ell}^{eq}\, \mathrm{I} + N_{\ell_1}\, \mathcal{P}^{(1)} - \frac{N_{\ell_1} + N_{\overline{\ell_1}}}{2}\, \mathcal{P}^{0(1)} \\ N^{\bar{\ell}} &= N_{\ell}^{eq}\, \mathrm{I} + N_{\overline{\ell_1}}\, \overline{\mathcal{P}}^{(1)} - \frac{N_{\ell_1} + N_{\overline{\ell_1}}}{2}\, \mathcal{P}^{0(1)}. \end{aligned} \tag{4.1.42}$$

Notice that being flavour-blind, the gauge interactions not only thermalise the leptons $|\ell_1\rangle$ and the antileptons $|\overline{\ell_1}\rangle$ independently of the strength of the neutrino Yukawa interactions, but also reconstruct the thermal abundances of the orthogonal states $|\ell_{1\perp}\rangle$ and $|\overline{\ell_{1\perp}}\rangle$. The first terms on the RHSs of the above equations are therefore accounting for this effect, while the second terms are the usual contributions of N_1 decays we discussed before. The third terms describe instead how the lepton doublet annihilations, mediated by gauge interactions, reveal the tree-level components of $|\ell_1\rangle$ and $|\overline{\ell_1}\rangle$ which are also thermalised[1].

Considering now eq.s (4.1.5) and (4.1.6) we linearise the above equations

$$\begin{aligned} N^{\ell} &= N_{\ell}^{eq}\, \mathrm{I} + \left(\frac{N_{\ell_1} + N_{\overline{\ell_1}}}{2}\right) (\mathcal{P}^{(1)} - \mathcal{P}^{0(1)}) - \frac{1}{2}\, N_{B-L}\, \mathcal{P}^{(1)} \\ N^{\bar{\ell}} &= N_{\ell}^{eq}\, \mathrm{I} + \left(\frac{N_{\ell_1} + N_{\overline{\ell_1}}}{2}\right) (\overline{\mathcal{P}}^{(1)} - \mathcal{P}^{0(1)}) + \frac{1}{2}\, N_{B-L}\, \overline{\mathcal{P}}^{(1)} \end{aligned} \tag{4.1.43}$$

[1] In this regard, notice that this contribution involves CP-conjugated states, hence its presence should not affect the calculation of the final $B - L$ asymmetry.

and performing the difference obtain an explicit expression for the $B-L$ asymmetry matrix:

$$N^{B-L} = \frac{N_{\ell_1} + N_{\overline{\ell_1}}}{2}\left(\overline{\mathcal{P}}^{(1)} - \mathcal{P}^{(1)}\right) + \frac{N_{B-L}}{2}\left(\mathcal{P}^{(1)} + \overline{\mathcal{P}}^{(1)}\right). \tag{4.1.44}$$

In analogy to eq. (4.1.28), the first term in the above equation accounts for the contribution to the flavoured asymmetries that arises from the discrepancies in the flavour compositions of $|\ell_1\rangle$ and $CP\,|\overline{\ell_1}\rangle$: the phantom terms. The second term, instead, represents the usual contribution proportional to the total asymmetry. Notice that the quantity $(N_{\ell_1} + N_{\overline{\ell_1}})/2$ should be regarded as dynamical, likewise the total asymmetry N_{B-L}[2].

At this stage we can also give an explicit expression for the sum $N^{\ell} + N^{\overline{\ell}}$, which will prove useful for later

$$N^{\ell+\overline{\ell}} \coloneqq N^{\ell} + N^{\overline{\ell}} = 2\,N_{\ell}^{eq}\,\mathrm{I} + \frac{N_{\ell_1} + N_{\overline{\ell_1}}}{2}\left(\delta\mathcal{P}^{(1)} + \delta\overline{\mathcal{P}}^{(1)}\right) + \frac{N_{B-L}}{2}\left(\overline{\mathcal{P}}^{(1)} - \mathcal{P}^{(1)}\right) \tag{4.1.45}$$

where we defined $\delta\mathcal{P}^{(1)} \coloneqq \mathcal{P}^{(1)} - \mathcal{P}^{0(1)}$ and $\delta\overline{\mathcal{P}}^{(1)} \coloneqq \overline{\mathcal{P}}^{(1)} - \mathcal{P}^{0(1)}$.

An equation for the asymmetry matrix, N^{B-L}, follows from the difference of the relation in eq. (4.1.36). Under the current assumptions we therefore neglect the effects due to charged-lepton interactions and by disregarding terms of order $\mathcal{O}(\varepsilon\,\Delta\mathcal{P})$ and $\mathcal{O}(\delta\mathcal{P}^2)$ we obtain:

$$\frac{\mathrm{d}\,N^{B-L}}{\mathrm{d}\,z} = \varepsilon^{(1)}\,D_1\,(N_{N_1} - N_{N_1}^{eq}) - \frac{1}{2}\,W_1\,\frac{N_{\ell_1} + N_{\overline{\ell}_1}}{2}\left(\overline{\mathcal{P}}^{(1)} - \mathcal{P}^{(1)}\right) - W_1\,\frac{N_{B-L}}{2}\left(\mathcal{P}^{(1)} + \overline{\mathcal{P}}^{(1)}\right). \tag{4.1.46}$$

Considering now that on the tree-level basis $i_0, j_0 = 1_0, 1_0^{\perp}$ it is

$$R^{0(1)}_{i_0\alpha}\,\delta\mathcal{P}^{1}_{\alpha\beta}\,(R^{0(1)\dagger})_{\beta j_0} = \delta\mathcal{P}^{(1)}_{i_0 j_0} = \begin{pmatrix} 0 & \delta p \\ \delta p^{\star} & 0 \end{pmatrix} \tag{4.1.47}$$

with $\delta p \coloneqq \mathcal{C}^0_{1\tau_1^{\perp}}\,\delta\mathcal{C}_{1\tau} - \mathcal{C}^0_{1\tau}\,\delta\mathcal{C}_{1\tau_1^{\perp}}$ and $\delta\mathcal{C}_{1\alpha} \equiv \mathcal{C}_{1\alpha} - \mathcal{C}^0_{1\alpha}$, we have

$$\left\{\mathcal{P}^{(1)}, \delta\mathcal{P}^{(1)}\right\} = \delta\mathcal{P}^{(1)} + \mathcal{O}(\delta\mathcal{P}^2), \qquad \left\{\overline{\mathcal{P}}^{(1)}, \delta\overline{\mathcal{P}}^{(1)}\right\} = \delta\overline{\mathcal{P}}^{(1)} + \mathcal{O}(\delta\overline{\mathcal{P}}^2) \tag{4.1.48}$$

hence we can simplify eq. (4.1.46) obtaining our final expression for the asymmetry matrix in the heavy neutrino flavour regime:

[2] In this regard, we emphasise that the above equation holds also when the gauge interactions are disregarded. In fact, differentiating eq. (4.1.44) with respect to z and considering the relations (4.1.2), (4.1.3) as well as the Boltzmann equation regulating N_{B-L} yields the expression for the asymmetry matrix we gave in eq. (4.1.27).

$$\frac{\mathrm{d}\, N^{B-L}}{\mathrm{d}\, z} = \varepsilon^{(1)}\, D_1\, (N_{N_1} - N_{N_1}^{\mathrm{eq}}) - \frac{1}{2}\, W_1\, \left\{\mathcal{P}^{0(1)}, N^{B-L}\right\}. \tag{4.1.49}$$

The above equation therefore generalises eq. (4.1.27) to the effect of gauge interactions. In this regard, an important remark follows. Equations (4.1.46) and (4.1.49) imply, non trivially, that accounting for the unflavoured thermal bath brought by the gauge interactions results in a washout of the phantom terms. More in detail. differently from the results presented in Section 4.1, the phantom terms undergo here a washout at the production which is half the one acting on the total $B - L$ asymmetry.

To show this explicitly we investigate the solutions encoded in the diagonal components of the asymmetry matrix, corresponding in the charged-lepton flavour basis to $N^{B-L}_{\tau\tau}$ and $N^{B-L}_{\tau_1^\perp\tau_1^\perp}$. To this purpose consider the tree-level basis in which $\varepsilon^{(1)}$, appearing on the RHS of eq. (4.1.28), specialises into

$$\varepsilon^{(1)}_{i_0 j_0} = \begin{pmatrix} \varepsilon_1 & 0 \\ 0 & 0 \end{pmatrix} + \begin{pmatrix} 0 & \delta\varepsilon \\ \delta\varepsilon^\star & 0 \end{pmatrix} \tag{4.1.50}$$

where $\delta\varepsilon = (\delta\overline{p} - \delta p)/2 = \Delta p/2$. The term $1_0 1_0$ clearly matches the total N_{B-L} asymmetry washed out by W_1 as prescript by eq. (4.1.7). The off-diagonal terms, instead, upon a rotation to the charged lepton flavour basis correspond to the phantom terms. Explicitly we have

$$\begin{aligned} N^{B-L,f}_{\tau\tau} &\simeq p^0_{1\tau}\, N^f_{B-L} + \frac{\Delta p_{1\tau}}{2}\, \kappa(K_1/2) \\ N^{B-L,f}_{\tau_1^\perp\tau_1^\perp} &\simeq p^0_{1\tau_1^\perp}\, N^f_{B-L} - \frac{\Delta p_{1\tau}}{2}\, \kappa(K_1/2). \end{aligned} \tag{4.1.51}$$

confirming what we anticipated.

4.1.1.2 N_1 Leptogenesis in the two flavour regime

We focus now on the two-flavour regime, in which the states $|\ell_1\rangle$ and $CP\,|\overline{\ell_1}\rangle$ break down to an incoherent mixture of $|\ell_\tau\rangle$, $|\ell_{\tau_1^\perp}\rangle$ and $|\overline{\ell_\tau}\rangle$, $|\overline{\ell_{\tau_1^\perp}}\rangle$ as a result of τ Yukawa interactions in the limit of full decoherence. As a first step, we take the difference of the equations (4.1.36), obtaining

$$\begin{aligned} \frac{\mathrm{d}\, N^{B-L}_{\alpha\beta}}{\mathrm{d}\, z} &= \varepsilon^{(1)}_{\alpha\beta}\, D_1\, N_{N_1} - \frac{1}{2}\, D_1 \left[\frac{\overline{\Gamma}_{ID,1}}{\Gamma_1 + \overline{\Gamma}_1} \left\{\overline{\mathcal{P}}^{(1)}, N^{\overline{\ell}}\right\}_{\alpha\beta} - \frac{\Gamma_{ID,1}}{\Gamma_1 + \overline{\Gamma}_1} \left\{\mathcal{P}^{(1)}, N^{\ell}\right\}_{\alpha\beta}\right] \\ &\quad + \Delta\Lambda_{\alpha\beta} \end{aligned} \tag{4.1.52}$$

with clear meaning of the notation. Hence, in analogy to eq.s (4.1.5) and (4.1.6), by recasting N^{ℓ} and $N^{\bar{\ell}}$ as

$$N^{\ell} = \frac{N^{\ell} + N^{\bar{\ell}}}{2} - \frac{N^{B-L}}{2}, \qquad N^{\bar{\ell}} = \frac{N^{\ell} + N^{\bar{\ell}}}{2} + \frac{N^{B-L}}{2} \tag{4.1.53}$$

it is

$$\begin{aligned} \frac{\mathrm{d}\, N^{B-L}_{\alpha\beta}}{\mathrm{d}\, z} &= \varepsilon^{(1)}_{\alpha\beta}\, D_1\, N_{N_1} - \frac{1}{4}\, D_1\, \frac{N^{eq}_{N_1}}{N^{eq}_{\ell}}\, \left\{\varepsilon^{(1)}_{\alpha\beta}, N^{\ell+\bar{\ell}}\right\}_{\alpha\beta} \\ &\quad -\frac{1}{4}\, D_1 \left[\frac{\overline{\Gamma}_{ID,1}}{\Gamma_1 + \overline{\Gamma}_1}\, \left\{\overline{\mathcal{P}}^{(1)}, N^{B-L}\right\}_{\alpha\beta} + \frac{\Gamma_{ID,1}}{\Gamma_1 + \overline{\Gamma}_1}\, \left\{\mathcal{P}^{(1)}, N^{B-L}\right\}_{\alpha\beta}\right] \\ &\quad +\Delta\Lambda_{\alpha\beta} \end{aligned} \tag{4.1.54}$$

and, by neglecting terms of order $\mathcal{O}(\Delta P\, N_{B-L})$, we finally have

$$\begin{aligned} \frac{\mathrm{d}\, N^{B-L}_{\alpha\beta}}{\mathrm{d}\, z} &= \varepsilon^{(1)}_{\alpha\beta}\, D_1\, N_{N_1} - \frac{1}{4}\, D_1\, \frac{N^{\mathrm{eq}}_{N_1}}{N^{\mathrm{eq}}_{\ell}}\, \left\{\varepsilon^{(1)}_{\alpha\beta}, N^{\ell+\bar{\ell}}\right\}_{\alpha\beta} - \frac{1}{2} W_1\, \left\{\mathcal{P}^{0(1)}, N^{B-L}\right\}_{\alpha\beta} \\ &\quad + \mathrm{i}\, \frac{\mathrm{Re}(\Lambda_\tau)}{H\, z} \left[\begin{pmatrix} 1 & 0 \\ 0 & 0 \end{pmatrix}, N^{\ell+\bar{\ell}}\right]_{\alpha\beta} - \frac{\mathrm{Im}(\Lambda_\tau)}{H\, z} \begin{pmatrix} 0 & N^{B-L}_{\tau\tau_1^{\perp}} \\ N^{B-L}_{\tau_1^{\perp}\tau} & 0 \end{pmatrix}. \end{aligned} \tag{4.1.55}$$

We now need to employ the Boltzmann equation regulating the quantity $N_{\ell+\bar{\ell}}$, given by

$$\frac{\mathrm{d}\, N^{\ell+\bar{\ell}}_{\alpha\beta}}{\mathrm{d}\, z} \simeq -\frac{\mathrm{Re}(\Lambda_\tau)}{H\, z} (\sigma_2)_{\alpha\beta} N^{B-L}_{\alpha\beta} - S_g\, (N^{\ell+\bar{\ell}}_{\alpha\beta} - 2\, N^{eq}_{\ell}\delta_{\alpha\beta}) \tag{4.1.56}$$

where $S_g \equiv \Gamma_g/(Hz)$ accounts for the gauge interactions rescaled rate. As shown in [116], this term has the effect of damping the flavour oscillations: gauge interactions force in fact $N^{\ell+\bar{\ell}}_{\alpha\beta} \simeq 2\, N^{eq}_{\ell_1}\delta_{\alpha\beta}$, as showed explicitly by eq. (4.1.45). The oscillatory term is therefore negligible and we obtain

$$\frac{\mathrm{d}\, N^{B-L}_{\alpha\beta}}{\mathrm{d}\, z} = \varepsilon^{(1)}_{\alpha\beta}\, D_1\, (N_{N_1} - N^{eq}_{N_1}) - \frac{1}{2}\, W_1\, \left\{\mathcal{P}^{0(1)}, N^{B-L}\right\}_{\alpha\beta} - \frac{\mathrm{Im}(\Lambda_\tau)}{H\, z} (\sigma_1)_{\alpha\beta}\, N^{B-L}_{\alpha\beta} \tag{4.1.57}$$

that generalises eq. (4.1.49).

When the tau interactions become effective, for $T \sim 10^{12}$ GeV, the off-diagonal elements of eq. (4.1.36) are therefore progressively suppressed and the quantum coherence of the original states is gradually lost. Eventually, when the off-diagonal terms are completely damped, the remaining entries in the above equation correctly reproduce the Boltzmann equations given for the considered fully flavoured regime: eq. (3.2.48) and (3.2.48). On the other hand, when the charged lepton interactions are negligible, the usual equation (4.1.7) for the total asymmetry in the unflavoured regime is also recovered upon a

rotation.

4.2 Heavy neutrino flavour effects, phantom terms and the projection effect

In this Section we investigate the heavy neutrino flavour effects and their consequences on the proposed formalism. For sake of clarity, we will first carry out our study assuming the presence of only two flavours τ and $\tau^{\perp}$, generalising the equations to a realistic three flavour case in the next Section.
For definiteness, we consider here masses $M_i \gg 10^9\,\mathrm{GeV}$, where only the tau lepton Yukawa interactions have to be taken into account. In order to further simplify our analysis we also assume that the heaviest neutrinos N_3 do not contribute to the final asymmetry, imposing $M_3 \gg T_{RH} \gg M_2$ to prevent the thermalisation of this neutrino species.
The two flavour regime that the above assumptions define can therefore be regarded as a special case in which the heavy neutrino flavour lepton states associated to N_1 and N_2 lie on the same plane orthogonal to the one identified by the light flavours e and μ. In particular we therefore impose $|\ell_{\tau_2^{\perp}}\rangle = |\ell_{\tau_1^{\perp}}\rangle = |\ell_{\tau^{\perp}}\rangle$ and consider the configuration depicted in Figure 4.2.

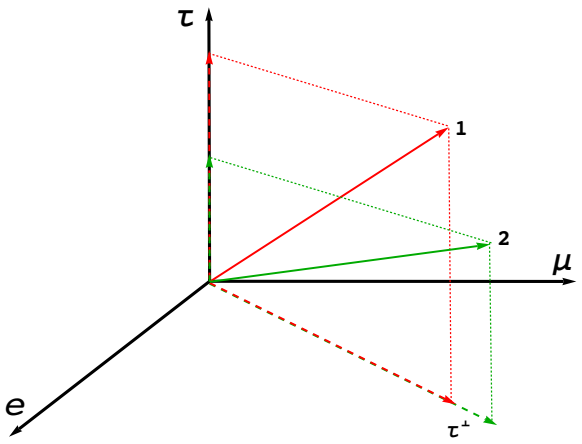

Figure 4.2: The flavour configuration of the two heavy neutrino lepton states considered in this Section.

Analogously, the two antilepton heavy neutrino flavour states $|\overline{\ell_1}\rangle$ and $|\overline{\ell_2}\rangle$, are also taken in the same plane orthogonal to e and μ, in a way that $|\overline{\ell_{\tau_2^{\perp}}}\rangle = |\overline{\ell_{\tau_1^{\perp}}}\rangle = |\overline{\ell_{\tau^{\perp}}}\rangle$ and by assuming here that $|\ell_{\tau^{\perp}}\rangle = CP\,|\overline{\ell_{\tau^{\perp}}}\rangle$ our analysis will be completely specified in terms of the flavours τ and $\tau^{\perp}$.

The density matrix in eq. (4.1.57), valid for N_1 Leptogenesis, is straightforwardly generalised to

$$\begin{aligned}\frac{\mathrm{d}\, N^{B-L}_{\alpha\beta}}{\mathrm{d}\, z} &= \varepsilon^{(1)}_{\alpha\beta}\, D_1\, (N_{N_1} - N^{eq}_{N_1}) - \frac{1}{2}\, W_1\, \left\{\mathcal{P}^{0(1)}, N^{B-L}\right\}_{\alpha\beta} \\ &+ \varepsilon^{(2)}_{\alpha\beta}\, D_2\, (N_{N_2} - N^{eq}_{N_2}) - \frac{1}{2}\, W_2\, \left\{\mathcal{P}^{0(2)}, N^{B-L}\right\}_{\alpha\beta} \\ &- \frac{\mathrm{Im}(\Lambda_\tau)}{H\, z}(\sigma_1)_{\alpha\beta}\, N^{B-L}_{\alpha\beta}\end{aligned} \tag{4.2.1}$$

where $(\alpha, \beta = \tau, \tau^\perp)$ and the N_{N_2} evolution is regulated as usual by eq. (3.1.2).
With this setup we now discuss three limit cases, characterised by $M_2 \gg 10^{12}\,\mathrm{GeV} \gg M_1$, $M_2, M_1 \gg 10^{12}\,\mathrm{GeV}$ and $M_1, M_2 \ll 10^{12}\,\mathrm{GeV}$, in which our density matrix formalism recovers the usual Boltzmann equations validating in this way the results presented in previous Chapters.

4.2.1 Three stages phantom Leptogenesis: $M_2 \gg 10^{12}\,\mathrm{GeV} \gg M_1$

The $B-L$ asymmetry, produced for $T \sim M_2$ by the out-of-equilibrium decays of N_2, is described by the equation

$$\frac{\mathrm{d}\, N^{B-L}_{\alpha\beta}}{\mathrm{d}\, z} = \varepsilon^{(2)}_{\alpha\beta}\, D_2\, (N_{N_2} - N^{\mathrm{eq}}_{N_2}) - \frac{1}{2}\, W_2\, \left\{\mathcal{P}^{0(2)}, N^{B-L}\right\}_{\alpha\beta} \tag{4.2.2}$$

obtained from eq. (4.1.49) through the change of label $1 \to 2$. Since $M_2 > 10^{12}$ GeV we neglected here any light flavour effect. For $T \simeq T_{L2} \equiv M_2/z_{L2}$, the τ and $\tau^\perp$ asymmetries are then described by the eqs. (4.1.51), again with the substitution $1 \to 2$:

$$\begin{aligned}N^{B-L}_{\tau\tau}(T \simeq T_{L2}) &\simeq p^0_{2\tau}\, N^{T\simeq T_{L2}}_{B-L} - \frac{\Delta p_{2\tau}}{2}\,\kappa(K_2/2) \\ N^{B-L}_{\tau^\perp\tau^\perp}(T \simeq T_{L2}) &\simeq p^0_{2\tau^\perp}\, N^{T\simeq T_{L2}}_{B-L} + \frac{\Delta p_{2\tau}}{2}\,\kappa(K_2/2).\end{aligned} \tag{4.2.3}$$

Notice that at this stage the phantom terms in the above equations mutually balance in the calculation of the total asymmetry. Therefore, so far, the description of the asymmetry evolution is completely analogous to the one given within N_1 Leptogenesis.

When the temperature drops below $T = T_\star \ll 10^{12}$ GeV the off-diagonal terms in $N^{B-L}_{\alpha\beta}$ are completely damped by the tau charged-lepton interactions. Hence, in this second stage, the diagonal elements N_{Δ_τ} and $N_{\Delta_{\tau^\perp}}$ can be treated as measured quantities.

The last stage we present takes into account the washout performed on the $B-L$ asymmetry by the lightest neutrino species. For $T \sim M_1$, the τ and the $\tau^\perp$ asymmetries are therefore washed out individually by the N_1 inverse-processes which proceed in the present fully flavoured regime. When the N_1 processes freeze-in , for $T \simeq T_{L1} = M_1/z_{L1}$

the values of the relevant flavoured asymmetries thus are

$$N^f_{\Delta\tau} \simeq \left[p^0_{2\tau}\, N^{T\simeq T_{L2}}_{B-L} - \frac{\Delta p_{2\tau}}{2}\,\kappa(K_2/2)\right] e^{-\frac{3\pi}{8}\,K_{1\tau}} \tag{4.2.4}$$

$$N^f_{\Delta\tau^\perp} \simeq \left[p^0_{2\tau^\perp}\, N^{T\simeq T_{L2}}_{B-L} + \frac{\Delta p_{2\tau}}{2}\,\kappa(K_2/2)\right] e^{-\frac{3\pi}{8}\,K_{1\tau^\perp}} \tag{4.2.5}$$

and for the final total asymmetry it follows

$$N^f_{B-L} \simeq N^f_{\Delta\tau} + N^f_{\Delta\tau^\perp}. \tag{4.2.6}$$

Consequently, if for the flavour $\alpha = \tau$ ($\tau^\perp$) it is $K_{1\alpha} \lesssim 1$ while for the other flavour $\beta = \tau^\perp$ (τ) we have $K_{1\beta} \gg 1$, the final asymmetry is dominated by the former component:

$$N^f_{B-L} \simeq p^0_{2\alpha}\, N^{T\simeq T_{L2}}_{B-L} - \frac{\Delta p_{2\alpha}}{2}\,\kappa(K_2/2). \tag{4.2.7}$$

Phantom Leptogenesis has been first discussed in the approximation of an instantaneous wave function collapse, neglecting the gauge interactions, in [117]. Here we have re-derived its main features within a density matrix formalism, showing the important impact of gauge interactions. Clearly, phantom Leptogenesis has some analogies with the particular scenario of N_1 Leptogenesis characterised by $\varepsilon_1 = 0$, discussed in [98]. In both the cases, in fact, the final asymmetry originates from the CP-violating terms $\propto \Delta p_{i\alpha}$ brought by the different flavour compositions of the lepton and antilepton heavy flavour states, provided an asymmetric washout act on the two flavoured asymmetries. There are however important differences. In particular, for N_1 Leptogenesis with $\varepsilon_1 = 0$, production, decoherence and washout occur simultaneously while, in the case of phantom Leptogenesis, these stages are effectively separated. In this regard, as we show below, phantom Leptogenesis does not require the N_2 production and the N_1 washout stages occur in two different fully-flavoured regimes.

4.2.2 The projection effect and two stages phantom Leptogenesis: $M_2 \gtrsim 3\,M_1 \gg 10^{12}$ GeV

We consider now the case in which the heavy neutrino masses satisfy $M_2, M_1 \gg 10^{12}$ GeV, so the charged-lepton Yukawa interactions do not affect the final $B-L$ asymmetry and we recover an heavy neutrino flavour scenario. The density matrix, eq. (4.2.1), is then recast as

$$\begin{aligned}\frac{\mathrm{d}\, N^{B-L}_{\alpha\beta}}{\mathrm{d}\, z} &= \varepsilon^{(1)}_{\alpha\beta}\, D_1\,(N_{N_1} - N^{eq}_{N_1}) - \frac{1}{2}\, W_1 \left\{\mathcal{P}^{0(1)}, N^{B-L}\right\}_{\alpha\beta} \\ &+ \varepsilon^{(2)}_{\alpha\beta}\, D_2\,(N_{N_2} - N^{eq}_{N_2}) - \frac{1}{2}\, W_2 \left\{\mathcal{P}^{0(2)}, N^{B-L}\right\}_{\alpha\beta}.\end{aligned} \tag{4.2.8}$$

4.2.2.1 The projection effect in isolation

For illustrative purposes we focus first on the interplay between the heavy neutrino flavour states involved in the N_1 and N_2 dynamics. To simplify our task we first impose $\Delta p_{1\alpha} = \Delta p_{2\alpha} = 0$, neglecting in a first approximation the differences in the flavour compositions of the states associated to each heavy neutrino and consequently obtaining

$$|\ell_1\rangle = \mathcal{C}_{1\tau}\,|\ell_\tau\rangle + \mathcal{C}_{1\tau^\perp}\,|\ell_{\tau^\perp}\rangle\,, \qquad |\overline{\ell_1}\rangle = \mathcal{C}^\star_{1\tau}\,|\overline{\ell_\tau}\rangle + \mathcal{C}^\star_{1\tau^\perp}\,|\overline{\ell_{\tau^\perp}}\rangle \tag{4.2.9}$$

and

$$|\ell_2\rangle = \mathcal{C}_{2\tau}\,|\ell_\tau\rangle + \mathcal{C}_{2\tau^\perp}\,|\ell_{\tau^\perp}\rangle\,, \qquad |\overline{\ell_2}\rangle = \mathcal{C}^\star_{2\tau}\,|\overline{\ell_\tau}\rangle + \mathcal{C}^\star_{2\tau^\perp}\,|\overline{\ell_{\tau^\perp}}\rangle\,. \tag{4.2.10}$$

In the hierarchical limit, $M_2 \gtrsim 3\,M_1$ [99], the Leptogenesis process comprises two different stages. In the first one, for $T \sim M_2$, the out-of-equilibrium decays of N_2 generate an amount of $B-L$ asymmetry. The lepton density matrix is given here by $\rho^\ell_{ij} = \mathrm{Diag}(1,0)$ in the basis $\ell_2 - \ell_2^\perp$. Analogously the antilepton density matrix is given by $\rho^{\bar\ell}_{ij} = \mathrm{Diag}(1,0)$ in the basis $\bar\ell_2 - \bar\ell_2{}^\perp$, that, under our assumptions, is CP-conjugated to $\ell_2 - \ell_2^\perp$. As in the previous case the asymmetry production from N_2 is described by eq. (4.2.2), hence disregarding the phantom terms we simply have

$$\begin{aligned} N^{B-L}_{\tau\tau}(T \simeq T_{L2}) &\simeq p^0_{2\tau}\, N_{B-L}(T \simeq T_{L2}) \\ N^{B-L}_{\tau^\perp\tau^\perp}(T \simeq T_{L2}) &\simeq p^0_{2\tau^\perp}\, N_{B-L}(T \simeq T_{L2}) \end{aligned} \tag{4.2.11}$$

where $N_{B-L}(T \simeq T_{L2}) \simeq \varepsilon_2\,\kappa(K_2)$. We now have to consider the N_1 washout stage, taking place for $T \sim M_1$. As usual we neglect the N_1 asymmetry production imposing $\varepsilon^{(1)}_{\alpha\beta} \equiv 0$ and assume furthermore that $|\ell_1\rangle = |\ell_\tau\rangle$ and $|\overline{\ell_1}\rangle = |\overline{\ell_\tau}\rangle$ to simplify our discussion.

For $T \sim M_1$, the eq.s (4.2.8) for the asymmetry evolution in the charged-lepton flavour basis are simply rearranged as $(\alpha, \beta = \tau, \tau^\perp)$

$$\frac{\mathrm{d}\, N^{B-L}_{\alpha\beta}}{\mathrm{d}\, z} = -W_1 \begin{pmatrix} N^{B-L}_{\tau\tau} & \frac{1}{2}\, N^{B-L}_{\tau\tau^\perp} \\ \frac{1}{2}\, N^{B-L}_{\tau^\perp\tau} & 0 \end{pmatrix} \tag{4.2.12}$$

and at the end of the N_1-washout we therefore have

$$\begin{aligned} N^{B-L}_{\tau\tau}(T \simeq T_{L1}) &\simeq e^{-\frac{3\pi}{8} K_1}\, p^0_{2\tau}\, N_{B-L}(T \simeq T_{L2}) \\ N^{B-L}_{\tau^\perp\tau^\perp}(T \simeq T_{L1}) &\simeq p^0_{2\tau^\perp}\, N_{B-L}(T \simeq T_{L2}). \end{aligned} \tag{4.2.13}$$

Finally, when $T \sim 10^{12}$ GeV the charged-lepton interactions damp the off-diagonal terms and the τ and $\tau^\perp$ asymmetries are measured.

The above result is easily generalised to a less specific flavour configuration of N_1. The eq. (4.2.12) is now to be written in the basis $\ell_1 - \ell_1^\perp$

$$\frac{\mathrm{d}\, N^{B-L}_{i_1 j_1}}{\mathrm{d}\, z} = -W_1 \begin{pmatrix} N^{B-L}_{11} & \frac{1}{2}\, N^{B-L}_{11^\perp} \\ \frac{1}{2}\, N^{B-L}_{1^\perp 1} & 0 \end{pmatrix} \tag{4.2.14}$$

where $i_1, j_1 = 1, 1^\perp$, yielding the washout of the 11 term

$$N^{B-L}_{11}(T \simeq T_{L1}) = e^{-\frac{3\pi}{8} K_1}\, N^{B-L}_{11}(T \simeq T_{L2}) \tag{4.2.15}$$

and of off-diagonal terms. The $1^\perp 1^\perp$ component is instead left untouched. The asymmetry matrix for $T \sim T_{L2}$ can be written in the $\ell_1 - \ell_1^\perp$ basis by employing the rotation matrices of eq. (4.1.20)

$$N^{B-L}_{i_1 j_1}(T \simeq T_{L2}) = N^{T \simeq T_{L2}}_{B-L}\, R^{0(1)}_{i_1 \alpha}\, R^{0(2)\dagger}_{\alpha i_2} \begin{pmatrix} 1 & 0 \\ 0 & 0 \end{pmatrix} R^{0(2)}_{j_2 \beta}\, R^{0(1)\dagger}_{\beta j_1} \tag{4.2.16}$$

or, in a more contained way, by considering that

$$N^{B-L}(T \simeq T_{L2}) = N^{T \simeq T_{L2}}_{B-L}\, |\ell_2\rangle \langle \ell_2|\,. \tag{4.2.17}$$

Hence, we have

$$N^{B-L}_{i_1 j_1}(T \simeq T_{L2}) = N_{B-L}(T \simeq T_{L2}) \begin{pmatrix} p_{12} & \langle \ell_1 | \ell_2 \rangle \langle \ell_2 | \ell_{1^\perp} \rangle \\ \langle \ell_{1^\perp} | \ell_2 \rangle \langle \ell_2 | \ell_1 \rangle & 1 - p_{12} \end{pmatrix} \tag{4.2.18}$$

where $p_{12} \coloneqq |\langle \ell_1 | \ell_2 \rangle|^2$ as prescript by eq. (3.1.22). The final asymmetry is then calculated through

$$N^f_{B-L} = \mathrm{Tr}[N^{B-L}_{i_1 j_1}(T \simeq T_{L1})] = e^{-\frac{3\pi}{8} K_1}\, p_{12}\, N_{B-L}(T \simeq T_{L2}) + (1 - p_{12})\, N_{B-L}(T \simeq T_{L2}) \tag{4.2.19}$$

and rotated to the charged-lepton flavour basis as follows:

$$N^{B-L}_{\alpha\beta}(T \simeq T_{L1}) = R^{0(1)^\dagger}_{\alpha i_1}\, N^{B-L}_{i_1 j_1}(T \simeq T_{L1})\, R^{0(1)}_{j_1 \beta}\,. \tag{4.2.20}$$

For $T \simeq 10^{12}$ GeV the charged lepton interactions damp the off-diagonal terms without affecting the total asymmetry which is given by the trace of the density matrix and therefore results in eq. (4.2.19).

This result confirms the description of the heavy neutrino flavour effects proposed in Chapter 3. Correctly, the component of the asymmetry along $|\ell_1\rangle$ undergoes the N_1 washout, while the orthogonal component is not modified by the latter [98, 103]. On top of that, even the washout strength is exactly quantified in the factor $\exp[-(3\pi K_1/8)]$, independently of the value of K_1 [2].

As a last comment, it is straightforward to generalise the presented result to a possible N_1 asymmetry production, in which case the final asymmetry reads

$$N^f_{B-L} = \varepsilon_1\,\kappa(K_1) + \left(e^{-\frac{3\pi}{8}K_1}\,p_{12} + 1 - p_{12}\right)\,\varepsilon_2\,\kappa(K_2). \tag{4.2.21}$$

4.2.2.2 Projection effect and phantom Leptogenesis

We now account for the projection effect releasing the assumption made before on the flavour composition of the involved heavy neutrino flavour states. As we are going to show the result is a generalisation of eq. (4.2.21), with the phantom terms contributing to the determination of the final asymmetry. A first complication arises in relation to the basis in which to describe the N_1 washout. In this regard, notice that the bases ℓ_1–$\ell_1^\perp$ and $\overline{\ell_1} - \overline{\ell_1^\perp}$ here do not coincide. Therefore, to solve this ambiguity, we choose to describe the Leptogenesis process on the tree-level basis $1^0 - 1^{0\perp}$.
The heavy neutrino flavour states $|\ell_2\rangle$ and $|\overline{\ell_2}\rangle$ are then decomposed according to

$$|\ell_2\rangle = \langle\ell_{1^0}|\ell_2\rangle\,|\ell_{1^0}\rangle + \langle\ell_{1^{0\perp}}|\ell_2\rangle\,|\ell_{1^{0\perp}}\rangle\,, \qquad |\overline{\ell_2}\rangle = \langle\overline{\ell_{1^0}}|\overline{\ell_2}\rangle\,|\overline{\ell_{1^0}}\rangle + \langle\overline{\ell_{1^{0\perp}}}|\overline{\ell_2}\rangle\,|\overline{\ell_{1^{0\perp}}}\rangle \tag{4.2.22}$$

and equation (4.2.2) is recast as

$$\frac{\mathrm{d}\,N^{B-L}_{i^0_1 j^0_1}}{\mathrm{d}\,z} = \varepsilon^{(2)}_{i^0_1 j^0_1}\,D_2\,(N_{N_2} - N^{\mathrm{eq}}_{N_2}) - \frac{1}{2}\,W_2\,\left\{\mathcal{P}^{0(2)}, N^{B-L}\right\}_{i^0_1 j^0_1} \tag{4.2.23}$$

where $i^0_1, j^0_1 = 1^0, 1^{0\perp}$ and the superscript "0" indicates the tree-level expression of the associated quantity. Defining now $\Delta p_{21^0} \coloneqq |\langle\ell_{1^0}|\ell_2\rangle|^2 - \left|\langle\overline{\ell_{1^0}}|\overline{\ell_2}\rangle\right|$, we therefore obtain the following expressions for the flavoured asymmetries on the tree-level basis

$$N^{B-L}_{1^0 1^0}(T \simeq T_{L2}) \;\simeq\; p^0_{12}\,\varepsilon_2\,\kappa(K_2) - \frac{\Delta p_{21^0}}{2}\,\kappa(K_2/2) \tag{4.2.24}$$

$$N^{B-L}_{1^{0\perp} 1^{0\perp}}(T \simeq T_{L2}) \;\simeq\; (1 - p^0_{12})\,\varepsilon_2\,\kappa(K_2) + \frac{\Delta p_{21^0}}{2}\,\kappa(K_2/2). \tag{4.2.25}$$

As a last step we account for the washout and the asymmetry production due to N_1, yielding the final asymmetry:

$$N^f_{B-L} = \varepsilon_1\,\kappa(K_1) + \left[p^0_{12}\,e^{-\frac{3\pi}{8}K_1} + (1 - p^0_{12})\right]\,\varepsilon_2\,\kappa(K_2) + \left(1 - e^{-\frac{3\pi}{8}K_1}\right)\,\frac{\Delta p_{21^0}}{2}\,\kappa(K_2/2). \tag{4.2.26}$$

As expected the phantom terms result in additional contributions to N^f_{B-L}. We underline that accounting for the different flavour compositions of $|\ell_1\rangle$ and $|\overline{\ell_1}\rangle$ also leads to phantom terms during the N_1 Leptogenesis stage. These contributions however undergo no washout as the Leptogenesis era is concluded, hence they reciprocally cancel in the final asymmetry.

4.2.3 The two-flavour regime: $10^{12}\,\mathrm{GeV} \gg M_1, M_2$

Under the condition $M_1, M_2 \ll 10^{12}\,\mathrm{GeV}$ the asymmetry production takes place in a two-flavour regime for both the heavy neutrino species considered. The N_2 Leptogenesis stage as usual results in

$$N^{B-L}_{\tau\tau}(T \simeq T_{L2}) = \varepsilon_{2\tau}\,\kappa(K_{2\tau}), \qquad N^{B-L}_{\tau^\perp\tau^\perp}(T \simeq T_{L2}) = \varepsilon_{2\tau^\perp}\,\kappa(K_{2\tau^\perp}) \tag{4.2.27}$$

and assuming a strong washout regime for the relevant flavours, $K_{2\tau^\perp}, K_{2\tau} \gg 1$, the total asymmetry recovers eq. (3.2.51).
Consequently, when the temperature drops down to $T \sim M_1$, the washout process of N_1 are active and for the configuration depicted in Figure 4.2 we have

$$N^{B-L}_{\tau\tau}(T \simeq T_{L2}) = \varepsilon_{2\tau}\,\kappa(K_{2\tau})\,e^{-\frac{3\pi}{8}K_{1\tau}} \tag{4.2.28}$$

$$N^{B-L}_{\tau^\perp\tau^\perp}(T \simeq T_{L2}) = \varepsilon_{2\tau^\perp}\,\kappa(K_{2\tau^\perp})\,e^{-\frac{3\pi}{8}K_{1\tau^\perp}}. \tag{4.2.29}$$

At the same time the out-of-equilibrium decays of N_1 add on to the asymmetry produced in the N_2 Leptogenesis stage, leading to our final formula

$$N^{B-L}_{\tau\tau}(T \simeq T_{L1}) = \varepsilon_{2\tau}\,\kappa(K_{2\tau})\,e^{-\frac{3\pi}{8}K_{1\tau}} + \varepsilon_{1\tau}\,\kappa(K_{1\tau}) \tag{4.2.30}$$

$$N^{B-L}_{\tau^\perp\tau^\perp}(T \simeq T_{L1}) = \varepsilon_{2\tau^\perp}\,\kappa(K_{2\tau^\perp})\,e^{-\frac{3\pi}{8}K_{1\tau^\perp}} + \varepsilon_{1\tau^\perp}\,\kappa(K_{1\tau^\perp}). \tag{4.2.31}$$

4.3 A general formula

To conclude this Chapter we extend our results to the realistic case in which the three light flavours e, μ and τ are considered. The density matrix equations we proposed are now to be written in terms of 3×3 matrices and the analysis must allow for general orientations of the heavy neutrino flavour states in the flavour space.
A straightforward generalisation of eq. (4.2.1) then yields

$$\frac{\mathrm{d}\, N^{B-L}_{\alpha\beta}}{\mathrm{d}\, z} = \varepsilon^{(1)}_{\alpha\beta}\, D_1 \left(N_{N_1} - N^{eq}_{N_1}\right) - \frac{1}{2}\, W_1 \left\{\mathcal{P}^{0(1)}, N^{B-L}\right\}_{\alpha\beta} \tag{4.3.1}$$

$$+ \varepsilon^{(2)}_{\alpha\beta}\, D_2 \left(N_{N_2} - N^{eq}_{N_2}\right) - \frac{1}{2}\, W_2 \left\{\mathcal{P}^{0(2)}, N^{B-L}\right\}_{\alpha\beta}$$

$$+ \varepsilon^{(3)}_{\alpha\beta}\, D_3 \left(N_{N_3} - N^{eq}_{N_3}\right) - \frac{1}{2}\, W_3 \left\{\mathcal{P}^{0(3)}, N^{B-L}\right\}_{\alpha\beta}$$

$$- \mathrm{Im}(\Lambda_\tau) \left[\begin{pmatrix} 1 & 0 & 0 \\ 0 & 0 & 0 \\ 0 & 0 & 0 \end{pmatrix}, \left[\begin{pmatrix} 1 & 0 & 0 \\ 0 & 0 & 0 \\ 0 & 0 & 0 \end{pmatrix}, N^{B-L} \right] \right]_{\alpha\beta} \tag{4.3.2}$$

$$- \mathrm{Im}(\Lambda_\mu) \left[\begin{pmatrix} 0 & 0 & 0 \\ 0 & 1 & 0 \\ 0 & 0 & 0 \end{pmatrix}, \left[\begin{pmatrix} 0 & 0 & 0 \\ 0 & 1 & 0 \\ 0 & 0 & 0 \end{pmatrix}, N^{B-L} \right] \right]_{\alpha\beta}$$

where $\alpha, \beta = \tau, \mu, e$. The effect of the gauge interactions has been addressed in the evolution of the lepton and antilepton abundances – cf. eq. (4.1.42), resulting in the anticommutators presented by the washout terms.

The master equation that we propose can now be employed to calculate the final $B - L$ asymmetry not only for the ten mass patterns presented in Figure 4.1, but also when the heavy neutrino masses fall in one of the indicated transition regimes.
In these cases, though, solving the above equation is clearly much more difficult as at least two of the five considered Yukawa-interactions would be simultaneously active. This goes beyond the purpose of the present Thesis and therefore, also in the remaining of this work, we will consider only Leptogenesis processes with hierarchical heavy neutrinos within the fully-flavoured regimes introduced in Chapter 3. On top of that, as our analysis proved that under these conditions a multiple-stage Boltzmann equations setup effectively describes the Leptogenesis process, we will employ this simple formalism to specify the evolution of the $B - L$ asymmetry.

As a final remark we emphasise that for the expression given in eq. (4.1.29) for the CP-asymmetry matrix, our master formula in eq. (4.3.1) applies exclusively to scenarios presenting hierarchical heavy neutrinos. It is however straightforward to generalise our result to the complementary class of resonant Leptogenesis scenarios, in which case eq. (4.1.29) is to be modified in order to account for the resonant contributions in $\varepsilon^{(1)}_{\alpha\beta}$ [120] that we previously neglected.

Chapter 5

The problem of initial conditions in Leptogenesis

As a result of flavour effects we are forced to move beyond N_1 Leptogenesis, considering a *minimal scenario* where the predicted final asymmetry depends on all the 18 parameters that the Lagrangian in eq. (2.0.15) introduced in the Theory [121]. These describe the masses and mixings of heavy and light neutrinos, and whereas informations on the latter are given by the neutrino experiments reviewed in Section 1.1, the high energy sector of the Theory remains unexplored. Clearly, the implications from the Cosmological measurements of a baryon asymmetry that we presented in Section 1.2 result in one additional constraint on the Seesaw parameter space, nevertheless performing a complete scan of the latter seems apparently impossible.
In order to overcome this difficulty two complementary strategies are usually considered. A first one consists in restricting the parameter space by imposing additional conditions suggested by models of new Physics. In this regard, a remarkable example of this approach is presented in the next Chapter, where we analyse in detail the $SO(10)$-inspired model.
The second strategy imposes additional phenomenological constraints on the Seesaw parameter space, adding on those already provided by the low energy neutrino experiments and Leptogenesis. In this case, important examples falling within the models of Physics beyond the SM involve lepton flavour violation processes, the study of electric dipole moments and the attempts to explain Dark Matter with RH neutrinos [122–128].

There is however a further issue that should be addressed in order to safely explore the Seesaw parameter space, as the predicted final $B-L$ asymmetry could depend, on top of these 18 parameters, on the details of the cosmological history. The initial abundances of the heavy neutrinos and $B-L$ asymmetry are in fact sensitive, in principle, to the particular dynamics involved in the evolution of the Early Universe. It could be then sustained that, in analogy to the case of BBN, imposing thermal initial conditions for the

heavy neutrinos abundances would be enough to define a *strong thermal Leptogenesis scenario*, in which the final $B-L$ asymmetry can be calculated independently of a detailed knowledge of the initial conditions and the many other possible cosmological ongoing processes. As we will now show, unfortunately, this is not the case.

5.1 On the consequences of a preexisting asymmetry and the importance of strong thermal Leptogenesis

Thermal scenarios, on one hand, indeed address the issues related to the initial abundances of the heavy neutrinos. Assuming a thermal production of these particles would effectively explain their origin, provided the reheating temperature is high enough for the neutrino Yukawa interactions to thermalise the relative abundances. On the other hand, the problem related to a possible amount of $B-L$ asymmetry present in our Universe before the Leptogenesis era is still open. In this regard, for the high reheating temperatures involved, there are many mechanisms which could generate a large $B-L$ asymmetry prior to the onset of Leptogenesis. Examples include the Affleck-Dine mechanism, gravitational Baryogenesis and even the more traditional decays of the GUT bosons [67, 111, 129–132].
The important consequences that this preexisting asymmetry N_{B-L}^{preex} has on Leptogenesis follow from the linearity of the Boltzmann equations employed. At the end of the Leptogenesis process, the final amount of $B-L$ asymmetry N_{B-L}^{f} comprises in fact two contributions:

$$N_{B-L}^{f} = N_{B-L}^{lept,f} + N_{B-L}^{preex,f}. \tag{5.1.1}$$

The first term is the product of the heavy neutrino decays, hence it is completely determined by the considered Leptogenesis process. The second term, differently, represents the residual amount of preexisting asymmetry. The washout performed by the inverse-processes of the heavy neutrinos on N_{B-L}^{preex} can be quantified within every Leptogenesis model, nevertheless a precise calculation of the initial abundance of preexisting asymmetry is not viable, as it relies on an accurate description of the state of the Universe after the Inflation era. The magnitude of $N_{B-L}^{preex,f}$ is therefore unknown and, a priori, there is no reason to exclude preexisting contributions large enough to dominate the final $B-L$ asymmetry and consequently the same baryon asymmetry of the Universe. In this way, if the preexisting contribution is not addressed, the informations that BBN and CMB provide cannot be used to constrain the Seesaw parameter space, as it is not clear how to disentangle the two components in the final asymmetry. In this sense N_{B-L}^{preex} thus represents an *unknown and problematic initial condition* for all the models of Leptogenesis.

As anticipated, a possible solution to this problem is given by strong thermal Leptogenesis. In these scenarios the same processes of Leptogenesis wash out any possible

preexisting contribution, in a way that after the Leptogenesis era the $B-L$ asymmetry is necessarily dominated by $N_{B-L}^{lept,f}$. Strong thermal Leptogenesis thus ensures the independence from possible preexisting asymmetries and the – unknown – initial conditions therein encapsulated. Under these conditions the baryon asymmetry of the Universe is therefore determined by Leptogenesis only, and the Cosmological measurements can be safely used to constrain the parameter space of the associated model. In this way, on more practical grounds, any kind of constraint that the strong thermal solution impose on the considered scenario is certainly more solid.

5.2 A systematic study

Attracted by the features of strong thermal Leptogenesis, we seek a scenario where the following strong condition is fulfilled

$$\left|N_{B-L}^{lept,f}\right| \gg \left|N_{B-L}^{preex,f}\right| \tag{5.2.1}$$

without preventing successful Leptogenesis, realised for

$$N_{B-L}^{lept,f} \times 0.0096 = \eta_B^{lept} \sim \eta_B^{CMB} = (6.19 \pm 0.15) \times 10^{-10}. \tag{5.2.2}$$

As we will see, this check will not require an explicit calculation of $N_{B-L}^{lept,f}$, hence we focus here on the evolution of the preexisting asymmetry. As for this, to quantify the strength of the washout imposed on the latter by the Leptogenesis process, we introduce the *washout parameter*

$$w(z) \coloneqq \frac{N_{B-L}^{preex}(z)}{N_{B-L}^{preex,0}} \tag{5.2.3}$$

where $N_{B-L}^{preex,0} \coloneqq N_{B-L}^{preex}(z=0)$. The final value of the washout parameter, w^f, is then the crucial quantity which we aim to calculate in order to check whether the condition (5.2.1) holds.
As an example, for a preexisting asymmetry $N_{B-l}^{preex,0} \sim \mathcal{O}(1)$ inherited from an Affleck-Dine scenario of Inflation [67], the independence of the initial conditions requires $w^f \ll 10^{-8}$.

Considering unflavoured Leptogenesis scenarios, the calculation of the washout parameter is actually straightforward. For N_1 Leptogenesis, given the Boltzmann equations reported below

$$\frac{\mathrm{d}\, N_{N_1}}{\mathrm{d}\, z} = -D_1(z)\left(N_{N_1}(z) - N_{N_1}^{eq}(z)\right) \tag{5.2.4}$$

$$\frac{\mathrm{d}\, N_{B-L}}{\mathrm{d}\, z} = \epsilon_1\, D_1(z)\left(N_{N_1} - N_{N_1}^{eq}\right) - N_{B-L}\, W_1^{ID}(z) \tag{5.2.5}$$

we obtain for the final $B-L$ asymmetry – eq. (2.2.32):

$$N^{f}_{B-L} = N^{preex,0}_{B-L}\, e^{-\frac{3\pi}{8}K_1} + \varepsilon_1 \kappa^{f}_{1}. \tag{5.2.6}$$

Hence, we have $N^{lept,f}_{B-L} = \varepsilon_1 \kappa^{f}_{1}$ while $w^f = e^{-\frac{3\pi}{8}K_1}$ and it enough to impose a strong washout regime $K_1 \gtrsim 10$ to ensure $w^f \lesssim 10^{-8}$ and therefore the washout of a preexisting asymmetry of order $\mathcal{O}(1)$[1].

When flavour effects are taken into account these conclusions change dramatically. In [133] it was shown that a simple condition $K_1 \gtrsim 10$ is not sufficient to guarantee the complete washout of an $\mathcal{O}(1)$ preexisting asymmetry. This is possible only if $M_1 \ll 10^9\,\text{GeV}$ and if $K_{1\alpha} \equiv p^0_{1\alpha} K_1 \gtrsim 10$ for all $\alpha = e, \mu, \tau$, where we defined $K_{i\alpha}$ according to eq. (3.2.44). Notice however that such a drastic condition is not compatible with successful Leptogenesis: any asymmetry produced from the heavier neutrinos is washed out together with the preexisting asymmetry and, at the same time, the CP-asymmetries of N_1 are far too suppressed – cf. eq. (2.2.55). We consequently must extend our analysis to more general cases where the assumption $M_3, M_2 \gg T_i \gg M_1$ is relaxed and more heavy neutrino species are involved. In order to pin down the conditions for successful strong thermal Leptogenesis, assuming again hierarchical heavy neutrinos $M_{i>j} > 3M_j$, we follow the evolution of the preexisting asymmetry through the resulting multiple-stage Leptogenesis process.
In this regard, notice that in order to account for the light and heavy neutrino flavour effects, we have to specialise the treatment of the heavy neutrinos dynamics depending on the relevant fully flavoured regime. In our discussion we must therefore distinguish between the possible mass patterns defined with respect to these regimes – Figure 4.1 – and the same *heavy neutrino mass spectrum* consequently plays a key role in the analysis we present. This is the novelty of our work: a systematic study of the evolution of N^{preex}_{B-L} for the many possible scenarios that the interplay between light and heavy neutrino flavour effects creates.

The preexisting asymmetry $N^{preex,0}_{B-L}$ is generally shared not only between lepton doublets, but also between the RH charged-leptons and quarks. Nevertheless, by assuming that $T < 10^{14}$ GeV throughout the analysis, the sphaleron processes are in equilibrium and the asymmetries in the different species are related according to the conditions that we presented in Section 2.2.0.1. In particular, the preexisting $B-L$ asymmetry in then related to the one in the lepton doublets by – cf. eq. (2.2.10)

$$N_{\ell_p} \simeq -\frac{2}{3} N^{preex}_{B-L} \tag{5.2.7}$$

hence, assuming that only the heavy neutrino decays and inverse processes modify the $B-L$ asymmetry, any change in N^{preex}_{B-L} can only be triggered by a variation in N_{ℓ_p}.

[1] In order to quantify the required w^f, in the present Chapter we will always refer to an abundance of initial preexisting asymmetry as large as $\mathcal{O}(1)$.

In analogy to the heavy neutrino flavour states, the leptons responsible for this preexisting asymmetry can also be regarded as a coherent superposition of light flavour states:

$$|\ell_p\rangle \coloneqq \sum_{\alpha=e,\mu,\tau} \mathcal{C}_{p\alpha} |\ell_\alpha\rangle , \qquad \mathcal{C}_{p\alpha} \coloneqq \langle \ell_\alpha | \ell_p \rangle \tag{5.2.8}$$

$$|\overline{\ell_p}\rangle \coloneqq \sum_{\alpha=e,\mu,\tau} \overline{\mathcal{C}}_{p\alpha} |\overline{\ell_\alpha}\rangle , \qquad \overline{\mathcal{C}}_{p\alpha} \coloneqq \langle \ell_\alpha | \ell_p \rangle . \tag{5.2.9}$$

In general, $\mathcal{C}^*_{p\alpha} \neq \overline{\mathcal{C}}_{p\alpha}$ and therefore the preexisting leptons $|\ell_p\rangle$ and antileptons $|\overline{\ell_p}\rangle$ are not CP-conjugated states. To simplify our analysis we will however impose $\mathcal{C}^*_{p\alpha} = \overline{\mathcal{C}}_{p\alpha}$[2] and introduce, with clear meaning of the notation, the probabilities

$$p_{p\alpha} \coloneqq |\mathcal{C}_{i\alpha}|^2 \tag{5.2.10}$$

and

$$p_{pi} \coloneqq |\langle \ell_i | \ell_p \rangle|^2 = \left| \sum_{\alpha=e,\mu,\tau} \mathcal{C}^*_{i\alpha} \mathcal{C}_{p\alpha} \right|^2 \tag{5.2.11}$$

respectively satisfying

$$\sum_{\alpha=e,\mu,\tau} p_{p\alpha} = 1 \tag{5.2.12}$$

and

$$p_{pi} + p_{pi^\perp_p} = 1, \qquad i = 1,2,3. \tag{5.2.13}$$

These sets of probabilities regulate the interplay between the preexisting leptons – and antileptons –, the heavy neutrino flavour states and the light flavour ones. As mentioned before, the preexisting leptons are in fact subject to the same flavour effects that we discussed in Chapter 3, the projection effect and consecutive washout due to the heavy neutrino inverse-decays in particular. Whether these processes will take place in a heavy neutrino flavour, two-flavour or three-flavour regime is strictly controlled by the heavy neutrino mass spectrum.

We start our discussion with the so-called heavy neutrino flavour scenario, where all the three heavy neutrino masses satisfy the condition $M_i > 10^{12}$ GeV and the three stages of the Leptogenesis process therefore take place in the heavy neutrino flavour regime.

5.2.1 Heavy neutrino flavour scenario

The heavy neutrino mass pattern associated to this scenario is presented in Figure 5.1. In this regime the relevant flavour directions are those associated to the heavy neautrino flavour states, since the charged-lepton Yukawa interactions are not fast enough to effectively measure the light flavour composition of the states involved. As a working hypothesis we assume an initial temperature $T_i \gg M_3$, so that all the three heavy

[2] We will review this assumption when presenting our conclusions in Chapter 7, especially in connection to the phantom terms of Section 4.1 .

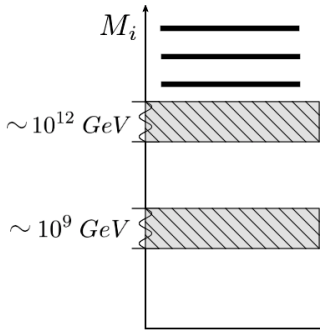

Figure 5.1: The heavy neutrino mass pattern defining the heavy neutrino flavour scenario.

neutrino species are effectively thermalised and can washout the preexisting asymmetry. Should we prove that some fraction of the preexisting asymmetry survives in this, most conservative, case, then some – at least equal – part will necessarily survive also in heavy neutrino flavour scenarios involving less neutrino species.

5.2.1.1 First stage: $T_i > T \gg M_3$

There are different stages in the evolution of $N^{preex}_{B-L}(z)$. In the first one, for $T_i > T \gg M_3$, all the heavy neutrino processes are ineffective and the $B-L$ asymmetry does not evolve. The preexisting leptons and antileptons can then be regarded as coherent superpositions of two flavour states: a component parallel to $|\ell_3\rangle$ and an orthogonal one. Explicitly we have

$$|\ell_p\rangle = \mathcal{C}_{p3}\,|\ell_3\rangle + \mathcal{C}_{p3^\perp_p}\,|\ell_{3^\perp_p}\rangle \tag{5.2.14}$$

and clearly

$$p_{p3} + p_{p3^\perp_p} = |\mathcal{C}_{p3}|^2 + \left|\mathcal{C}_{p3^\perp_p}\right|^2 = 1. \tag{5.2.15}$$

This decomposition is depicted in the upper-right panel of Figure 5.2, and a similar analysis holds and is understood for the preexisting antileptons. In this regard, under the given assumptions we have $\overline{p}_{p3} = p_{p3}$ and also $\overline{p}_{p3^\perp_p} = p_{p3^\perp_p}$, hence the preexisting $B-L$ asymmetry can be decomposed as

$$N^{preex,0}_{B-L} = N^{preex,0}_{\Delta_3} + N^{preex,0}_{\Delta_{3^\perp_p}} \tag{5.2.16}$$

where we defined $N^{preex,0}_{\Delta_3} = p_{p3}\,N^{preex,0}_{B-L}$ and $N^{preex,0}_{\Delta_{3^\perp_p}} = (1-p_{p3})\,N^{preex,0}_{B-L}$.

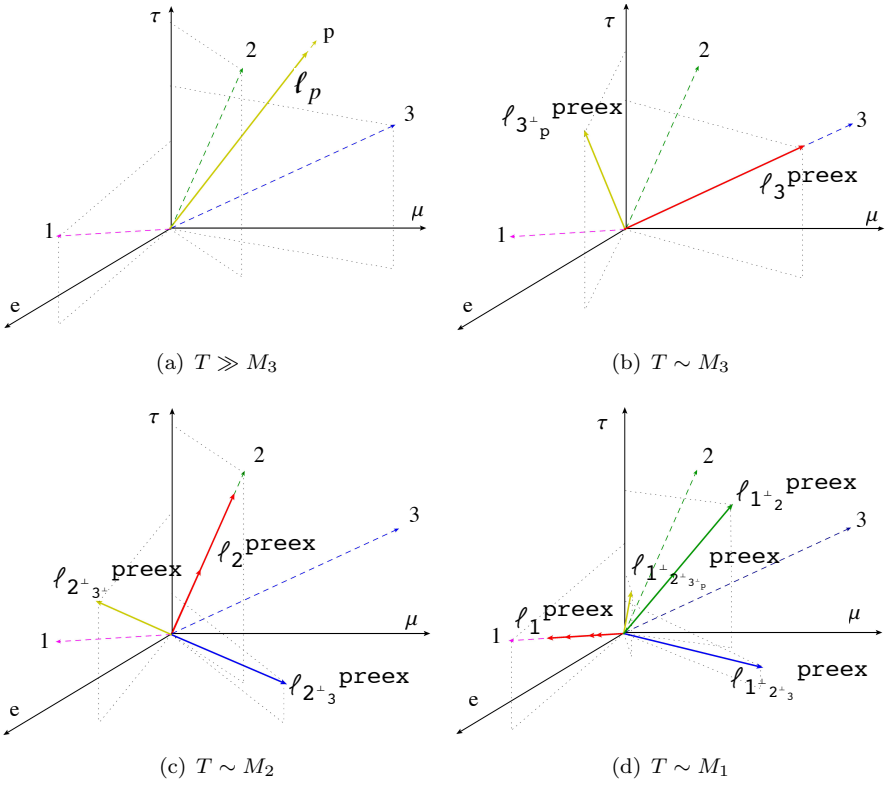

Figure 5.2: The four stages of the heavy neutrino flavour scenario. In a first step, for $T \gg M_3$ (a), the preexisting leptons are a coherent superposition of light flavour states. When $T \sim M_3$ (b), the N_3 decays and inverse-processes break the coherent evolution of $|\ell_p\rangle$ that becomes an incoherent mixture comprising an $|\ell_3\rangle$ and an $|\ell_{3^{\perp}_{p}}\rangle$ states. The ket notation represents here the direction of the associated preexisting component in the flavour space. For $T \sim M_2$ (c), these states are both re-projected with respect to the direction associated to the heavy neutrino decay direction "2". We indicate respectively with ℓ_i^{preex} and $\ell_{i^{\perp}_{j}}^{preex}$ the preexisting leptons components of flavour compositions "i" and "j" that contribute to the residual preexisting asymmetry and experienced a different washout history. For example, ℓ_i^{preex} is the component of ℓ^{preex} that underwent a washout performed by the inverse-decays of N_i. In the same way $\ell_{1^{\perp}_{2}}^{preex}$ is the component of ℓ^{preex} that has been first measured along ℓ_2, underwent the relevant washout, and finally has been measured on a direction orthogonal to ℓ_1. This component will therefore escape the washout from the latter. In each stage the red arrows indicate the components which are subject to a washout, the yellow ones instead represent those left untouched. We remark that at any stage components with a different washout history might be measured in the same quantum state and therefore be projected on a common direction.
For $T \sim M_1$ (d), the $|\ell_2\rangle$ and the orthogonal components are finally projected along "1" and the relative orthogonal directions, identified by the states $|\ell_1\rangle$ and $|\ell_{1^{\perp}_{i}}\rangle$. This stage therefore comprises 8 contributions to the final asymmetry that experienced different washout histories. Notice the yellow component which is completely 'unwashed'.

5.2.1.2 Second stage: $M_3 \gtrsim T \gtrsim T_{L3}$

We discuss now the second stage of the heavy neutrino flavour scenario, taking place for $M_3 \gtrsim T \gtrsim T_{L3}$, where $T_{L3} \simeq M_3/z_{L3}$ is the freeze-in temperature of the N_3 inverse processes and $z_{B3} = \mathcal{O}(1-10)$ is defined in eq. (2.2.43). The interaction of a quantum lepton state $|\ell_p\rangle$ with a Higgs doublet can be regarded, in a statistical picture, as a measurement process. We thus have a probability p_{p3} that $|\ell_p\rangle$ *collapse* on $|\ell_3\rangle$, producing a N_3 in the inverse-decay, and a probability $1-p_{p3}$ that the same state be measured as $|\ell_{3^\perp p}\rangle$. In the latter case no inverse-process occurs[3]. In this way, supposing a strong washout regime, only the component $N^{preex,0}_{\Delta_3}$ of the preexisting $B-L$ asymmetry is erased, while the orthogonal component $N^{preex,0}_{\Delta_{3^\perp_p}}$ is left untouched – Figure 5.2 (b).

Beside the preexisting asymmetry, we should take also into account the $B-L$ production due to the states $|\ell_3\rangle$ and $|\overline{\ell_3}\rangle$ arising from the CP-violating decays of the heaviest neutrinos N_3. Within the adopted classical description we can employ the Boltzmann equations to describe the relevant dynamics. For the present stage these simply read – cf. Section 3.1.2 –

$$\frac{\mathrm{d}\, N_{N_3}}{\mathrm{d}\, z_3} = -D_3\,(N_{N_3} - N^{eq}_{N_3}) \tag{5.2.17}$$

$$\frac{\mathrm{d}\, N_{\Delta_3}}{\mathrm{d}\, z_3} = \varepsilon_3\, D_3\,(N_{N_3} - N^{eq}_{N_3}) - W_3\, N_{\Delta_3} \tag{5.2.18}$$

$$\frac{\mathrm{d}\, N_{\Delta_{3^\perp_p}}}{\mathrm{d}\, z_3} = 0. \tag{5.2.19}$$

The evolution of the asymmetry produced from the heavy neutrino decays within the heavy neutrino flavour regime has already been discussed in Section 3.1.2. As previously mentioned, we focus here here only the dynamics involving the residual preexisting asymmetry. After this stage, for $T \sim T_{L3}$, the latter is then

$$N^{preex}_{B-L}(T_{L3}) = N^{preex,0}_{\Delta_3}\, e^{-\frac{3\pi}{8} K_3} + N^{preex,0}_{\Delta_{3^\perp_p}} = \tag{5.2.20}$$

$$= p_{p3}\, N^{preex,0}_{B-L}\, e^{-\frac{3\pi}{8} K_3} + (1-p_{p3})\, N^{preex,0}_{B-L} \tag{5.2.21}$$

and the corresponding washout factor is therefore

$$w(T_{L3}) = p_{p3}\, e^{-\frac{3\pi}{8} K_3} + 1 - p_{p3}. \tag{5.2.22}$$

Clearly no condition can be imposed on the Seesaw parameters in order to guarantee an efficient washout of the preexisting asymmetry characterised by a generic flavour composition – $p_{p3} \neq 1$. If we impose $K_3 \gg 1$, at the end of the present stage the lepton doublets are an incoherent mixture of $|\ell_3\rangle$ and $|\ell_{3^\perp_p}\rangle$ states. Analogously the antileptons

[3] An analogous situation is presented by active-sterile neutrino oscillations when described in terms of classical Boltzmann equations [134, 135]. The orthogonal component plays here the role of the sterile component.

are an incoherent mixture of $|\overline{\ell_3}\rangle$ and $|\overline{\ell_{3_p^\perp}}\rangle$ and only the asymmetry in the components along "3" is efficiently washed out.

5.2.1.3 Third stage: $T_{L3} \gtrsim T \gtrsim T_{L2}$

In the subsequent stage, for $T \sim M_2$ the N_2 inverse processes are active. The quantum states $|\ell_3\rangle$ and the $|\ell_{3_p^\perp}\rangle$ either collapse onto $|\ell_2\rangle$ or on the orthogonal directions containing $|\ell_{2_i^\perp}\rangle$, $i = 3, p$. We therefore perform exactly the same decomposition as in the previous stage, writing the inherited residual preexisting asymmetry as the sum of two terms

$$N_{B-L}^{preex}(T_{L3}) = N_{\Delta_2}^{preex}(T_{L3}) + N_{\Delta_{2^\perp}}^{preex}(T_{L3}) \tag{5.2.23}$$

where

$$\begin{aligned} N_{\Delta_2}^{preex}(T_{L3}) &= p_{32}\, N_{\Delta_3}^{preex}(T_{L3}) + p_{3_p^\perp 2}\, N_{\Delta_{3_p^\perp}}^{preex}(T_{L3}) = \\ &= p_{32}\, p_{p3}\, N_{B-L}^{preex,0}\, e^{-\frac{3\pi}{8} K_3} + p_{3_p^\perp 2}\,(1 - p_{p3})\, N_{B-L}^{preex,0} \end{aligned} \tag{5.2.24}$$

and

$$\begin{aligned} N_{\Delta_{2^\perp}}^{preex}(T_{L3}) &= (1 - p_{32})\, N_{\Delta_3}^{preex}(T_{L3}) + (1 - p_{3_p^\perp 2})\, N_{\Delta_{3_p^\perp}}^{preex}(T_{L3}) = \\ &= (1 - p_{32})\, p_{p3}\, N_{B-L}^{preex,0}\, e^{-\frac{3\pi}{8} K_3} + (1 - p_{3_p^\perp 2})\,(1 - p_{p3})\, N_{B-L}^{preex,0}. \end{aligned} \tag{5.2.25}$$

These are the two terms of the asymmetry that provide the initial conditions for the processes involving N_2. The relevant Boltzmann equations are obtained from the eq.s (5.2.18) presented in the previous stage, by means of a simple replacement of the labels $3 \to 2$. Explicitly we have

$$\frac{\mathrm{d}\, N_{N_2}}{\mathrm{d}\, z_2} = -D_2\,(N_{N_2} - N_{N_2}^{eq}) \tag{5.2.26}$$

$$\frac{\mathrm{d}\, N_{\Delta_2}}{\mathrm{d}\, z_2} = \varepsilon_2\, D_2\,(N_{N_2} - N_{N_2}^{eq}) - W_2\, N_{\Delta_2} \tag{5.2.27}$$

$$\frac{\mathrm{d}\, N_{\Delta_{2^\perp}}}{\mathrm{d}\, z_2} = 0. \tag{5.2.28}$$

and it is straightforward to give an expression for the residual preexisting asymmetry at $T \sim T_{L2}$:

$$N_{B-L}^{preex}(T_{L2}) = N_{\Delta_2}^{preex}(T_{L3})\, e^{-\frac{3\pi}{8} K_2} + N_{\Delta_{2^\perp}}^{preex}(T_{L3}). \tag{5.2.29}$$

Imposing now $K_2, K_3 \gtrsim 10$, we neglect all the terms which are exponentially suppressed, hence[4]

$$N_{B-L}^{preex}(T_{L2}) = N_{\Delta_{2^\perp_{3^\perp_p}}}^{preex}(T_{L3}) \tag{5.2.30}$$

and the washout factor reduces to

$$w(T_{L2}) \simeq (1 - p_{3^\perp_p 2})\,(1 - p_{p3}). \tag{5.2.31}$$

This result shows that in general, even at this stage that comprises the washout processes performed by two heavy neutrinos, no condition can be imposed on the Seesaw parameters to guarantee an efficient washout of a generic preexisting asymmetry.

5.2.1.4 Fourth stage: $T_{L2} \gtrsim T \gtrsim T_{L1}$

The washout process from the lightest heavy neutrino species can now be calculated along the same lines as above. At the end of the present stage, for $T \sim T_{L1}$, the asymmetry freezes-in at its final value, given by

$$N_{B-L}^{preex}(T_{L1}) \equiv N_{B-L}^{preex,f} = N_{\Delta_1}^{preex}(T_{L2})\, e^{-\frac{3\pi}{8} K_1} + N_{\Delta_{1^\perp}}^{preex}(T_{L1}). \tag{5.2.32}$$

By splitting the last term on the RHS of the previous equation into two components, the residual preexisting asymmetry can now be written as

$$N_{B-L}^{preex,f} = N_{\Delta_1}^{preex,f}(T_{L1}) + N_{\Delta_{1^\perp_2}}^{preex,f}(T_{L1}) + N_{\Delta_{1^\perp_{2^\perp}}}^{preex,f}(T_{L1}) \tag{5.2.33}$$

and comprises eight different contributions. More in detail, the first term accounts for the residual preexisting asymmetry found along the states of heavy neutrino decay direction "1"

$$\begin{aligned} N_{\Delta_1}^{preex,f}(T_{B1}) \;=\; & N_{B-L}^{preex,0} \Big[p_{21}\, p_{32}\, p_{p3}\, e^{-\frac{3\pi}{8}(K_1+K_2+K_3)} + \\ & + p_{21}\, p_{3^\perp_p 2}\,(1 - p_{p3})\, e^{-\frac{3\pi}{8}(K_1+K_2)} + \\ & + p_{2^\perp_3 1}\,(1 - p_{32})\, p_{p3}\, e^{-\frac{3\pi}{8}(K_1+K_3)} + \\ & + p_{2^\perp_{3^\perp_p} 1}\,(1 - p_{3^\perp_p 2})\,(1 - p_{p3})\, e^{-\frac{3\pi}{8} K_1} \Big]. \end{aligned} \tag{5.2.34}$$

[4] Notice that the notation $\ell_{x^\perp_{y^\perp}}^{preex}$ indicates components obtained by projecting the preexisting quantum state $|\ell_p\rangle$ and $|\overline{\ell_p}\rangle$ first on a plane orthogonal to the flavour y, and then on the plane orthogonal to the flavour x. Hence, with $N_{\Delta_{x^\perp_{y^\perp}}}^{preex}$ we indicate the asymmetry stored in these states.

The second term is the contribution brought by the $|\ell_{1_2^\perp}\rangle$ leptons and the relative anti-leptons, quantified in

$$N^{preex,f}_{\Delta_{1_2^\perp}}(T_{B1}) = N^{preex,0}_{B-L}\left[(1-p_{21})\,p_{32}\,p_{p3}\,e^{-\frac{3\pi}{8}(K_2+K_3)} + \right. \\ \left. +(1-p_{21})\,p_{3_p^\perp 2}\,(1-p_{p3})\,e^{-\frac{3\pi}{8}K_2}\right]. \tag{5.2.35}$$

Finally, the third contribution arising from the lepton states $|\ell_{1_{2^\perp}^\perp}\rangle$ and the associated antileptons, is given by

$$N^{preex,f}_{\Delta_{1_{2^\perp}^\perp}}(T_{B1}) = N^{preex,0}_{B-L}\left[(1-p_{2_3^\perp 1})\,(1-p_{32})\,p_{p3}\,e^{-\frac{3\pi}{8}K_3} + \right. \\ \left. +(1-p_{2_{3_p^\perp}^\perp 1})\,(1-p_{3_p^\perp 2})\,(1-p_{p3})\right]. \tag{5.2.36}$$

This is our final result for the residual value of the preexisting asymmetry. Of the reported eight terms, seven undergo at least one washout process resulting in an exponential suppression and only one component escapes the washout of the three heavy neutrinos. Imposing $K_1, K_2, K_3 \gtrsim 10$ therefore erases seven contributions and the final value of the washout factor is then dominated by the remaining one, left completely unwashed. Explicitly we have

$$w^f \simeq (1-p_{2_{3_p^\perp}^\perp 1})\,(1-p_{3_p^\perp 2})\,(1-p_{p3}). \tag{5.2.37}$$

It is clear that, barring very special situations, the washout of a preexisting asymmetry cannot be enforced in the considered scenario. These special situations are realised either when the preexisting leptons and antileptons lie along the decay direction of the heaviest neutrino – $p_{p3} = 1$ – or when the heavy neutrino flavour states form an orthonormal basis – in which case, necessarily $p_{3_{2_p^\perp}^\perp 1} = 1$. The latter configuration corresponds to a special Dirac mass matrix obtained by an orthogonal matrix Ω – eq. (2.2.48) that is either the identity or one of its permutations. These special forms correspond to so called form dominance models [136] and are enforced typically by discrete flavour symmetries, such as $A4$ [137], invoked in order to reproduce the tri-bimaximal mixing [138]. However, notice that in the limit of exact form dominance, the total [139] and the flavour CP-asymmetries vanish [140] and deviations from the orthogonality condition are therefore necessary. In models employing discrete symmetries, for example, this deviation has to be of the order of the symmetry breaking parameter $\xi \sim 10^{-2}$ to generate the correct $B-L$ asymmetry. Nevertheless, the same small deviations yields $w^{\rm f} \sim \xi$ in our case, which still is not sufficient to guarantee an efficient washout of an asymmetry as large as $\mathcal{O}(1)$.

5.2.2 Light flavour scenarios

In this Section we consider heavy neutrino mass patterns in which at least one M_i is below 10^{12} GeV. The preexisting lepton states $|\ell_p\rangle$ and $|\overline{\ell_p}\rangle$ are therefore partially or fully projected on the light flavour basis, depending on whether the N_i decays and inverse-processes are active in a two or three-flavour regime.

5.2.2.1 Two-flavour scenarios

We start by analysing the three mass patterns obtained for $M_1 \gg 10^9$ GeV, reported in Figure 5.3, where only the τ component is 'measured' through the tau charged-lepton Yukawa interactions.

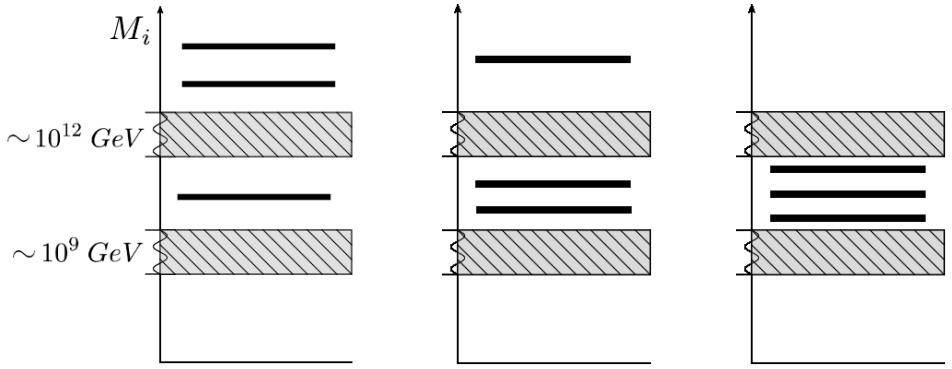

Figure 5.3: The three mass patterns of the two-flavour scenarios, where at least for one heavy neutrino 10^9 GeV $< M_i < 10^{12}$ GeV.

- **Pattern I: $\mathbf{M_2, M_3 \gg 10^{12}}$ GeV**
  The first case we consider presents the two heaviest neutrinos with masses $M_2, M_3 \gg 10^{12}$ GeV, while the mass of the lightest heavy neutrino satisfies 10^{12} GeV$\gg M_1 \gg 10^9$ GeV. The evolution of the residual preexisting asymmetry, N_{B-L}^{preex}, proceeds here through the same steps which we discussed in the heavy neutrino flavour scenario until the end of the N_2 washout, for $T \sim T_{L2}$. At that stage the asymmetry is given by eq. (5.2.29) and by supposing that $K_3 \geqslant 10$ we can safely neglect the terms suppressed by the associated exponential factor. An important difference arises now between the two scenarios. In the light flavour case we are considering, before the onset of the N_1 washout processes, the tau charged-lepton interactions enter equilibrium. The τ component of the involved quantum states are consequently 'measured' and the resulting incoherent mixture therefore comprises components along the following three states: $|\ell_\tau\rangle$, the projection of $|\ell_2\rangle$ on the plane orthogonal to τ $|\ell_{\tau_2^\perp}\rangle$, and $|\ell_{\tau_{2^\perp}^\perp}\rangle$, resulting from the projection of the remaining preexisting

leptons on the $\tau^{\perp}$ plane[5]. The residual value of the preexisting asymmetry can then be decomposed accordingly:

$$N^{preex}_{B-L}(10^{12}\,\mathrm{GeV} \gg T \gg M_1) = N^{preex}_{\Delta_\tau} + N^{preex}_{\Delta_{\tau^{\perp}_2}} + N^{preex}_{\Delta_{\tau^{\perp}_{2^{\perp}}}} \tag{5.2.38}$$

where

$$\begin{aligned} N^{preex}_{\Delta_\tau} &= p_{2\tau}\, N^{preex}_{\Delta_2}(T_{L3})\, e^{-\frac{3\pi}{8} K_2} + p_{2^{\perp}\tau}\, N^{preex}_{\Delta_{2^{\perp}}}(T_{L3}) && (5.2.39)\\ N^{preex}_{\Delta_{\tau^{\perp}_2}} &= (1-p_{2\tau})\, N^{preex}_{\Delta_2}(T_{L3})\, e^{-\frac{3\pi}{8} K_2} \\ N^{preex}_{\Delta_{\tau^{\perp}_{2^{\perp}}}} &= (1-p_{2^{\perp}\tau})\, N^{preex}_{\Delta_{2^{\perp}}}(T_{L3}). && (5.2.40) \end{aligned}$$

The N_1 washout processes act then on the preexisting asymmetry and, in this regard, we must distinguish between the washout acting along the τ direction, controlled by $K_{1\tau} \equiv p^0_{1\tau} K_1$ – cf eq. (3.2.44) – and the one acting on $N^{preex}_{\Delta_{\tau^{\perp}_1}}$, regulated by $K_{1\tau^{\perp}} := (1-p^0_{1\tau})\, K_1$. At the end of this stage, for $T \sim T_{L1}$, $N^{preex}_{\Delta_\tau}$ is therefore given by

$$N^{preex}_{\Delta_\tau}(T_{L1}) = \left[p_{2\tau}\, N^{preex}_{\Delta_2}(T_{L3})\, e^{-\frac{3\pi}{8} K_2} + p_{2^{\perp}\tau}\, N^{preex}_{\Delta_{2^{\perp}}}(T_{L3})\right] e^{-\frac{3\pi}{8} K_{1\tau}} \tag{5.2.41}$$

and by imposing $K_{1\tau} \gtrsim 10$ this component is completely washed out. In the same way, for $K_2 \gtrsim 10$, the washout of $N^{preex}_{\Delta_{\tau^{\perp}_2}}$ is also enforced. The contribution $N^{preex}_{\Delta_{\tau^{\perp}_{2^{\perp}}}}$ is not modified by either of the above conditions and is to be now decomposed as the sum of two terms: $N^{preex}_{\Delta_{\tau^{\perp}_1}}$, accounting for the asymmetry stored in the states resulting from the projection of $|\ell_{\tau^{\perp}_{2^{\perp}}}\rangle$ on the direction delineated by $|\ell_{\tau^{\perp}_1}\rangle$, and $N^{preex}_{\Delta_{\tau^{\perp}_{1^{\perp}}}}$, due to the states orthogonal both to $|\ell_1\rangle$ and to $|\ell_\tau\rangle$. The first term is then exponentially washed out by N_1 inverse processes

$$N^{preex}_{\Delta_{\tau^{\perp}_1}}(T_{L1}) = p_{\tau^{\perp}_{2^{\perp}}\tau^{\perp}_1}\,(1-p_{2^{\perp}\tau})\, N^{preex}_{\Delta_{2^{\perp}}}(T_{L3})\, e^{-\frac{3\pi}{8}(K_1-K_{1\tau})} \tag{5.2.42}$$

while the second one is not:

$$N^{preex}_{\Delta_{\tau^{\perp}_{1^{\perp}}}}(T_{L1}) = (1-p_{\tau^{\perp}_{2^{\perp}}\tau^{\perp}_1})\,(1-p_{2^{\perp}\tau})\, N^{preex}_{\Delta_{2^{\perp}}}(T_{L3}). \tag{5.2.43}$$

Employing now eq. (5.2.25) for an explicit expression of $N^{preex}_{\Delta_{2^{\perp}}}(T_{L3})$, it is clear that also in the limit $K_3 \geqslant 10$ there is still a completely unwashed term, generated by the preexisting states orthogonal to the heavy neutrino decay direction "3". In

[5] In principle for these states we should distinguish between the preexisting leptons, $\ell^{preex}_{\tau^{\perp}_{2^{\perp}_{3^{\perp}_p}}}$ and $\ell^{preex}_{\tau^{\perp}_{2^{\perp}_3}}$, anyway the strong washout regime we imposed for the dynamics of N_3 already erased the asymmetry associated to the latter and we can safely disregard its further evolution.

detail

$$N^{preex}_{\Delta_{\tau_{1^\perp}^\perp \tau_{1^\perp}^\perp}}(T_{L1}) = (1 - p_{\tau_{2^\perp}^\perp \tau_{1^\perp}^\perp})\,(1 - p_{2^\perp \tau})\,(1 - p_{3_{\tilde{p}}^\perp 2})\,(1 - p_{p3})\,N^{preex,0}_{B-L} \tag{5.2.44}$$

and it follows that, even by imposing $K_{1\tau}, K_2, K_3, (K_1 - K_{1\tau}) \gtrsim 10$, it is

$$w^f \simeq (1 - p_{\tau_{2^\perp}^\perp \tau_{1^\perp}^\perp})\,(1 - p_{2^\perp \tau})\,(1 - p_{3_{\tilde{p}}^\perp 2})\,(1 - p_{p3}). \tag{5.2.45}$$

Consequently, in this scenario, there is no efficient washout of the preexisting asymmetry which is affected here only by the reduction resulting from the proposed geometrical projections. It is therefore clear that, also in the present case, a sensible fraction of a large preexisting asymmetry escapes the washout performed by the three heavy neutrinos inverse-processes. The fundamental stages of our analysis are summarised in Figure 5.4.

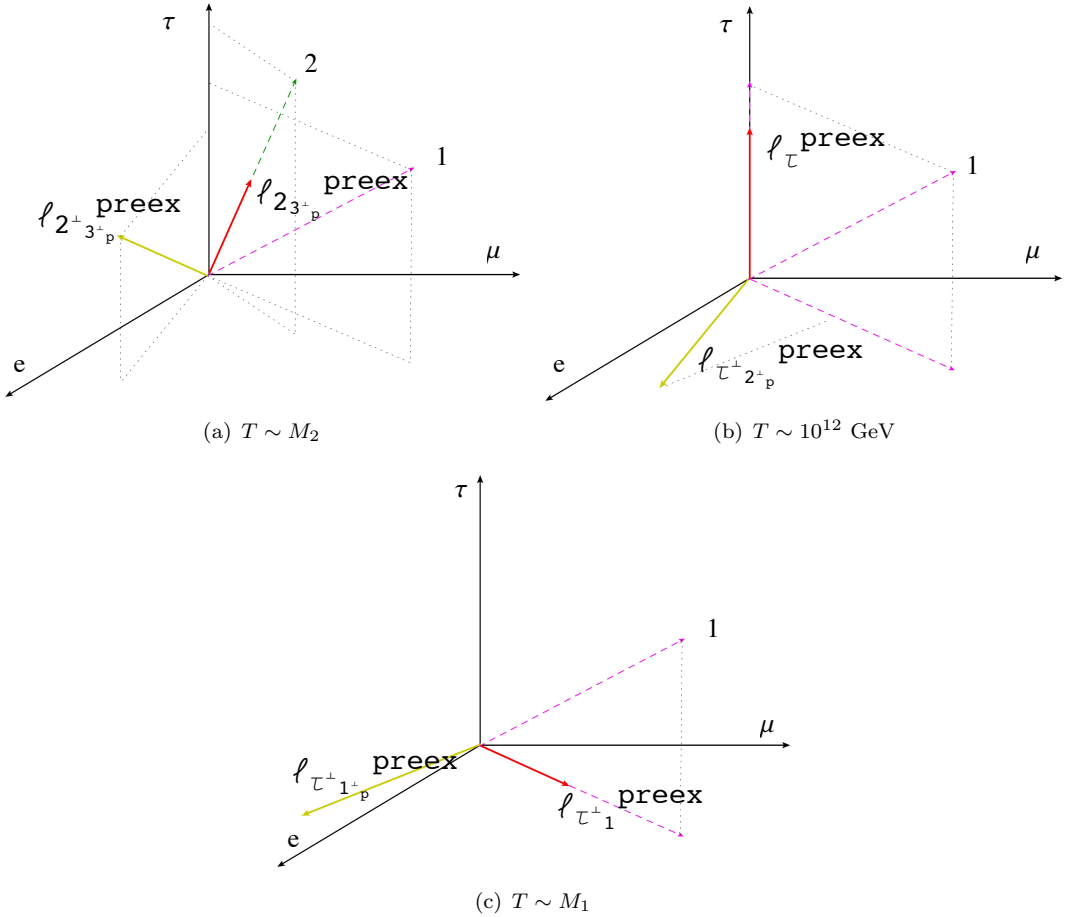

(a) $T \sim M_2$

(b) $T \sim 10^{12}$ GeV

(c) $T \sim M_1$

Figure 5.4: The three main steps for the evolution of the residual preexisting asymmetry in the two-flavour scenario characterised by $M_2, M_3 \gg 10^{12}$ GeV and 10^{12} GeV $\gg M_1 \gg 10^9$ GeV.

- **Pattern II: $\mathbf{M_3 \gg 10^{12}\ GeV \gg M_2 \gg M_1 \gg 10^9\ GeV}$**
  It is straightforward to extend the result in eq. (5.2.45) to a scenario where $M_3 \gg 10^{12}$ GeV $\gg M_2 \gg M_1 \gg 10^9$ GeV. The derivation of the washout factor is in fact slightly different from the one in the previous case.
  As before, we impose the condition $K_3 \gtrsim 10$ to washout at $T \sim M_3$ the component $N_{\Delta_3}^{preex} = p_{p3}\, N_{B-L}^{preex,0}$. At $T \sim 10^{12}$ GeV then, the lepton quantum states become an incoherent mixture of a τ component and of a $\tau^{\perp}$ one. The condition $K_{1\tau} + K_{2\tau} \gtrsim 10$ hence clearly guarantees the washout of the asymmetry due to the former. For $T \sim M_2$, the preexisting quantum states orthogonal to τ are then to be regarded as an incoherent mixture composed by $|\ell_{\tau_2^{\perp}}\rangle$, lying along the projection of the heavy neutrino decay direction "2" on the $\tau^{\perp}$ plane, and by $|\ell_{\tau_{2^{\perp}}^{\perp}}\rangle$, which instead represent the projection of the states orthogonal to the heavy neutrino decay direction "2" on the considered plane. The condition $K_{2\tau^{\perp}} \coloneqq K_{2e} + K_{2\mu} \gtrsim 10$ thus guarantees the washout of the preexisting asymmetry component stored in the former, but does not affect the one due to the latter. Finally, in the last stage for $T \sim M_1$, the surviving components of the preexisting leptons and antileptons are projected with respect to the direction $\tau_1^{\perp}$ that the decay direction of N_1 defines. The resulting incoherent mixtures therefore comprise components along the states $|\ell_{\tau_1^{\perp}}\rangle$ and $|\ell_{\tau_{1^{\perp}}^{\perp}}\rangle$, and imposing $K_{1\tau^{\perp}} \coloneqq K_{1e} + K_{1\mu} \gtrsim 10$ only the washout of the asymmetry along the former is enforced. Consequently, at the end of the Leptogenesis process there will still be a completely unwashed fraction of the preexisting asymmetry given by

$$N_{B-L}^{preex,f} \simeq (1 - p_{\tau_{2^{\perp}}^{\perp}\tau_1^{\perp}})\,(1 - p_{\tau_{3^{\perp}}^{\perp}\tau_2^{\perp}})\,(1 - p_{\tau_{3^{\perp}}^{\perp}})\,(1 - p_{p3})\, N_{B-L}^{preex,0} \tag{5.2.46}$$

  showing that, also in this scenario, the washout of $N_{B-L}^{preex,0}$ is not complete.

- **Pattern III: $\mathbf{10^{12}\ GeV \gg M_3 \gg M_2 \gg M_1 \gg 10^9\ GeV}$**
  In this last scenario, characterised by $10^{12}\,\text{GeV} \gg M_3 \gg M_2 \gg M_1 \gg 10^9\,\text{GeV}$, the result for the final washout factor is a straightforward generalisation of the two previous cases. We can directly write our final result as

$$w^f \simeq (1 - p_{\tau_{2^{\perp}}^{\perp}\tau_1^{\perp}})\,(1 - p_{\tau_{3^{\perp}}^{\perp}\tau_2^{\perp}})\,(1 - p_{\tau_{p^{\perp}}^{\perp}\tau_3^{\perp}})\,(1 - p_{p\tau}) \tag{5.2.47}$$

  proving that in general, also in this case, $N_{B-L}^{preex,0}$ cannot be completely washed out.

  We can conclude, therefore, that for all the mass patterns with $M_1 \gg 10^9$ GeV it is not possible to enforce an efficient washout of a large preexisting asymmetry.

5.2.2.2 Three-flavour scenarios

We discuss now the mass patterns where at least one $M_i \ll 10^9$ GeV, sketched in Figure 5.5.

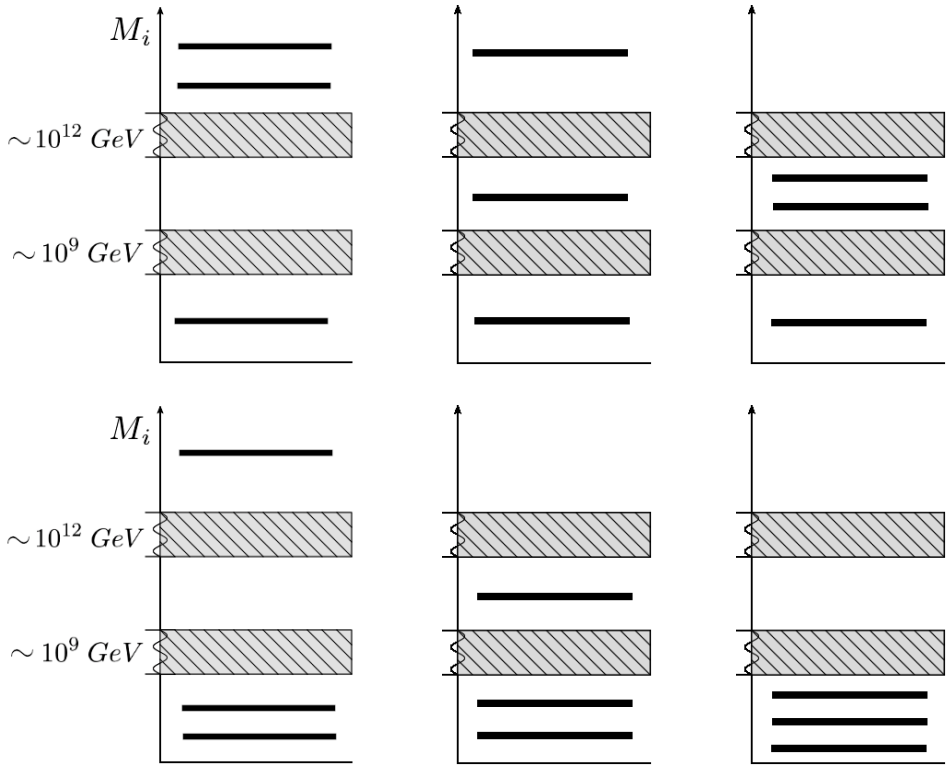

Figure 5.5: The six possible mass patterns with $M_1 \ll 10^9$ GeV. Only the second and the third configurations allow for successful strong thermal Leptogenesis.

It is clear, from our previous discussions, that in all the proposed cases it is always possible to enforce here a strong washout of the preexisting asymmetry by imposing $K_{1e}, K_{1\mu}, K_{1\tau} \gtrsim 10$ [133]. In fact, for $T \sim T_{L2}$ when the N_2 inverse-processes that drive the washout freeze-out, the residual value of the preexisting asymmetry is given by $N_{B-L}^{preex}(T \sim T_{L2})$. Consequently, for $T \sim M_1 \ll 10^9$ GeV and irrespectively of the value of T_{L2}, this asymmetry is re-distributed on the light flavour states that constitute the incoherent mixture of the three-flavour regime. The N_1 washout will then act separately on each flavour contribution $N_{\Delta_\alpha}^{preex}$, $\alpha = e, \mu, \tau$, and the final value of the residual preexisting asymmetry is therefore given by

$$N_{B-L}^{preex,f} = \sum_{\alpha=e,\mu,\tau} N_{\Delta_\alpha}^{preex}\, e^{-\frac{3\pi}{8} K_\alpha}. \tag{5.2.48}$$

Consequently, the condition $K_{1e}, K_{1\mu}, K_{1\tau} \gtrsim 10$ always ensures a sufficiently strong washout also for a large preexisting asymmetry – $w^f \lesssim 10^{-8}$. Yet, notice that such a strong condition would also washout the contribution $N_{B-L}^{lept,f}$ produced from the decays of the heaviest neutrino species. Furthermore, for $M_1 \ll 10^9$ GeV, the CP-asymmetries

of N_1 are too suppressed to guarantee the production of a BAU compatible with the Cosmological observations – cf. eq. (2.2.55) –, hence we conclude that the proposed condition is incompatible with successful Leptogenesis [6].

We have then to find a weaker condition, for which simultaneously $w^f \lesssim 10^{-8}$ and $N_{B-L}^{lept,f} \sim 10^{-7}$, so that successful strong thermal Leptogenesis is allowed. Clearly at least in one flavour it must therefore be $K_{1\alpha} \lesssim 1$ and the washout of the preexisting asymmetry stored in this flavour is then to be carried out by the heaviest neutrinos. Notice that, consequently, the decays of these neutrino species will necessary produce an asymmetry $N_{B-L}^{lept,f}$ stored in the same flavour α.

- **A first attempt: $\mathbf{M_3, M_2 \gg 10^{12}}$ GeV**

  Our first attempt is focused on a mass pattern where M_3, $M_2 \gg 10^{12}$ GeV. For $T \sim T_{L2}$ the residual value of the preexisting asymmetry is given by the eq. (5.2.29). Hence, imposing $K_2 \gtrsim 10$, only the contribution from the components orthogonal to the $|\ell_2\rangle$ and $|\overline{\ell_2}\rangle$ states survives – the second term on the RHS of eq. (5.2.29). The asymmetry produced from the N_2 decays at $T \sim T_{L2}$ is, by definition, contained on the direction associated to the decays of this heavy neutrino species, hence

  $$N_{B-L}^{lept}(T_{L2}) = N_{\Delta_2}^{lept}(T_{L2}). \tag{5.2.49}$$

  For $T \sim 10^{12}$ GeV, all the involved quantum states become an incoherent mixture of a τ component and of a $\tau^{\perp}$ one. Below $T \sim 10^9$ GeV the contributions to the final asymmetry that come from states orthogonal to τ, comprising both the residual preexisting asymmetry and the one produced by heavy neutrino decays are further reprocessed. As the μ Yukawa interactions are fast enough to break the coherence of the heavy neutrino flavour states, these asymmetries are re-distributed to an incoherent mixture of muon and electron components. Therefore, there is a residual fraction of the preexisting asymmetry in each light flavour and consequently it is impossible to impose a condition for which all the residual preexisting asymmetry is washed out and, at the same time, the contribution due to the heavy neutrino decays is maintained.

5.3 The τ $\mathbf{N_2}$-dominated scenario

We consider finally a scenario with $M_1 \ll 10^9$ GeV and 10^{12} GeV $\gg M_2 \gg 10^9$ GeV. As usual, for $T \sim M_2$ the lepton and antilepton states are to be described as an incoherent mixture of a τ and $\tau^{\perp}$ components. We again impose $K_{2\tau} \gtrsim 10$, in a way

[6] There is a loophole. In [107] it was shown that the flavour CP-asymmetries contain a term that is not upper bounded if strong cancellations in the light neutrino masses from the seesaw formula are allowed. In these particular situations successful Leptogenesis from the N_1 decays is then possible for $M_1 \ll 10^9$ GeV.

that any residual preexisting asymmetry $\lesssim \mathcal{O}(1)$ in the tau flavour is completely washed out. Differently from before, in the present two-flavour regime where the dynamics of N_2 takes place, a part of $B-L$ asymmetry sufficient to have successful Leptogenesis is now produced by the out-of-equilibrium decays in the tau flavour. Then, by imposing $K_{1e}, K_{1\mu} \gtrsim 10$ we get rid of the preexisting asymmetry also along the remaining light flavour directions and therefore we have finally pinned down a configuration in which successful strong thermal Leptogenesis is allowed, defining *the τ N_2-dominated scenario*. Notice that successful Leptogenesis requires $\varepsilon_{2\tau} \sim 10^{-6}$ so that, eventually – Section 3.2.1.1

$$\eta_B \sim \varepsilon_{2\tau}\, \kappa(K_{2\tau}) \sim 10^{-9}. \tag{5.3.1}$$

In this regard, we remark that in the τ N_2-dominated scenario the presence of a third heavy neutrino species, N_3, is necessary for $\varepsilon_{2\tau}$ not to be suppressed as – cf. eq. (3.2.31)

$$\varepsilon_{2\tau} \propto \frac{M_1}{M_2} \times 10^{-6} \frac{M_1}{10^{10}\ \text{GeV}}. \tag{5.3.2}$$

We also underline that *there cannot be a scenario of successful strong thermal Leptogenesis where the final asymmetry is dominantly in the electron or in the muon flavour*. Suppose, in fact, that we imposed $K_{2e} + K_{2\mu} \gtrsim 10$ so that all the preexisting asymmetry in the $\tau_2^{\perp}$ component was washed out at $T \sim M_2$. Suppose also that, afterwards, a sufficiently high $B-L$ asymmetry was generated in the same $\tau_2^{\perp}$ component by the out-of-equilibrium decays of N_2 at $T \sim T_{L2}$. Hence, we would have a $\tau_{2^{\perp}}^{\perp}$ component, $N^{preex}_{\Delta_{\tau_{2^{\perp}}^{\perp}}}(T_{L2})$, that escapes the washout. Indeed, for $T \ll 10^9$ GeV, the lepton quantum states would become an incoherent mixture of electron and muon components and if we imposed $K_{1\tau} + K_{2\tau} \gtrsim 10$ we could washout efficiently the residual preexisting asymmetry in the tau flavour. However, either K_{1e} or $K_{1\mu}$ have now to necessarily satisfy $K_{1\beta} \lesssim 1$, otherwise also N^{lept}_{B-L} would be washed out. Suppose then $K_{1e} \lesssim 1$, consequently there would still be a residual value of the preexisting asymmetry in the electron flavour given by

$$N^{preex,f}_{\Delta_e} = p_{\tau_{2^{\perp}}^{\perp} e}\, N^{preex}_{\Delta_{\tau_{2^{\perp}}^{\perp}}}(T_{L2}) \tag{5.3.3}$$

that cannot be washed out. Clearly the same would happen if we were to choose $K_{1\mu} \lesssim 1$ instead of $K_{1e} \lesssim 1$.

This being said, notice that for the mass pattern presenting both M_2 and M_3 in the range $(10^9 - 10^{12})$ GeV, things work exactly as for the τ N_2-dominated scenario. In this case, in fact, the less restrictive condition $K_{2\tau} + K_{3\tau} \gtrsim 10$ can be imposed in order to washout the preexisting asymmetry stored in the tau flavour. A τ N_3-dominated scenario is also in principle possible if $K_{3\tau} \gtrsim 10$ and $K_{2\tau} \lesssim 1$, however the maximal value of $\varepsilon_{3\tau}$ is suppressed as $\propto M_2/M_3$ with respect to $\varepsilon_{2\tau}$. Therefore, the asymmetry produced from N_2 decays tends to be larger, both for the lower washout and the much

larger CP-asymmetry. Still this possibility can be realised for a very fine tuned choice of the Seesaw parameters and, in any case, only for a not too strong hierarchy between M_2 and M_3. For the same reasons the mass patterns presenting $M_2 \ll 10^9$ GeV and $M_3 \gg 10^9$ GeV do not lead to successful Leptogenesis.

We have finally shown that, assuming three hierarchical heavy neutrino species within a framework involving only one Higgs doublet and neglecting the effects due to the light flavour coupling, the only possible scenario which allows for successful strong thermal Leptogenesis is the τ N_2-dominated scenario. In this configuration, obtained for $M_1 \ll 10^9$ GeV and 10^{12} GeV$\gg M_2 \gg 10^9$ GeV, the final $B-L$ asymmetry is dominantly produced in the τ flavour and the washout procedure of the preexisting asymmetry N_{B-L}^{preex} follows the lines depicted in Figure 5.6.

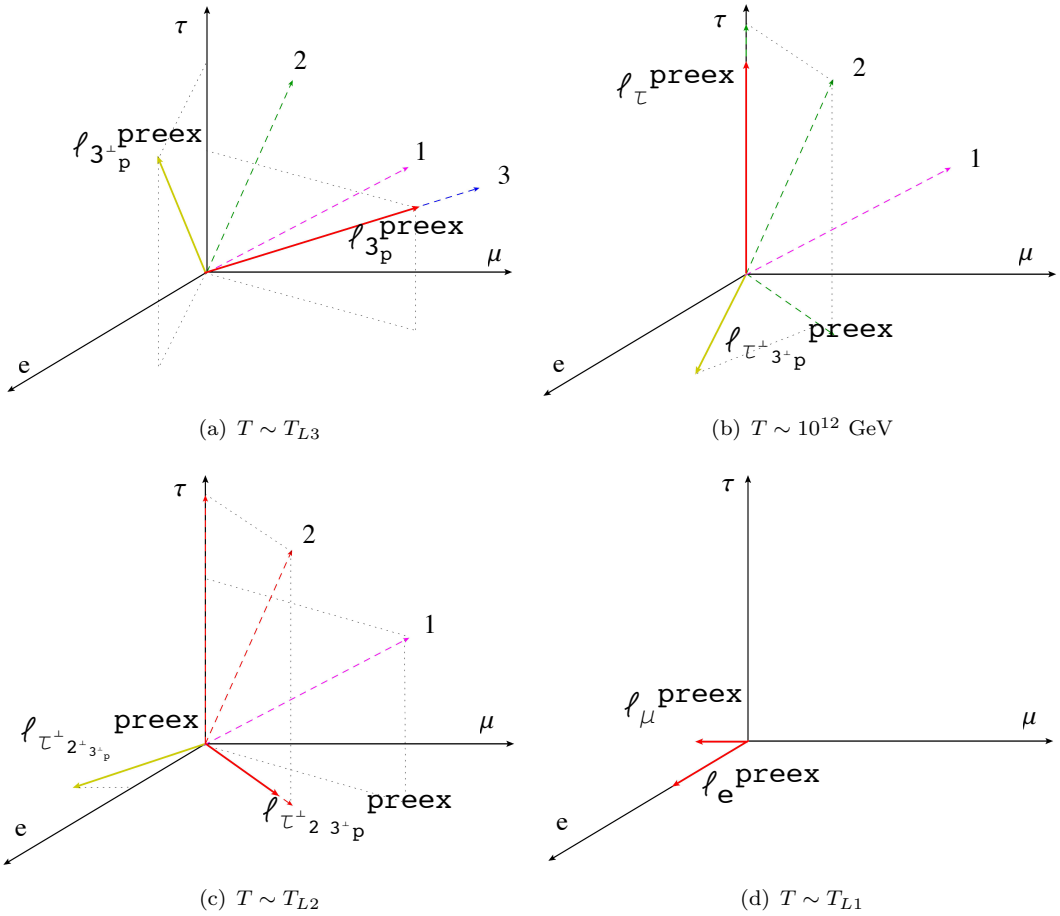

(a) $T \sim T_{L3}$ (b) $T \sim 10^{12}$ GeV

(c) $T \sim T_{L2}$ (d) $T \sim T_{L1}$

Figure 5.6: The τ N_2-dominated scenario: the evolution of the preexisting asymmetry.
As in the previous Figures, the red arrows represent components that are undergoing a washout process. The yellow arrows, instead, are reserved for the components that escape the latter and in particular track the lepton states carrying an unwashed fraction of the preexisting asymmetry. Notice that no yellow arrow is present after the final N_1 washout stage, for $T \sim M_1$. This is the only configuration for which successful strong thermal Leptogenesis is possible.

Chapter 6

The $SO(10)$-inspired model of Leptogenesis and its predictions

In this Chapter we introduce the $SO(10)$-inspired model of Leptogenesis [79, 141–144] and discuss the resulting scenario accounting for light and heavy neutrino flavour effects and considering the impact of a potential preexisting asymmetry. After reviewing the hypothesis which are beyond the definition of the model, we will detail the steps that the Leptogenesis process here comprises. The novelty of our work [3, 145, 146] is in the consequent study of the compatibility between the proposed model and the strong Leptogenesis condition. In particular, as clear from the treatment of the preexisting asymmetry exposed in the previous Chapter, it is our aim to investigate whether the restrictive requirements defining the τ N_2-dominated scenario are satisfied within the $SO(10)$-inspired model of Leptogenesis. Our analysis will therefore highlight the regions in the parameter space associated to the model where successful strong thermal Leptogenesis is realised, identifying in this way a class of solutions for which the dependence on the initial conditions is negligible. The result is indeed intriguing: adopting these strong solutions of the $SO(10)$-inspired model delivers sharp predictions on the same low energy neutrino parameters that experiments currently aim to measure.

6.1 The $SO(10)$-inspired model

We begin our review of the $SO(10)$-inspired model by introducing the parameters that this scenario involves. The Seesaw mechanism we adopt is the minimalistic type I already introduced in Chapter 2, relying on three RH neutrino species. The Lagrangian behind our model, once written on a basis where the matrices of the charged-lepton Yukawa

couplings and the heavy neutrino Majorana masses are diagonal, therefore reads:

$$\mathcal{L} = \mathcal{L}_{SM} + \mathcal{L}_{Seesaw} \supset i \sum_{i=1}^{3} \overline{N_{iR}}\, \partial^{\mu}\, \gamma_{\mu}\, N_{iR} - \sum_{\alpha=e,\mu,\tau} (D_y)_{\alpha}\, \overline{\ell_{\alpha L}}\, l_{\beta R}\, \Phi + \\ - \sum_{\substack{\alpha=e,\mu,\tau \\ i=1,2,3}} h_{\alpha i}\, \overline{\ell_{\alpha L}}\, N_{iR}\, \tilde{\Phi} - \frac{1}{2} \sum_{i=1,2,3} \overline{N_{iR}^{c}}\, (D_M)_i\, N_{iR} + \text{ H.c.} \tag{6.1.1}$$

where $N_{iR} = P_R\, N_i$ and the helicity projectors are defined according to eq. (2.2.1).
The Seesaw mechanism provides the following light neutrino mass matrix – eq. (2.1.10)

$$m_{\nu} \coloneqq -m_D\, D_M^{-1}\, (m_D)^T \tag{6.1.2}$$

which, for the basis we chose, is here diagonalised by the same PMNS mixing matrix introduced in Section 1.1.2.1:

$$U^{\dagger} m_{\nu} U^{*} =: -D_{m_{\nu}}. \tag{6.1.3}$$

In its usual parametrisation the matrix U depends on three mixing angles, θ_{ij}, two Majorana phases ρ and σ and one Dirac phase δ. Explicitly we have

$$U := \begin{pmatrix} c_{12}c_{13} & s_{12}c_{13} & s_{13}e^{-i\delta} \\ -s_{12}c_{23} - c_{12}s_{23}s_{13}e^{i\delta} & c_{12}c_{23} - s_{12}s_{23}s_{13}e^{i\delta} & s_{23}c_{13} \\ s_{12}s_{23} - c_{12}c_{23}s_{13}e^{i\delta} & -c_{12}s_{23} - s_{12}c_{23}s_{13}e^{i\delta} & c_{23}c_{13} \end{pmatrix} \cdot \begin{pmatrix} e^{i\rho} & 0 & 0 \\ 0 & 1 & 0 \\ 0 & 0 & e^{i\sigma} \end{pmatrix} \text{ (NO)} \tag{6.1.4}$$

and

$$U := \begin{pmatrix} s_{13}e^{-i\delta} & c_{12}c_{13} & s_{12}c_{13} \\ s_{23}c_{13} & -s_{12}c_{23} - c_{12}s_{23}s_{13}e^{i\delta} & c_{12}c_{23} - s_{12}s_{23}s_{13}e^{i\delta} \\ c_{23}c_{13} & s_{12}s_{23} - c_{12}c_{23}s_{13}e^{i\delta} & -c_{12}s_{23} - s_{12}c_{23}s_{13}e^{i\delta} \end{pmatrix} \cdot \begin{pmatrix} e^{i\sigma} & 0 & 0 \\ 0 & e^{i\rho} & 0 \\ 0 & 0 & 1 \end{pmatrix} \text{ (IO)} \tag{6.1.5}$$

where s_{ij} and c_{ij} indicate sines and cosines of the mixing angles and we distinguished between the two configurations that neutrino oscillation experiments allow for the light neutrino mass spectrum encoded in $D_{m_{\nu}}$: normal ordering (NO) and inverted ordering (IO). Adopting the convention $m_1 < m_2 < m_3$ for the eigenvalues of $D_{m_{\nu}}$ and by defining

$$m_{sol} := \sqrt{\Delta m_{sol}^2} \simeq (0.00875 \pm 0.00012) \quad \text{eV} \tag{6.1.6}$$

and

$$m_{atm} := \sqrt{\Delta m_{sol}^2 + \Delta m_{atm}^2} \simeq (0.050 \pm 0.001) \quad \text{eV} \tag{6.1.7}$$

results in the following possible light neutrino mass patterns –Figure 1.1:

$$\begin{aligned} &m_1, \qquad m_2 = \sqrt{m_1^2 + m_{sol}^2}, \qquad m_3 = \sqrt{m_1^2 + m_{atm}^2} \qquad \text{(NO)} \\ &m_1, \qquad m_2 = \sqrt{m_1^2 + m_{atm}^2 - m_{sol}^2}, \qquad m_3 = \sqrt{m_1^2 + m_{atm}^2} \qquad \text{(IO)}. \end{aligned} \tag{6.1.8}$$

In order to specify the assumptions which define the $SO(10)$-inspired model, we consider now the different relations that exist between the parameters introduced above. In particular, by inverting the eq. (6.1.3) end employing the Seesaw formula (6.1.2) we obtain

$$D_{m_D}^{-1} V_L U D_{m_\nu} U^T V_L^T D_{m_D}^{-1} = U_R D_M^{-1} U_R^T \tag{6.1.9}$$

where the following bi-unitary decomposition was considered for m_D:

$$m_D = V_L^\dagger D_{m_D} U_R. \tag{6.1.10}$$

We underline the importance of eq. (6.1.9), which connects the high energy parameters describing the RH neutrinos, presented on the RHS, to the low energy ones on the left-hand side. By defining now [79]

$$M^{-1} \coloneqq U_R D_M^{-1} U_R^T \tag{6.1.11}$$

it follows that

$$M^{-1} \left(M^{-1}\right)^\dagger = U_R D_M^{-2} U_R^\dagger \tag{6.1.12}$$

and therefore through the relation (6.1.9) we can also determine unambiguously the heavy neutrino mass spectrum and the matrix U_R[1].
As a result of the proposed exercise in the Seesaw algebra, we can parametrize the 18 new quantities that the Lagrangian (6.1.1) yields in the following way:

- 3 Dirac masses in D_{m_D}
- 3 mixing angles and 3 phases in the unitary matrix V_L
- 3 mixing angles and 3 phases in the leptonic mixing matrix U
- 3 light neutrino masses in D_{m_ν}.

Despite the neutrino oscillation experiments and the efforts in pinning down the neutrino absolute mass scale provide some informations on U and D_{m_ν}, performing a complete test of the Seesaw parameter space clearly requires further constraints. In this regard, owing to the adopted parametrization, we are free to impose additional requirements on the matrix V_L and the masses in D_{m_D} which will implicitly define our model. Our

[1]The details regarding the precise determination of the phases in U_R are discussed in [143].

choice is the $SO(10)$-*inspired relations* [79, 141, 144].

In these scenarios, which draw from the spirit of $SO(10)$ GUT theories, the matrix V_L would play the same role as the CKM matrix of the quark sector, if we had no Seesaw mechanism. Within $SO(10)$-inspired models the mixing angles in the former thus are limited according to the range of their counterparts in the latter:

$$\theta_{ij}^{L} \simeq \theta_{ij}^{CKM}. \tag{6.1.13}$$

We remark that, in the present scheme, the large mixing angles that neutrino experiments detect are therefore to be interpreted as an effective consequence of the Seesaw mechanism.
The second constraint we impose regards the Dirac masses of neutrinos. In particular we parametrize the eigenvalues λ_i of m_D according to

$$\lambda_1 := \alpha_1 m_u, \qquad \lambda_2 := \alpha_2 m_c, \qquad \lambda_3 := \alpha_3 m_t \tag{6.1.14}$$

where m_u, m_c and m_t are, respectively, the masses of the up, charm and top quarks. For the similarity between neutrinos and the up-type quarks that $SO(10)$ GUT scenarios propose we then expect $\alpha_i \sim \mathcal{O}(1)$ and replace the Dirac masses with these quantities in our parametrization of the model.
The assumptions in eq.s (6.1.13) and (6.1.14) constitute the framework of our $SO(10)$-inspired model. Of the 18 original parameter, beside the 6 phases which are limited to their natural intervals, the proposed conditions constrain 5 masses and the 6 mixing angles. On top of that we have the informations on the baryon asymmetry of the Universe and, in this regard, as we will see in the next Section for the characteristic of the Leptogenesis process α_1 and α_3 will also decouple from our analyses.

6.1.1 The Leptogenesis process

Through the Seesaw formula (6.1.2) the mass hierarchy of the quark sector is transferred to the heavy neutrinos. If we exclude particular choices of parameters which result in a degenerate mass spectrum, the heavy neutrino masses obey the relation [141]

$$M_1 \ : \ M_2 \ : \ M_3 \ = \ (\alpha_1 m_u)^2 \ : \ (\alpha_2 m_c)^2 \ : \ (\alpha_3 m_t)^2 \, . \tag{6.1.15}$$

By means of the $SO(10)$-inspired condition $\alpha_i \sim \mathcal{O}(1)$ we therefore have

$$M_1 \ll 10^9 \text{ GeV} \lesssim M_2 \lesssim 10^{12} \text{ GeV} \ll M_3 \tag{6.1.16}$$

and the $B-L$ asymmetry production is generally dominated by the next-to-the-lightest of the heavy neutrinos. In other words, the natural Leptogenesis scenario emerging from

$SO(10)$-inspired conditions is N_2-*dominated*. In our analysis we will focus on strongly hierarchical solutions, characterised by $M_i > 10\, M_{j<i}$. As long as the condition (6.1.16) holds, we can therefore neglect the contributions to the generated asymmetry, N^{lept}_{B-L}, brought by the out-of-equilibrium decays of N_1 and N_3. The former neutrino species is in fact too light for the associated CP-asymmetries to be sizeable, whereas the contribution of the latter is suppressed by the strong mass hierarchy imposed. Under these conditions, it turns out that the values of α_1 and α_3 are actually irrelevant to the Leptogenesis process[2], which proceeds as detailed below.

Due to the hierarchy imposed on the heavy neutrinos, the Leptogenesis era is effectively composed by separated stages. As usual we neglect many complications by considering only the picture that decays and inverse-decays provide. Furthermore we address all flavour effects only in the fully flavoured regimes presented in Chapter 3, where the classic description provided by the Boltzmann equations is a good approximation. Under our working assumptions, the impact of N_3 Leptogenesis is absolutely negligible. The presence of a third heavy neutrino species in the model, in fact, is only required for ε_2 not to be suppressed as explained in the previous Chapter. The Leptogenesis process therefore comprises only two effective stages:

- **Stage I: $\mathbf{N_2}$ Leptogenesis.**
  This first effective stage takes place for $T \sim M_2$, when the processes of N_2 are active. In the present two-flavour regime the τ components of the involved heavy neutrino flavour states are measured, hence the Boltzmann equations describing the evolution of the resulting incoherent mixture are

$$\frac{\mathrm{d}\, N_{N_2}}{\mathrm{d}\, z} = -D_2(z) \left(N_{N_2}(z) - N^{eq}_{N_2}(z) \right), \qquad i = 1,2,3 \tag{6.1.17}$$

  and

$$\frac{\mathrm{d}\, N_{\Delta_\tau}}{\mathrm{d}\, z} = \varepsilon_{2\tau}\, D_2(z) \left(N_{N_2}(z) - N^{eq}_{N_2}(z) \right) - p^0_{2\tau}\, W^{ID}_2(z) N_{\Delta\tau} \tag{6.1.18}$$

$$\frac{\mathrm{d}\, N_{\Delta_{\tau_2^\perp}}}{\mathrm{d}\, z} = \varepsilon_{2\tau_2^\perp}\, D_2(z) \left(N_{N_2}(z) - N^{eq}_{N_2}(z) \right) - p^0_{2\tau_2^\perp}\, W^{ID}_2(z) N_{\Delta\tau_2^\perp}. \tag{6.1.19}$$

  In analogy to eq. (3.2.50) we can consequently write the generated $B-L$ asymmetry as

$$N^{lept}_{B-L}(T \sim M_2/z_{L2}) \simeq \varepsilon_{2\tau} \kappa_2(K_2, p^0_{2\tau}) + \varepsilon_{2\tau_2^\perp} \kappa_2(K_2, p^0_{2\tau_2^\perp}) \tag{6.1.20}$$

  where, for the considered thermal scenario, the efficiency factor $\kappa_2(K_2, p^0_{2\gamma})$, $\gamma = \tau, \tau_2^\perp$ comprise two contributions

$$\kappa_2(K_2, p^0_{2\gamma}) = \kappa^{f-}_2(K_2, p^0_{2\gamma}) + \kappa^{f+}_2(K_2, p^0_{2\gamma}) \tag{6.1.21}$$

[2]Equation (6.1.16) holds for a broad range of values of α_is, provided that α_1 be not as large as required to push $M_1 \gtrsim 10^9$ GeV and achieve successful N_1 Leptogenesis.

previously introduced in eq.s (3.2.42) and (3.2.43).

- **Stage II: the N_1 washout.**
  As a consequence of the hierarchical heavy neutrino mass spectrum, eq. (6.1.20) effectively describes the $B-L$ asymmetry until $T \sim M_1$, when the N_1 processes become active and the second Leptogenesis stage begins. As mentioned before we can safely neglect the N_1 asymmetry production, as $M_1 \ll 10^9$ GeV. Nevertheless, the washout processes driven by the N_1 inverse-decays cannot be neglected. For $T \sim 10^9$ GeV the quantum coherence of the states $|\ell_{\tau_2^\perp}\rangle$ and $|\overline{\ell_{\tau_2^\perp}}\rangle$ is broken by the μ Yukawa interactions. The washout process is therefore performed in a three-flavour regime, where the involved states are fully projected on the light flavour basis. The final $B-L$ asymmetry is then given by a sum of three flavoured contributions $N^{lept,f}_{\Delta_\alpha}$:

$$\begin{aligned} N^{lept,f}_{B-L} &= \sum_{\alpha=e,\mu,\tau} N^{lept,f}_{\Delta_\alpha} = \\ &= \frac{p^0_{2e}}{p^0_{2\tau_2^\perp}} \varepsilon_{2\tau_2^\perp} \kappa_2(K_2, p^0_{2\tau_2^\perp}) e^{-\frac{3\pi}{8} K_{1e}} + \\ &+ \frac{p^0_{2\mu}}{p^0_{2\tau_2^\perp}} \varepsilon_{2\tau_2^\perp} \kappa_2(K_2, p^0_{2\tau_2^\perp}) e^{-\frac{3\pi}{8} K_{1\mu}} + \\ &+ \varepsilon_{2\tau} \kappa(K_2, p^0_{2\tau}) e^{-\frac{3\pi}{8} K_{1\tau}}. \end{aligned} \tag{6.1.22}$$

From our previous discussion it is clear that successful Leptogenesis can only be achieved in the $SO(10)$-inspired model when, at least for one flavour, $K_{1\alpha} \lesssim 1$. As we will explicitly show in the next Section, in concordance to previous analyses [142, 143], this regions delineate a well-defined subspace in the parameter space of the model. If, as we hope, the same subspace is then further refined by the strong Leptogenesis condition we are going to investigate, the predictions of the $SO(10)$-inspired model will consequently become even sharper.

6.1.2 The washout factor

In the previous Section we addressed the evolution of the asymmetry that the out-of-equilibrium decays of N_2 generate. We can therefore focus now on the preexisting component N^{preex}_{B-L} and on the strong Leptogenesis condition which ensures its complete washout. Our analysis [2] already pointed out that, considering light and heavy neutrino flavour effects as well as hierarchical heavy neutrinos, only the setup corresponding to the τ N_2-dominated scenario is able to guarantee successful and strong Leptogenesis at the same time. Hence, although the $SO(10)$-inspired model naturally proposes a N_2-dominated scenario, we still have to verify whether the restrictive conditions on the flavoured decay parameters which define the τ N_2-dominated scenario are satisfied.

Proceeding along the same lines as before, we introduce the washout parameter $w(T)$, such that

$$N_{B-L}^{preex}(T) = w(T) N_{B-L}^{preex,0} \tag{6.1.23}$$

and follow the evolution of N_{B-L}^{preex} step-by-step to quantify the final value w^f of $w(T)$.

- **Stage 1: $\mathbf{T > 10^{12}}$ GeV**
  Given the initial amount of preexisting asymmetry $N_{B-L}^{preex,0}$, the first step in the evolution of this component takes place for $T \sim M_3$, when the processes of N_3 Leptogenesis are active. Barring specific flavour configurations, within the present framework the N_3 processes have only a little impact on the evolution of the preexisting asymmetry and therefore can be safely neglected. In this way we can assume that
  $$N_{B-L}^{preex}(T_{L3}) = N_{B-L}^{preex,0} \tag{6.1.24}$$
  where we defined $T_{L3} \coloneqq M_3/z_{L3}$, denoting the freeze-in temperature for the N_3 processes.

- **Stage 2: $\mathbf{10^{12}}$ GeV $\mathbf{> T > 10^9}$ GeV**
  The preexisting asymmetry starts effectively to evolve only when $T \sim M_2$ and the processes of N_2 are active. We remark that in the $SO(10)$-inspired model the mass of the next-to-the-lightest heavy neutrino respects the condition 10^9 GeV $< M_2 < 10^{12}$ GeV, implying that N_2 Leptogenesis takes place in a two-flavour regime. Therefore, we decompose N_{B-L}^{preex} into the flavoured asymmetries corresponding to the components resulting from the action of the relevant Yukawa interactions [2]. Explicitly we have
  $$N_{B-L}^{preex}(T \sim M_2) = N_{\Delta_\tau}^{preex}(T \sim M_2) + N_{\Delta_{\tau^\perp 2}}^{preex}(T \sim M_2) + N_{\Delta_{\tau_{2^\perp}^\perp}}^{preex}(T \sim M_2) \tag{6.1.25}$$
  where
  $$N_{\Delta_\tau}^{preex} = p_{p\tau} N_{B-L}^{preex,0} \tag{6.1.26}$$
  $$N_{\Delta_{\tau^\perp 2}}^{preex} = p_{p\tau_2^\perp}(1 - p_{p\tau}) N_{B-L}^{preex,0} \tag{6.1.27}$$
  $$N_{\Delta_{\tau^\perp 2^\tau}}^{preex} = (1 - p_{p\tau_2^\perp})(1 - p_{p\tau}) N_{B-L}^{preex,0}. \tag{6.1.28}$$
  After the N_2 washout has been performed, the preexisting $B - L$ asymmetry is then given by
  $$\begin{aligned} N_{B-L}^{preex}(T_{L2}) &= N_{\Delta_\tau}^{preex}(T_{L2}) + N_{\Delta_{\tau^\perp 2}}^{preex}(T_{L2}) + N_{\Delta_{\tau_{2^\perp}^\perp}}^{preex}(T_{L2}) = \\ &= p_{p\tau} e^{-\frac{3\pi}{8} K_{2\tau}} N_{B-L}^{preex,0} + \\ &+ p_{p\tau_2^\perp}(1 - p_{p\tau}) e^{-\frac{3\pi}{8}(K_2 - K_{2\tau})} N_{B-L}^{preex,0} + \\ &+ (1 - p_{p\tau_2^\perp})(1 - p_{p\tau}) N_{B-L}^{preex,0} \end{aligned} \tag{6.1.29}$$

and at this stage the washout factor is therefore

$$w(T_{L2}) = p_{p\tau} e^{-\frac{3\pi}{8} K_{2\tau}} + p_{p\tau_2^\perp}(1 - p_{p\tau}) e^{-\frac{3\pi}{8}(K_2 - K_{2\tau})} + (1 - p_{p\tau_2^\perp})(1 - p_{p\tau}). \quad (6.1.30)$$

Even if the $SO(10)$-inspired model imposed a strong washout regime, $K_{2\gamma} \geqslant 10$ for $\gamma = \tau, \tau_2^\perp$, the last term in eq. (6.1.29) would still survive. This component corresponds in fact to the fraction of preexisting $B-L$ asymmetry stored in lepton and antilepton states which are orthogonal both to τ and the projection of the decay direction of N_2 on the e–μ plane.

- **Stage 3: 10^9 GeV $>$ T**
  Again, for the heavy neutrino mass hierarchy, the expression (6.1.29) for the preexisting asymmetry holds until the temperature reaches $T \sim 10^9$ GeV, when the μ Yukawa interactions are no longer negligible. The quantum states contributing into N_{B-L}^{preex} are then to be regarded as incoherent mixtures of the light flavour states which form the basis of our flavour space. Accordingly, each term in eq. (6.1.29) has also to be decomposed in the flavoured asymmetries $N_{\Delta_\alpha}^{preex}$, where $\alpha = e, \mu, \tau$. Then, for $T \sim M_1$, the N_1 inverse-processes perform the final washout of these asymmetries in a three-flavour regime. Proceeding along the same lines as before, at the end of the Leptogenesis era we therefore have

$$\begin{aligned}
N_{B-L}^{preex,f} &= N_{B-L}^{preex}(T_{L1}) = N_{\Delta_\tau}^{preex}(T_{L1}) + N_{\Delta_\mu}^{preex}(T_{L1}) + N_{\Delta e}^{preex}(T_{L1}) = \\
&= p_{p\tau} e^{-\frac{3\pi}{8} K_{2\tau}} e^{-\frac{3\pi}{8} K_{1\tau}} N_{B-L}^{preex,0} + \\
&+ p_{\tau_2^\perp \mu} p_{p\tau_2^\perp}(1 - p_{p\tau}) e^{-\frac{3\pi}{8}(K_2 - K_{2\tau})} e^{-\frac{3\pi}{8} K_{1\mu}} N_{B-L}^{preex,0} + \\
&+ p_{\tau_{2^\perp}^\perp \mu}(1 - p_{p\tau_2^\perp})(1 - p_{p\tau}) e^{-\frac{3\pi}{8} K_{1\mu}} N_{B-L}^{preex,0} + \qquad (6.1.31) \\
&+ (1 - p_{\tau_2^\perp \mu}) p_{p\tau_2^\perp}(1 - p_{p\tau}) e^{-\frac{3\pi}{8}(K_2 - K_{2\tau})} e^{-\frac{3\pi}{8} K_{1e}} N_{B-L}^{preex,0} + \\
&+ (1 - p_{\tau_{2^\perp}^\perp \mu})(1 - p_{p\tau_2^\perp})(1 - p_{p\tau}) e^{-\frac{3\pi}{8} K_{1e}} N_{B-L}^{preex,0} \qquad (6.1.32)
\end{aligned}$$

and, from the above equation, we can easily extract our final expression for w^f

$$\begin{aligned}
w^f &= p_{p\tau} e^{-\frac{3\pi}{8}(K_{2\tau} + K_{1\tau})} + p_{\tau_2^\perp \mu} p_{p\tau_2^\perp}(1 - p_{p\tau}) e^{-\frac{3\pi}{8}(K_{1\mu} + K_2 - K_{2\tau})} + \\
&+ p_{\tau_{2^\perp}^\perp \mu}(1 - p_{p\tau_2^\perp})(1 - p_{p\tau}) e^{-\frac{3\pi}{8} K_{1\mu}} + (1 - p_{\tau_2^\perp \mu}) p_{p\tau_2^\perp}(1 - p_{p\tau}) e^{-\frac{3\pi}{8}(K_{1e} + K_2 - K_{2\tau})} + \\
&+ (1 - p_{\tau_{2^\perp}^\perp \mu})(1 - p_{p\tau_2^\perp})(1 - p_{p\tau}) e^{-\frac{3\pi}{8} K_{1e}}. \qquad (6.1.33)
\end{aligned}$$

6.2 Predictions on the Seesaw parameter space

With the final formula for the produced $B-L$ asymmetry given by eq. (6.1.22) and the above result on the washout factor, we can finally perform a systematic examination of the parameter space of the model. Our aim is to detect the regions corresponding to successful strong thermal solutions of the theory, giving rise to solid predictions which are not affected by the details of the history of our Universe before the Leptogenesis era.

6.2.1 Methodology and successful Leptogenesis

From a procedural point of view, we performed a scan of the parameter space of the model restricting the involved quantities to the intervals that neutrino experiments and the $SO(10)$-inspired conditions delineate. In Table 6.1 we report the values denoting the boundaries of the explored region.

Neutrino parameters		
$\theta_{12} \in (31.30 - 36.27)^\circ$, $\delta \in (-\pi - \pi)$,	$\theta_{23} \in (35.06 - 52.54)^\circ$, $\rho, \sigma \in (0 - 2\pi)$,	$\theta_{13} \in (0.00 - 11.54)^\circ$, $m_1, m_{ee} \in (0 - 10^{-4})$ eV.
Remaining parameters		
$\theta_{12}^L \in (0.00 - 13.00)^\circ$, $\delta^L \rho^L, \sigma^L \in (0 - 2\pi)$,	$\theta_{23}^L \in (0.00 - 2.37)^\circ$, $\alpha_2 = 5.$	$\theta_{13}^L \in (0.00 - 0.21)^\circ$,

Table 6.1: The explored region in the parameter space of the $SO(10)$-inspired model. The lower bounds for m_1 and m_{ee}, respectively the lightest neutrino mass and the Majorana effective mass – cf. eq. (1.1.16) –, have been limited to the presented values after a preliminary analysis excluded the region 10^{-10} – 10^{-4} eV. The quantities carrying a superscript "L" denote the parameters of the matrix V_L.

As a first step we focused on the implications of successful $SO(10)$-inspired Leptogenesis only. The relevant condition has been quantified in

$$\eta_B^{lept} \coloneqq 0.0096 \times N_{B-L}^{lept,f} \in (5.9 - 6.5) \times 10^{-10} \tag{6.2.1}$$

yielding the results reported in Figure 6.1 and 6.2 respectively for a normal and inverted ordering of the light neutrino mass spectrum.

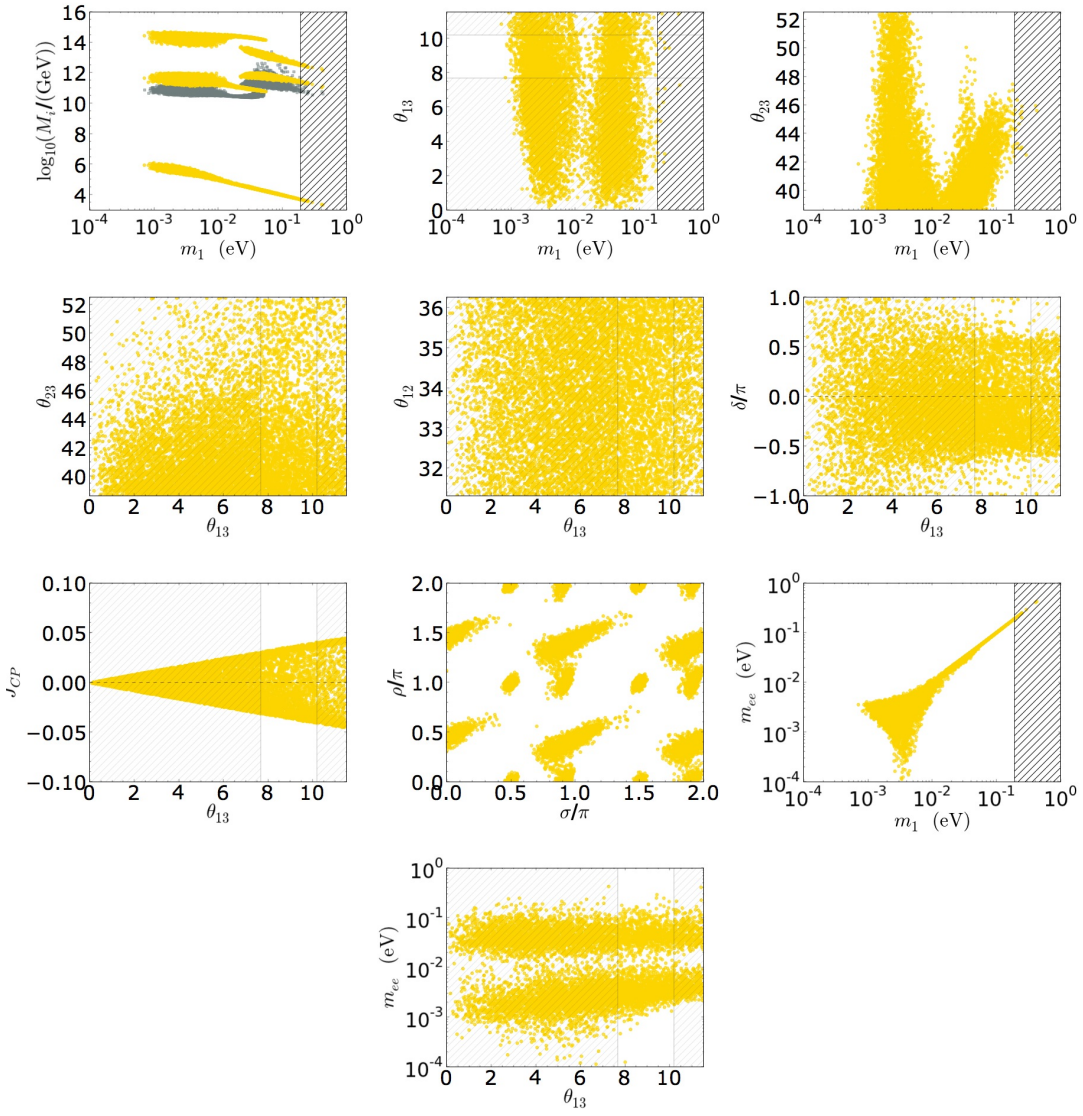

Figure 6.1: Results from successful Leptogenesis in the $SO(10)$-inspired model on the low energy neutrino parameters for normal ordering, based on [142, 143]. The hatched area for $m_1 > 0.19$ eV is due to the upper-bound obtained by Cosmology on the sum of the neutrino masses [46]. The areas presenting a lighter hatching indicate instead the range of θ_{13} values falling outside the current 2σ region $7.7^\circ \leqslant \theta_{13} \leqslant 10.2^\circ$.

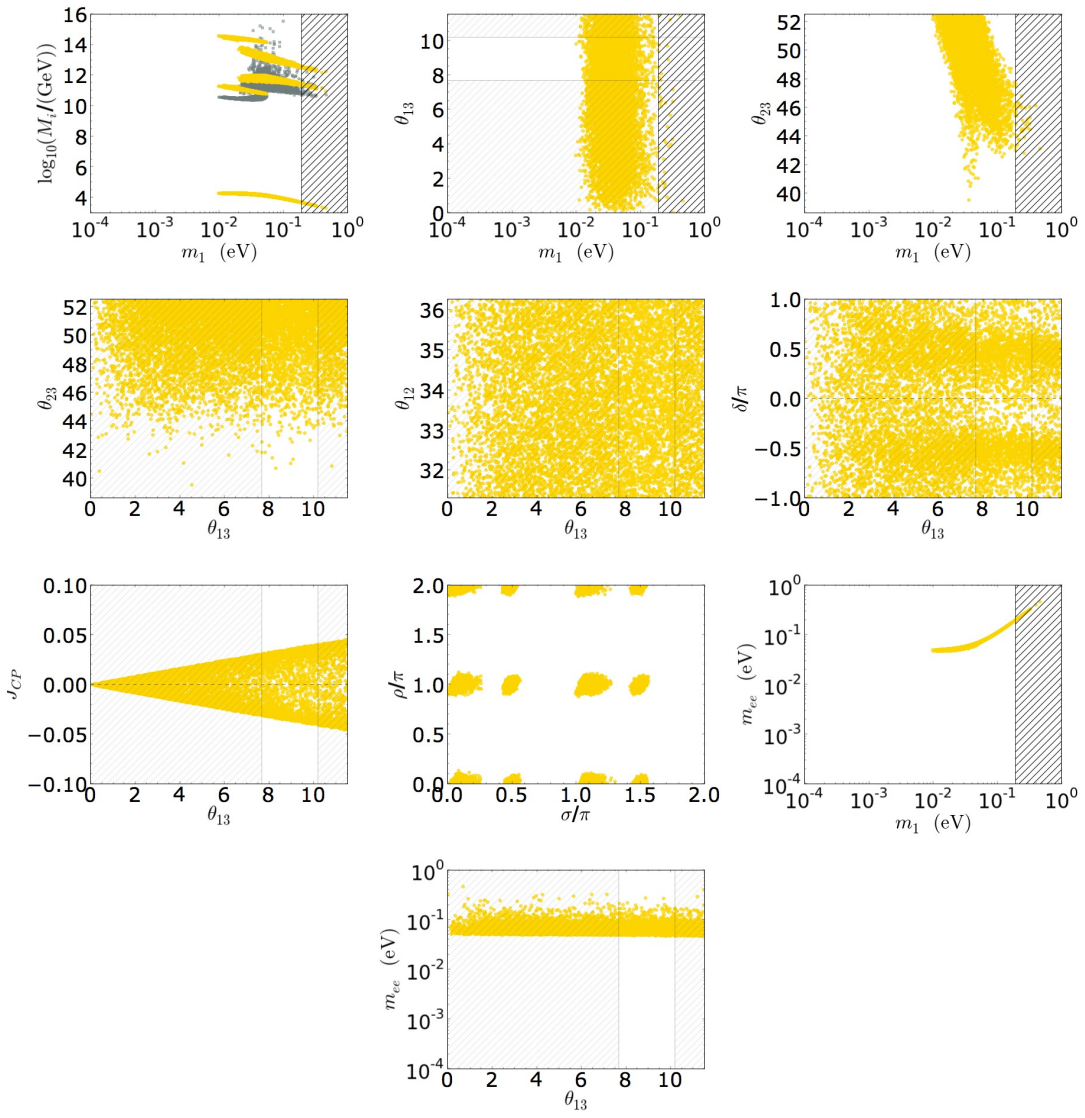

Figure 6.2: Results from successful Leptogenesis in the $SO(10)$-inspired model on the low energy neutrino parameters for inverted ordering, based on [142,143]. As in the normal ordering case, the hatched area for $m_1 > 0.19$ eV represents the upper-bound due to Cosmology [46] and indicate for θ_{13} the values falling outside the current 2σ region $7.7° \leqslant \theta_{13} \leqslant 10.2°$.

In both the Figures, the hatched area for $m_1 > 0.19$ eV is due to the upper-bound that Cosmology places, already discussed in eq. (1.1.19). The areas presenting a lighter exclusion pattern refer instead to the values of θ_{13} which fall outside the current 2σ range $7.7^\circ \leqslant \theta_{13} \leqslant 10.2^\circ$ [38, 39]. Relying on a larger statistics, our analysis refines the one already presented in [143]. For an easier comparison between the two works – a necessary cross-check for the codes employed – we restricted here θ_{23} to the range $(35.65 - 52.54)^\circ$.

Notice first that, for both the schemes, the $SO(10)$-inspired conditions effectively lead to the required hierarchical heavy neutrino mass spectrum. The resulting Leptogenesis process is therefore indeed N_2-dominated.

Focusing now on the results obtained for normal ordering – Figure 6.1 – our work confirms the presence of two adjacent regions that lead to successful Leptogenesis, outlined by the boundary at $m_1 \simeq 10^{-2}$ eV. A similar situation is presented in the last plot, where $m_{ee} \simeq 10^{-2}$ eV delineates two regions both linear in θ_{13}. This should not surprise, as due to the required values of the Majorana phases ρ and σ, in this model there is a strong correlation between m_1 and m_{ee}, testified by the relative plot.

As for the inverted ordering, the lower-bound on θ_{23} is less strong but still present. More importantly, the prediction emerging from this scheme on m_1 and m_{ee} confirms the previous analyses and will hopefully allow in the next years for a first experimental test of the light neutrino mass spectrum within this model.

6.2.2 Successful strong thermal Leptogenesis

On top of the previous constraint we impose now the strong Leptogenesis condition and scan on the full range proposed for θ_{23} in Table 6.1. Starting form eq. (6.1.33) we therefore seek regions in the parameter space where $w^f \ll 10^{-8}$. Using the same averaged flavour configuration for $|\ell_p\rangle$ and $|\overline{\ell_p}\rangle$ [3]

$$p_{p\tau} = 1/3, \qquad p_{p\tau_2^\perp} = p_{\tau_2^\perp \mu} = p_{\tau_{2^\perp}^\perp \mu} = 1/2 \tag{6.2.2}$$

the strong Leptogenesis condition has been tested at every considered point for three different values of the initial preexisting asymmetry: $N_{B-L}^{preex,0} = 10^{-1}, 10^{-2}, 10^{-3}$. We remark that the strong Leptogenesis solutions we identify are a subset of the successful ones, therefore they effectively delineate the regions in the parameter space of the model where successful strong thermal Leptogenesis is allowed.

Before presenting our results, we have however to face a last consistency check regarding the conditions which define the τ N_2-dominated scenario we aim to identify.

[3] Ad-hoc flavour configurations would result in changes of order $\mathcal{O}(1)$ in the final preexisting asymmetry and therefore in w^f. As we are concerned here with the magnitude of the latter, for our analysis we can clearly adopt the proposed averaged flavour configuration.

6.2.2.1 An explicit check of the successful strong thermal Leptogenesis condition

In Chapter 5 we identified in the τ N_2-dominated scenario the unique setup which allows for successful and strong Leptogenesis at the same time. The DNA of this solution is summarised in the following points

- a heavy neutrino mass spectrum leading to N_2-dominated Leptogenesis: $M_3 > 10^{12}$ GeV $> M_2 > 10^9$ GeV $> M_1$.
- a strong washout in the flavour τ driven by the N_2 inverse-decays: $K_{2\tau} \gtrsim 10$.
- a strong washout in the flavours e and μ performed by the N_1 inverse-processes: K_{1e}, $K_{1\mu} \gtrsim 10$.
- a weak washout by N_1 in the τ flavour: $K_{1\tau} \ll 10$.

The solutions we seek must therefore match this profile in order to be associated to the scenario we proposed. In this regard, our analysis highlighted the results in Figure 6.3

Starting with the normal ordering case, reported in the left column, the strong solutions we identified clearly respect the characteristics of the τ N_2-dominated scenario. Beside presenting the required mass spectrum, the flavoured decay parameter $K_{2\tau}$ respects the strong washout condition $K_{2\tau} \gtrsim 10$. The preexisting asymmetry lying on the τ direction is therefore washed out during the N_2 Leptogenesis phase while, at the same time, the out-of-equilibrium decays of N_2 generate the amount of $B - L$ asymmetry required to satisfy the successful Leptogenesis condition. Notice that the strong condition selected those regions in the parameter space where, beside $K_{2\tau} \geqslant 10$, also $K_{\tau_2^\perp} \geqslant 10$. The washout performed along the $\tau_2^\perp$ directions has the net effect of reducing the preexisting asymmetry which is confined on the $e - \mu$ plane, adding on to the washout that N_1 will perform. This further condition is here necessary because, as shown in Figure 6.3, in the $SO(10)$-inspired model the values of K_{1e} and $K_{1\mu}$ cannot be both arbitrarily large at the same time. In particular, K_{1e} is bounded to $K_{1e} \lesssim 30$ by the requirement $K_{1\tau} \lesssim 1$, necessary for successful Leptogenesis. Strong successful Leptogenesis is therefore only allowed in those regions of the parameter space where a compromises between K_{1e}, $K_{1\mu}$ and $K_{1\tau}$ is found. The former must be large enough to suppress the residual preexisting asymmetry while the latter should be small, not to compromise the product of N_2 Leptogenesis. In this regard, as $K_{1\tau} \lesssim 1$, the resulting asymmetry is necessarily produced mainly in the τ flavour.
We can then safely affirm that the presented results carry, for the normal ordering case, the trademark of the τ N_2-dominated scenario.

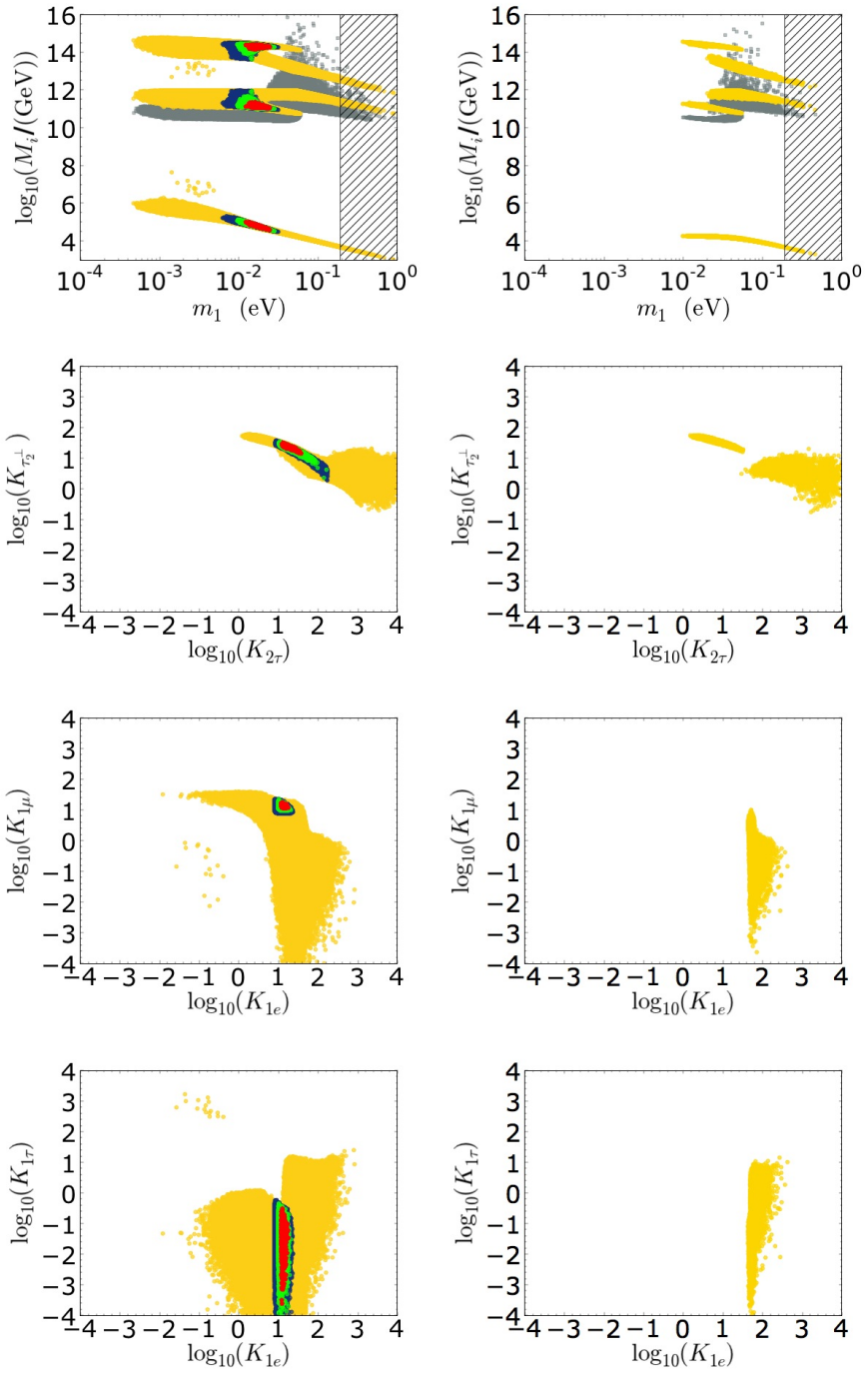

Figure 6.3: Strong Leptogenesis condition in the $SO(10)$-inspired model for normal and inverted ordering, from [3, 145]. The colour code indicates the magnitude of the preexisting $B - L$ asymmetry which can be washed out in the corresponding point of the parameter space. Blue dots are for $\mathcal{O}(10^{-3})$, the green dots for $\mathcal{O}(10^{-2})$ and red stars are for $\mathcal{O}(10^{-1})$. The points indicated by yellow dots correspond to the regions where only the successful Leptogenesis condition is satisfied – eq. (6.2.1). The grey squares represent the necessary reheating temperature. The left column corresponds to the result obtained for a normal ordering of the light neutrino mass spectrum, the right one is for inverted ordering. In the latter, for the considered initial values of the preexisting asymmetry, the strong Leptogenesis condition is never satisfied in the investigated portion of the parameter space.

Interestingly, the situation is dramatically different if we consider inverted ordering. As clear from the corresponding plots, in spite of the correct mass pattern, the flavour decay parameters of N_1 do not match the requirement imposed by the τ N_2-dominated scenario. More in detail, notice that $K_{1\mu}$ is limited to $K_{1\mu} \lesssim 10$. Consequently, a sizeable fraction of preexisting asymmetry is always found in the corresponding flavour at the end of the Leptogenesis process.
These preliminary analyses therefore yield an important conclusion: successful strong thermal Leptogenesis within the $S0(10)$-inspired model is allowed *only for a normal ordering* of the light neutrinos.

6.2.2.2 Results on the Seesaw parameters

We present in Figure 6.4 the results on the Seesaw parameters that we obtained by constraining the parameter space with successful strong thermal Leptogenesis in the $SO(10)$-inspired model. Obviously, the study is for a normal ordering of the light neutrino mass spectrum only.
At a first glance, the regions corresponding to the solutions we seek appear remarkably well-defined. The contours corresponding to more severe strong Leptogenesis conditions are included in the ones obtained for lower initial abundances of preexisting asymmetry. This is an important point which testifies the stability of our analysis with respect to the value of $N_{B-L}^{preex,0}$.

A striking feature of these solutions is the presence of new bounds affecting two of the three mixing angles contained in the PMNS mixing matrix. In particular, requiring the washout of a preexisting asymmetry as large as $\mathcal{O}(10^{-1})$ implies the following lower-bound for θ_{13}:

$$\theta_{13} \gtrsim 2^\circ. \tag{6.2.3}$$

We underline that this is a genuine prediction arising from the strong Leptogenesis solutions: no informations on the distribution function of θ_{13} have been employed in performing the present analysis. The presence of a lower-bound on θ_{13} can therefore be regarded as a first proof of the compatibility between the solutions we propose and the latest experimental trend [37–39]. On top of this result, the sharp upper-bound proposed for θ_{23}

$$\theta_{23} \lesssim 41^\circ \tag{6.2.4}$$

is also in line with the latest global analyses of neutrino data [34]. Furthermore this feature potentially offers a first way to discriminate between the successful strong thermal

solutions and other models of neutrino phenomenology.

The third panel of Figure 6.4 shows traces of a linear correlation between the maximum values of the implied mixing angles that our solutions allow. This is interpreted as a remnant of the relation between θ_{23} and θ_{13}, noticed first in [143], that the $SO(10)$-inspired model imposes for small values of m_1. As for the last mixing angle, θ_{12}, the successful strong thermal solutions deliver no predictions in this case, being rather insensitive to changes in this parameter for the considered range.

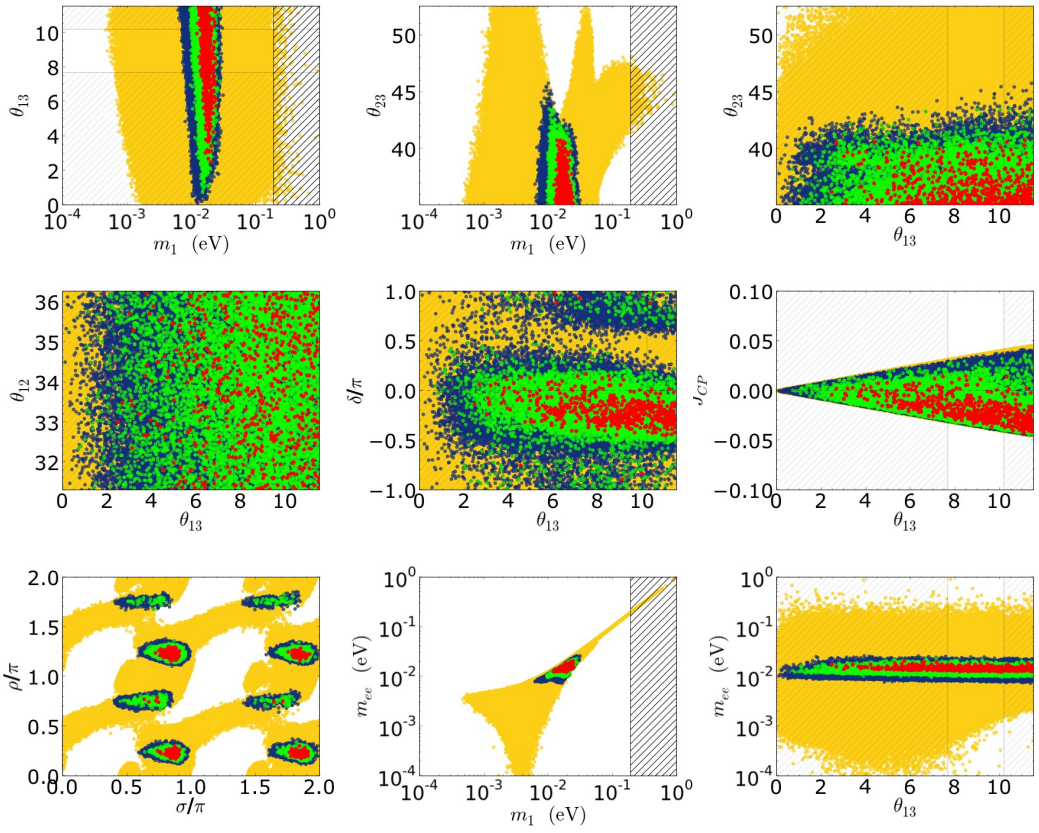

Figure 6.4: Successful strong thermal Leptogenesis: predictions on the low energy neutrino parameters for normal ordering, [142,143]. As before, the hatched area indicate the exclusion limit due to Cosmology and the current 2σ interval for θ_{13}. The yellow regions in the present plots differ from the corresponding ones of Figure 6.1 due to the larger statistics and the extended range for θ_{23} employed here. The remaining colour code is intended as in Figure 6.3.

The next two panels of Figure 6.4, regarding δ and J_{CP}, are particularly important in the light of the latest experimental results on θ_{13}. As we mentioned before, large values of this parameter open up the possibility for a direct testing of the CP-asymmetry in the lepton sector of the SM, controlled by the Dirac phase δ. Considering the latest 2σ interval for θ_{13}, the bulk of our solutions predicts a negative value for δ and, accordingly, for the *Jarlskog invariant* given by

$$J_{CP} = \cos(\theta_{12})\sin(\theta_{12})\ \cos(\theta_{23})\sin(\theta_{23})\ \cos^2(\theta_{13})\sin(\theta_{13})\sin(\delta). \tag{6.2.5}$$

Hence, the successful strong thermal Leptogenesis solutions will be almost completely ruled out if the future experiments will measure positive value of these quantities. Conversely, negative entries for δ and J_{CP} would provide a first strong hint in their support. To conclude, we consider now the prediction on the neutrino mass scales m_{ee} and m_1 which indeed represent the signature of our framework. Due to the rather specific values of the Majorana phases that our conditions selected, successful strong thermal Leptogenesis leads in the $SO(10)$-inspired model to a remarkably sharp prediction:

$$m_1,\, m_{ee} \in (1 - 3) \times 10^{-2} \text{ eV}. \tag{6.2.6}$$

According to our scenario the value of m_1 falls between the two regimes considered before, while m_{ee} is substantially insensitive to variations in θ_{13}. This behaviour is explained considering that for $m_1 \lesssim 0.01$ eV we have $K_{1\mu} \gg 1$, while the solutions for $m_1 \gtrsim 0.01$ eV are characterised by $K_{1e} \gg 1$ [143]. Both these conditions are required in strong thermal Leptogenesis, therefore our analysis correctly selected the points around $m_1 \simeq 0.01$ eV for which these constraints are simultaneously satisfied. This being said, we also remark that both the predictions on m_1 and m_{ee} fall nicely within the reach of the next-generation neutrinoless double-β decay and absolute mass scale experiments.

Owing to the many predictions that the $SO(10)$-inspired model delivers through its successful strong thermal solutions, we have presented a simple and predictive framework in which the parameter space of the Seesaw mechanism can be effectively constrained. In this regard, it is our hope that the investigations of future neutrino experiments will probe our predictions, consequently providing an exhaustive test of this appealing Leptogenesis scenario.

To conclude our discussion, we present in Figure 6.5 our results on the mixing angles and the phases contained in the matrix V_L. Potentially these could provide indications on possible rigorous $SO(10)$ GUT scenarios, where a small misalignment of order U_{CKM} [79] is expected between the basis diagonalising $yy^\dagger$ and $hh^\dagger$ – cf. eq. (6.1.1). Unfortunately in this case our solutions provides no indications, being basically insensitive to these parameters barring a slight preference for the limiting values of ρ^L.

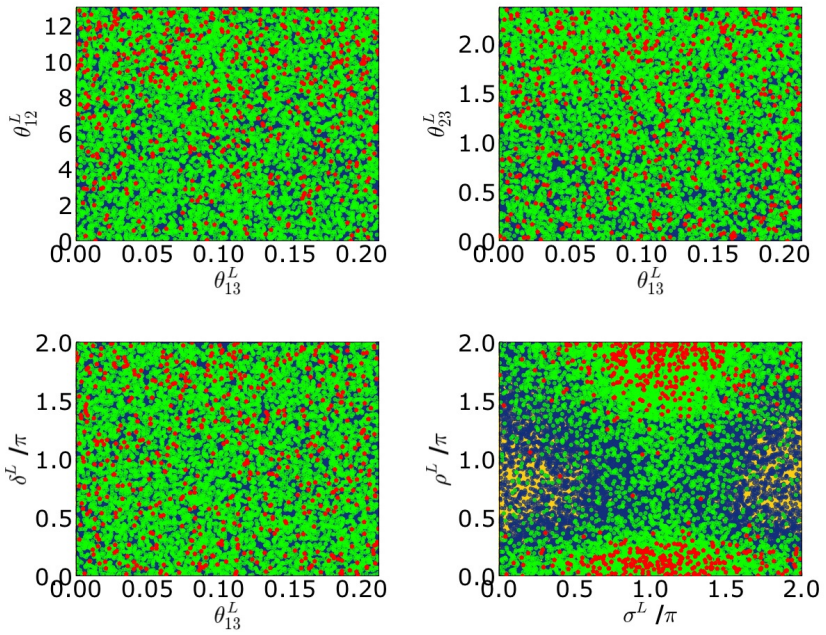

Figure 6.5: Successful strong thermal Leptogenesis: predictions on the parameters in V_L for normal ordering, [142, 143]. The colour code is intended as in Figure 6.3: blue dots are for $\mathcal{O}(10^{-3})$, the green dots for $\mathcal{O}(10^{-2})$ and red stars are for $\mathcal{O}(10^{-1})$. The points indicated by yellow dots correspond to the regions where only the successful Leptogenesis condition is satisfied.

6.3 Refining our analysis

The analyses we presented so far disregard the detailed informations that neutrino experiments provide on the probability distribution functions of the low energy parameters. Our conclusions are therefore based on a scan of the Seesaw parameter space which is not sensitive to the likelihood of the configuration under examination. In particular, the condition that we employed to identify the regions corresponding to successful Leptogenesis, eq. (6.2.1), does not account for the statistical significances of the values adopted for the low energy parameter during the calculation of the asymmetry produced. Likewise, for the latter, the indications of CMB measurements have not been completely exploited. Hence, whereas on one hand the yellow regions proposed in the previous Section indeed indicate the combinations of the low energy parameters for which Leptogenesis is successful, on the other our analysis is not able to discriminate against the likelihood of the selected configurations.

In the present Section we therefore intend to add to our study by better employing the indications that neutrino experiments and CMB measurements provide. In particular, we aim to investigate the impact of these experimental informations on the solutions that we previously identified. We therefore specialise our discussion to the regions where the successful Leptogenesis condition is met, moving by net toward a first statistical

analysis of the successful Leptogenesis solution presented by the $SO(10)$-inspired model. Successful strong thermal Leptogenesis will then be allowed in the $SO(10)$-inspired model if the corresponding sub-regions are not ruled out by the improved treatment of the experimental constraints that we consider here.

6.3.1 Toward a statistical analysis

The first step toward a statistical analyses is modelling the experimental informations that neutrino oscillations experiments and CMB provide. In this regard, we remark that a complete statistical analysis is beyond our current purposes. This would in fact require to derive the probability distribution functions (PDFs) of the involved parameters from scratch, by fitting the dataset of the relevant experiments and consequently marginalising to extract the required PDF from the joint one. In a first approximation, to understand the impact of statistics on our scatterplots, we therefore neglect the correlations that exist between the neutrino oscillation parameters and perform our analyses adopting the following distributions:

- Mixing angles:
  The indications on the mixing angles that neutrino oscillation experiments provide have been modelled in the gaussian distributions reported in the following Table:

Parameter:	Best fit:	Standard deviation:
$\sin^2\theta_{12}$	0.312	0.016
$\sin^2\theta_{23}$	0.450	0.050
$\sin^2\theta_{13}$	0.025	0.007

Table 6.2: The distributions adopted for the PMNS mixing angles in light of the results from neutrino oscillation experiments [34, 147, 148]. The reported values have been chosen to reproduce the actual 1σ and 2σ ranges as accurately as possible in the adopted approximation. The standard deviation adopted for $\sin^2\theta_{13}$ reflects the design sensitivity of the Daya Bay experiment [149].

- The remaining low energy parameters:
  The Dirac phase δ and the Majorana phases ρ and σ –cf. eq. (6.1.4), are not constrained by the current experiments. To our purposes we consequently assume for these parameters flat probability distributions over the relevant intervals.
  In the absence of a signal from the absolute mass scale experiments, the same conservative choice has been also employed in modelling m_1. The light neutrino mass spectrum is then calculated according to eq. (6.1.8) by assuming the mean values for m_{sol} and m_{atm}.

In order to quantify the likelihood of the configurations that successful Leptogenesis selected, we intend to derive now the joint probability distributions for the same quantities which appear in the plots of Figure 6.4 and 6.5. In this regard, it could be indeed sustained that under our working assumption the functions we seek are simply given by the product of the relevant one-parameter PDFs we presented. We therefore remark that, beside the informations resulting from the neutrino experiments encapsulated in the above distributions, our analysis aims to account also for the details in the profile of the baryon asymmetry of the Universe that CMB reveals. More in detail, the joint probability distributions we seek must describe the low energy parameters of the Seesaw mechanism *under the assumption that the baryon asymmetry of the Universe be generated as prescript by the* $SO(10)-$*inspired model of Leptogenesis*. Within the proposed scheme, the informations that the CMB measurements provide on the baryon asymmetry of the Universe are then to be combined to those of the neutrino experiments and consequently result in a further constraint on the parameters we aim to describe. An additional step in the derivation of the relevant PDFs is therefore necessary.

The results of CMB fittings, on top of the Baryon Acoustic Oscillations and the latest measurements of H_0 are extensively discussed in [46, 47]. With a good approximation, the baryon asymmetry of the Universe is then described by the following gaussian distribution

Parameter:	Best fit:	Standard deviation:
η_B	$\eta_B^{CMB} = 6.19 \times 10^{-10}$	$\sigma_\eta = 0.15 \times 10^{-10}$

Table 6.3: The distributions adopted for the baryon asymmetry of the Universe, [46, 47].

We need now to find a proper way to combine these informations. To this purpose let $\boldsymbol{\theta}$ be the seven low energy parameters[4] and let the function p_θ be their joint probability distribution function, obtained by normalising the product of the individual PDFs proposed before. In the same way we also introduce the gaussian distribution p_η, which characterises the baryon asymmetry of the Universe. Quantitatively, our aim is to calculate the joint probability distribution for the low energy parameters *given that* the baryon asymmetry calculated through the $SO(10)$-inspired model is distributed as specified by p_η:

$$p_{SO(10)}\left(\boldsymbol{\theta}|\eta_B^{lept} = \eta_B\right) = p_{SO(10)}(\eta_B^{CMB}, \sigma_\eta, \boldsymbol{\theta}^{best}, \sigma_\theta). \tag{6.3.1}$$

The distribution $p_{SO(10)}$ is then specified by the same parameters, η_B^{CMB}, σ_η, $\boldsymbol{\theta}^{best}$ and σ_θ which regulate the individual PDFs. From a formal point of view, a relation between $p_{SO(10)}$, p_η and p_θ can be obtained by employing the *Bayes' theorem* [150–153]

$$p_{SO(10)}\left(\boldsymbol{\theta}|\eta_B^{lept} = \eta_B\right) = p\left(\eta_B^{lept} = \eta_B|\boldsymbol{\theta}\right)\, p_\theta(\boldsymbol{\theta}) \tag{6.3.2}$$

[4] As remarked before, we neglect the errors associated to m_{atm} and m_{sol}.

Here we neglected a normalisation factor by choosing to normalise our final distribution function in a second moment. We now employ the following decomposition property

$$p(x) = \int p(x|y)\, p(y)\, \mathrm{d}\, y \tag{6.3.3}$$

where $p(x|y)$ is the conditional probability of x given the parameter y. In our case we have

$$p\left(\eta_B^{lept} = \eta_B|\boldsymbol{\theta}\right) = \int p\left(\eta_B^{lept} = \eta_B|\eta_B, \boldsymbol{\theta}\right)\, p(\eta_B|\boldsymbol{\theta})\, \mathrm{d}\, \eta_B. \tag{6.3.4}$$

We recall that η_B is a quantity distributed according to the function p_η, characterised in turn by the parameters of Table 6.3. As the experimental distribution p_η is obtained through the CMB measurements only, independently of the low energy Seesaw parameters, it follows $p(\eta_B|\boldsymbol{\theta}) \equiv p_\eta(\eta_B)$ and therefore

$$p_{SO(10)}\left(\boldsymbol{\theta}|\eta_B^{lept} = \eta_B\right) = \int p\left(\eta_B^{lept} = \eta_B|\eta_B, \boldsymbol{\theta}\right)\, p_\eta(\eta_B)\, p_\theta(\boldsymbol{\theta})\, \mathrm{d}\, \eta_B. \tag{6.3.5}$$

At this stage, to require that the $SO(10)$-inspired model explain the baryon asymmetry of the Universe, we impose

$$p_{SO(10)}\left(\eta_B^{lept} = \eta_B|\eta_B, \boldsymbol{\theta}\right) = \delta\left(\eta_B^{lept}(\boldsymbol{\theta}) - \eta_B\right) \tag{6.3.6}$$

leading to our final result that, once properly normalised, reads:

$$p_{SO(10)}\left(\eta_B^{lept}\eta_B|\boldsymbol{\theta}\right) = \frac{p_\eta\left(\eta_B^{lept}(\boldsymbol{\theta})\right)\, p_\theta(\boldsymbol{\theta})}{\int p_\eta\left(\eta_B^{lept}(\boldsymbol{\theta})\right)\, p_\theta(\boldsymbol{\theta})\, \mathrm{d}\, \boldsymbol{\theta}}. \tag{6.3.7}$$

The joint distribution function we seek is therefore given by the PDFs which describes the Seesaw low energy parameters alone, $p_\theta(\boldsymbol{\theta})$, weighted at every point of the parameter space by the distribution that the CMB measurements propose for the baryon asymmetry. The two-parameter joint PDFs, that quantify the likelihood of the successful Leptogenesis regions we identified before, can be consequently obtained from $p_{SO(10)}$ by marginalization. The results of our procedure are proposed in Figure 6.6 and 6.7, where the scatterplots of our previous analysis are compared with the corresponding probability distribution functions.

The impact of the adopted statistical treatment is clearly visible. By comparing the yellow regions of the left column to the light green areas presented in the right one, which denote a confidence level as large as $CL \simeq 95\%$, the subspace characterised by the successful Leptogenesis condition appears noticeably reduced. A first, obvious, effect of the profiles adopted for the low energy parameter and the baryon asymmetry of the Universe is in fact to collapse the viable subspace, disfavouring the regions characterised by extremal values of the involved quantities. Notice that while such a reduction was expected, the presence of regions that still allow for successful strong thermal solutions of

the model could not be given for granted. The fact that many of these solutions survived can therefore be regarded as a further important proof of the compatibility between the picture we propose and the one that neutrino experiments and CMB provide. Consider for definiteness the red regions presented by the scatterplots in the left column, which correspond to successful strong thermal solutions obtained for an initial preexisting asymmetry of order $\mathcal{O}(10^{-1})$. As clear from the comparison we propose, even by restricting our discussion to a confidence level of $CL \simeq 68\%$ indicated by the dark green areas of the PDFs in the right column, the regions corresponding to successful strong thermal solutions are not ruled out.

Allowing for a confidence level as high as $CL \simeq 95\%$, we reconsider the predictions we made on the low energy parameters, discussed in Section 6.2.2.2, in light of the new statistical treatment adopted. Starting with θ_{13}, successful strong thermal solutions placed a lower-bound for $\theta_{13} \gtrsim 2^\circ$. Now, the statistical treatment alone places a lower-bound $\theta_{13} \gtrsim 4.5^\circ$, for $m_1 \in (1 - 5) \times 10^{-3}$ eV at $CL \simeq 95\%$. Accounting for the strong leptogenesis conditions this constraint is basically unmodified, yielding $\theta_{13} \gtrsim 4.5 - 5^\circ$ for $m_1 \in (1 - 3) \times 10^{-2}$ eV at the same CL.
Differently, for θ_{23} our prediction maintains its full strength. For $m_1 > 10^{-3}$ eV, current experiments indicate values of the mixing angle as high as $\theta_{23} = 48^\circ$ as possible. The successful strong Leptogenesis solutions in this case once again restrict the viable subspace re-proposing the same upper-bound $\theta_{23} = 41^\circ$ for $m_1 \in (1 - 3) \times 10^{-2}$ eV at $CL = 95\%$.
As for the Majorana phases of the PMNS matrix, ρ and σ, our original analysis proposes four main regions – Figure 6.7 – delineated by $\rho \in (0.6\pi - \pi)$ or $\rho \in (1.6\pi - 2\pi)$ and, correspondingly, $\sigma \in (0.1\pi - 0.3\pi)$ or $\sigma \in (1.1\pi - 1.3\pi)$. These are supported by four subdominant configurations, which could play an important role in case of initial preexisting asymmetries as large as $\mathcal{O}(10^{-2})$ but are strongly disfavoured by our refined treatment. In spite of that, the important prediction that successful strong thermal solutions deliver for m_{ee} are unaffected by this selection. This is a crucial point, as the bounds that the solutions we consider place on m_1 and m_{ee} represent, in fact, the signature of the proposed framework. Interestingly, the current experimental information do not discriminate between the values of these quantities on the broad interval m_1, $m_{ee} \in (10^{-3} - 10^{-1})$ eV. On the contrary, once again the successful strong thermal solution are able to place a sharp bound, as only for $m_1 \simeq m_{ee} \in (1 - 3) \times 10^{-2}$ eV the washout of a preexisting asymmetry of order $\mathcal{O}(10^{-1})$ can be ensured.

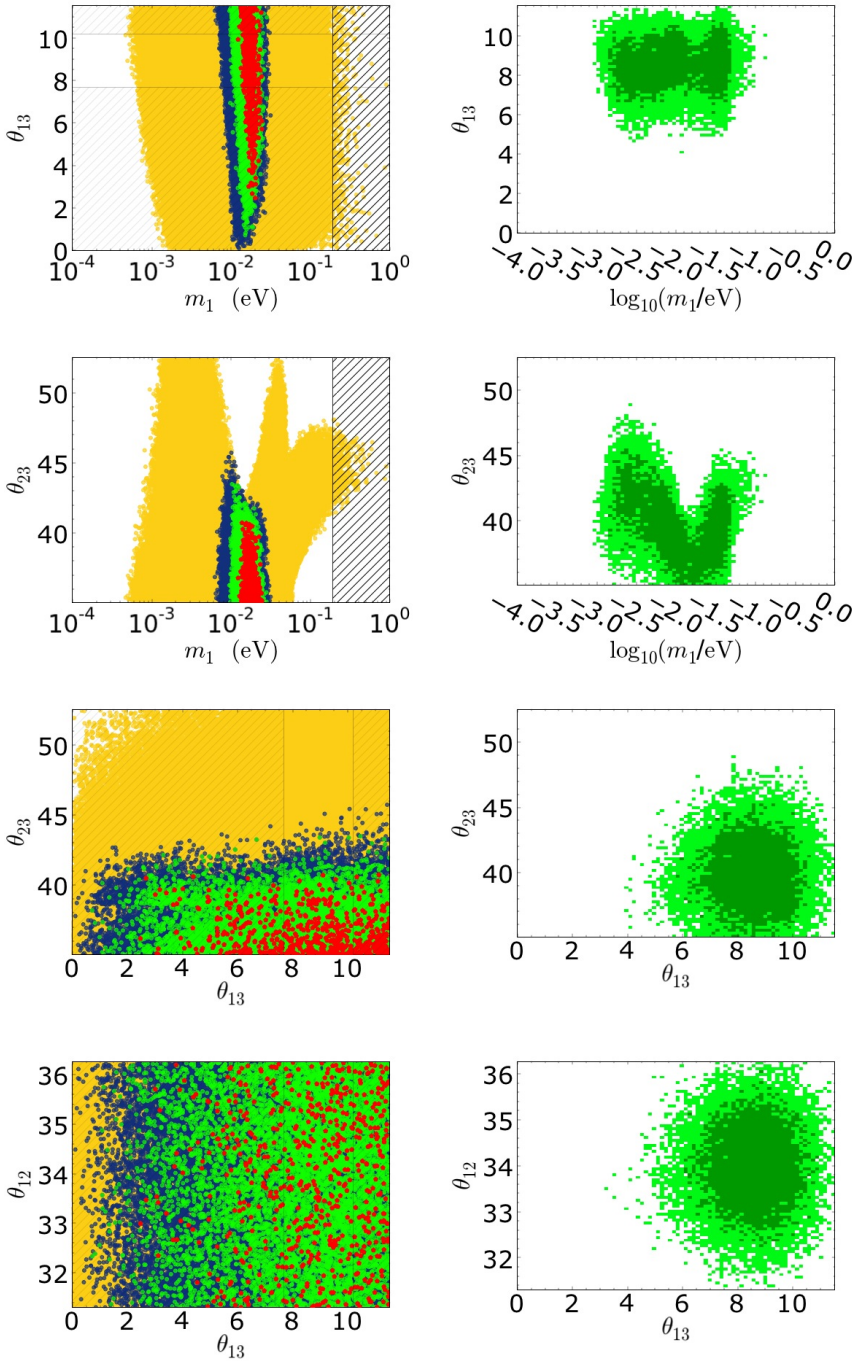

Figure 6.6: A statistical analysis of the successful Leptogenesis condition in the $SO(10)$-inspired model: results on the lepton mixing angles, [146]. We compare the yellow regions of the results in Figure 6.4, presented in the left column, to the corresponding two-parameter joint probability distribution functions, in the right column. For the latter, the dark green regions indicate a confidence level (CL) $CL \simeq 68\%$ while the light green areas correspond to $CL \simeq 95\%$. The direct comparison of scatterplots and PDFs highlights the regions of the Seesaw parameter space which are disfavoured by a statistical treatment. The proposed PDFs are based on the latest global analyses of the neutrino oscillation data [34] and encapsulate the assumption that the $SO(10)$-inspired model of Leptogenesis explains the baryon asymmetry of the Universe, modelled according to Table 6.3.

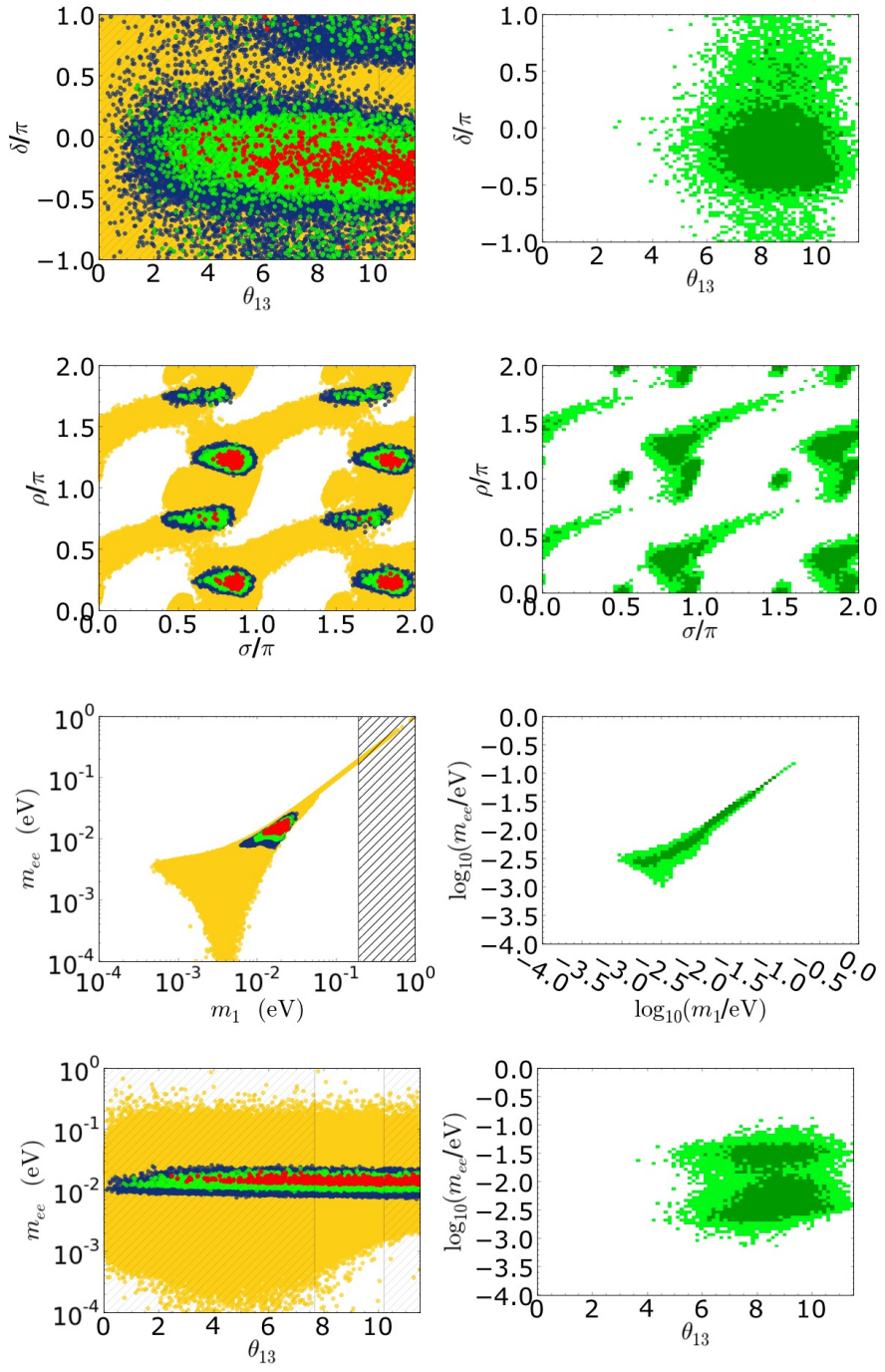

Figure 6.7: A statistical analysis of the successful Leptogenesis condition in the $SO(10)$-inspired model: results on the PMNS phases and neutrino mass scales, [146]. We compare again the scatterplots of Figure 6.4 to the corresponding two-parameter joint probability distribution functions. The colour codes for the latter are intended as in Figure 6.7.

Chapter 7

Epilogue

In this conclusive Chapter we summarise our work and comment on the validity of the presented original results in light of the underlying assumptions we made. The discussion we propose is organised in sections, each corresponding to one of the Chapters that delineate the structure of this Thesis.

On the present status of the Standard Model and Physics

The Standard Model of Particle Physics is indeed one of the most elegant and successful theories ever formulated. The precision of its predictions and the numerous successful experimental confirmations lead to an impressive list of achievement for which this Theory can be regarded as the paradigm of contemporary Particle Physics.
In the normal evolution of Science, however, after a paradigm is established, a number of anomalies which cannot be explained within the corresponding framework is accumulated over the time. These anomalies, when unsolved, reveal the weaknesses of the old theory, test its boundaries, and eventually lead to a *paradigm shift*. Science then enters its revolutionary phase and a new Theory is consequently formulated [154].
It is exciting that we are witnessing this transition right now in Physics. In the last decades, in fact, many experiment underlined results which are left unexplained within the framework of the Standard Model. We focused in particular on a first issue which arises in the lepton sector of the Theory, in connection to the properties of neutrinos.

For the last fifty years these elusive particles have been the subject of an extensive testing, resulting in an increasing disagreement between theory and experiments. On one hand, in fact, the neutrino oscillation experiments underline that at least two neutrino species must be massive in order to reproduce the measured oscillation pattern [33, 66]. On the other, the Standard Model requires its three neutrinos be purely massless particles [4–6, 155, 156], leaving no space for any oscillation. In Section 1.1 we exposed this clash,

reviewing the current description of neutrinos and pointing out its incompatibility with the oscillation mechanism that the experiments support.

We also discussed a further issue that recent Cosmological observations arise within the Standard Model. Beside the fundamental puzzles posed by the Dark Energy and the Dark Matter components of the Universe, we reviewed how the analyses of the Cosmic Microwave Background [46, 47] and the measurement of the primordial nuclear abundances within the Big Bang Nucleosynthesis [52, 53] point out the existence of a baryon asymmetry in our Universe. Interestingly the Standard Model possesses all the ingredients required to develop such an asymmetry [56], nevertheless the emerging scenario of Electro-Weak Baryogenesis [62] is unfortunately not viable [63, 64].

The neutrino mass puzzle and the baryon asymmetry of the Universe are therefore two problems that currently find no solution within the boundaries of the Standard Model. Consequently, the results that the neutrino oscillation experiments and the recent Cosmological measurements expose can be regarded as solid evidences for new Physics and it follows the *present requirement* for new, testable, theoretical frameworks in which the Physics beyond the current paradigms can be modelled.

On the Seesaw mechanism and Leptogenesis

To address the neutrino mass puzzle and the problem raised by the baryon asymmetry of the Universe at once, we consider the minimal *type I Seesaw extension* of the Standard Model [68–71] in which three right-handed neutrinos are added to the particle content of the Theory. These particles, which transform as singlets under the symmetry group of the Standard Model, are provided a Majorana mass term and couple to the lepton and Higgs doublets through a new set of Yukawa couplings. As the RH neutrinos are typically introduced within GUTs theories, where they complete the representations occupied by the remaining particles of the model, the associated mass scale is naturally of order Λ_{GUT}. As we saw in Chapter 2, it is then possible in this setup to explain the mass scale of ordinary neutrinos and the baryon asymmetry of the Universe, respectively through the Seesaw mechanism and Leptogenesis.

- **The origin of neutrino masses: the Seesaw mechanism.**
  Owing to the right-handed neutrinos and the new set of Yukawa coupling introduced by the Seesaw extension, a Dirac mass term is generated in the theory for the ordinary neutrinos after the Electro-Weak symmetry breaking. In the proposed framework the mass scale associated to the three right-handed neutrinos is much larger than the the Electro-Weak scale Λ_{EW}, which characterises the new Dirac masses. Then, as a consequence of the *Seesaw mechanism* introduced in Section 2.1, the neutrino mass spectrum effectively splits into two sectors. The

high energy one presents three heavy Majorana neutrinos N_i with masses of order Λ_{GUT}, whose right-handed components roughly correspond to the new particles originally introduced by the Seesaw extension. The low energy sector comprises instead three light Majorana neutrinos, associated to the energy scale $\sim \Lambda_{EW}^2/\Lambda_{GUT}$ which, surprisingly, matches the typical neutrino mass scale inferred through the oscillation experiments. The three light neutrinos are therefore ideal candidates to address the neutrino mass puzzle and the fact that the detected neutrino mass scale emerges in the theory as a natural consequence of the Seesaw mechanism is indeed a very attractive feature of the proposed scenario.
We remark that the neutrino oscillation and absolute mass scale experiments have therefore the potential to probe at least part of the Seesaw parameter space. In this regard we also underline the importance of the experiments dedicated to the neutrinoless double-β decays, which directly probe the Seesaw prediction made on the Dirac/Majorana nature of neutrinos.

- **Generating the baryon asymmetry: Leptogenesis.**
  There is another fundamental consequence of the Seesaw mechanism, entangling the dynamics of the heavy neutrino species which populate the high energy sector of the theory to the latest Cosmological measurements. In this regard, consider that through the Yukawa interactions introduced by the Seesaw extension the heavy neutrinos can decay into lepton and Higgs doublets or antilepton and antiHiggs doublets, owing to their Majorana nature. We can therefore sketch a new scenario of baryogenesis, *Leptogenesis*, in which the baryon asymmetry of the Universe is explained as a product of an original lepton asymmetry generated by the decays of these particles. In order to effectively give rise to a lepton asymmetry, the heavy neutrino decays must satisfy the restrictive conditions originally detailed by A. D. Sakharov [56] that we reviewed in Section 2.2. The generated asymmetry is then distributed to the remaining particle species through the network of reactions that the active gauge and Yukawa interactions imply in the Early Universe. In particular, to recast the lepton asymmetry as a baryon asymmetry, the Seesaw extension of the Standard Model relies on the non-perturbative *sphaleron* effects, which violate both the lepton and baryon numbers but conserve their difference.
  By net a Leptogenesis process is then able to account for an amount of baryon asymmetry roughly speaking given by 1/100 of the produced $B - L$ asymmetry.

Attracted by the features offered by the Seesaw extension of the Standard Model, in Section 2.2 we presented a first model of Leptogenesis in which the contributions of the heaviest neutrino species and the impact of flavour were neglected. In discussing the resulting N_1-*dominated scenario* we first reviewed how the Sakharov conditions are satisfied within Leptogenesis, introducing consequently the Boltzmann equations which regulate the evolution of the heavy neutrino abundance and the $B - L$ asymmetry. In this simplified scenario we detailed the Leptogenesis process focusing in particular

on the *strong washout regime*, which currently the neutrino experiment indicate – cf. eq. (2.2.24). Supposing a strong washout regime and a thermal production of the relevant heavy neutrinos, within N_1 Leptogenesis, the final $B-L$ asymmetry amount does not depend on the initial conditions adopted to solve the Boltzmann equations. Additionally, in this regime, the simple picture that decays and inverse-decays provide allows an accurate description of the final asymmetry even if scattering processes and thermal corrections are neglected [89].
On top of that, interestingly, even in the simple case of N_1-Leptogenesis a few constraints on the parameters of the model can be derived. As we showed it is the case of M_1, the mass of the lightest of the heavy neutrino species, that for successful Leptogenesis cannot be lighter than about 10^9 GeV [87, 92].
Once the corrections due to the $|\Delta L| = 2$ scattering are taken into account, the amount of asymmetry produced becomes sensitive to the light neutrino mass scale $\bar{m}$ – Section 2.2.1.2 – which regulates the strength of the corresponding washout process. Consequently, successful Leptogenesis also implies within this framework a second bound $\bar{m} < (0.20 - 0.30)$ eV [87, 96].

Flavour effects and the minimal Leptogenesis scenario

In Chapter 3 we improved our description of the Leptogenesis process addressing the flavour effects. To investigate the modifications that flavour introduces, we distinguished between light and heavy neutrino flavour effects when referring, respectively, to the impact of charged-lepton and neutrino Yukawa interactions.

- **The impact of neutrino Yukawa interactions: heavy neutrino flavour states and their interplay.**
  The flavour compositions of the leptons and antileptons produced in the decays of the heavy neutrinos are regulated by neutrino Yukawa interactions according to the diagrams of Figure 2.1. This suggests the definition of the heavy neutrino flavour states $|\ell_i\rangle$ and $|\overline{\ell_i}\rangle$, $i = 1, 2, 3$ as the particular coherent superpositions of flavoured lepton doublets or antidoublets involved in the dynamics of a specific heavy neutrino species N_i. Explicitly, the decay of a neutrino N_i therefore results in a Higgs doublet (or antiHiggs doublet) and in a lepton (or antilepton) specified by the heavy neutrino flavour state $|\ell_i\rangle$ ($|\overline{\ell_i}\rangle$).
  Following the analysis presented in Appendix C, it is clear that the lepton and antilepton states associated to the same heavy neutrino species possess, in general, different flavour compositions and therefore $CP(|\ell_i\rangle) \neq |\overline{\ell_i}\rangle$.

  Under the assumption of hierarchical heavy neutrinos [99], $M_{i+1} > 3M_i$ for $i = 1, 2$, the Leptogenesis process comprises three distinct phases, corresponding to the separated dynamics of these particles which take place for $T \sim M_i$. All these stages

individually resemble the scenario proposed for N_1 Leptogenesis, therefore it is straightforward to generalise the adopted description accounting for the two heaviest neutrino species.

Taking now into account the heavy neutrino flavour effects, the decays and inverse-decays of an heavy neutrino species affect only leptons and antileptons associated to the corresponding heavy neutrino flavour states. We remark, however, that these states do not generally satisfy any orthogonality relation, hence some interplay between the processes and particles associated to different heavy neutrinos is allowed.

Consider for instance the coherent state $|\ell_i\rangle$ ($|\overline{\ell_i}\rangle$), associated to the leptons (antileptons) which participate in the processes of N_i. As soon as active, the inverse processes of a different heavy neutrino $N_{j\neq i}$ are fast enough to effectively resolve in the considered state a component lying along the relative heavy neutrino state $|\ell_j\rangle$ ($|\overline{\ell_j}\rangle$). Within the classical approximation of an instantaneous collapse of the wave-function of the involved quantum states, this process can be regarded as a 'measurement' leading to the *decoherence* of $|\ell_i\rangle$ ($|\overline{\ell_i}\rangle$). The resulting incoherent mixture therefore comprises a state $|\ell_j\rangle$ ($|\overline{\ell_j}\rangle$), involbed in the dynamics of N_j, and an orthogonal state $|\ell_{j_i^\perp}\rangle$ ($|\overline{\ell_{j_i^\perp}}\rangle$), which does not take part in the latter [103, 104]. The inverse-decays of N_j can consequently washout only a part of the asymmetry produced by N_i, corresponding to the components of the original heavy neutrino lepton and antilepton states measured along the heavy neutrino flavour states associated to N_j. The asymmetry stored in the states $|\ell_{j_i^\perp}\rangle$ and $|\overline{\ell_{j_i^\perp}}\rangle$ is instead protected from the washout, hence is not modified by the dynamics of N_j – *the projection effect*. The described interplay clearly depends on the probabilities p_{ij} for a lepton, or antilepton, associated to the dynamics of N_i to be actually measured as the corresponding particle of involved in the processes of a different heavy neutrino N_j. These can be specified in terms of the same coefficient which detail the flavour composition of the heavy neutrino flavour states.

The projection effect is a first, important consequence of flavour effects within Leptogenesis. As a result of the former, the $B-L$ asymmetry produced by the heaviest neutrino species is given a new way to evade the washout of the lightest one, yielding a non-negligible contribution at the end of the Leptogenesis era. In this sense the projection effect provides a first motivation to move beyond the simple N_1-dominated scenario, underlining the importance of the other Leptogenesis stages toward the final amount of $B-L$ asymmetry generated.

- **The role of charged-lepton Yukawa interactions: the light flavour effects.**

  As the temperature of the Universe drops consequently to its expansion, the charged-lepton Yukawa interactions progressively come into equilibrium. When

the associated rate Γ_α, $\alpha = e, \mu, \tau$, satisfy $\Gamma_\alpha \gtrsim \sum_i \Gamma_{ID,i}$ for at least one flavour, the impact of these interactions on the Leptogenesis process cannot be neglected [106]. Metaphorically, we are witnessing a duel between the lepton Yukawa interactions, that compete to identify the relative flavours in the involved lepton and antilepton states. When the above condition is satisfied, the heavy neutrino flavour lepton (antilepton) states generated by the decays of N_i interact, on average, first with the right-handed components of the charged-lepton (antilepton) fields of flavour α and then with a Higgs doublet. Assuming again a classical picture, the involved charged-lepton Yukawa interactions are therefore fast enough to break the coherence of the heavy neutrino flavour states $|\ell_i\rangle$ ($|\overline{\ell_i}\rangle$) prior to their absorption in inverse-decay processes. In this full decoherence limit, which defines a *fully flavoured regime*, the inverse-decays thus involve the Higgs doublets and an incoherent mixture that comprises the following components: *the light flavour states* $|\ell_\alpha\rangle$ ($|\overline{\ell_\alpha}\rangle$), of definite flavour $\alpha = e, \mu, \tau$, and possibly an orthogonal state $|\ell_{\alpha_i^\perp}\rangle$ ($|\overline{\ell_{\alpha_i^\perp}}\rangle$), remnant of the original heavy neutrino flavour state.

The light flavour states correspond to lepton doublets of ordinary flavours e, μ, τ, associated to the corresponding charged leptons. Differently from the case of heavy neutrino flavour states, they satisfy the orthogonality condition $\langle \ell_\alpha | \ell_\beta \rangle = \delta_{\alpha\beta}$, as well as $CP(|\ell_\alpha\rangle) = |\overline{\ell_\alpha}\rangle$. For these reasons, in our depictions of the heavy neutrino flavour effects, the light flavours have been employed as a basis of the flavour space.

This being said, in the limit of full decoherence, the resulting incoherent mixtures comprise statistically independent components whose evolutions must consequently be individually tracked. The associated flavoured $B - L$ asymmetries are therefore to be regulated by dedicated *flavoured Boltzmann equations* [97, 98].

From the condition $\Gamma_\alpha \gtrsim \sum_i \Gamma_{ID,i}$, owing to the hierarchy of the charged-lepton Yukawa couplings, we identify the following fully flavoured regime

- $T \gtrsim 10^{12}$ GeV: *heavy neutrino flavour regime.*
  In this regime no charged-lepton Yukawa interaction satisfies the above condition and the Leptogenesis process is therefore regulated by the interplay of the heavy neutrino flavour states only.
- 10^{12} GeV $\gtrsim T \gtrsim 10^9$ GeV: *two-flavour regime.*
  Here the τ Yukawa interactions are in equilibrium and fast enough to break the quantum coherence of heavy neutrino flavour lepton and antilepton states. The resulting incoherent mixture therefore comprises $|\ell_\tau\rangle$ and $|\overline{\ell_\tau}\rangle$ states, together with the orthogonal $|\ell_{\tau_i^\perp}\rangle$ and $|\overline{\ell_{\tau_i^\perp}}\rangle$. The latter, being a remnant of the original heavy neutrino flavour states, are still a coherent superposition of e and μ leptons. In this regime the Leptogenesis process is detailed by the flavoured asymmetries N_{Δ_τ} and $N_{\Delta_{\tau_i^\perp}}$.
- 10^9 GeV $\gtrsim T$: *three-flavour regime.*
  On top of τ reactions, in this regime also the μ Yukawa interactions satisfy the

equilibrium condition. The heavy neutrino flavour states are therefore completely projected on the tree light flavours states $|\ell_\alpha\rangle$ (or $|\overline{\ell_\alpha}\rangle$). Notice that the electron component of $|\ell_i\rangle$ ($|\overline{\ell_i}\rangle$) is effectively measured in this regime as a non-τ, non-μ state. Under these conditions, the Boltzmann equations must track the evolution of the flavoured asymmetry N_{Δ_α}, $\alpha = e, \mu, \tau$, introduced in eq. (3.2.5).

To expose the impact of light flavour effects within Leptogenesis, we introduced in Section 3.2.1 the flavoured probabilities $p_{i\alpha}$ and $\overline{p}_{i\alpha}$ to detail the flavour content of the heavy neutrino flavour states $|\ell_i\rangle$ and $|\overline{\ell_i}\rangle$. The resulting flavoured Boltzmann equations, which describe the Leptogenesis process within a two or three-flavour regime, present three key differences with respect to the case where the light flavour effects are disregarded:

- The source term of the flavoured Boltzmann equation regulating the $B-L$ production is proportional to the *flavoured CP-asymmetry* $\varepsilon_{i\alpha}$.
- The strength of the washout performed on a flavour α is reduced, with respect to the unflavoured case, by the flavoured probabilities.
- The dynamics of different flavour components is coupled through the *flavour coupling matrix* $\mathrm{C}_{\alpha\beta}$ – Section 3.2.1.1.

Starting with the flavoured CP-asymmetries, our analysis showed that these quantities comprise two distinct contributions. Beside the averaged flavour branching of the usual 'unflavoured' contribution, quantified by ε_i, the flavoured CP-asymmetries encapsulate in fact a new source of CP-violation. This is driven by the possible differences in the flavour compositions of $|\ell_i\rangle$ and $|\overline{\ell_i}\rangle$, measured by $\Delta p_{i\alpha} \coloneqq p_{i\alpha} - \overline{p}_{i\alpha}$. When calculating the total $B-L$ asymmetry, the former contribution yield an enhancement of a factor 2 or 3 with respect to the unflavoured calculation, considering respectively a two or a three-flavour regime. The remarkable novelty that flavour effects introduce is however related to the second contribution, quantified in $\Delta p_{i\alpha}$, which is *not* proportional to the total CP-asymmetry ε_i. This new source of CP-asymmetry therefore evades the bounds that constrain ε_i [87,92] and, provided the washout affects different flavour with different strengths, could potentially dominate the final asymmetry production relaxing the bounds given for N_1 Leptogenesis [107].

Focusing now on the washout term, the presence of the flavoured projectors is explained considering that, within a fully flavoured regime, the evolution of a flavoured asymmetry N_{Δ_α} is only sensitive to the abundances of leptons and antileptons of the corresponding flavour α. Since the relative abundances of light flavour states, with respect to the unflavoured case, are clearly suppressed by the same flavoured probabilities, it follows that the rate of the washout process acting on N_{Δ_α} is correspondingly suppressed.

Lastly, to explain the presence of the flavour coupling matrix [97,98,103,108], we

recall that the asymmetries stored in the different species are correlated through the network that the active gauge and Yukawa interactions form in the Early Universe. Considering all these constraints, as well as the ones imposed by the neutrality of the plasma and the sphaleron processes leads to the formulation of the matrix under examination. However, as remarked before, owing to the hierarchy that the entries of the flavour coupling matrix present, it is a usual practise to approximate $C_{\alpha\beta} \simeq \delta_{\alpha\beta}$, decoupling by net the evolution of the different flavour asymmetries.

As a result of light and heavy neutrino flavour effects the Leptogenesis process is now to be described through different sets of Boltzmann equations corresponding to the different stages that the Leptogenesis era comprises. Within this setup it is not possible to disregard the role that the heaviest neutrino species play in the production of the final $B - L$ asymmetry [103, 113]. Owing to the flavour effects, we are therefore forced to move beyond the N_1 Leptogenesis scenario, considering more complex frameworks, the *minimal leptogenesis scenarios* [121], in which the $B - L$ asymmetry depends on all the 18 parameters that the Seesaw extension introduced.

An introspective analysis: density matrix formalism and Boltzmann equations

Within the classical formalism of Boltzmann equations, the interplay of light and heavy neutrino flavour effects distinguishes between the ten different heavy neutrino mass patterns reported in Figure 4.1. These are obtained in the limits where the masses obey the hierarchical constraint $M_{i+1} > 3M_i$ for $i = 1, 2$ and do not fall in the transition regimes which cannot be described within the proposed classical picture.
Given this premise, in Chapter 4 we generalised the density matrix formalism for the calculation of the matter-antimatter asymmetry in Leptogenesis [103, 112, 114] accounting for the heavy neutrino flavour effects. Our result is a set of density matrix equations which can be employed to describe the evolution of the $B - L$ asymmetry for *any choice* of the heavy neutrino masses.

Within this more general description, the ten hierarchical mass patterns of Figure 4.1 correspond to the cases in which only one of the five relevant Yukawa interactions is effective within each given range of temperatures. As we showed, in these cases the evolution of the asymmetry can be described through separated stages where the density matrix equations always recover one of the sets of Boltzmann equations proposed in the Chapter 3, depending on the temperature regime and therefore on the relevant lepton Yukawa interaction. We consequently confirmed and extended the results that we derived within the simpler description previously proposed, based on the instantaneous collapse of the wave function of the involved quantum states.

In particular, the *projection effect* that characterises the interplay between heavy neutrino flavour states, is confirmed. In fact, also within the rigorous density matrix description of Leptogenesis, the orthogonal component of the $B - L$ asymmetry that the heaviest neutrino species generate escapes the washout performed by the lightest heavy neutrinos. At the same time we also proved that the parallel components of these asymmetries are instead washed out, with the resulting suppression factor that recovers the value previously given within a classical treatment, independently of the considered washout regime – cf. Section 4.2.2.

Beside this, the *phantom terms* emerge as genuine feature of flavoured Leptogenesis. As proved by eq. (4.1.51) , differently from the expectations of the classical calculation, these contributions should be taken into account even in thermal scenarios where a vanishing initial abundance is imposed to the heavy neutrinos.
In this regard, the discrepancy between the density matrix formulation and the classical treatment of the phantom terms that we highlighted is due to the gauge interactions, which were neglected in the latter approach. Once the efficient thermalisation that these interactions imply for the lepton and antilepton abundances is taken into account – cf. eq. (4.1.42) – we are lead to conclude that, likewise the contributions proportional to the total CP-asymmetry ε_i, the phantom terms also undergo a washout process at the production. Interestingly, the corresponding washout rate is half the one acting on the total asymmetry.
This being said, notice that the phantom terms contribute to the final asymmetry even in scenarios where the production, due to a certain heavy neutrino, is followed by the washout performed by a lighter neutrino species within the same fully flavoured regime. Their presence therefore goes beyond the N_2-dominated scenario where they were originally discussed [117].

It would be desirable in future to calculate the asymmetry beyond the ten asymptotic limits presented, solving the full density matrix equations in which more than one lepton Yukawa interactions are simultaneously active. In this way our description of the matter-antimatter asymmetry evolution would be suitable for a generic heavy neutrino mass pattern, including also the cases in which the Leptogenesis process of a heavy neutrino species falls within one of the indicated transition regimes. These general solutions should therefore also hold when the quantum decoherence effects, induced by the charged-lepton Yukawa interactions, are balanced by the neutrino Yukawa interactions that drive the asymmetry generation and the washout process. In this way an effective interpolation between the asymptotic limits of the two regimes under analysis could be given, consequently allowing for the identification of the exact conditions under which the density matrix formalism proposed can be abandoned in favour of a simpler classical treatment.

The problem of initial conditions in Leptogenesis

The rigorous density matrix formulation that we proposed in Chapter 4 availed the classical description of Leptogenesis proposed within the different fully flavoured regimes in Chapter 3. Adopting the latter for its simplicity, we subsequently focused in Chapter 5 on the evolution of the preexisting asymmetry N_{B-L}^{preex}. We already remarked how, within N_1 Leptogenesis, this component is easily controlled by imposing a strong washout regime. Nevertheless, when the interplay of light and heavy neutrino flavour effects is considered, the preexisting asymmetry is given many ways to evade an efficient washout.

The importance of this tedious component follows form the linearity of the Boltzmann equations. The amount of $B-L$ asymmetry present in our Universe at the end of the Leptogenesis process, in general, comprises in fact two contributions. The first one is due to the out-of-equilibrium decays of the heavy neutrinos, therefore is completely determined by the Leptogenesis process. The other contribution is given instead by the residual value of the preexisting asymmetry, as found after the Leptogenesis era – cf eq. (5.1.1). Whereas within every Leptogenesis model we can calculate the suppression that this preexisting contribution receives, owing to the washout processes operated by the inverse-decays of the heavy neutrinos, a precise calculation of its initial abundance is not viable at the moment. The latter would in fact rely on an accurate description of the state of the Universe after the Inflation era and the magnitude of the residual preexisting asymmetry is therefore unknown. A priori, there is consequently no reason to exclude preexisting contributions large enough to dominate the final $B-L$ asymmetry and therefore the same baryon asymmetry of the Universe. In this way, if this component is not addressed, the informations that BBN and CMB provide cannot be used to constrain the Seesaw parameter space, as it is not clear how to disentangle the two contributions in the final $B-L$ asymmetry. In this sense N_{B-L}^{preex} thus represents an *unknown and problematic initial condition* for all the models of Leptogenesis.

To address the problem that N_{B-L}^{preex} poses, we presented a systematic study in which the light and heavy neutrino flavour effects have been exhaustively addressed. Considering all the mass patterns of Figure 4.1, we followed the evolution of the preexisting asymmetry through the resulting Leptogenesis scenarios. Our procedure then selected only the configurations leading to *strong thermal Leptogenesis*, which allows for the complete washout of the preexisting component even if an initial abundance as large as $\mathcal{O}(1)$ is assumed.

It is quite intriguing that there is only one well defined case, corresponding to the τ N_2 dominated scenario, in which successful and strong thermal Leptogenesis are possible at the same time. On one hand, the flavour effects therefore seem to spoil the attractiveness of thermal Leptogenesis, providing many ways for the preexisting asymmetry to avoid the washout process. On the other, they indicate a well defined scenario in which the Leptogenesis contribution necessarily dominates the baryon asymmetry of the Universe

and, at the same time, the independence from possible preexisting asymmetries and the initial conditions therein incapsulated is ensured.

In the setup we propose, as a consequence of the strong thermal Leptogenesis conditions we identified, the final $B-L$ asymmetry is necessarily produced by the decays of the next-to-the-lightest heavy neutrino species, N_2, prevalently in the τ flavour. It is remarkable that this kind of model emerges naturally within the context of grand unified theories. An important example that we discussed in detail is provided by the $SO(10)$-inspired model [3,141–143,145,146], that could therefore explain the observed baryon asymmetry. A detailed analysis of the strong thermal conditions and their implications within the $SO(10)$-inspired model has been presented in Chapter 6 and will be discussed in the next Section.

To conclude our review of Chapter 5 we comment on the assumptions at the basis of our analyses and indicate some caveats regarding the results that we have found.

- **Beyond the hierarchical limit.**
  Our conclusions have been derived assuming the heavy neutrino masses obey the hierarchy imposed by $M_{i+1} > 3M_i$ for $i = 1, 2$. Releasing this assumption, if the two lightest heavy neutrinos have a similar mass below $10^9\,\mathrm{GeV}$ successful Leptogenesis is possible owing to the resonant enhancement presented by the CP-asymmetries [85]. On top of that, as in this configuration the relevant dynamics takes place in the three flavour regime, before the onset of Leptogenesis the preexisting leptons and antileptons responsible for the preexisting asymmetry break down to an incoherent mixture comprising all the light flavour states. In this case, as discussed in Chapter 5, an efficient washout of the preexisting component is enforced simply by imposing $K_{1\alpha} \gtrsim 10$ on all the light flavours. Clearly this would not spoil the successful Leptogenesis condition, leading for example to the scenario described in [93].

  Less trivially, also a scenario where all the heavy neutrino masses are quasi-degenerate should realise successful strong thermal leptogenesis for any value of M_i. In this regard, our results were obtained under the assumption that the washout processes operated by different heavy neutrinos occur at different stages. In this way we can employ the projection effect, as validated by our analysis in Chapter 4. Under these assumptions, in fact, at any stage there is a well defined flavour basis where the density matrix can be taken of the diagonal form. If the washout processes of different heavy neutrinos occur simultaneously along three different directions, it is seems clearly enough the latter be linearly independent to carry out an efficient washout of a preexisting asymmetry. However, we remark, this heuristic argument should first be proven within a rigorous density matrix formulation.

- **Supersymmetry and multiple Higgs scenarios.**
  In the case of supersymmetric models, and likewise in framework invoking more than one Higgs doublet, the charged-lepton Yukawa interactions proceed faster than in the Standard Model and the condition $M_i \lesssim 10^9$ GeV, denoting the beginning of the three flavour regime, is relaxed to [157] $M_i \ll 10^9\,\mathrm{GeV}\,(1+\tan^2\beta)$. On the other hand, the lower bound on the heavy neutrino mass for successful Leptogenesis does not change significantly. Therefore, if $1+\tan^2\beta \gtrsim 20$, it is possible to have a complete washout of the preexisting asymmetry by imposing $K_{1e}, K_{1\mu}, K_{1\tau} \gtrsim 10$ and, at the same time, successful Leptogenesis from the N_1 decays. In other words, within this class of models, it is possible that the traditional N_1-dominated scenario lead to strong thermal Leptogenesis.

- **Phantom Leptogenesis.** In our analysis we assumed that the flavour compositions of the preexisting leptons and antileptons are the same. If the corresponding quantum states are instead allowed a different flavour composition, we have to take into account the possible presence of phantom terms, as well as the additional contributions to the flavoured asymmetries that is consequently originated. Phantom terms clearly provide further ways for a preexisting asymmetry to avoid an efficient washout in all the proposed scenarios but the τ N_2-dominated one [2]. In fact, for the proposed setup, within the N_2 Leptogenesis phase the possible phantom term in the τ flavour is exposed owing to the effect of the corresponding Yukawa interaction. The condition $K_{2\tau} \gtrsim 10$ then ensures its complete washout. The remaining phantom terms, hidden in the e and μ flavours, are washed out in a similar way during the N_1 Leptogenesis stage: first these components are singularly resolved within a three-flavour regime, then the remaining strong conditions $K_{1e}, K_{1\mu} \gtrsim 10$ ensure their suppression.

  The further aspect concerning the different flavour compositions of the involved heavy neutrino flavour states is addressed in a similar way. Within the τ N_2-dominated scenario, phantom terms could only appear in connection to possible differences in the flavour compositions of the heavy neutrino flavour states $|\ell_2\rangle$ and $|\overline{\ell_2}\rangle$, It is then clear that in the proposed setup the same strong conditions $K_{2\tau}, K_{1e}, K_{1\mu} \gtrsim 10$ would ensure again the complete washout of these elusive components. The solutions which respect the strong thermal leptogenesis conditions are consequently independent of the unknown initial conditions encapsulated in the preexisting asymmetry, and also *unaffected by possible discrepancies in the flavour compositions of the heavy neutrino flavour states* which generated the $B-L$ asymmetry.

A well defined framework: $SO(10)$-inspired Leptogenesis

The subject of Chapter 6 is a concrete example of minimal Leptogenesis scenario: the $SO(10)$-inspired model. As we remarked before, the type I Seesaw extension we consider brings *eighteen new parameters* in the game, which regulate the masses and mixings of the heavy and light neutrinos. Currently the dedicated experiments provide only indications on five of these quantities, hence the predictive power of the proposed framework could indeed be questioned.
In order to perform a first test of the Seesaw parameter space it is therefore necessary to provide further constraints, invoking models of new Physics or extending the involved phenomenology. In this regard, after adopting a suitable parametrization, we consider the additional conditions provided by the $SO(10)$-*inspired relations* [79,141,144]. Within this framework, which draws from the $SO(10)$ grand unified theories, the neutrino Dirac masses resulting form the new Yukawa interactions that the Seesaw extension introduced are proportional to the ones of the up-type quarks. Furthermore the matrix V_L, that regulates the mixing of the left-handed components of the light neutrino fields, is to be modelled here after the CKM matrix. In total the low energy neutrino experiments and the $SO(10)$-inspired conditions therefore provide eleven constraints, adding on to the information regarding the baryon asymmetry of the Universe that we can employ owing to Leptogenesis. Hence, as the parameters which remain unconstrained are six phases, an exploration of the parameter space associated to the model is now in reach.

Considering a thermal scenario and negligible discrepancies in the flavour composition of the heavy neutrino flavour states, we began our investigation by reproducing and extending the results previously obtained in [142,143] under the assumptions of successful Leptogenesis. We performed this preliminary analysis for both the possible orderings of the light neutrino mass spectrum, confirming that the $SO(10)$-inspired relations indeed lead to a N_2-dominated scenario under the current assumptions. In the case of normal ordering, reported in Figure 6.1, our work confirmed the presence of two adjacent regions of the parameter space which lead to successful Leptogenesis. The parameter discriminating between these solutions is m_1, with a boundary found for $m_1 \simeq 10^{-2}$ eV. A similar situation is presented by m_{ee}, where $m_{ee} \simeq 10^{-2}$ eV delineates two separated regions both linear in θ_{13}. This coincidence is explained by the strong correlation that the required values of the Majorana phases impose in this model between m_1 and m_{ee}, testified by the relative plot.
Regarding the results obtained for the inverted ordering of the light neutrino mass spectrum, this preliminary analysis confirmed the presence of a lower-bound on θ_{23}. More importantly, the predictions on m_1 and m_{ee} are significantly different from the corresponding solutions presented by normal ordering. In fact, as delineated in previous studies [143], this could allow for a future test of the neutrino mass ordering itself within the $SO(10)$-inspired model.

Attracted by the features of strong thermal Leptogenesis, we investigated the compatibility of the proposed model with the τ N_2-dominated scenario discussed in Chapter 5. Assuming different values for the initial preexisting asymmetry, we performed a scan of the parameter space of the model selecting only the regions were successful and strong thermal Leptogenesis are allowed at the same time. Our results show that a well defined subset of the proposed successful solutions respects the non trivial conditions which allow for the complete washout of the preexisting asymmetry. Interestingly, even the cross-check presented in Figure 6.3 highlights some important results. At a first glance, in fact, it is already clear that the successful strong thermal solutions of the $SO(10)$-inspired model *exclude the inverted ordering* of the light neutrino mass spectrum. Further to that, our analysis confirms the results in [2], proposing a τ N_2-dominated scenario as the only possible setup that allows for the required kind of solutions. In this regard, notice that the values that our procedure selected for the flavoured decay parameters and the heavy neutrino mass spectrum recover the same bounds that our previous study pointed out. In light of these results, the failure of strong thermal Leptogenesis solutions for an inverted ordering of the light neutrino masses can be attributed to $K_{1\mu}$, which here satisfies $K_{1\mu} \lesssim 10$.

Encouraged by the successful outcome of our cross-check, we consequently focused on the impact that the successful strong thermal solutions have on the predictions of the $SO(10)$-inspired model. Disregarding the possibilities offered by the inverted order, the solutions we propose selected once again well defined subspaces in the parameter space of the model, giving rise to sharp predictions which the neutrino experiments are already testing – Figure 6.4.

It is the case of θ_{13}, one of the angles contained in the PMNS matrix, which recently has been subject of an extensive investigation [35–39]. In trend with the latest results, the successful strong thermal solutions show a net preference for large values of this mixing angle, placing the *lower-bound* $\theta_{13} \gtrsim 2^\circ$. We stress on the importance of this first result, which underlines the agreement between the proposed theoretical framework and the latest experimental picture.

A further important result concerns another mixing angle: θ_{23}. The successful strong thermal solutions of the model predict in fact a *stringent upper-bound*, $\theta_{23} \lesssim 41^\circ$, which also is in line with the latest global analyses of neutrino data [34] and, potentially, allows the identification of the framework we are proposing.

Another important indication supporting our scenario is potentially provided by J_{CP}, the Jarlskog invariant, which barring a little number of configurations is negative within this scheme.

On top of that, we showed the remarkable predictions that the model delivers for m_1 and m_{ee}, respectively the lightest neutrino mass and the Majorana effective mass. Owing to the precise values that our procedure selected for the Majorana phases, the $SO(10)$-inspired model highlights for both these quantities the bound $m_1, m_{ee} \in$

$(1-3)\times 10^{-2}$ eV. These constraints, which nicely fall within the reach of the dedicated next generation experiments, encapsulate the signature of the proposed framework and therefore provide a straightforward way to test the strong thermal solutions of the $SO(10)$-inspired model.

The last topic we faced in our exploration of this attractive scenario is the stability of the above conclusions with respect to the experimental data. The proposed analysis disregarded, so far, any information on the likelihood of the selected configurations that neutrino oscillations experiments and CMB provide. To address this issue and refine our investigation, we consequently modelled the available experimental informations in a set of independent probability distribution functions. Then we derived a collective distribution function, which describes the parameter space of the model under the assumption that the baryon asymmetry of the Universe is effectively produced according to the proposed framework. We remark that the adopted method clearly neglects any possible correlation between the involved parameters, relying furthermore on approximate probability distribution functions to describe the behaviour of the latter. Hence, far from being a rigorous statistical analysis of the model, our attempt is to be regarded as a first step in this direction.
Given this premise, in Figure 6.6 and 6.7 we compare the scatterplots previously obtained to the corresponding joint probability distribution functions, derived under the hypothesis of successful $SO(10)$-inspired Leptogenesis.
The impact of our improved treatment is clearly exposed by the visible reduction of the subspace associated to the successful Leptogenesis solutions. In this regard, we emphasise that the adopted statistical considerations nevertheless confirm the presence of the same regions that were previously associated to the τ N_2-dominated scenario. This fact can therefore be regarded as the proof supporting the stability of our conclusions that we were seeking. More in detail, *the bounds that we previously derived are substantially unmodified* by this refined analysis and consequently maintain their full predictive power, with the only notable exception of θ_{13}. In the case of this quantity, in fact, the statistical analysis alone implies the stringent lower-bound $\theta_{13} \gtrsim 4.5^\circ$, for $m_1 \in (1-5)\times 10^{-3}$ eV at a confidence level of 95%, which clearly overrides our previous result. The new constraint is then substantially left unmodified if the strong thermal conditions are imposed, yielding $m_1 \in (1-5)\times 10^{-3}$ eV at the same confidence level.

Summing up, we presented an extensive analysis of the attractive scenario of Leptogenesis provided by $SO(10)$-inspired model. Our investigation focused on the compatibility of this framework with the successful strong thermal solutions identified in the τ N_2-dominated scenario. It would be interesting in the future to test the stability of the proposed results accounting for the effects introduced by the flavour coupling and addressing the running of the involved Yukawa couplings. Beside this, it would be also interesting to investigate the impact of a proper statistical treatment, improving on the method that we adopted in our investigation.

Appendices

Appendix A

Leptons in The Standard Model

In this Appendix we settle down our conventions by reviewing selected topics regarding leptons within the Standard Model.

A.1 Fields and Symmetries

Before the symmetry breaking, the lepton sector of the Standard Model is described in terms of a non-Abelian field theory, built on the $SU(2)_L \times U(1)_Y$ symmetry group of Weak Isospin and Hypercharge [7].

The interactions associated to the $SU(2)_L$ group of Weak Isospin couple non-trivially only the left-handed components of the leptonic fields, denoted by a subscript "L". The generators of $SU(2)$, I_a for $a = 1, 2, 3$, form the Lie algebra of the group and obey the commutation relation

$$[I_a, I_b] = i\varepsilon_{abc}\, I_c, \qquad a, b, c = 1, 2, 3 \tag{A.1.1}$$

with the tensor ε_{abc}, the structure constant of the group, being totally antisymmetric under permutations of its indices and such that $\varepsilon_{123} = 1$. A representation of the Lie algebra of $SU(2)$ is a mapping of the generators onto a set of traceless Hermitian matrices which respect the relation (A.1.1). In particular, an important bi-dimensional representation of the algebra is obtained by mapping the generators onto the three Pauli matrices:

$$I_a \to \frac{\sigma_a}{2}, \qquad a = 1, 2, 3 \tag{A.1.2}$$

where

$$\sigma_1 = \sigma_x = \begin{pmatrix} 0 & 1 \\ 1 & 0 \end{pmatrix}, \qquad \sigma_2 = \sigma_y = \begin{pmatrix} 0 & -i \\ i & 0 \end{pmatrix}, \qquad \sigma_3 = \sigma_z = \begin{pmatrix} 1 & 0 \\ 0 & -1 \end{pmatrix}. \tag{A.1.3}$$

Once the fields are assigned to representations of the symmetry group, the action of an element of $SU(2)$ is defined by the transformation it induces on the fields themselves. For Lie groups we can consider each finite transformation as a series of infinitesimal ones, continually connected to the identity. As a consequence, we can relate the particular transformation induced by an element of the group to a specific linear combination of the group generators $\boldsymbol{\theta} \cdot \mathbf{I}$:

$$\mathcal{G}_{SU(2)}(\boldsymbol{\theta}) = 1 + i\boldsymbol{\theta} \cdot \mathbf{I} + \cdots \simeq \exp\left(i\boldsymbol{\theta} \cdot \mathbf{I}\right). \tag{A.1.4}$$

It is therefore clear that representations of the group elements can be obtained from the ones given for the generators by exponentiation. For example, in case of the bi-dimensional representation discussed above, we have:

$$\mathcal{G}_{SU(2)}(\boldsymbol{\theta}) \to U_{SU(2)}(\boldsymbol{\theta}) = \exp\left(\frac{i}{2}\boldsymbol{\theta} \cdot \boldsymbol{\sigma}\right). \tag{A.1.5}$$

The $U(1)_Y$ group accounts for the Hypercharge symmetry in the Standard Model. Its generator is the Hypercharge operator Y, connected to I_3 and the generator Q of Quantum ElectroDynamics by the relation

$$Q = I_3 + \frac{Y}{2}. \tag{A.1.6}$$

Again a representation of the group elements, $\mathcal{G}_Y$, is given by exponentiating the representation of the generator, Y:

$$\mathcal{G}_Y(\eta) \to U_Y(\eta) = \exp\left(i\eta\frac{Y}{2}\right). \tag{A.1.7}$$

Thus, for the total symmetry group acting on the leptonic sector of the Standard Model, we have

$$SU(2)_L \times U(1)_Y \ni \mathcal{G}(\boldsymbol{\theta}, \eta) = \mathcal{G}_{SU(2)}(\boldsymbol{\theta})\mathcal{G}_Y(\eta). \tag{A.1.8}$$

and the generic element is given by:

$$\mathcal{G}(\boldsymbol{\theta}, \eta) \to U(\boldsymbol{\theta}, \eta) = U_{SU(2)}(\boldsymbol{\theta})U_Y(\eta) \tag{A.1.9}$$

With respect to $SU(2)_L$, leptons are assigned to three generations of doublets

$$\ell'_{\alpha L} \coloneqq \begin{pmatrix} \nu'_{\alpha L} \\ l'_{\alpha L} \end{pmatrix}, \qquad \alpha = e, \mu, \tau \tag{A.1.10}$$

and three singlets $l'_{\alpha R}$, which provide, after the Electro-Weak symmetry breaking, the right-handed components to the fields corresponding to the massive charged-lepton. The phase transition associated to this symmetry breaking is instead triggered by the Higgs

doublet:

$$\Phi \coloneqq \begin{pmatrix} \phi^+ \\ \phi^0 \end{pmatrix}. \tag{A.1.11}$$

The Hypercharge is assigned to fields as prescript by Table A.1, in order to produce the correct electric charge for the associated particles after the symmetry breaking, eq. (A.1.6). The transformations laws of the considered fields therefore are

$$\ell'_{\alpha L} \longrightarrow U(\boldsymbol{\theta}, \eta)\, \ell'_{\alpha L} = e^{\frac{i}{2}\boldsymbol{\theta}\cdot\boldsymbol{\sigma} - \frac{i}{2}\eta}\, \ell'_{\alpha L} \tag{A.1.12}$$

$$\Phi \longrightarrow U(\boldsymbol{\theta}, \eta)\, \Phi = e^{\frac{i}{2}\boldsymbol{\theta}\cdot\boldsymbol{\sigma} + \frac{i}{2}\eta}\, \Phi \tag{A.1.13}$$

$$l'_{\alpha R} \longrightarrow U(\boldsymbol{\theta}, \eta)\, l'_{\alpha R} = e^{-i\eta}\, l'_{\alpha R} \tag{A.1.14}$$

where $\alpha = e, \mu, \tau$. For local transformations, $\eta, \theta \equiv \eta(x), \theta(x)$, the invariance of the Standard Model Lagrangian requires the adoption of the covariant derivative

$$D_\mu \coloneqq \partial_\mu - ig\, \mathbf{A}_\mu \cdot \mathbf{I} - ig'\, B_\mu \frac{Y}{2} \tag{A.1.15}$$

which introduces four gauge bosons and their interactions in the theory.

Field	$\lvert I \rvert$	I_3	Y
$\nu_{\alpha L}$	1/2	1/2	-1
$l_{\alpha L}$	1/2	-1/2	-1
$l_{\alpha R}$	0	0	-2
ϕ^+	1/2	1/2	+1
ϕ^0	1/2	-1/2	+1

Table A.1: Standard Model, the matter content of the leptonic sector.

A.2 Neutrinos and the charged current interaction

We focus now on a specific aspect of Weak Interactions after the phase transition, the charged current interactions, which couple neutrinos to charged leptons and W bosons:

$$\mathcal{L}_{cc}^{lep} = -\frac{g}{2\sqrt{2}}\, j_W^\mu\, W_\mu + \text{H.c.}. \tag{A.2.1}$$

$$j_W^\mu = 2 \sum_{\alpha=e,\mu,\tau} \overline{\ell'_{\alpha L}}\, \gamma^\mu\, I_+\, \ell'_{\alpha L} \tag{A.2.2}$$

The matrix $I_+ \coloneqq (\sigma_1 + i\sigma_2)/2$ of eq. (A.2.2) is the raising operator in the $SU(2)_L$ algebra, associated to the gauge field $W^\mu \coloneqq: (A_1 - iA(2))/\sqrt{2}$. Then, considering the

explicit form of I_+, eq. (A.2.2) and (A.2.1) become

$$\mathcal{L}_{cc}^{lep} = -\frac{g}{\sqrt{2}} \sum_{\alpha,\beta=e,\mu,\tau} \left[\overline{\nu'_{\alpha L}}\,\gamma^\mu\,(U_L^{l\dagger})_{\alpha\beta}\,l_{\beta L}\right] W_\mu + \text{H.c.} \tag{A.2.3}$$

where $l_{\beta L}$ are the left handed components of the fields corresponding to the charged lepton mass eigenstates, defined by the diagonalisation of the charged lepton Yukawa term

$$\mathcal{L}_{SM} \supset \mathcal{L}_m^{lep} = -v \sum_{\alpha,\beta=e,\mu,\tau} \overline{l'_{\alpha L}}\,y_{\alpha\beta}\,l'_{\beta R} + \text{ H.c.} \tag{A.2.4}$$

$$= -v \sum_{\alpha=e,\mu,\tau} (D_y)_\alpha\,\overline{l_{\alpha L}} l_{\alpha R} + \text{ H.c.} \tag{A.2.5}$$

with $y = U_L^{l\dagger}\,D_y\,U_R^l$ and

$$\begin{pmatrix} l_{eL} \\ l_{\mu L} \\ l_{\tau L} \end{pmatrix} \coloneqq U_L^l \begin{pmatrix} l'_{eL} \\ l'_{\mu L} \\ l'_{\tau L} \end{pmatrix} = \begin{pmatrix} e_L \\ \mu_L \\ \tau_L \end{pmatrix}, \qquad \begin{pmatrix} l_{eR} \\ l_{\mu R} \\ l_{\tau R} \end{pmatrix} \coloneqq U_R^l \begin{pmatrix} l'_{eR} \\ l'_{\mu R} \\ l'_{\tau R} \end{pmatrix} = \begin{pmatrix} e_R \\ \mu_R \\ \tau_R \end{pmatrix}. \tag{A.2.6}$$

It should be now stressed that the Lagrangian of the SM does not provide a mass term for neutrinos, which are therefore purely massless particles within this theory. Consequently we can pick an arbitrary basis for the fields associated to the degenerate neutrino mass eigenstates, as no unique prescription for a rotation corresponding to eq. (A.2.6) is given for these particles. In particular we can choose the mass eigenstate basis in a way that the related field n_i satisfy

$$n_{iL} = \sum_{\alpha=e,\mu,\tau} (U_L^l)_{i\alpha}\,\nu'_{\alpha L}, \qquad i = 1,2,3 \tag{A.2.7}$$

diagonalising by net equation eq. (A.2.3) in the flavour space:

$$\mathcal{L}_{SM} \supset -\frac{g}{\sqrt{2}} \sum_{\substack{i=1,2,3 \\ \alpha=e,\mu,\tau}} [\overline{n_{iL}}\,\gamma^\mu\,\delta_{i\alpha}\,l_{\alpha L}]\,W_\mu + \text{H.c.}. \tag{A.2.8}$$

As a consequence the neutrino mass eigenstates created by the fields in eq. (A.2.7) possess a definite flavour, determined by the coupling to a specific charged lepton mass eigenstate.

Differently, in theories which allow for massive neutrinos, the matrix U_L^ν and the associated left-handed components of the fields describing the neutrino mass eigenstates, n_{iL}, are completely defined by the diagonalisation of the neutrino mass term. Hence

eq. (A.2.3) generalises to

$$\mathcal{L}_{SM} \not\supset \mathcal{L}_{cc}^{m_\nu \neq 0} = -\frac{g}{\sqrt{2}} \sum_{\substack{i=1,2,3 \\ \alpha=e,\mu,\tau}} \left[\overline{n_{iL}}\, \gamma^\mu \, (U^\dagger)_{i\alpha}\, l_{\alpha L} \right] W_\mu + \text{H.c.} \tag{A.2.9}$$

where the PMNS mixing matrix U is given by:

$$U \coloneqq U_L^l \, U_L^{\nu\dagger}. \tag{A.2.10}$$

The PMNS matrix thus provides a measure of the mismatch between two basis, which respectively diagonalise the charged-lepton mass matrix and the neutrino one. The flavour neutrino fields involved in the charged current interactions are, therefore, superpositions of the left-handed components of the fields n_i

$$\nu_{\alpha L} \equiv \sum_{i=1}^{3} U_{\alpha i}\, n_{iL}, \qquad \alpha = e, \mu, \tau. \tag{A.2.11}$$

corresponding to the neutrino mass eigenstates.

Appendix B

On the definition of baryon asymmetry

In this Appendix we focus on the definition of baryon asymmetry given in eq. (1.2.1).

In the expanding Universe a unitary comoving volume corresponds to a physical volume of size $V(t) = R(t)^3 = \big(a(t)R_0\big)^3$, where $R(t)$ is the scale factor of the Friedmann-Robertson-Walker metric and the subscript "0" refers to quantities calculated at the reference time t_0. Hence, for the definition of entropy

$$S \propto g_{\star S} T^3 a^3 R_0^3 \tag{B.0.1}$$

it is clear that the entropy per coming volume is conserved during the expansion of the Universe, provided that $g_{\star S}$ is constant. The latter quantifies the contribution to the entropy of a relativistic species i in thermal equilibrium with radiation. Explicitly

$$g_{\star S} \coloneqq \sum_{i=\text{bosons}} g_i + \sum_{i=\text{fermions}} \frac{7}{8} g_i. \tag{B.0.2}$$

where g_i is the internal number of degrees of freedom that the species i possesses. Going further, eq. (B.0.1) implies

$$T \propto g_{\star S}^{-1/3} (a R_0)^{-1} \tag{B.0.3}$$

and therefore

$$T = T_0 \left(\frac{g_{\star S,0}}{g_{\star S}} \right)^{1/3} a^{-1}. \tag{B.0.4}$$

Recalling now that the photon number density

$$n_\gamma = \frac{\zeta(3)}{\pi^2} g_\gamma T^3 \tag{B.0.5}$$

scales with the Universe expansion as

$$n_\gamma \propto a^{-3} R_0^{-3} \qquad \text{if } g_{\star S} = \text{const.} \tag{B.0.6}$$

it follows that n_γ is implicitly a measure of the physical size of a unitary comoving volume. Notice also that equation (B.0.4) implies

$$n_\gamma = n_{\gamma,0} \frac{g_{\star S,0}}{g_{\star S}} a^{-3} \tag{B.0.7}$$

while the net baryon density is diluted by the Universe expansion in the same way as n_γ:

$$n_B - n_{\overline{B}} = \left(n_B - n_{\overline{B}}\right)_0 a^{-3}. \tag{B.0.8}$$

Hence, the baryon asymmetry of the Universe defined by

$$\eta_B := \frac{n_B - n_{\overline{B}}}{n_\gamma} \tag{B.0.9}$$

implicitly provides a measure of the net number of baryons contained in a unitary comoving volume. Furthermore, in absence of baryon violating interactions, the evolution of η_B is regulated by

$$\eta_{B,0} = \eta_B \frac{g_{\star S,0}}{g_{\star S}}. \tag{B.0.10}$$

accounting for the dilution factor due to photon production.

Appendix C

The rescaled amplitudes $\mathcal{C}_{i\alpha}$ and the CP-asymmetries

The present Appendix is dedicated to the relation between the CP-asymmetries and the rescaled amplitudes $\mathcal{C}_{i\alpha}$ and $\overline{\mathcal{C}}_{i\alpha}$.

The CP-asymmetries are traditionally evaluated through an explicit calculation of the diagrams in Figure 2.1 [85, 102, 158]. This straightforward approach, despite leading to the correct result for $\varepsilon_{i\alpha}$, is however not well-formulated under a formal point of view. In fact, the employed S-matrix formalism is able to describe only processes between input and output asymptotic states that correspond to stable physical particles. In the depiction of Quantum Field theories offered by the Feynman diagrams, these states are associated to *fully-renormalised external legs*, involving *dressed propagators* that account for all the relevant quantum corrections. For stable particles, the S-matrix element under investigation can then be evaluated considering the necessary *amputated diagrams*, as well as the renormalisation factors that the external lines involve [159]. Unfortunately the same procedure does not hold in case of unstable particles: the associated self-energy diagrams have non-zero imaginary parts, consequently the corresponding counterterms spoil the unitarity of the S-matrix as the renormalised Lagrangian is no longer Hermitian. The properties of unstable particles are then to be inferred only from the study of the on-shell scattering processes that the same particles mediate. This rigorous approach has been previously applied to Leptogenesis, [160] and [120], confirming the results obtained from a naive calculation of the decay diagrams.

Adopting the formalism proposed in [160] and [120], we provide now a rigorous definition for the factors $\mathcal{C}_{i\alpha}$ and $\overline{\mathcal{C}}_{i\alpha}$ which appear in the expressions for the heavy neutrino flavour states

$$|\ell_i\rangle \coloneqq \sum_{\alpha=e,\mu,\tau} \mathcal{C}_{i\alpha} |\ell_\alpha\rangle \tag{C.0.1}$$

$$|\overline{\ell_i}\rangle \coloneqq \sum_{\alpha=e,\mu,\tau} \overline{\mathcal{C}}_{i\alpha}\, |\overline{\ell_\alpha}\rangle\,. \tag{C.0.2}$$

The relations presented in Section 3.2.1, reported below for convenience

$$|\mathcal{C}_{i\alpha}|^2 = \frac{\Gamma_{i\alpha}}{\Gamma_i} \tag{C.0.3}$$

$$\left|\overline{\mathcal{C}}_{i\alpha}\right| = \frac{\overline{\Gamma}_{i\alpha}}{\overline{\Gamma}_i} \tag{C.0.4}$$

suggest that $\mathcal{C}_{i\alpha}$ and $\overline{\mathcal{C}}_{i\alpha}$ can be interpreted as rescaled flavoured amplitudes for the associated decay process of a heavy neutrino N_i. At the tree-level, we therefore identify

$$\begin{aligned} \mathcal{C}^0_{i\alpha} &= \frac{h_{\alpha i}}{\sqrt{(h^\dagger\, h)_{ii}}} \\ \overline{\mathcal{C}}^0_{i\alpha} &= \frac{h^*_{\alpha i}}{\sqrt{(h^\dagger\, h)_{ii}}} \end{aligned} \tag{C.0.5}$$

while, at one-loop level, our rescaled amplitudes read

$$\mathcal{C}_{i\alpha} = \frac{1}{\sqrt{(h^\dagger h)_{ii} - 2\Re(h^\dagger h \xi_u)_{ii}}} \left[h_{\alpha i} - (h\, \xi_u)_{\alpha i}\right] \tag{C.0.6}$$

$$\overline{\mathcal{C}}_{i\alpha} = \frac{1}{\sqrt{(h^\dagger h)_{ii} - 2\Re(h^\dagger h \xi^*_v)_{ii}}} \left[h^*_{\alpha i} - (h^*\, \xi_v)_{\alpha i}\right] \tag{C.0.7}$$

and the quantum correction generated by the self-energies and the vertex diagrams have been modelled in the functions ξ_u and ξ_v. More in detail, introducing the diagonal mass matrix $M_{ki} \coloneqq M_i \delta_{ki}$, the proposed corrections comprise two contributions [160], [120]:

$$\begin{aligned} \left[\xi_u(M_i^2)\right]_{ki} &\coloneqq \left[u^T(M_i^2) + M b(M_i^2)(h^\dagger\, h)^T M\right]_{ki} \\ \left[\xi_v(M_i^2)\right]_{ki} &\coloneqq \left[v^T(M_i^2) + M b(M_i^2)(h^\dagger\, h) M\right]_{ki}. \end{aligned} \tag{C.0.8}$$

The functions u and v enter the diagonalisation of the heavy neutrino propagator and depend on the on-shell part of the latter, $\omega_{ik}(q^2 = M_i^2)$, as well as on the self-energies $\Sigma_{N,ki}(q^2) \equiv a(q^2)(h^\dagger\, h)_{ki}$, where the involved loop factor $a(q^2)$ is also to be evaluated on the mass-shell:

$$\begin{aligned} u_{ki}(M_i^2) &\coloneqq \omega_{ki}(M_i^2)\left[M_k \Sigma_{N,ik}(M_i^2) + M_i \Sigma_{N,ki}(M_i^2)\right] \\ v_{ki}(M_i^2) &\coloneqq \omega_{ki}(M_i^2)\left[M_k \Sigma_{N,ki}(M_i^2) + M_i \Sigma_{N,ik}(M_i^2)\right]. \end{aligned} \tag{C.0.9}$$

The second term on the RHS of eq. (C.0.8) is instead due to the vertex correction, being $b(q^2)$ the relevant loop factor.

It can be easily checked that generally $\xi_v \neq \xi_u^*$, therefore $\overline{\mathcal{C}}_{i\alpha} \neq \mathcal{C}^*_{i\alpha}$ and a different flavour composition of leptons and antileptons is implied.

We can now employ the presented rescaled amplitudes to calculate the flavoured and the total CP-asymmetries. Defining the difference within the flavoured branching ratios $\Delta p_{i\alpha} \coloneqq |\mathcal{C}_{i\alpha}|^2 - \left|\overline{\mathcal{C}}_{i\alpha}\right|^2$, from eq. (3.2.27) in fact it follows

$$\Delta p_{i\alpha} \simeq 2(p^0_{i\alpha}\,\varepsilon_i - \varepsilon_{i\alpha}) \tag{C.0.10}$$

where we neglected terms of orders higher than $\mathcal{O}(h^6_{\alpha i})$ and the factor "2" on the RHS is due to the fact that decay rates have been summed over the $SU(2)_L$ index. A straightforward calculation of $\Delta p_{i\alpha}$ can be performed starting from eq.s (C.0.6) and (C.0.7), resulting in

$$\begin{aligned}|\mathcal{C}_{i\alpha}|^2 - \left|\overline{\mathcal{C}}_{i\alpha}\right|^2 = \frac{1}{(h^\dagger\,h)_{ii}} \sum_k \Big\{ & 4M_i M_k \,\mathrm{Im}\left[b_{ki}(M_i^2)\right]\,\mathrm{Im}\left[h^*_{\alpha i} h_{\alpha k} (h^\dagger\,h)_{ik}\right] \\ & + 4M_k \,\mathrm{Re}\left[\omega_{ki}(M_i^2)\right]\,\mathrm{Im}\left[a(M_i^2)\right]\,\mathrm{Im}\left[h^*_{\alpha i} h_{\alpha k} (h^\dagger\,h)_{ik}\right] \\ & + 4M_i \,\mathrm{Re}\left[\omega_{ki}(M_i^2)\right]\,\mathrm{Im}\left[a(M_i^2)\right]\,\mathrm{Im}\left[h^*_{\alpha i} h_{\alpha k} (h^\dagger\,h)_{ki}\right] \\ & - 4\frac{|h_{\alpha i}|^2}{(h^\dagger h)_{ii}} M_k \left(M_i \,\mathrm{Im}\left[b_{ki}(M_i^2)\right] + \,\mathrm{Re}\left[\omega_{ki}(M_i^2)\right]\mathrm{Im}\left[a(M_i^2)\right]\right)\,\mathrm{Im}\left[(h^\dagger\,h)^2_{ik}\right]\Big\}\,.\end{aligned} \tag{C.0.11}$$

As a next step we plug in the expression for the on-shell loop coefficients, given by

$$\mathrm{Im}\left[a(M_i^2)\right] = -1/(16\pi) \tag{C.0.12}$$

and

$$\mathrm{Im}\left[b_{ki}(M_i^2)\right] = \frac{1}{16\pi M_i M_k} f(x_k/x_i) \tag{C.0.13}$$

where $x_i \equiv M_i^2/M_1^2$ and $f(x) = \sqrt{x}\left(1 - (1+x)\log\left(\frac{1+x}{x}\right)\right)$. As for the real part of the on-shell propagator we have

$$\mathrm{Re}\left[\omega_{ki}(M_i^2)\right] = \frac{M_i(M_k^2 - M_i^2)}{(M_k^2 - M_i^2)^2 + (M_k\Gamma_i - M_i\Gamma_k)^2} \tag{C.0.14}$$

which further simplifies by neglecting the term $(M_k\Gamma_i - M_i\Gamma_k)^2$ in the denominator, corresponding to the assumption of hierarchical heavy neutrinos. In this way from the last line of eq. (C.0.11) it follows by inspection

$$\varepsilon_i = \frac{3}{16\,\pi\,(h^\dagger\,h)_{ii}} \sum_{j\neq i} \mathrm{Im}\left[(h^\dagger h)^2_{ij}\right] \frac{\xi(x_j/x_i)}{\sqrt{x_j/x_i}} \tag{C.0.15}$$

where the function $\xi(x)$ is as usual defined according to:

$$\xi(x) = \frac{2}{3}\,x\,\left[(1+x)\,\ln\left(\frac{1+x}{x}\right) - \frac{2-x}{1-x}\right]. \tag{C.0.16}$$

The flavoured CP-asymmetries are instead contained in the first three lines of eq. (C.0.11), which correctly read

$$\varepsilon_{i\alpha} = \frac{3}{16\,\pi (h^\dagger\, h)_{ii}} \sum_{j\neq i} \left\{ \text{Im}\, \left[h^*_{\alpha i} h_{\alpha j} (h^\dagger h)_{ij} \right] \frac{\xi(x_j/x_i)}{\sqrt{x_j/x_i}} + \frac{2}{3(x_j/x_i - 1)} \text{Im}\, \left[h^*_{\alpha i} h_{\alpha j} (h^\dagger h)_{ji} \right] \right\}. \tag{C.0.17}$$

Bibliography

[1] S. Blanchet, P. Di Bari, D.A. Jones and L. Marzola, (2011), 1112.4528.

[2] E. Bertuzzo, P. Di Bari and L. Marzola, Nuclear Physics B 849 (2011) 521, 1007.1641.

[3] L. Marzola, Proceedings presented for the Electroweak Interaction and Unified Theories session of the 47th edition of the Recontres de Moriond, 2012.

[4] S. Glashow, Nucl.Phys. 22 (1961) 579.

[5] A. Salam, Conf.Proc. C680519 (1968) 367.

[6] S. Weinberg, Phys. Rev. Lett. 19 (1967) 1264.

[7] E. Abers and B.W. Lee, Physics Reports 9 (1973) 1.

[8] UA1 Collaboration, G. Arnison et al., Phys.Lett. B122 (1983) 103.

[9] UA1 Collaboration, G. Arnison et al., Phys.Lett. B126 (1983) 398.

[10] UA2 Collaboration, P. Bagnaia et al., Phys.Lett. B129 (1983) 130.

[11] UA2 Collaboration, M. Banner et al., Phys.Lett. B122 (1983) 476.

[12] S. Herb et al., Phys.Rev.Lett. 39 (1977) 252.

[13] D0 Collaboration, S. Abachi et al., Phys.Rev.Lett. 74 (1995) 2632, hep-ex/9503003.

[14] CDF Collaboration, F. Abe et al., Phys.Rev.Lett. 74 (1995) 2626, hep-ex/9503002.

[15] DONUT Collaboration, K. Kodama et al., Phys.Lett. B504 (2001) 218, hep-ex/0012035.

[16] CMS Collaboration, CERN preprint CMS-PAS-HIG-12-020 (2012).

[17] ATLAS Collaboration, CERN preprint ATLAS-CONF-2012-093 (2012).

[18] B. Pontecorvo, Soviet Journal of Experimental and Theoretical Physics 26 (1968) 984.

[19] B. Pontecorvo, Soviet Journal of Experimental and Theoretical Physics 6 (1958) 429.

[20] Z. Maki, M. Nakagawa and S. Sakata, Progress of Theoretical Physics 28 (1962) 870.

[21] R. Davis, Phys. Rev. Lett. 12 (1964) 303.

[22] J.N. Bahcall, Phys. Rev. Lett. 12 (1964) 300.

[23] Kamiokande Collaboration, Y. Fukuda et al., Phys.Rev.Lett. 77 (1996) 1683.

[24] Super-Kamiokande Collaboration, J. Hosaka et al., Phys.Rev. D73 (2006) 112001, hep-ex/0508053.

[25] GALLEX Collaboration, W. Hampel et al., Phys.Lett. B447 (1999) 127.

[26] GNO Collaboration, M. Altmann et al., Phys.Lett. B616 (2005) 174, hep-ex/0504037.

[27] SAGE Collaboration, J. Abdurashitov et al., J.Exp.Theor.Phys. 95 (2002) 181, astro-ph/0204245.

[28] Super-Kamiokande Collaboration, Y. Fukuda et al., Phys. Rev. Lett. 81 (1998) 1562.

[29] SNO Collaboration, Q. Ahmad et al., Phys.Rev.Lett. 89 (2002) 011301, nucl-ex/0204008.

[30] KamLAND Collaboration, K. Eguchi et al., Phys.Rev.Lett. 90 (2003) 021802, hep-ex/0212021.

[31] K2K Collaboration, M. Ahn et al., Phys.Rev.Lett. 90 (2003) 041801, hep-ex/0212007.

[32] MINOS Collaboration, D. Michael et al., Phys.Rev.Lett. 97 (2006) 191801, hep-ex/0607088.

[33] S.F. King, Contemporary Physics 48 (2007) 195.

[34] G. Fogli et al., Phys.Rev. D86 (2012) 013012, 1205.5254.

[35] CHOOZ Collaboration, M. Apollonio et al., Phys.Lett. B466 (1999) 415, hep-ex/9907037.

[36] MINOS Collaboration, P. Adamson et al., Phys.Rev.Lett. 107 (2011) 181802, hep-ex/1108.0015.

[37] T2K Collaboration, K. Abe et al., Phys.Rev.Lett. 107 (2011) 041801, hep-ex/1106.2822.

[38] DAYA-BAY Collaboration, F. An et al., Phys.Rev.Lett. 108 (2012) 171803, hep-ex/1203.1669.

[39] RENO collaboration, J. Ahn et al., Phys.Rev.Lett. 108 (2012) 191802, hep-ex/1204.0626.

[40] C. Kraus et al., Eur.Phys.J. C40 (2005) 447, hep-ex/0412056.

[41] V. Lobashev et al., Physics Letters B 460 (1999) 227 .

[42] S.M. Bilenky and S.T. Petcov, Rev. Mod. Phys. 59 (1987) 671.

[43] Majorana Collaboration, R. Gaitskell et al., (2003), nucl-ex/0311013.

[44] GERDA Collaboration, A.A. Smolnikov, (2008), nucl-ex/0812.4194.

[45] F. Feruglio, A. Strumia and F. Vissani, Nucl.Phys. B637 (2002) 345, hep-ph/0201291.

[46] WMAP Collaboration, E. Komatsu et al., Astrophys.J.Suppl. 192 (2011) 18, 1001.4538.

[47] WMAP Collaboration, N. Jarosik et al., Astrophys.J.Suppl. 192 (2011) 14, 1001.4744v1.

[48] A. Beach et al., Phys.Rev.Lett. 87 (2001) 271101, astro-ph/0111094.

[49] G. Steigman, Ann.Rev.Astron.Astrophys. 14 (1976) 339.

[50] A.G. Cohen, A. De Rujula and S. Glashow, Astrophys.J. 495 (1998) 539, astro-ph/9707087.

[51] E. Kolb and M. Turner, The Early Universe (Westview Press, 1994).

[52] G. Steigman, Ann.Rev.Nucl.Part.Sci. 57 (2007) 463, 0712.1100.

[53] D. Kirkman et al., Astrophys.J.Suppl. 149 (2003) 1, astro-ph/0302006.

[54] G.F. Smoot et al., Astrophys.J. 396 (1992) L1.

[55] A. Strumia, Les Houches Summer School on Theoretical Physics, pp. 655–680, 2005, hep-ph/0608347.

[56] A. Sakharov, Pisma Zh.Eksp.Teor.Fiz. 5 (1967) 32.

[57] G. 't Hooft, Phys. Rev. Lett. 37 (1976) 8.

[58] F.R. Klinkhamer and N.S. Manton, Phys. Rev. D 30 (1984) 2212.

[59] M. Kobayashi and T. Maskawa, Progress of Theoretical Physics 49 (1973) 652.

[60] CKMfitter Group, J. Charles et al., Eur.Phys.J. C41 (2005) 1, hep-ph/0406184.

[61] W. Bernreuther, Lect.Notes Phys. 591 (2002) 237, hep-ph/0205279.

[62] V. Rubakov and M. Shaposhnikov, Usp.Fiz.Nauk 166 (1996) 493, hep-ph/9603208.

[63] M. Gavela et al., Mod.Phys.Lett. A9 (1994) 795, hep-ph/9312215.

[64] K. Jansen, Nucl.Phys.Proc.Suppl. 47 (1996) 196, hep-lat/9509018.

[65] N. Arkani-Hamed et al., 65 (2002) 024032, arXiv:hep-ph/9811448.

[66] M.C. Gonzalez-Garcia and M. Maltoni, Phys. Rept. 460 (2008) 1, 0704.1800.

[67] I. Affleck and M. Dine, Nucl.Phys. B249 (1985) 361.

[68] M. Gell-Mann, P. Ramond and R. Slansky, Conf.Proc. C790927 (1979) 315.

[69] P. Minkowski, Physics Letters B 67 (1977) 421.

[70] R.N. Mohapatra and G. Senjanovic, Physical Review Letters 44 (1980) 912.

[71] T. Yanagida, Conf.Proc. C7902131 (1979) 95.

[72] M. Magg and C. Wetterich, Phys.Lett. B94 (1980) 61.

[73] R.N. Mohapatra and G. Senjanovic, Phys.Rev. D23 (1981) 165.

[74] G. Lazarides, Q. Shafi and C. Wetterich, Nucl.Phys. B181 (1981) 287.

[75] R. Foot et al., Z.Phys. C44 (1989) 441.

[76] E. Ma, Phys. Rev. D 73 (2006) 077301.

[77] C. Aulakh et al., Physics Letters B 588 (2004) 196 .

[78] A. Hartanto and L. Handoko, Phys.Rev. D71 (2005) 095013, hep-ph/0504280.

[79] G.C. Branco et al., Nuclear Physics B 640 (2002) 202, arXiv:hep-ph/0202030.

[80] S.L. Glashow, J. Iliopoulos and L. Maiani, Physical Review D 2 (1970) 1285.

[81] W. Buchmuller, R.D. Peccei and T. Yanagida, Ann. Rev. Nucl. Part. Sci. 55 (2005) 311, hep-ph/0502169.

[82] J.A. Harvey and M.S. Turner, Phys. Rev. D 42 (1990) 3344.

[83] E. Nardi et al., Journal of High Energy Physics 1 (2006) 68, arXiv:hep-ph/0512052.

[84] E.W. Kolb and M.S. Turner, Annual Review of Nuclear and Particle Science 33 (1983) 645, http://www.annualreviews.org/doi/pdf/10.1146/annurev.ns.33.120183.003241.

[85] L. Covi, E. Roulet and F. Vissani, Phys. Lett. B384 (1996) 169, hep-ph/9605319.

[86] M. Flanz, E.A. Paschos and U. Sarkar, Phys.Lett. B345 (1995) 248, hep-ph/9411366.

[87] W. Buchmüller, P.D. Bari and M. Plümacher, Nuclear Physics B 665 (2003).

[88] M. Fukugita and T. Yanagida, Phys. Lett. B174 (1986) 45.

[89] W. Buchmuller, P. Di Bari and M. Plumacher, Ann. Phys. 315 (2005) 305, hep-ph/0401240.

[90] J. Casas and A. Ibarra, Nucl.Phys. B618 (2001) 171, hep-ph/0103065.

[91] W. Buchmüller, P.D. Bari and M. Plümacher, Nuclear Physics B (2002).

[92] S. Davidson and A. Ibarra, Phys. Lett. B535 (2002) 25, hep-ph/0202239.

[93] A. Pilaftsis and T.E. Underwood, Nucl.Phys. B692 (2004) 303, hep-ph/0309342.

[94] G. Giudice et al., Nucl.Phys. B685 (2004) 89, hep-ph/0310123.

[95] M.A. Luty, Phys. Rev. D 45 (1992) 455.

[96] W. Buchmüller, P.D. Bari and M. Plümacher, Physics Letters B 547 (2002) 128.

[97] A. Abada et al., JHEP 0609 (2006) 010, hep-ph/0605281.

[98] E. Nardi et al., JHEP 01 (2006) 164, hep-ph/0601084.

[99] S. Blanchet and P. Di Bari, JCAP 0606 (2006) 023, hep-ph/0603107.

[100] A. Pilaftsis and T.E. Underwood, Phys.Rev. D72 (2005) 113001, hep-ph/0506107.

[101] G. Branco et al., Phys.Rev. D67 (2003) 073025, hep-ph/0211001.

[102] M. Plümacher, Zeitschrift fur Physik C Particles and Fields 74 (1997) 549, arXiv:hep-ph/9604229.

[103] R. Barbieri et al., Nuclear Physics B 575 (2000) 61 .

[104] G. Engelhard et al., Physical Review Letters 99 (2007) 081802, arXiv:hep-ph/0612187.

[105] J.M. Cline, K. Kainulainen and K.A. Olive, Phys.Rev. D49 (1994) 6394, hep-ph/9401208.

[106] S. Blanchet, P. Di Bari and G.G. Raffelt, JCAP 3 (2007) 12, arXiv:hep-ph/0611337.

[107] S. Blanchet and P. Di Bari, Nucl. Phys. B807 (2009) 155, 0807.0743.

[108] S. Davidson, E. Nardi and Y. Nir, Phys. Rept. 466 (2008) 105, 0802.2962.

[109] S. Blanchet and P. Di Bari, JCAP 0703 (2007) 018, hep-ph/0607330.

[110] A. Dolgov and Y. Zeldovich, Rev.Mod.Phys. 53 (1981) 1.

[111] E.W. Kolb and S. Wolfram, Nucl.Phys. B172 (1980) 224.

[112] A. Abada et al., JCAP 0604 (2006) 004, hep-ph/0601083.

[113] O. Vives, Phys. Rev. D 73 (2006) 073006.

[114] A.D. Simone and A. Riotto, JCAP 0702 (2007) 005, hep-ph/0611357v3.

[115] J.J. Sakurai, Modern Quantum Mechanics (Revised Edition), 1 ed. (Addison Wesley, 1993).

[116] M. Beneke et al., Nucl.Phys. B843 (2011) 177, 1007.4783.

[117] S. Antusch et al., Nucl.Phys. B856 (2012) 180, 1003.5132.

[118] G. Sigl and G. Raffelt, Nucl.Phys. B406 (1993) 423.

[119] H.A. Weldon, Phys.Rev. D26 (1982) 2789.

[120] A. Anisimov, A. Broncano and M. Plumacher, Nucl.Phys. B737 (2006) 176, hep-ph/0511248.

[121] P. Di Bari, Contemporary Physics Volume 53 (4) 2012, 1206.3168.

[122] A. Anisimov and P. Di Bari, Phys.Rev. D80 (2009) 073017, 0812.5085.

[123] S. Davidson and A. Ibarra, JHEP 0109 (2001) 013, hep-ph/0104076.

[124] F. Deppisch et al., Phys.Rev. D73 (2006) 033004, hep-ph/0511062.

[125] B. Dutta and R.N. Mohapatra, Phys.Rev. D68 (2003) 113008, hep-ph/0307163.

[126] A. Ibarra and G.G. Ross, Phys.Lett. B591 (2004) 285, hep-ph/0312138.

[127] F. Joaquim, I. Masina and A. Riotto, Int.J.Mod.Phys. A22 (2007) 6253, hep-ph/0701270.

[128] S. Pascoli, S. Petcov and C. Yaguna, Phys.Lett. B564 (2003) 241, hep-ph/0301095.

[129] H. Davoudiasl et al., Phys.Rev.Lett. 93 (2004) 201301, hep-ph/0403019.

[130] S. Dimopoulos and L. Susskind, Phys.Rev. D18 (1978) 4500.

[131] R. Kallosh et al., Phys.Rev. D52 (1995) 912, hep-th/9502069.

[132] M. Yoshimura, Phys.Rev.Lett. 41 (1978) 281.

[133] G. Engelhard et al., Phys.Rev.Lett. 99 (2007) 081802, hep-ph/0612187.

[134] R. Barbieri and A. Dolgov, Phys.Lett. B237 (1990) 440.

[135] P. Di Bari, P. Lipari and M. Lusignoli, Int.J.Mod.Phys. A15 (2000) 2289, hep-ph/9907548.

[136] M.C. Chen and S.F. King, JHEP 0906 (2009) 072, 0903.0125.

[137] E. Ma, Phys.Rev. D70 (2004) 031901, hep-ph/0404199.

[138] P. Harrison, D. Perkins and W. Scott, Phys.Lett. B530 (2002) 167, hep-ph/0202074.

[139] P.D. Bari, Nuclear Physics B 727 (2005) 318 .

[140] E.E. Jenkins and A.V. Manohar, Phys.Lett. B668 (2008) 210, 0807.4176.

[141] E.K. Akhmedov, M. Frigerio and A.Y. Smirnov, JHEP (2003).

[142] P. di Bari and A. Riotto, Physics Letters B 671 (2009) 462, 0809.2285.

[143] P. Di Bari and A. Riotto, JCAP 1104 (2011) 037, 1012.2343.

[144] A. Abada et al., Nucl.Phys. B809 (2009) 183, 0808.2058.

[145] P. Di Bari and L. Marzola, in preparation .

[146] P. Di Bari et al., in preparation .

[147] G. Fogli et al., Phys.Rev. D84 (2011) 053007, 1106.6028.

[148] T. Schwetz, M. Tortola and J. Valle, New J.Phys. 13 (2011) 063004, 1103.0734.

[149] Daya-Bay Collaboration, J. Ochoa-Ricoux, Nucl.Phys.Proc.Suppl. 217 (2011) 140.

[150] R.J. Barlow, Statistics - A Guide and Reference to the Use of Statistical Methods in the Physical Sciences (John Wiley Sons, 1989).

[151] G. D'Agostini, Reports on Progress in Physics 66 (2003) 1383, arXiv:physics/0304102.

[152] H.B. Prosper, physics/0606179v1.

[153] B.P. Roe, Probability and Statistics in Experimental Physics (Springer, 1997).

[154] T.S. Kuhn, The Structure of Scientific Revolutions, 3rd ed. (University of Chicago Press, 1996).

[155] D. Bardin and G. Passarino, The Standard model in the making (Clarendon Press, 1999).

[156] W. Buchmuller and C. Ludeling, (2006), hep-ph/0609174.

[157] S. Antusch, S. King and A. Riotto, JCAP 0611 (2006) 011, hep-ph/0609038.

[158] J. Liu and G. Segrè, Phys. Rev. D 48 (1993) 4609.

[159] M. Peskin and D. Schroeder, An Introduction To Quantum Field Theory (Frontiers in Physics) (Westview Press, 1995).

[160] W. Buchmüller and M. Plümacher, Physics Letters B 431 (1998) 354, arXiv:hep-ph/9710460.